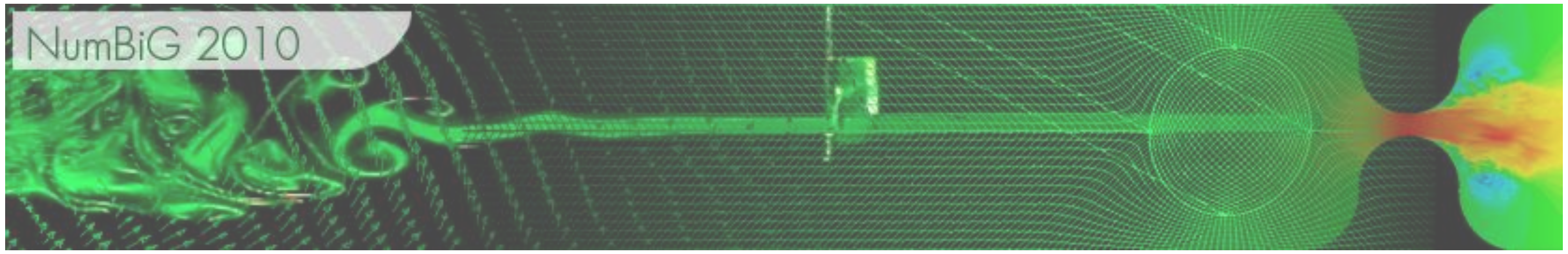

Pierre-Yves Lagrée

"Flow over an erodible bed, limits of the Saint Venant approach."

Grenoble 01/04/10

Institut Jean Le Rond d'Alembert *ex LMM*

Olivier Devauchelle, Christophe Josserand
(Daniel Lhuillier, Lydie Staron): FCIH IJLRA

Kouamé Kouakou, Kanh-Dang Nguyen Thu-Lam

Luce Malverti, Eric Lajeunesse, François Métivier: IPGP

- introduction
- the problem
- the flow: Saint Venant and other
- first granular model
- first coupling: bars
- improved granular model: saturation length
- ripples
- bars & ripples
- conclusions perspectives

meander

braided river

Iceland

Ornain, Bar-Le-Duc

photo Jorzan

photo IGN

Dunes Ripples

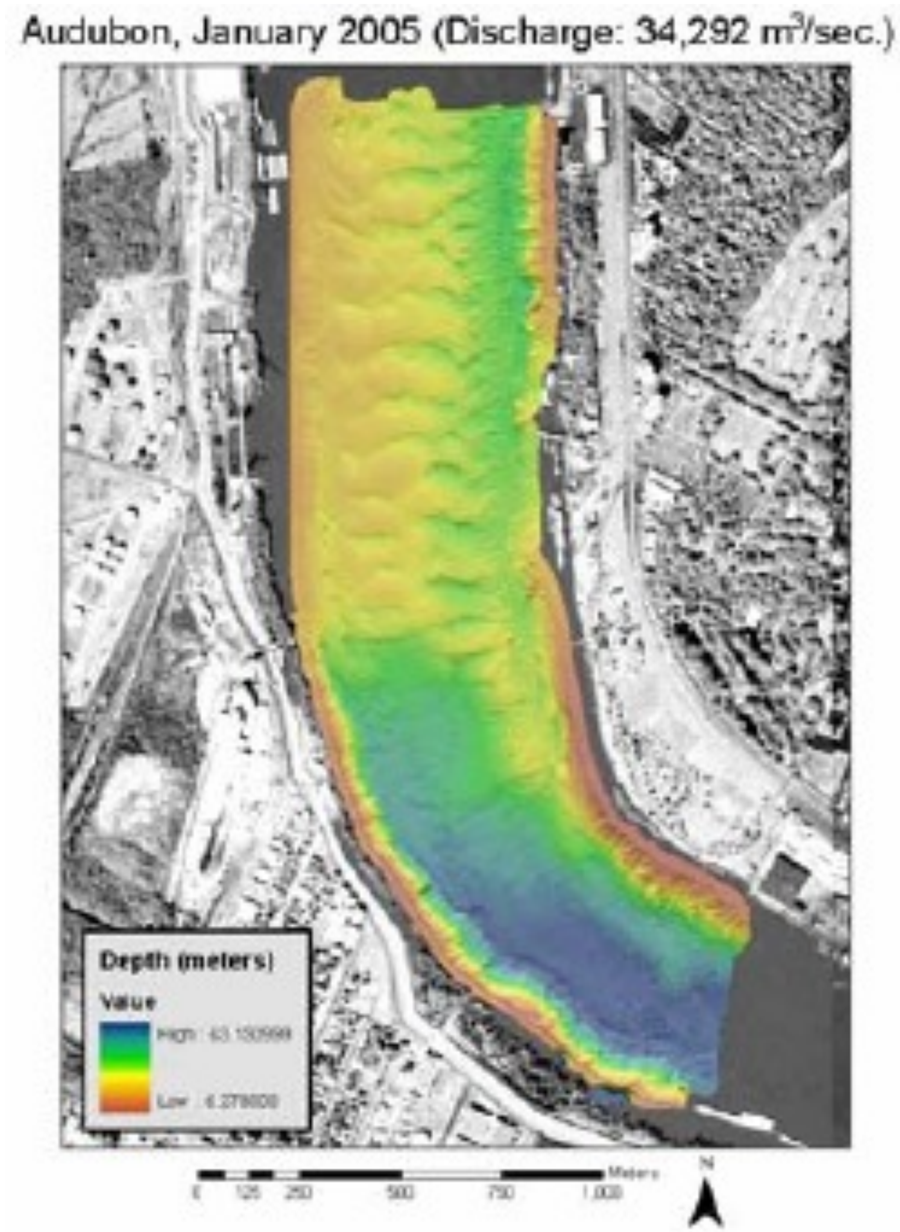

Dunes in the Mississippi
(L. Malverti et al., *Fluvial and Subaqueous Morphodynamics of Laminar Flow*, Sedimentology)

Dunes or Rhomboid bars in a micro-river

Laboratoire de Dynamique des Systèmes Géologiques

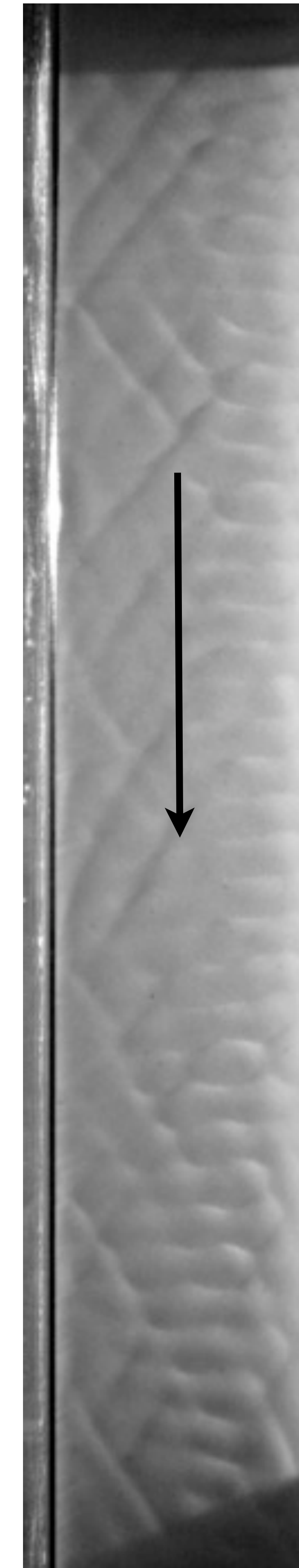

« linguoid bars»

Fuefuki river, Japon
(S. Ikeda)

笛吹市

in a micro-river
Laboratoire de Dynamique des Systèmes Géologiques

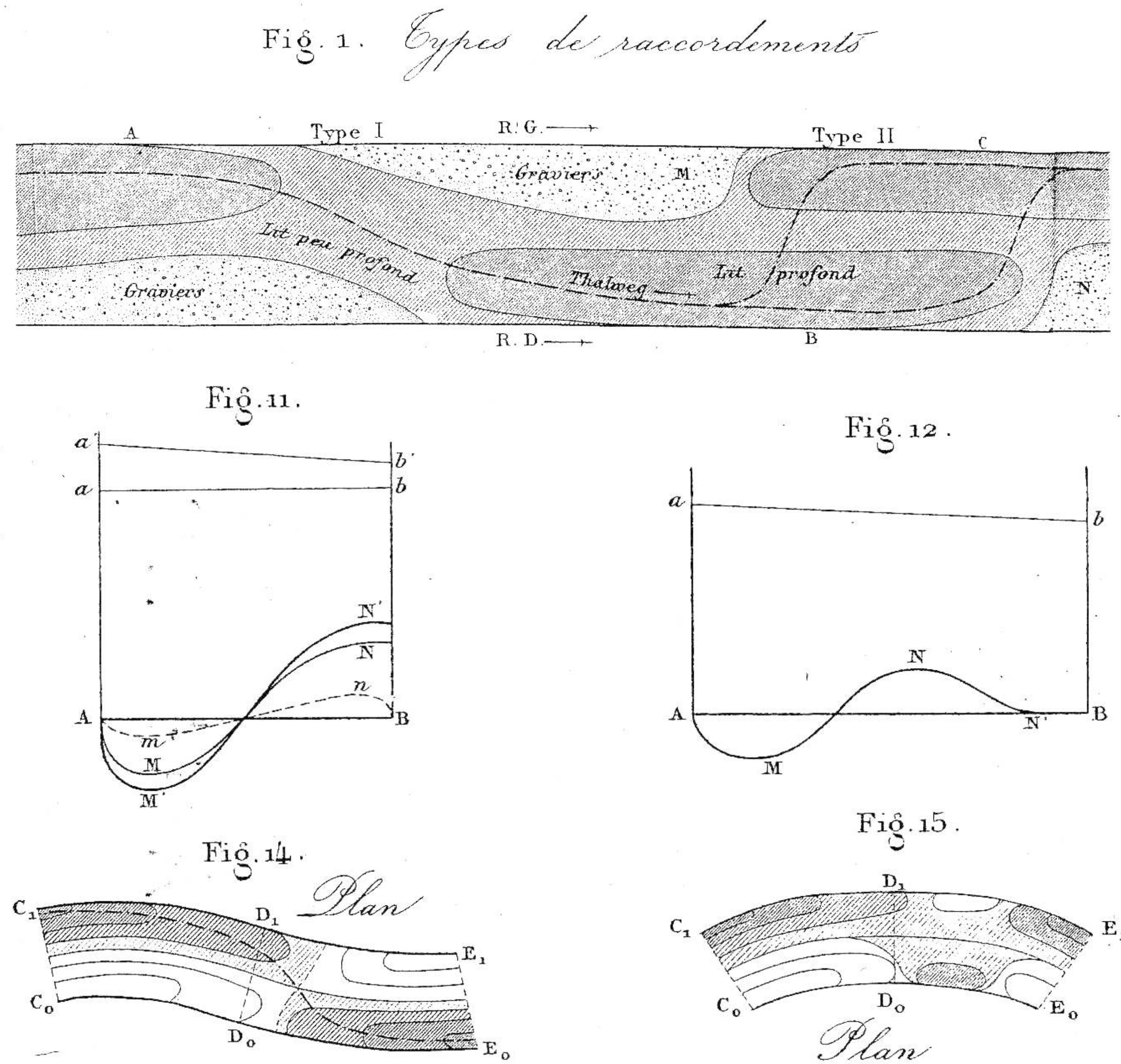

Fig. 1. Types de raccordements
Type I
R. G.
Type II
Graviers
Lit peu profond
Thalweg
Lit profond
Graviers
R. D.
Fig. 11.
Fig. 12.
Fig. 14.
Plan
Fig. 15.
Plan

Du Boys 1879

- introduction
- the problem
- the flow: Saint Venant and other
- first granular model
- first coupling: bars
- imporved granular model: saturation length
- ripples
- bars & ripples
- conclusions perspectives

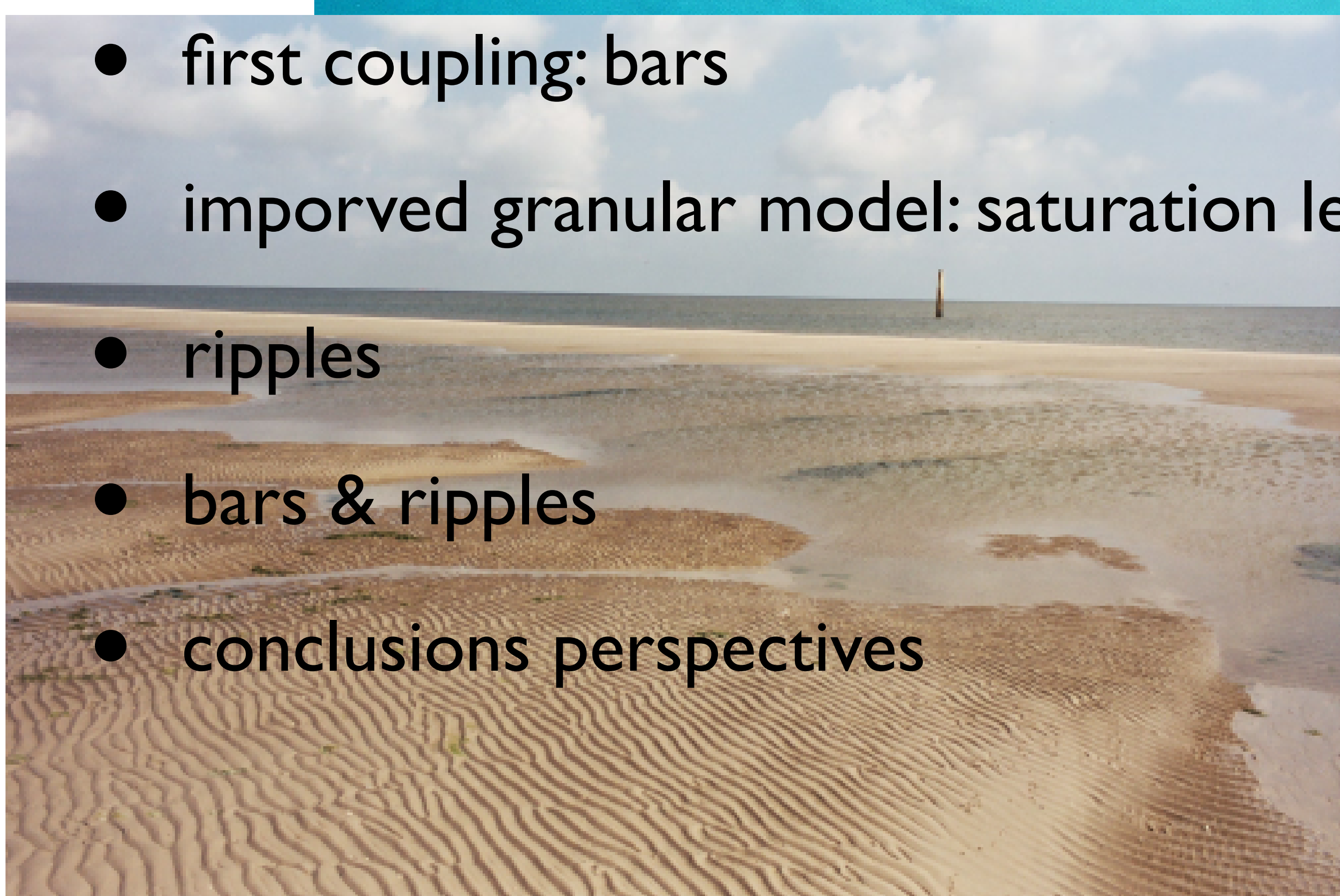

The problem:

Simplified model of interaction: erodible bed/ flow

- simplified transport laws

- asymptotic models for the flow (Saint Venant, pure shear flow at large Reynolds)

=> good physics, good terms in the equation but maybe too simple...

easy model to solve

stability, pattern formation

conservation of mass of granulars bed load

$$\frac{\partial f}{\partial t} = -\frac{\partial q}{\partial x}.$$

Problem :
What is the relationship between q and the flow?
hint: the larger u the larger the erosion, the larger q
q seems to be proportional to the skin friction

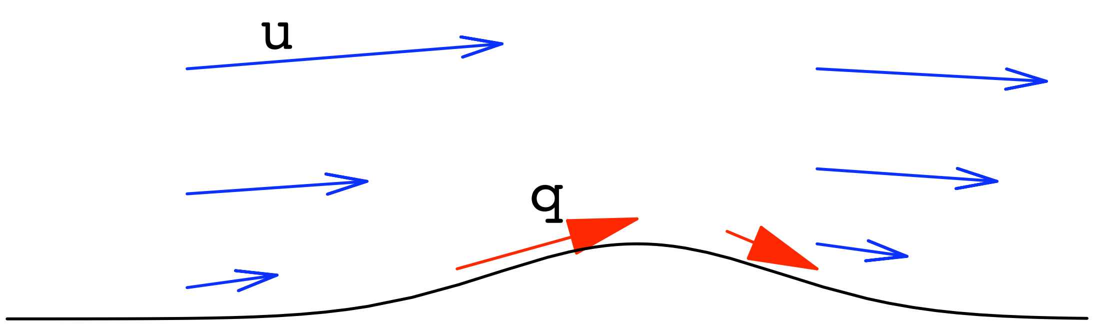

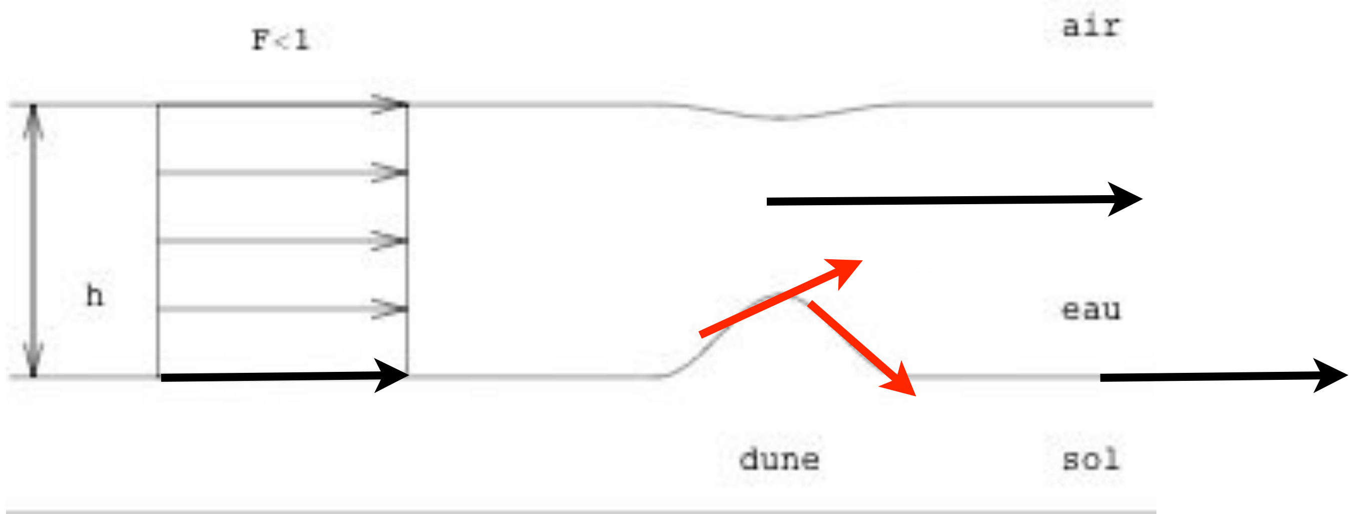

u increases & deacreases over the bump,

flux of granulars increases on the «wind» side

flux of granulars decreases on the «lee» side

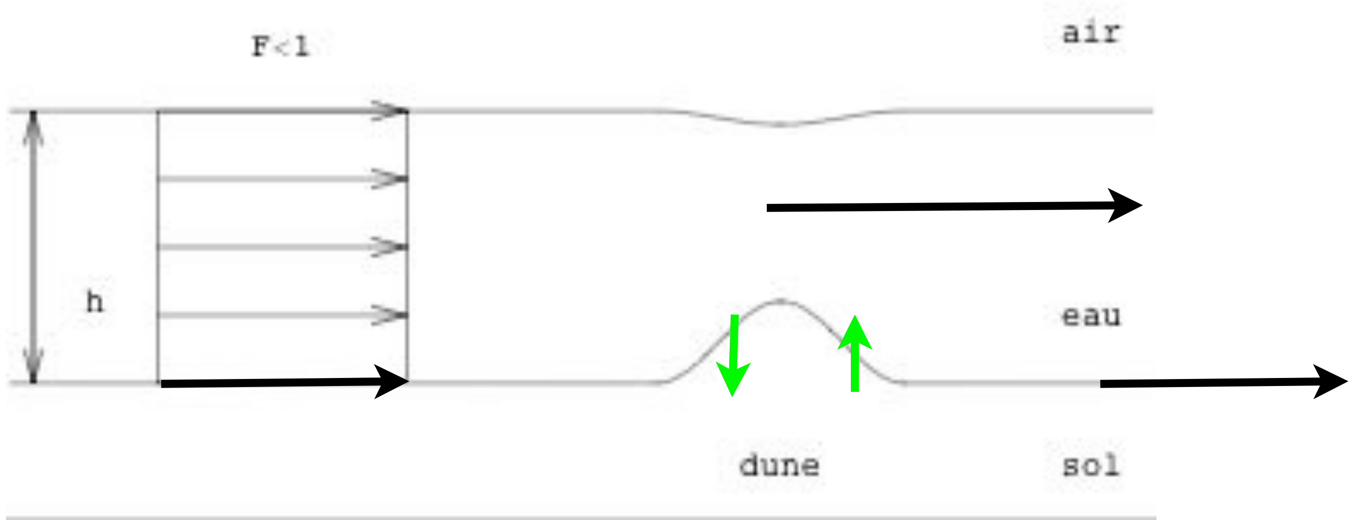

u increases & deacreases over the bump,

flux of granulars increases on the «wind» side

flux of granulars decreases on the «lee» side

the bump is eroded and sedimented

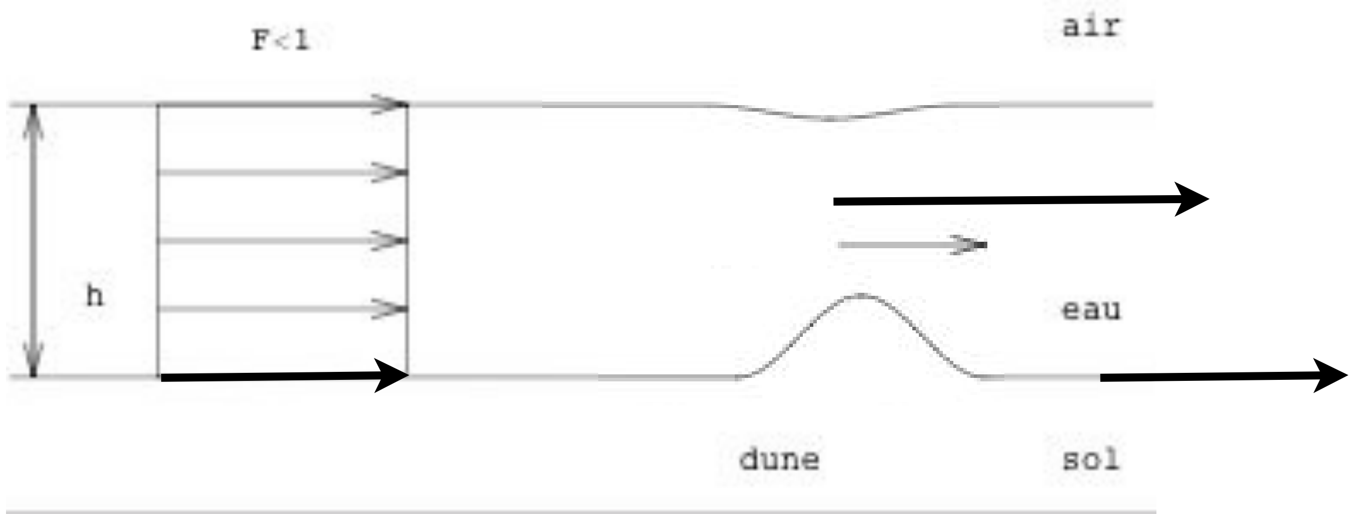

u increases & deacreases over the bump,

flux of granulars increases on the «wind» side

flux of granulars decreases on the «lee» side

the bump is eroded and sedimented

- case of the antidune!

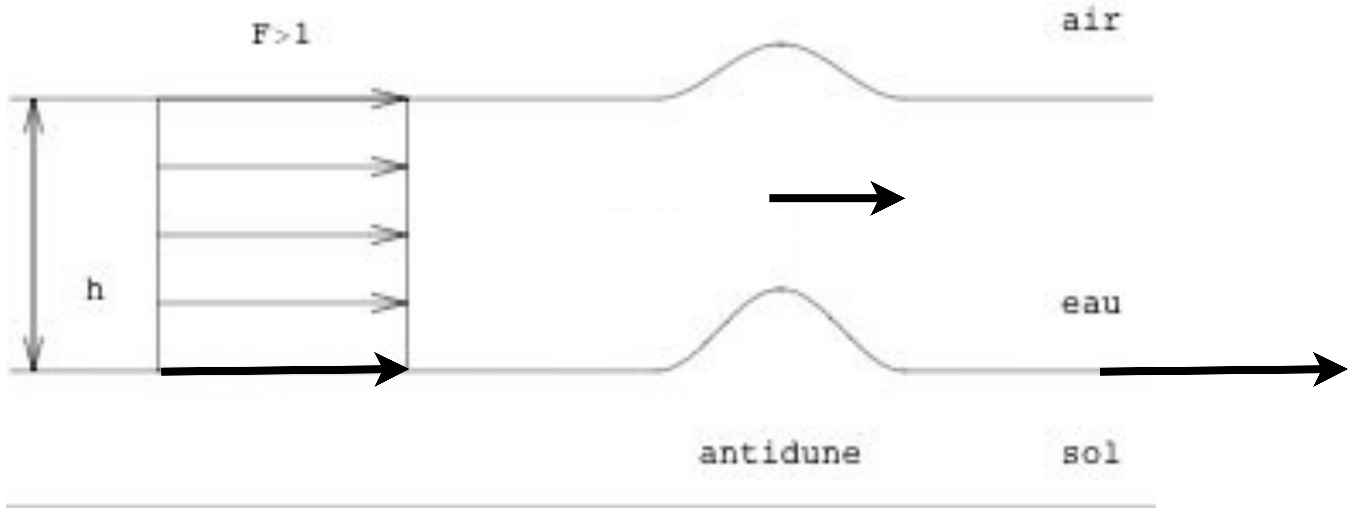

u increases & deacreases over the bump,

flux of granulars increases on the «wind» side

flux of granulars decreases on the «lee» side

the bump is eroded and sedimented

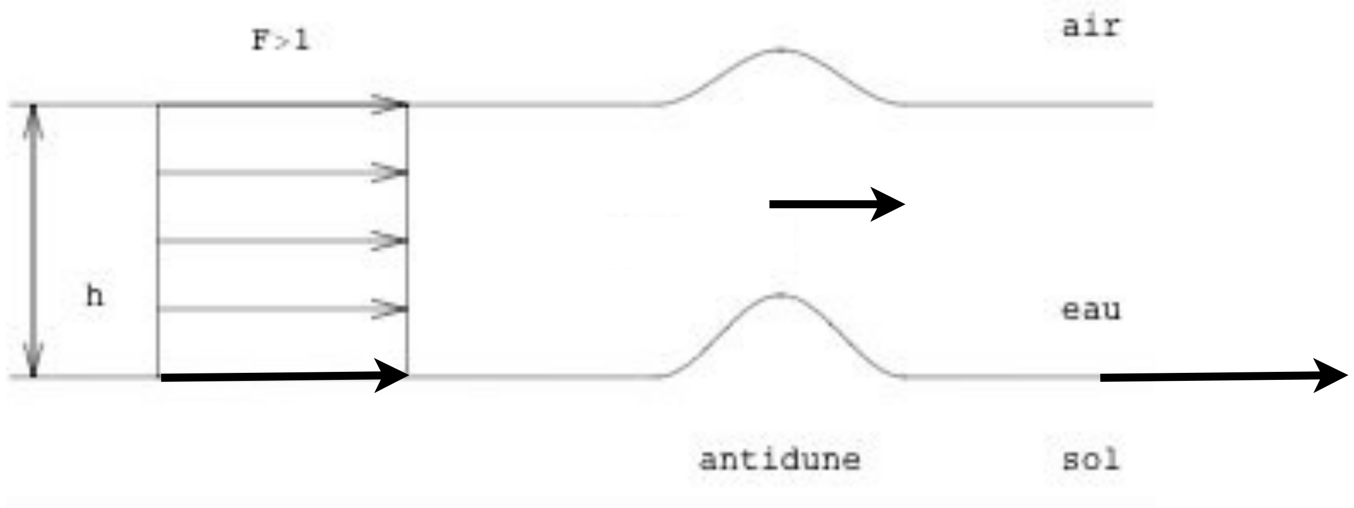

u increases & deacreases over the bump,

flux of granulars increases on the «wind» side

flux of granulars decreases on the «lee» side

the bump is eroded and sedimented

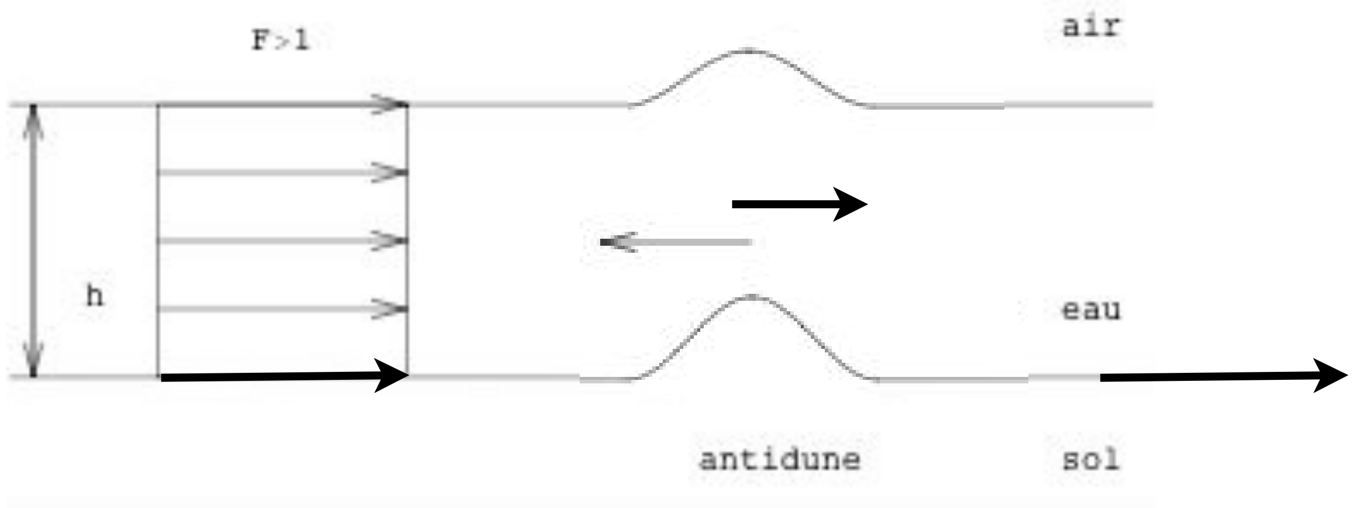

u increases & deacreases over the bump,

flux of granulars increases on the «wind» side

flux of granulars decreases on the «lee» side

the bump is eroded and sedimented

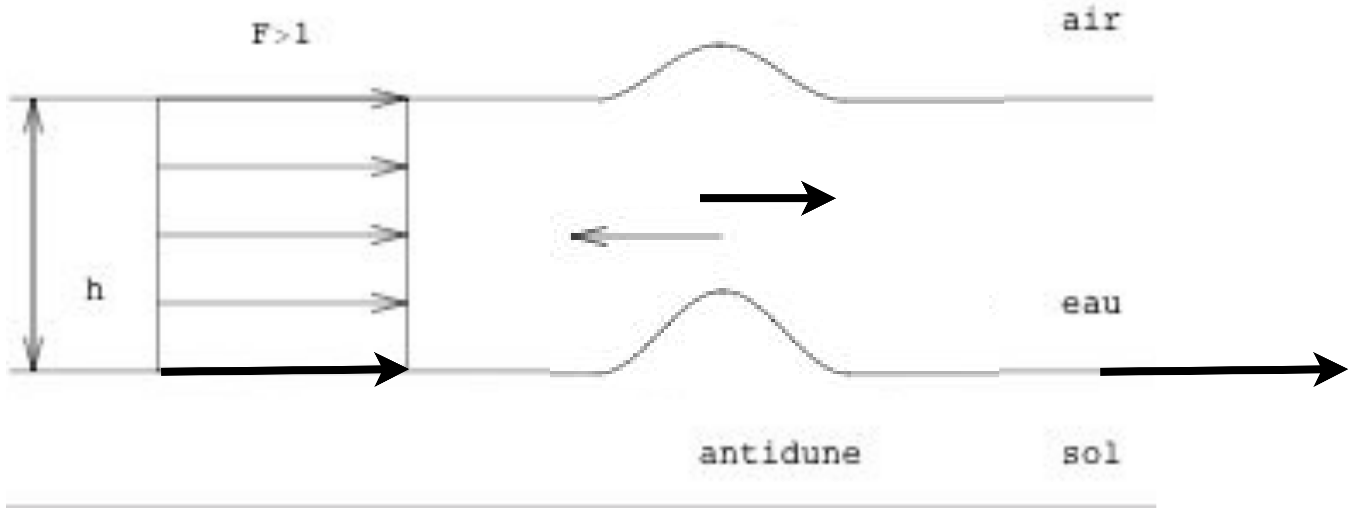

u increases & deacreases over the bump,

flux of granulars increases on the «wind» side

flux of granulars decreases on the «lee» side

the bump is eroded and sedimented

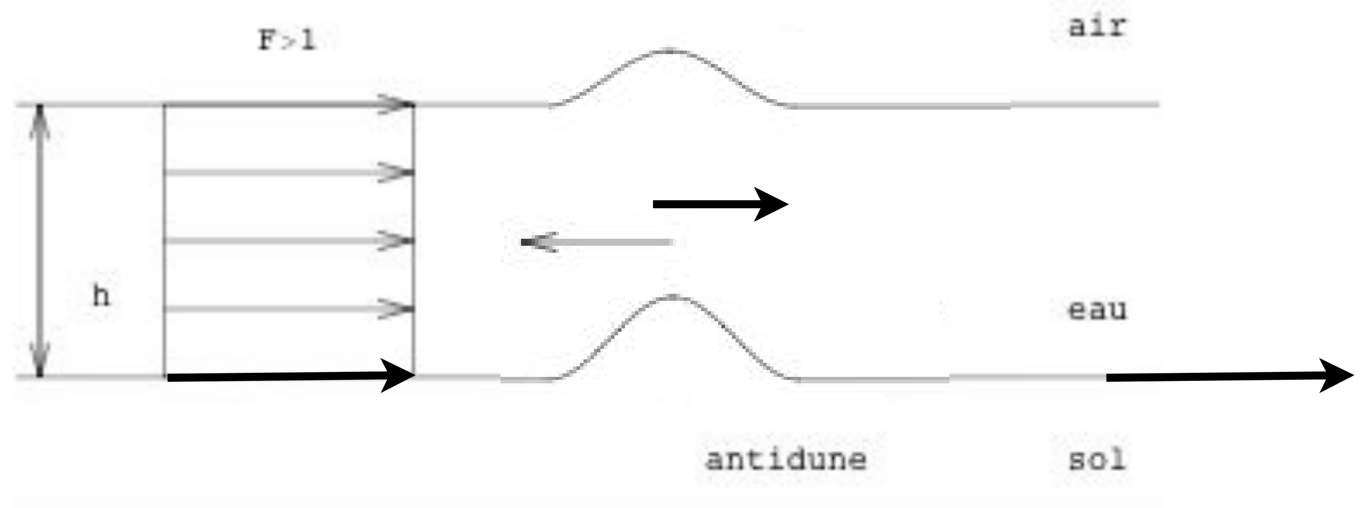

u increases & deacreases over the bump,

flux of granulars increases on the «wind» side

flux of granulars decreases on the «lee» side

the bump is eroded and sedimented

port An Dro Belle Ile

PATTERNS

Alternate bars

Meanders

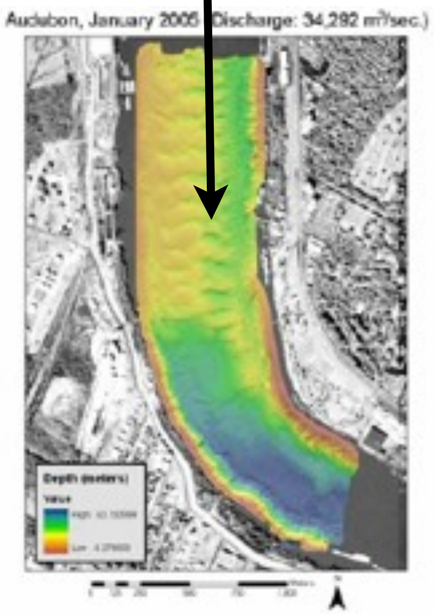

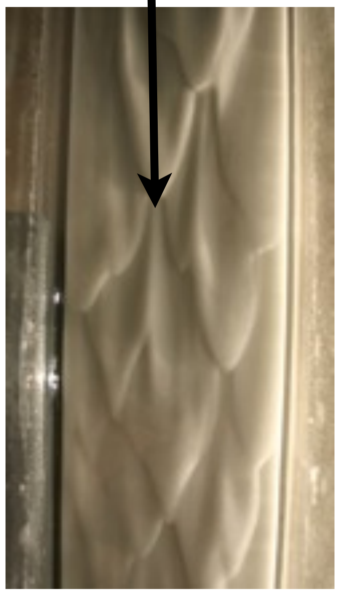

Rhomboid patterns

Lingoid bars

Ripples

Dunes

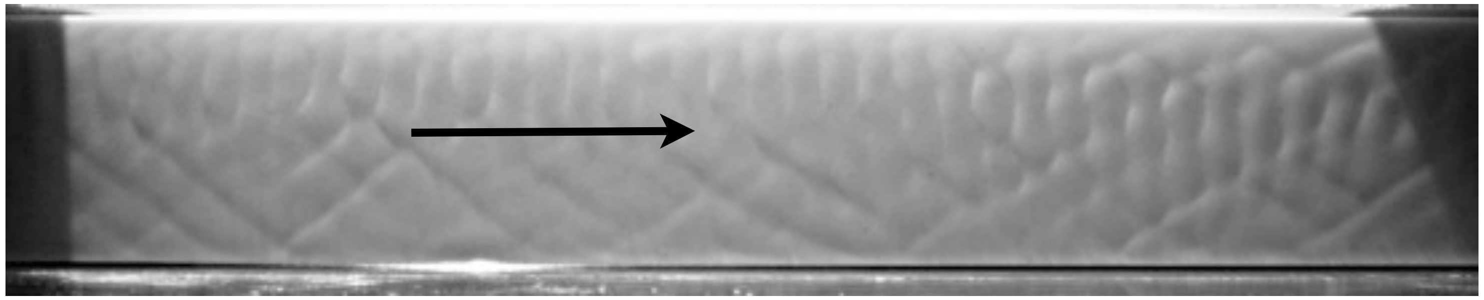

PATTERNS

Alternate bars

Meanders

Point meanders

Rhomboid patterns

Lingoid bars

Ripples

Dunes

Flow model?

Erosion model?

- introduction
- the problem
- the flow: Saint Venant and other
- first granular model
- first coupling: bars
- imporved granular model: saturation length
- ripples
- bars & ripples
- conclusions perspectives

the models

- Fluid Models
- Erosion models

steady flow configurations

fast, but with enough Physics

aimed at river flow, but OK for coastal

Saint-Venant approach

Flow Model

$$\int_{z=f}^{z=\eta} dz \qquad \text{(Navier Stokes)}$$

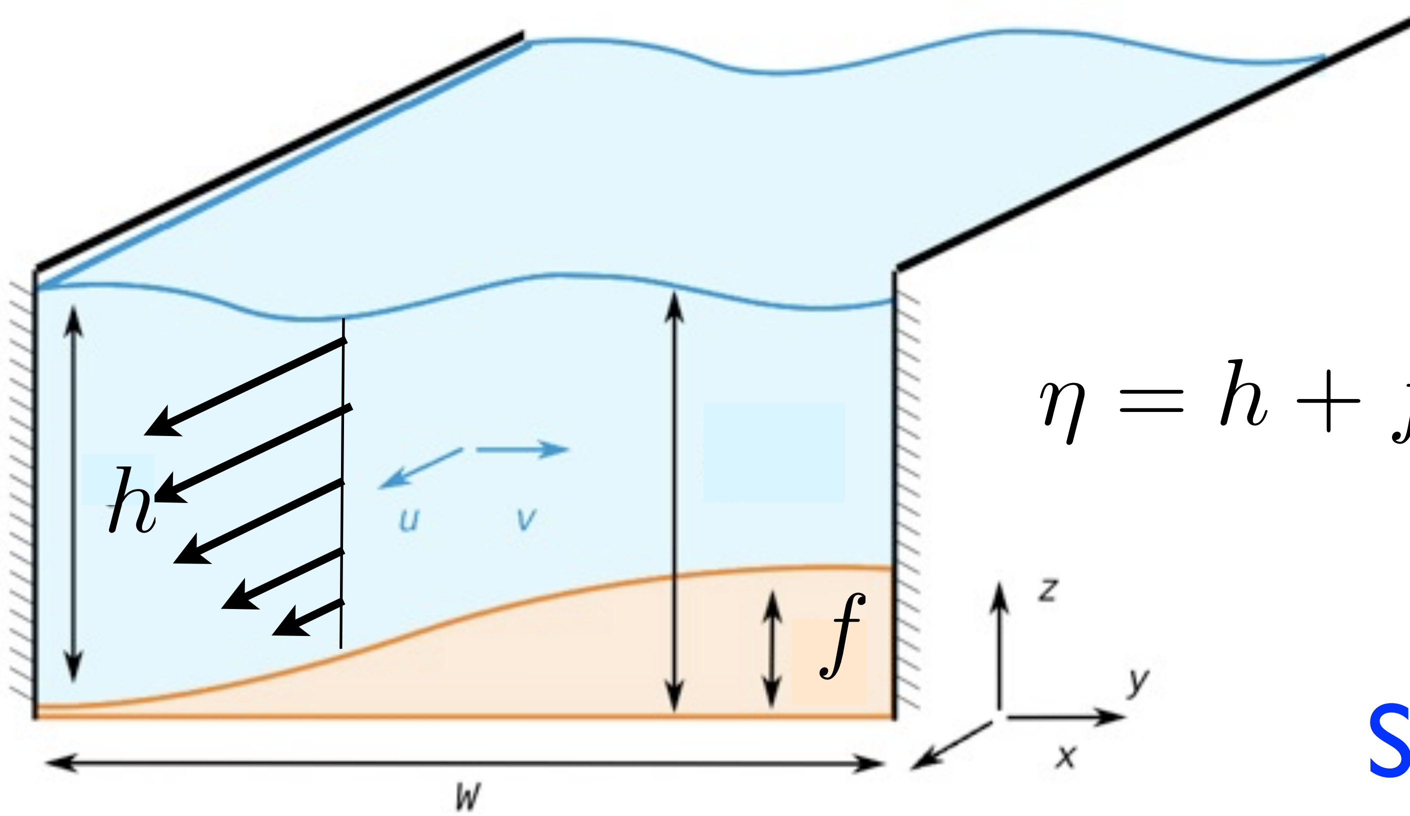

$$\eta = h + f$$

+Poiseuille profile

+ hydrostatic balance

Shallow water - Saint Venant

Saint-Venant approach

Flow Model

$$\frac{6}{5}(\overrightarrow{u} \cdot \overrightarrow{\nabla})\overrightarrow{u} = -g(\overrightarrow{\nabla}\eta + sin(\theta)\overrightarrow{e}_x) - \frac{3\nu\overrightarrow{u}}{(h)^2}$$

$$\overrightarrow{\nabla} \cdot (h\overrightarrow{u}) = 0$$

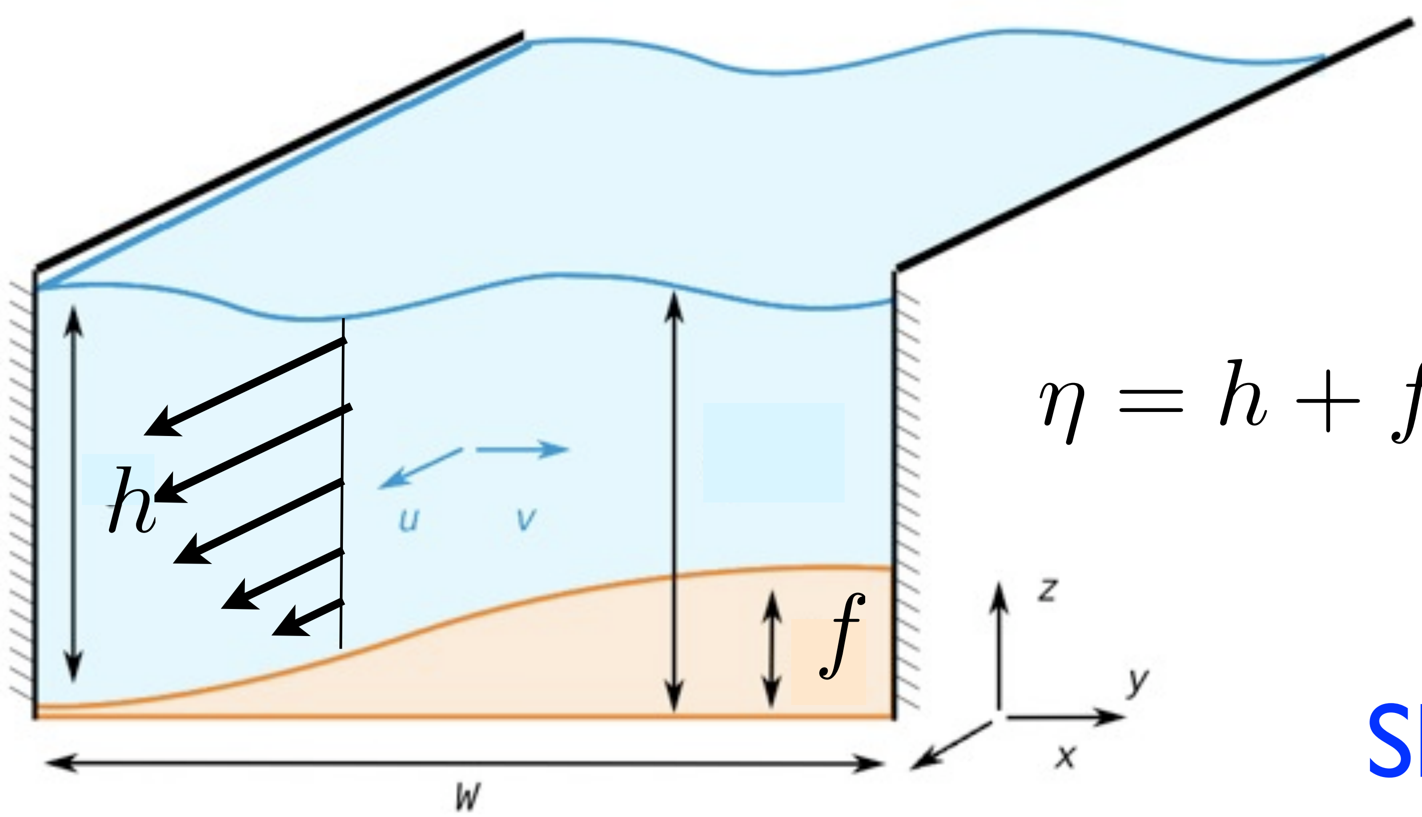

$$\eta = h + f$$

+Poiseuille profile

+ hydrostatic balance

Shallow water - Saint Venant

Saint-Venant approach

Flow Model

laminar $$\frac{6}{5}F^2 u_k \partial_k u_i = S\delta_{i1} - \partial_i(h+f) - S\frac{u_i}{h^2}$$

turbulent $$F^2 u_k \partial_k u_i = S\delta_{i1} - \partial_i(h+f) - S\frac{||u||}{h}u_i$$

$$\partial_k(hu_k) = 0$$

$$F^2 = \frac{U_0}{gh_0}$$

$$\mathrm{Re} = \frac{3F^2}{S}.$$

$$\boxed{\tau_i = ||u||u_i}$$

Saint-Venant approach

Flow Model

laminar $$\frac{6}{5}F^2 u_k \partial_k u_i = S\delta_{i1} - \partial_i(h+f) - S\frac{u_i}{h^2}$$

$$\partial_k(hu_k) = 0$$

$$F^2 = \frac{U_0}{gh_0}$$

$$\mathrm{Re} = \frac{3F^2}{S}.$$

$$\boxed{\tau_i = \frac{u_i}{h}}$$

Saint-Venant approach

Flow Model

laminar $$\frac{6}{5}F^2 u_k \partial_k u_i = S\delta_{i1} - \partial_i(h+f) - S\frac{u_i}{h^2}$$

$$\partial_k(hu_k) = 0$$

$$F^2 = \frac{U_0}{gh_0}$$

$$(x, y) \to h_0/S$$

$$\mathrm{Re} = \frac{3F^2}{S}.$$

$$\boxed{\tau_i = \frac{u_i}{h}}$$

Saint-Venant approach

Flow Model

laminar $$\frac{6}{5}F^2 u_k \partial_k u_i = \delta_{i1} - \partial_i(h+f) - \frac{u_i}{h^2}$$

$$\partial_k(hu_k) = 0$$

$$F^2 = \frac{U_0}{gh_0}$$

$$(x,y) \to h_0/S$$

$$\mathrm{Re} = \frac{3F^2}{S}.$$

$$\boxed{\tau_i = \frac{u_i}{h}}$$

SV

$$\frac{6}{5}F^2 u_k \partial_k u_i = \delta_{i1} - \partial_i (h+f) - \frac{u_i}{h^2}$$

$$\partial_k (h u_k) = 0$$

Long Wave perturbation

$$\frac{6}{5}\varepsilon F^2 u_k \partial_k u_i = \delta_{i1} - \frac{u_i}{h^2} - \varepsilon \partial_i (h+f)$$

$$\partial_k (h u_k) = 0$$

Short Wave perturbation

$$\frac{6}{5}F^2 u_k \partial_k u_i = \varepsilon(\delta_{i1} - \frac{u_i}{h^2}) - \partial_i (h+f)$$

$$\partial_k (h u_k) = 0$$

SV

$$\frac{6}{5}F^2 u_k \partial_k u_i = \delta_{i1} - \partial_i(h+f) - \frac{u_i}{h^2}$$

$$\partial_k(hu_k) = 0$$

equations «before» transverse integration:

Reduced Navier Stokes Prandtl

$$F^2\left(\frac{\partial \bar{U}_1}{\partial \bar{t}} + \bar{U}_1\frac{\partial \bar{U}_1}{\partial \bar{x}} + \bar{U}_2\frac{\partial \bar{U}_1}{\partial \bar{z}}\right) = 1 - \frac{\partial \bar{p}}{\partial \bar{x}} + \frac{\partial^2 \bar{U}_1}{\partial \bar{z}^2}.$$

$$\frac{\partial \bar{U}_1}{\partial \bar{x}} + \frac{\partial \bar{U}_2}{\partial \bar{z}} = 0$$

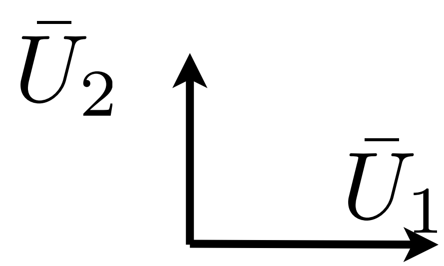

parabolic system

not primitive equations

equations «before» transverse integration

Short Wave perturbation

$$\frac{6}{5}F^2 u_k \partial_k u_i = \varepsilon(\delta_{i1} - \frac{u_i}{h^2}) - \partial_i(h+f)$$

$$\partial_k(hu_k) = 0$$

equations «before» transverse integration

Short Wave perturbation

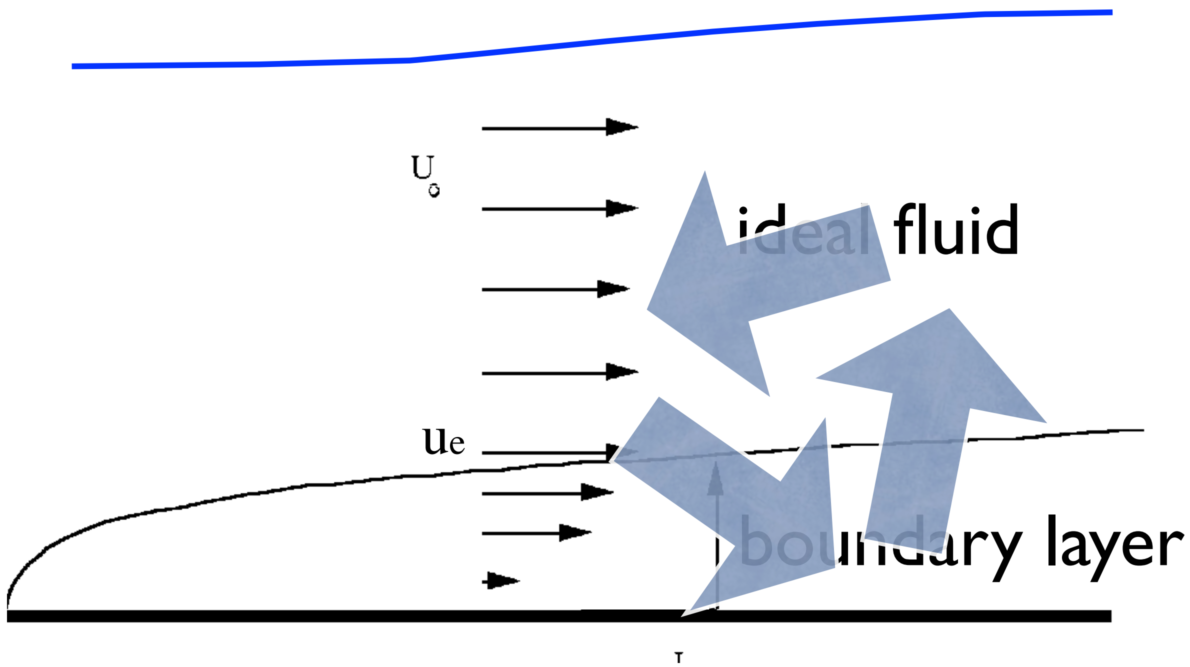

$$\frac{6}{5}F^2 u_k \partial_k u_i = -\partial_i(h+f)$$

$$\partial_k(hu_k) = 0$$

Ideal Fluid + Boundary Layer

INTERACTING BOUNDARY LAYER

VISCOUS INVISCID INTERACTIONS

$$\bar{u}_e = 1 + \frac{1}{1-F}[\bar{f}(\bar{x}) + \tilde{\delta}_1 Re^{-1/2}]$$

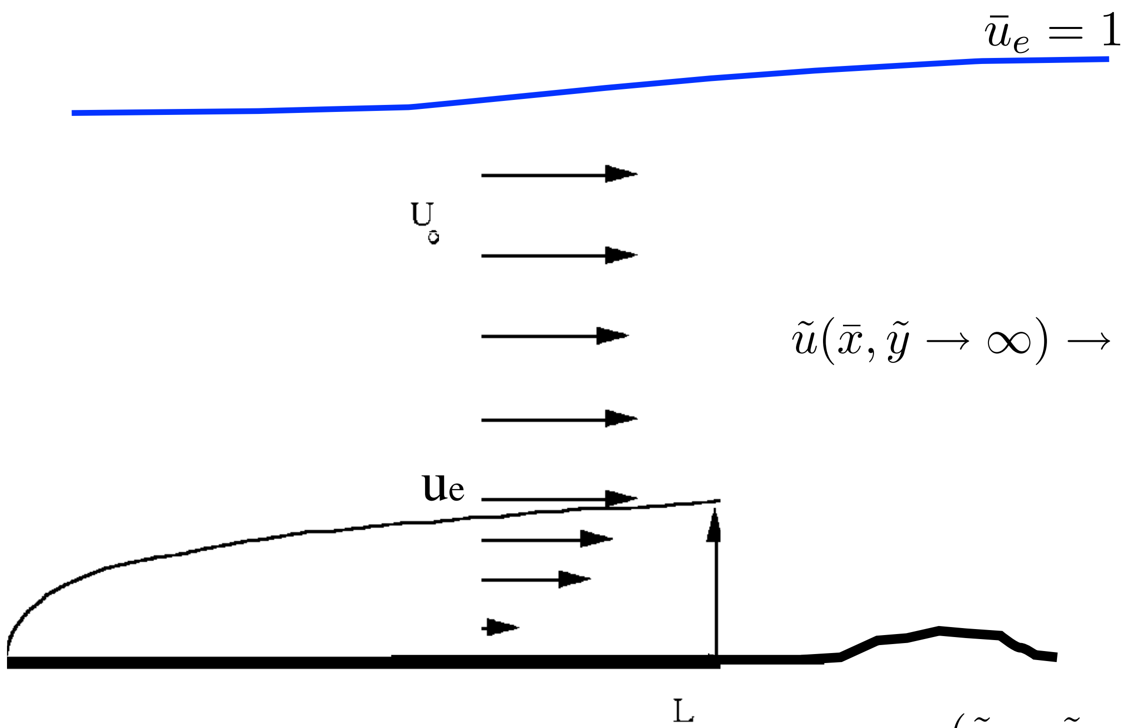

$$\tilde{u}(\bar{x}, \tilde{y} \to \infty) \to \bar{u}_e(\bar{x}) \qquad \bar{v}_e = Re^{-1/2}\frac{d(\tilde{\delta}_1 \bar{u}_e)}{d\bar{x}}$$

$$\frac{\partial \tilde{u}}{\partial \bar{x}} + \frac{\partial \tilde{v}}{\partial \tilde{y}} = 0,$$

$$\tilde{u}\frac{\partial \tilde{u}}{\partial \bar{x}} + \tilde{v}\frac{\partial \tilde{u}}{\partial \tilde{y}} = \bar{u}_e\frac{d\bar{u}_e}{d\bar{x}} + \frac{\partial^2 \tilde{u}}{\partial \tilde{y}^2},$$

$$(\tilde{u} = \tilde{v} = 0 \text{ on the body } \bar{f}(\bar{x}))$$

inviscid viscous interaction

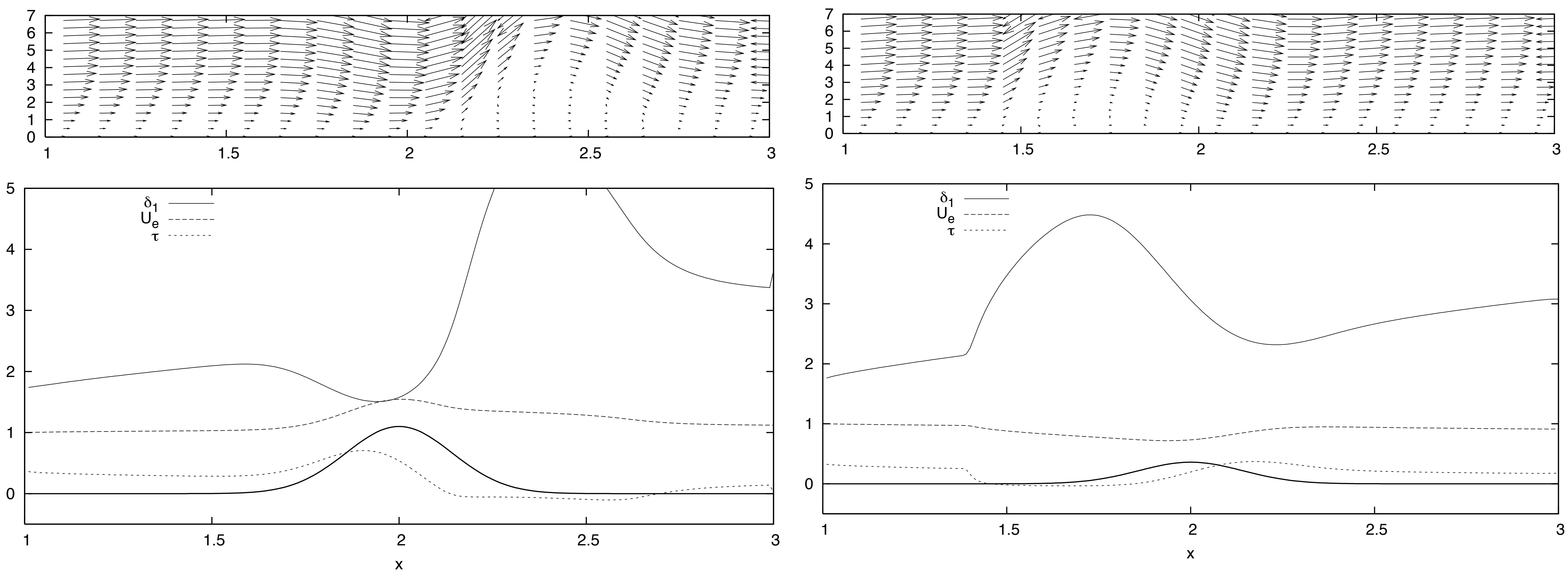

we think that:

IBL is a better closure than Saint Venant in the Short Wave case

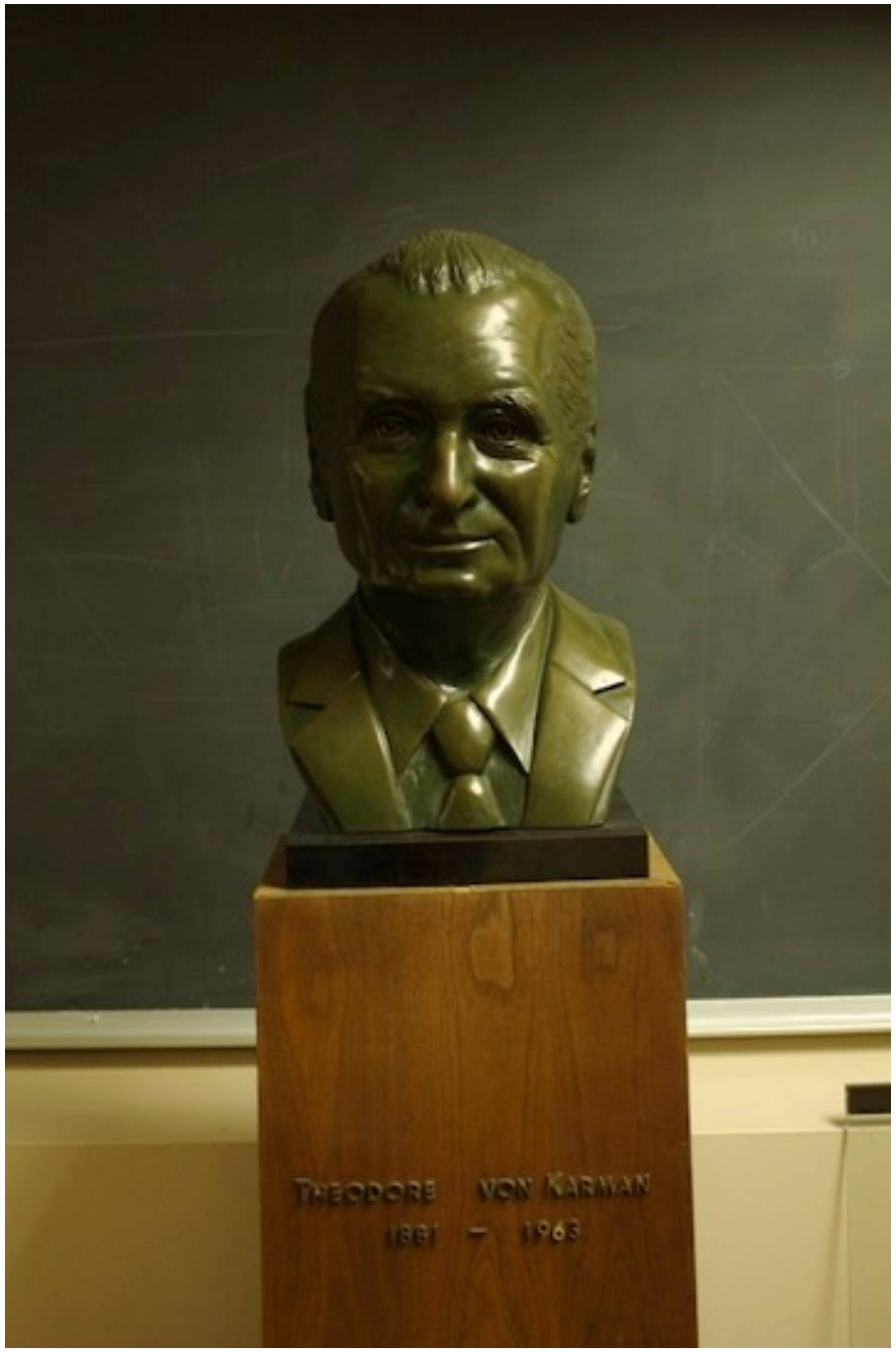

photo PYL

Adhémar BARRÉ de SAINT-VENANT 1797 1886

sabix

But maybe the best model is NAVIER STOKES ;-)

linear perturbation of a quasisteady flow with a given wavy bed

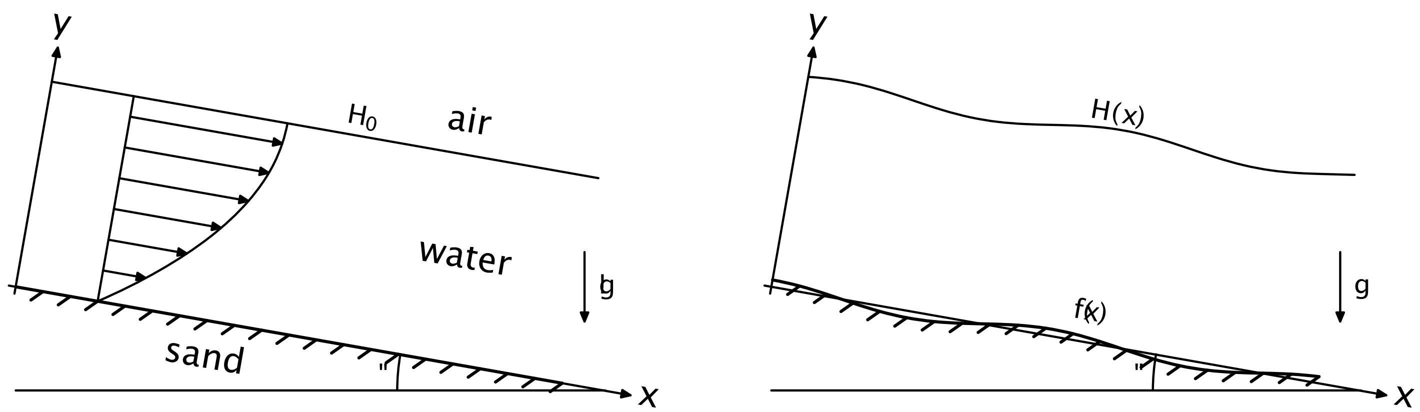

basic flow is Nuβelt (half Poiseuille)

linear perturbation of a quasisteady flow with a given wavy bed

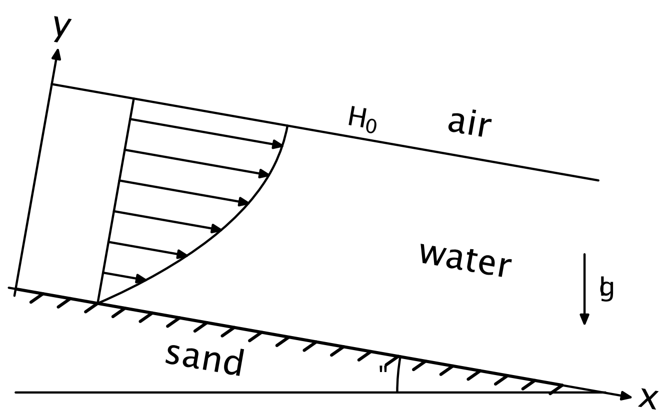

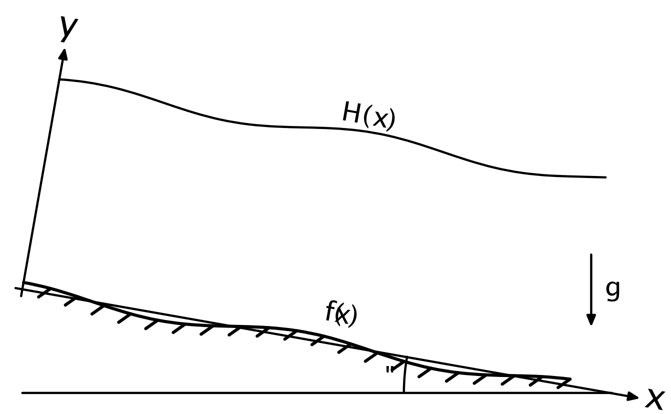

basic flow is Nuβelt (half Poiseuille)

+ linear perturbation

$$u = U_0 + \varepsilon\psi'(y)e^{ikx} \quad v = -\varepsilon ik\psi(y)e^{ikx}$$

$$\psi'''' - 2k^2\psi'' + k^4\psi = ikRe\{U_0(\psi'' - k^2\psi) - U_0''\psi\}$$

linear perturbation of a quasisteady flow with a given wavy bed

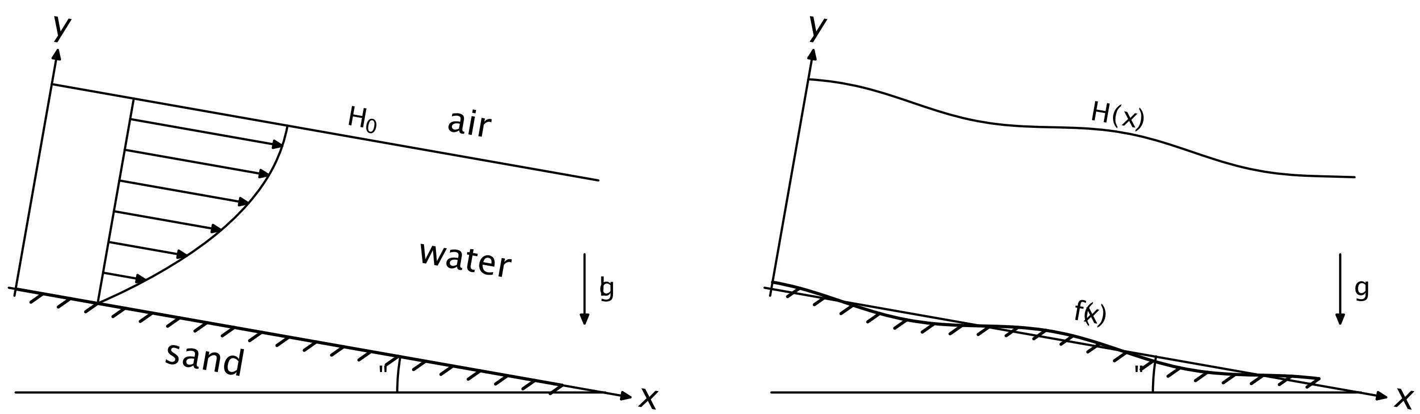

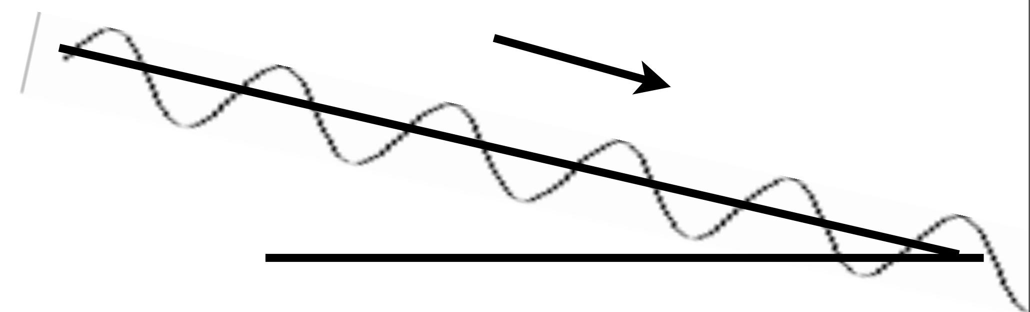

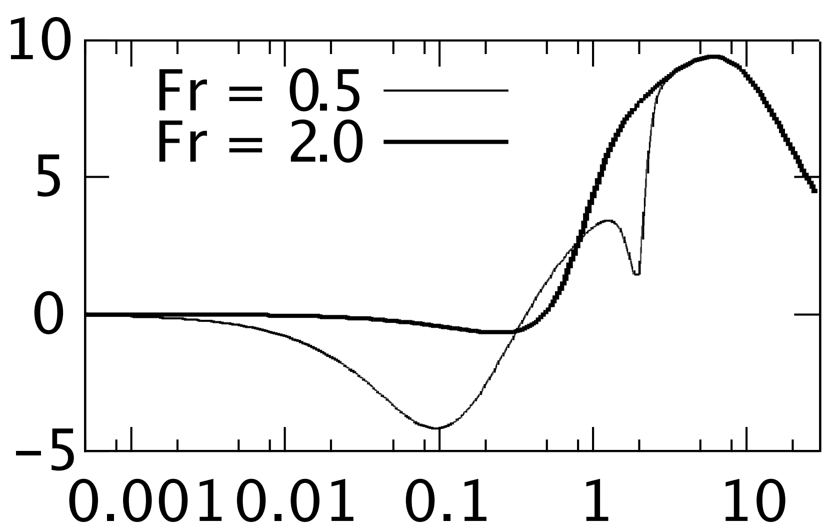

Re=50

skin friction response

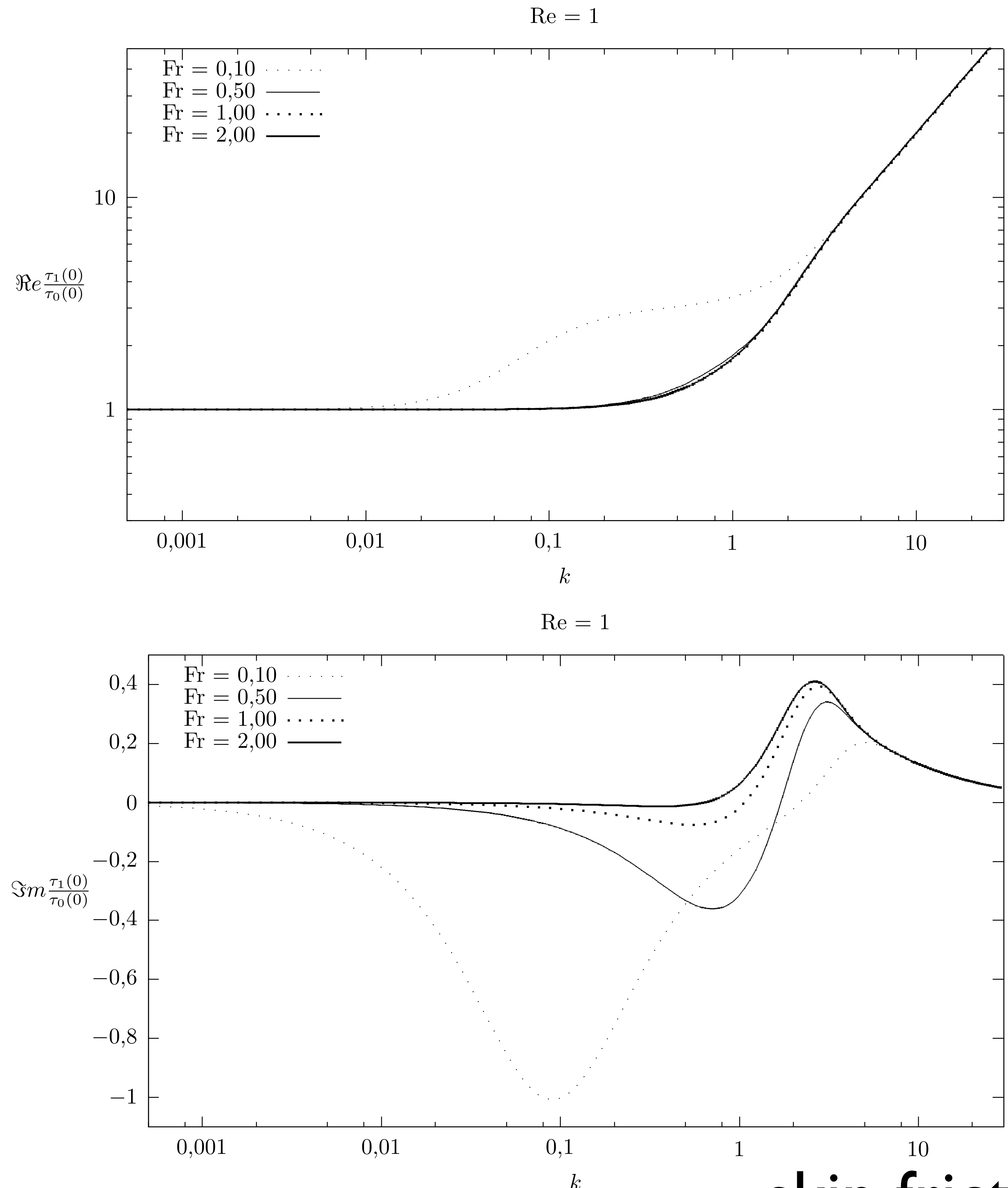

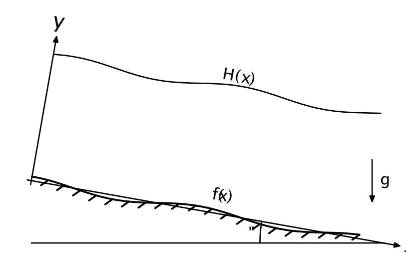

skin friction response

FIG. 2.3 – *Parties réelles (en haut) et parties imaginaires (en bas) de la perturbation du cisaillement au fond renormalisée, pour $Re = 1$ et différentes valeurs de Fr.*

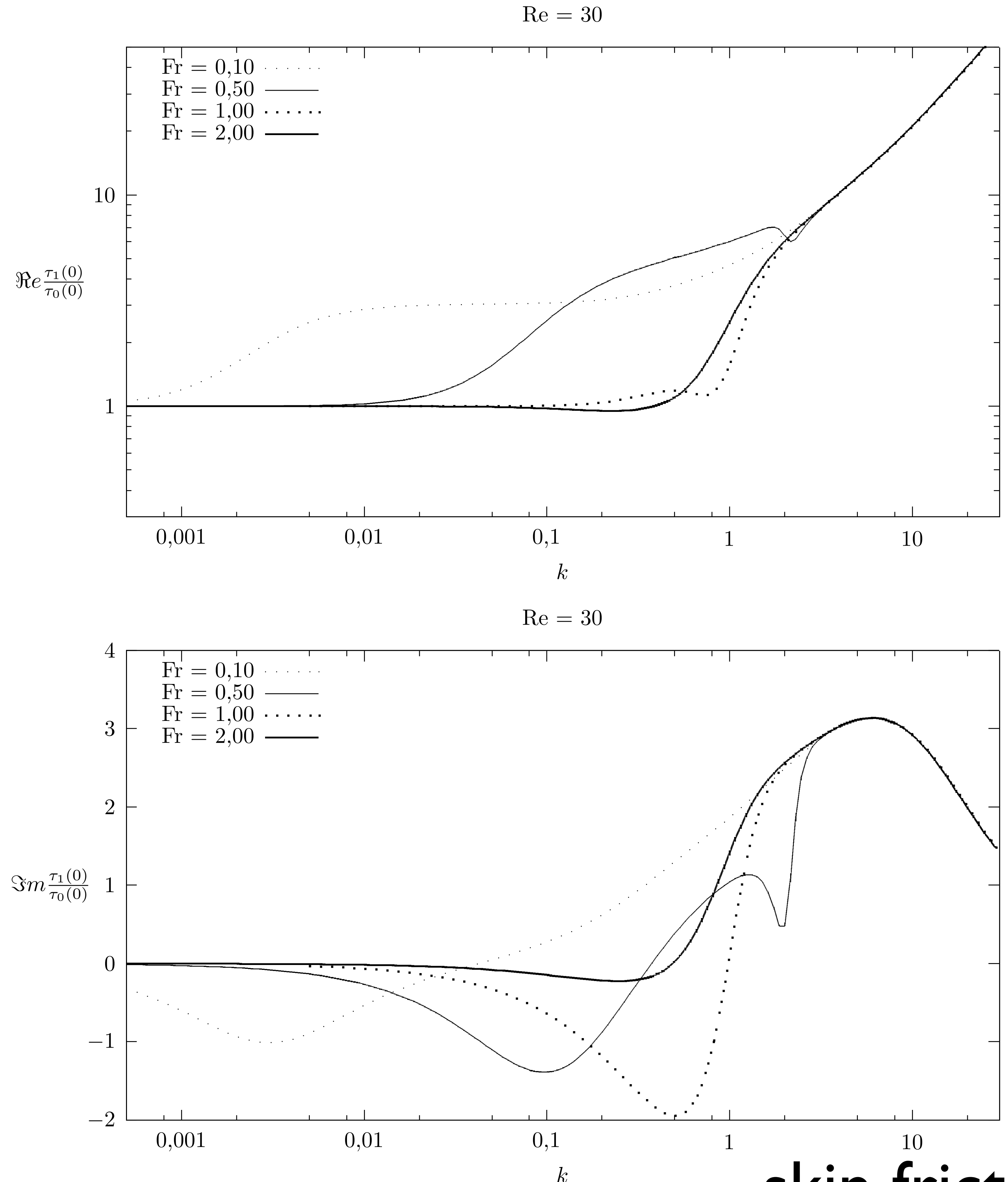

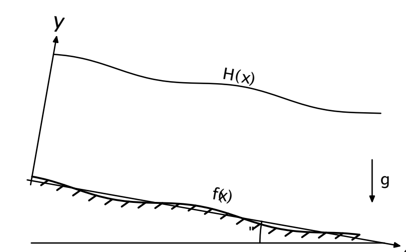

skin friction response

FIG. 2.4 – *Parties réelles (en haut) et parties imaginaires (en bas) de la perturbation du cisaillement au fond renormalisée, pour $Re = 30$ et différentes valeurs de Fr.*

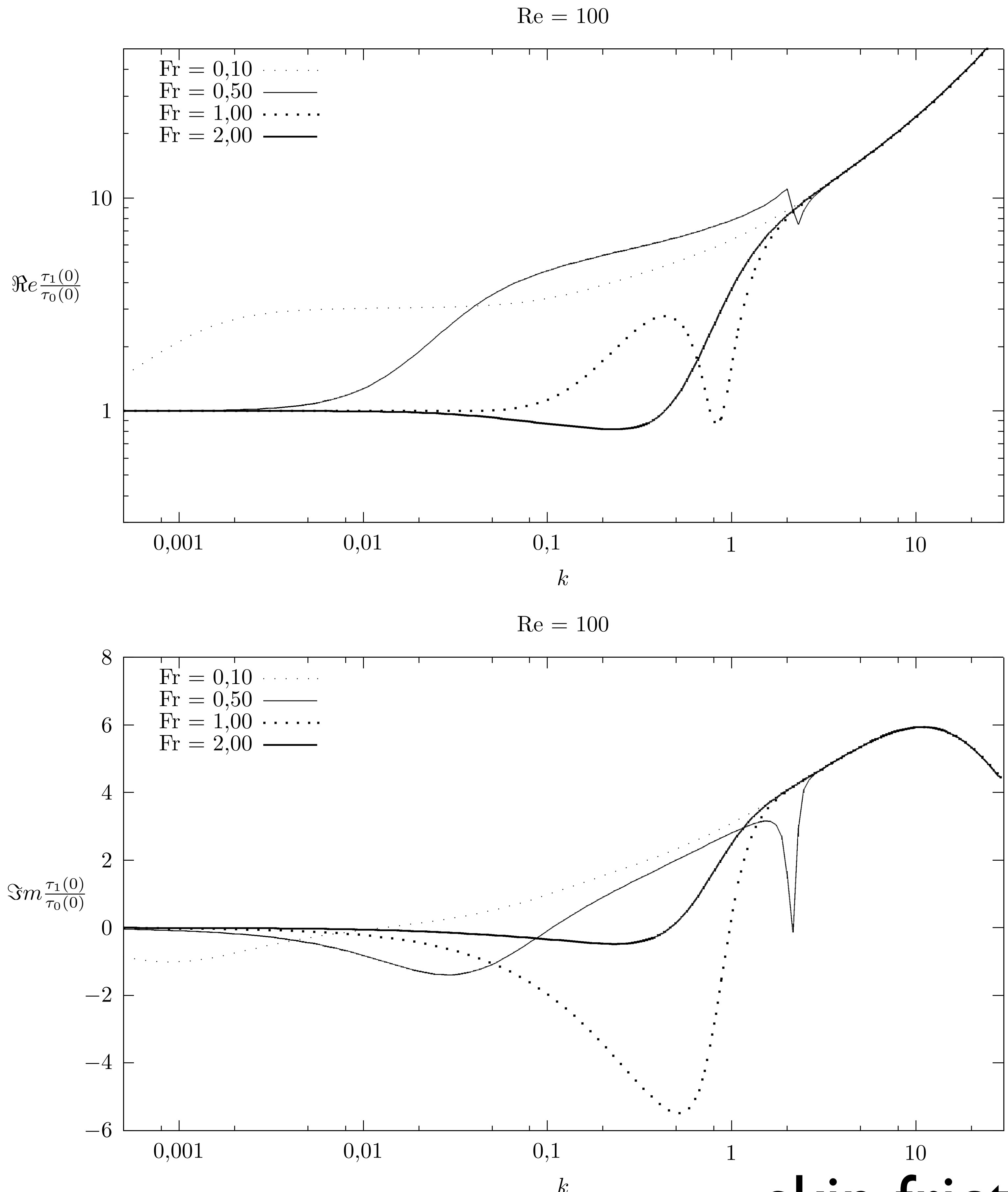

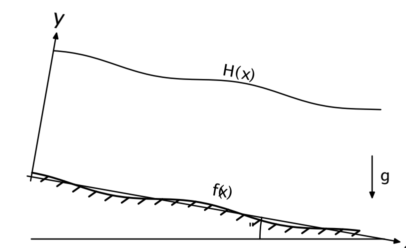

skin friction response

FIG. 2.5 – *Parties réelles (en haut) et parties imaginaires (en bas) de la perturbation du cisaillement au fond renormalisée, pour $Re = 100$ et différentes valeurs de Fr.*

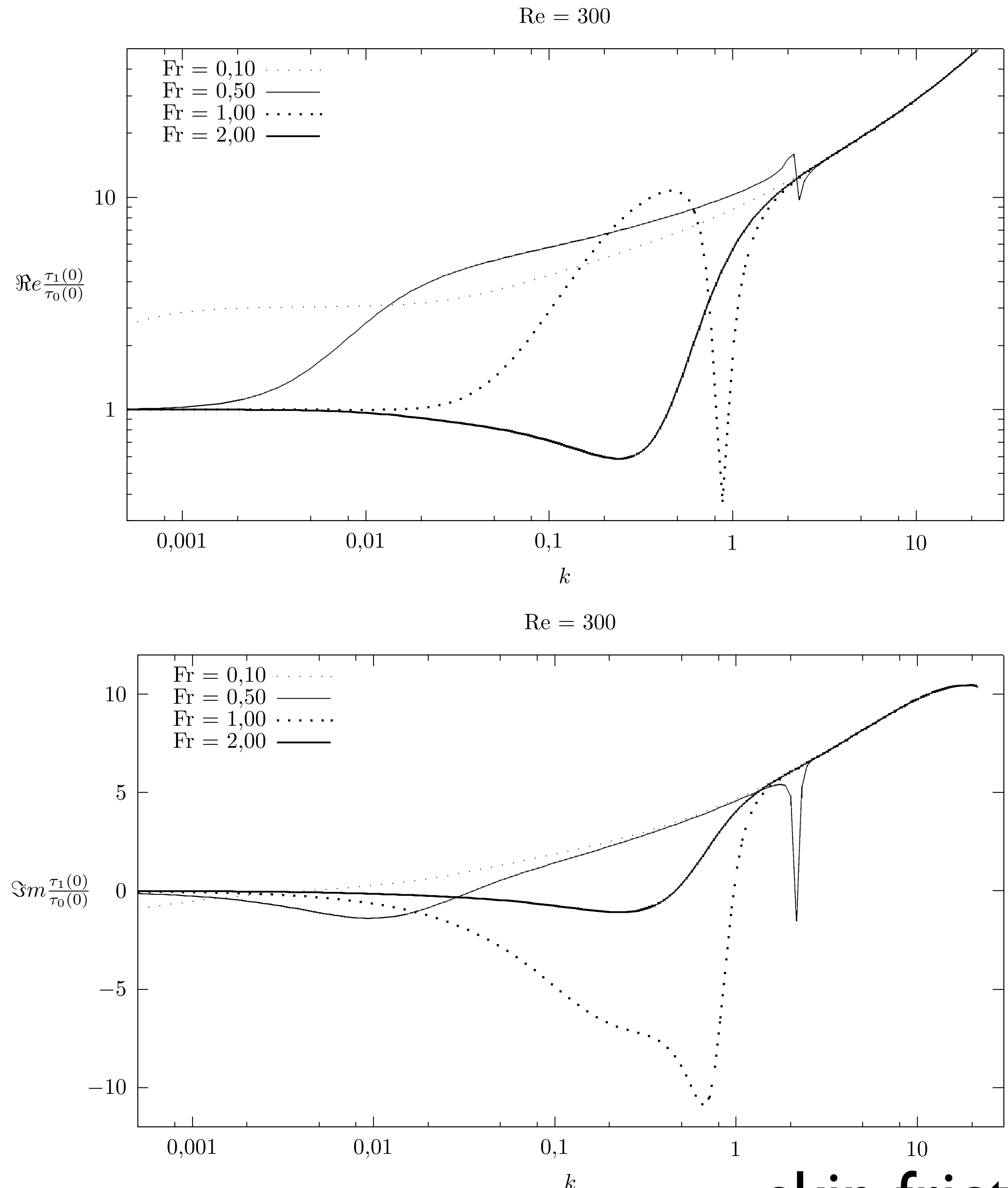

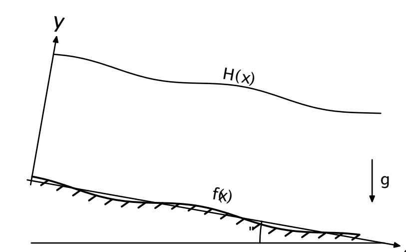

skin friction response

FIG. 2.6 – *Parties réelles (en haut) et parties imaginaires (en bas) de la perturbation du cisaillement au fond renormalisée, pour $Re = 300$ et différentes valeurs de Fr.*

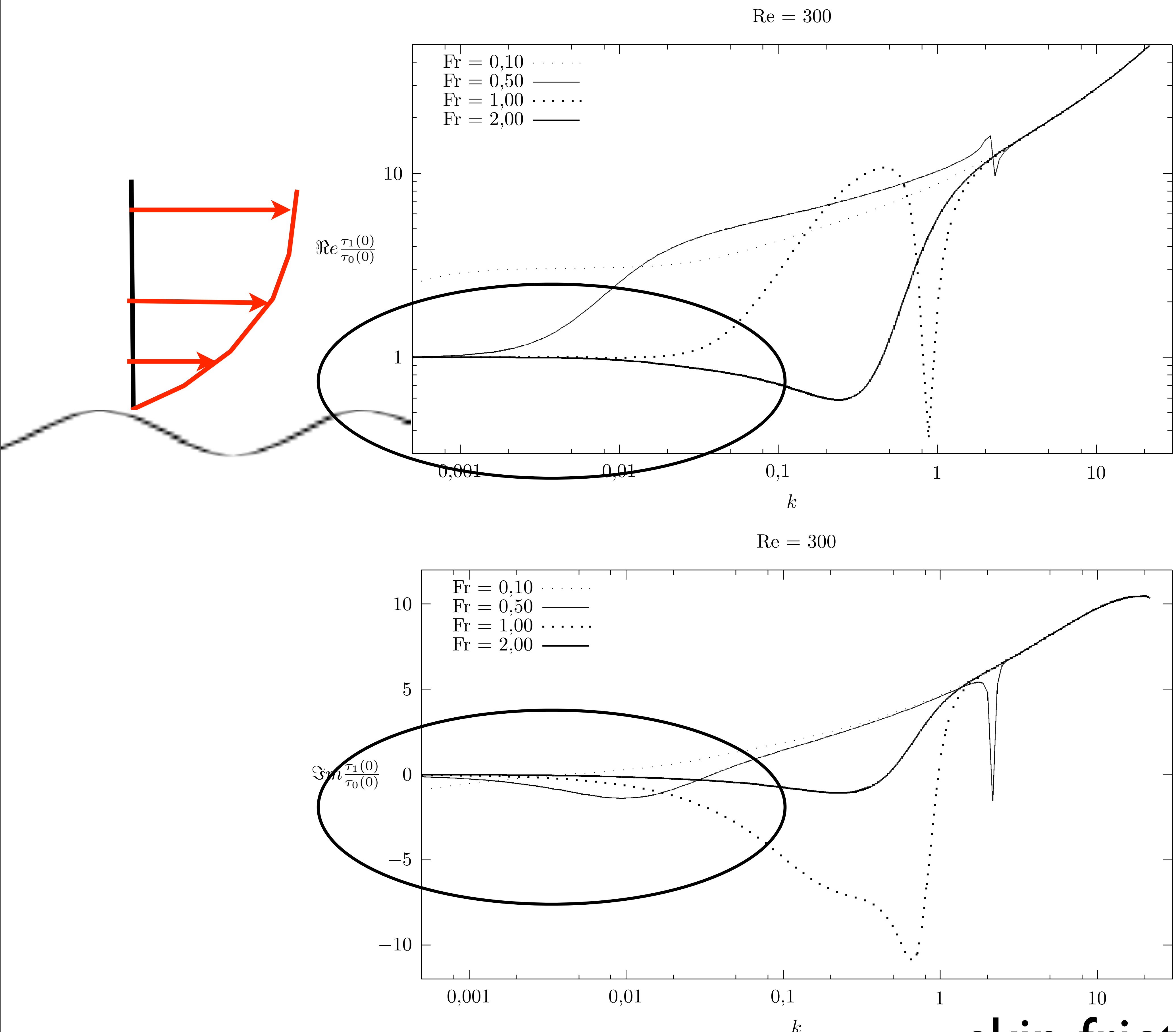

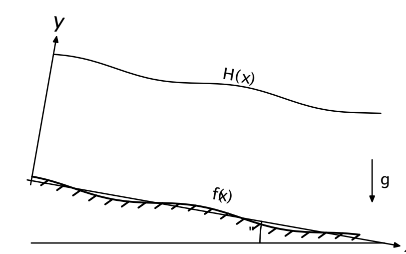

skin friction response

FIG. 2.6 – *Parties réelles (en haut) et parties imaginaires (en bas) de la perturbation du cisaillement au fond renormalisée, pour Re = 300 et différentes valeurs de Fr.*

Saint Venant/ Orr Sommerfeld Stationnaire 2D

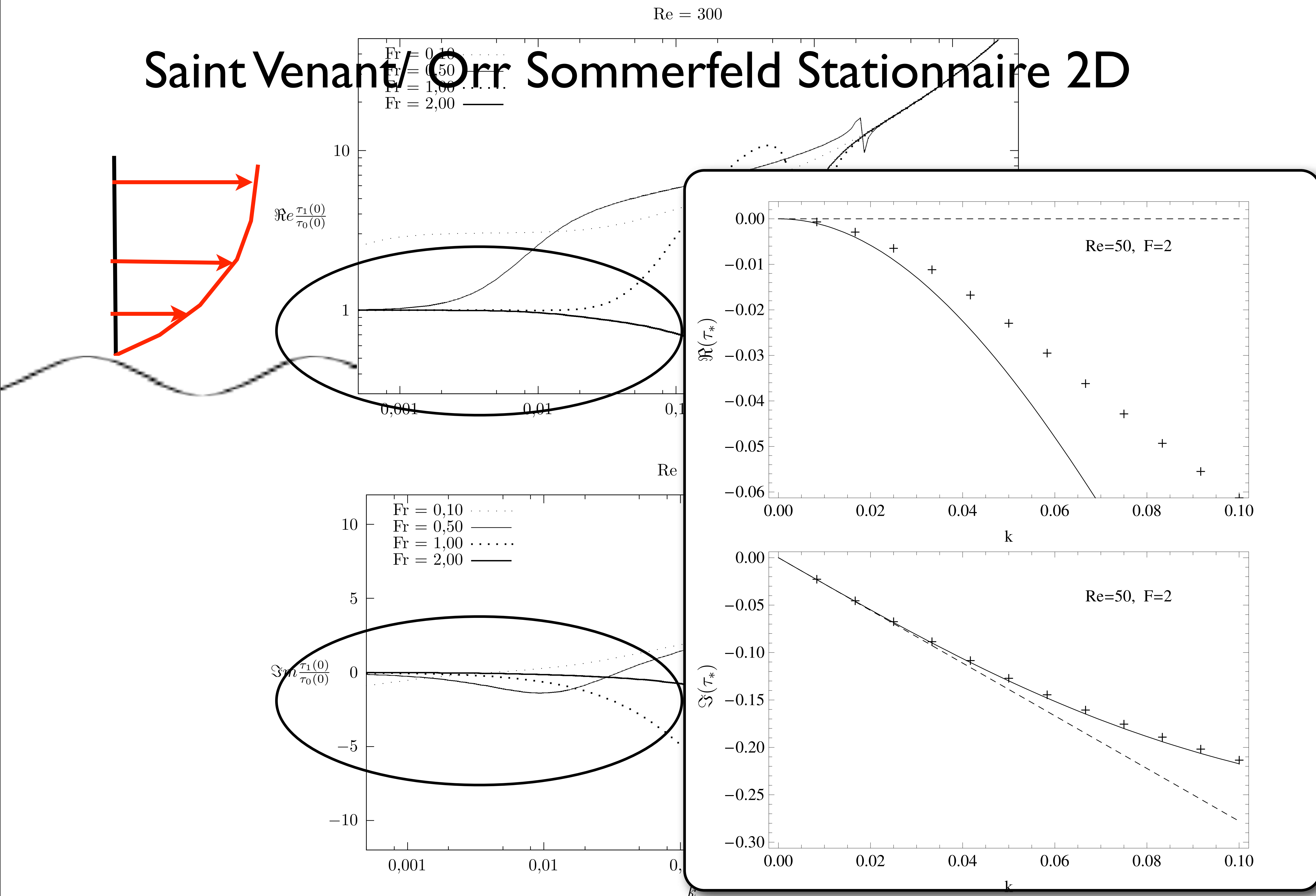

c’est bien toujours stable

FIG. 2.6 – *Parties réelles (en haut) et parties imaginaires (en bas) de la perturbation du cisaillement au fond renormalisée, pour Re = 300 et différentes valeurs de Fr.*

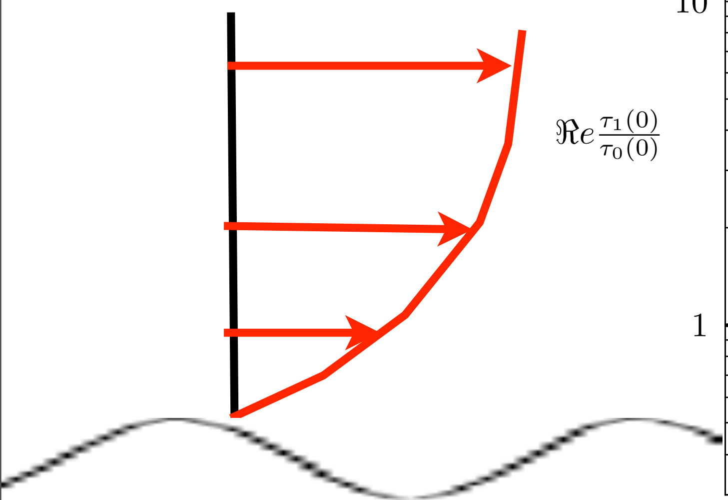

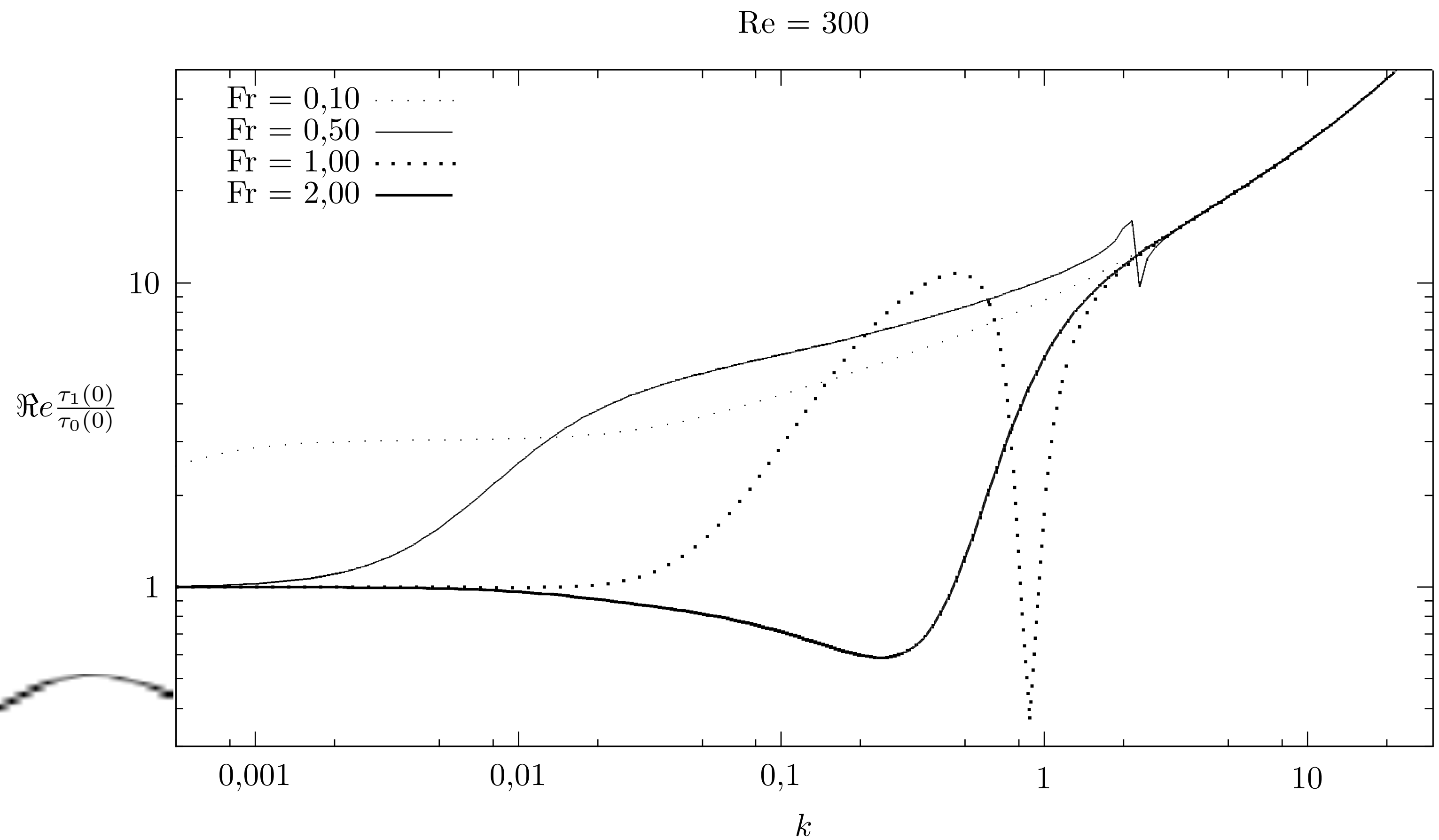

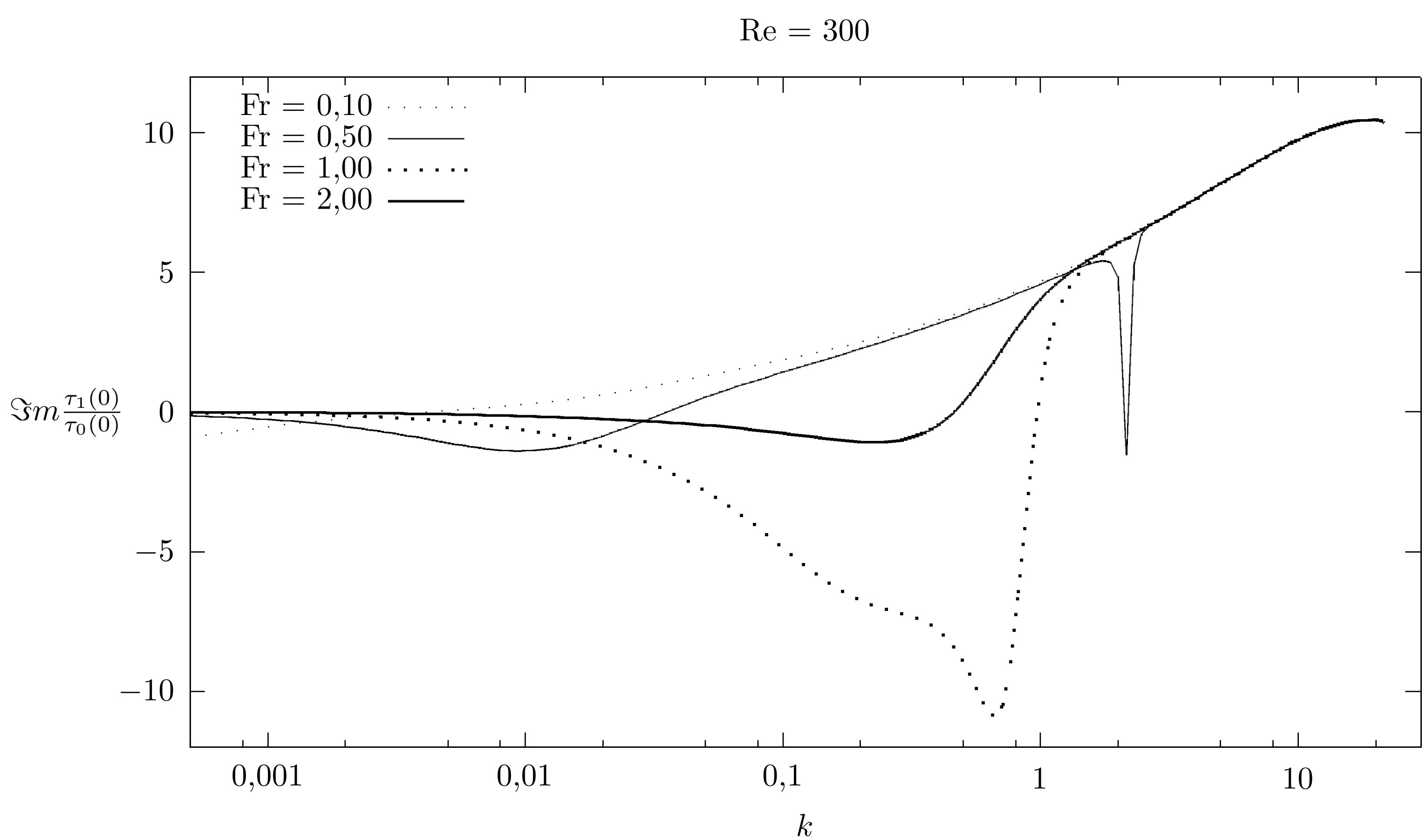

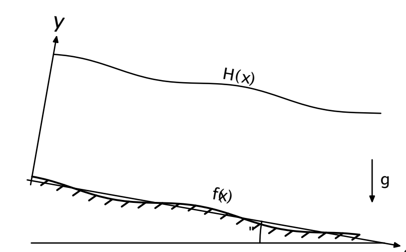

FIG. 2.6 – *Parties réelles (en haut) et parties imaginaires (en bas) de la perturbation du cisaillement au fond renormalisée, pour Re = 300 et différentes valeurs de Fr.*

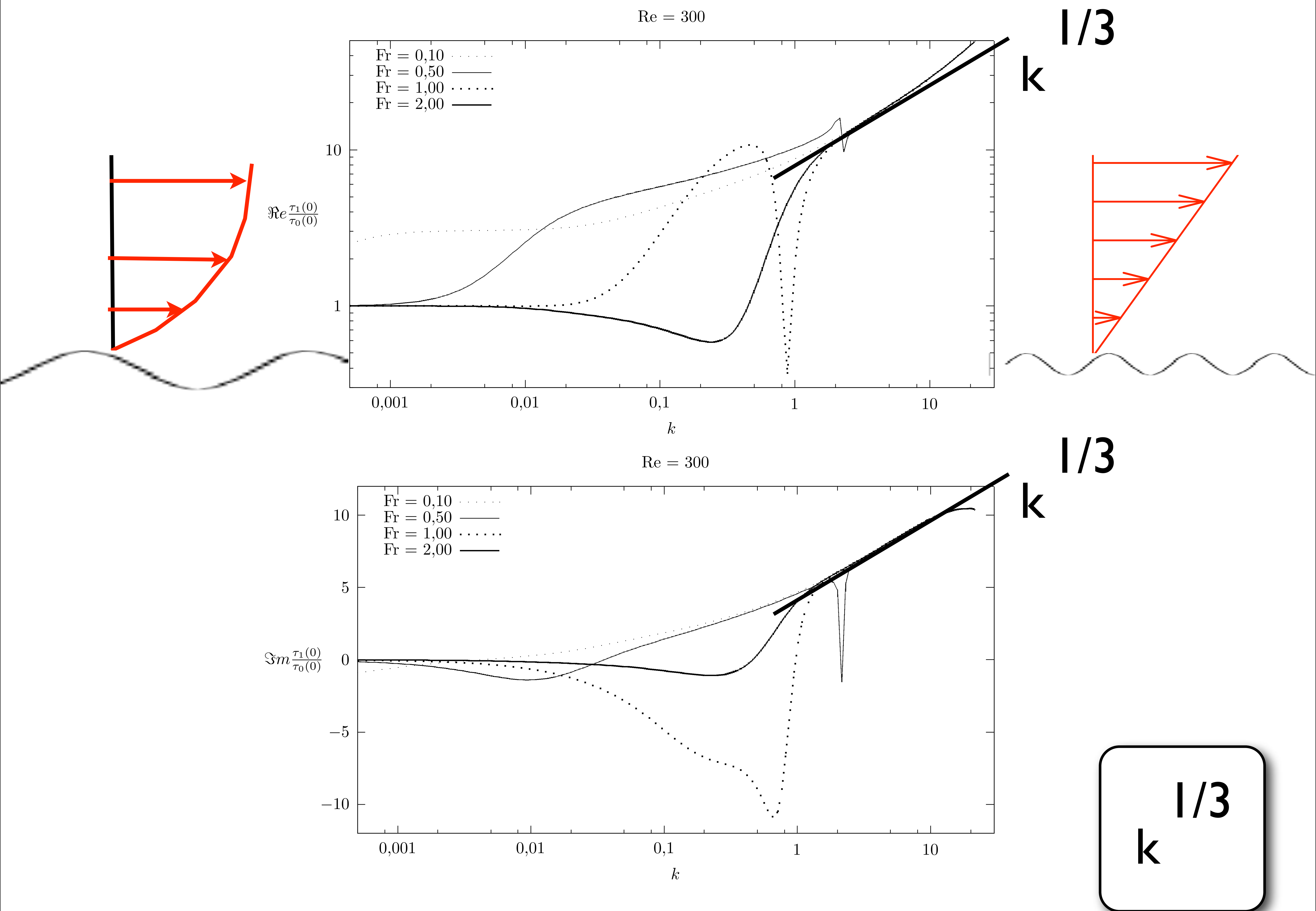

FIG. 2.6 – *Parties réelles (en haut) et parties imaginaires (en bas) de la perturbation du cisaillement au fond renormalisée, pour $Re = 300$ et différentes valeurs de Fr.*

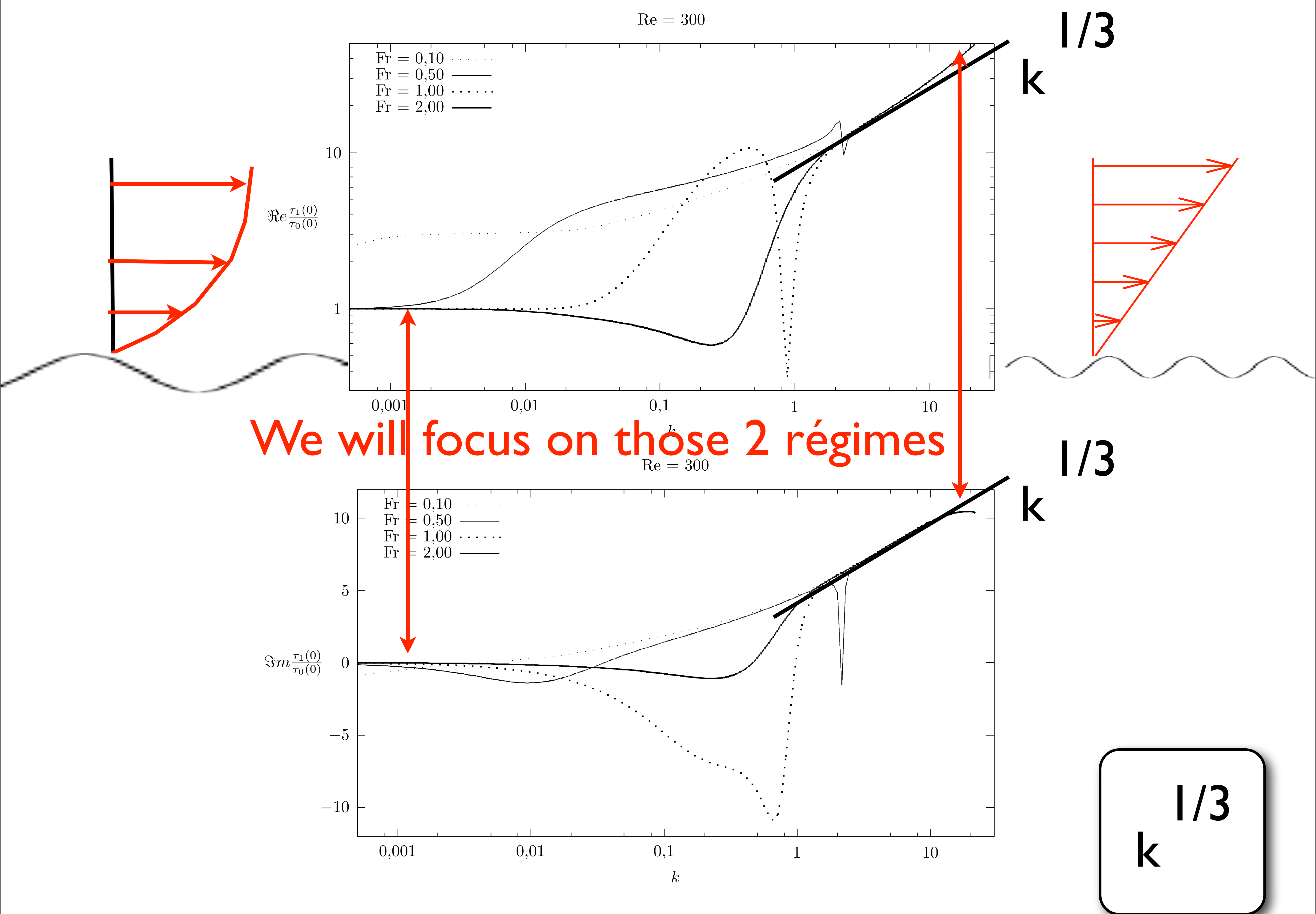

FIG. 2.6 – *Parties réelles (en haut) et parties imaginaires (en bas) de la perturbation du cisaillement au fond renormalisée, pour Re = 300 et différentes valeurs de Fr.*

Viscous effects are important near the wall

Perturbation of a shear flow Non linear resolution (with flow separation) possible

But first we linearise

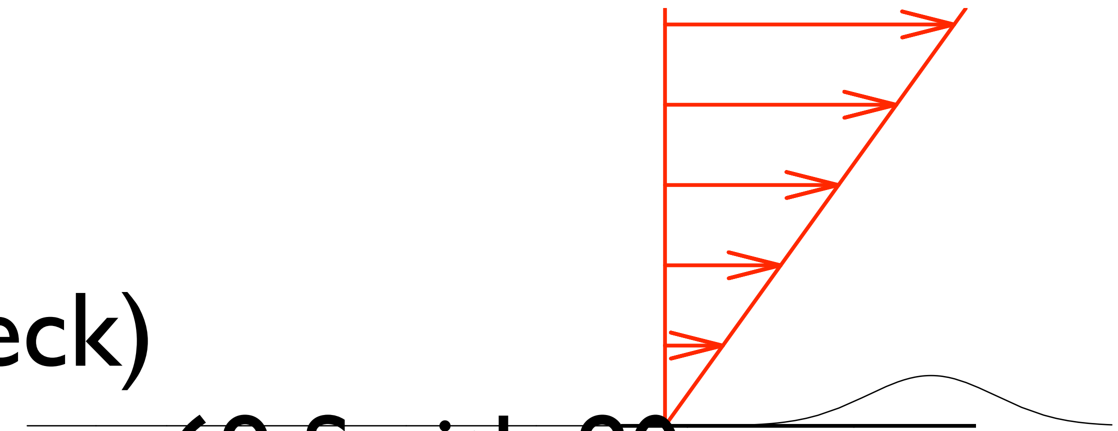

It is called Double Deck (Triple Deck)

Introduced by Neiland 69 Stewartson 69 Smith 80...

$$k^{1/3}$$

Viscous effects are important near the wall

Perturbation of a shear flow Non linear resolution (with flow separation) possible

But first we linearise

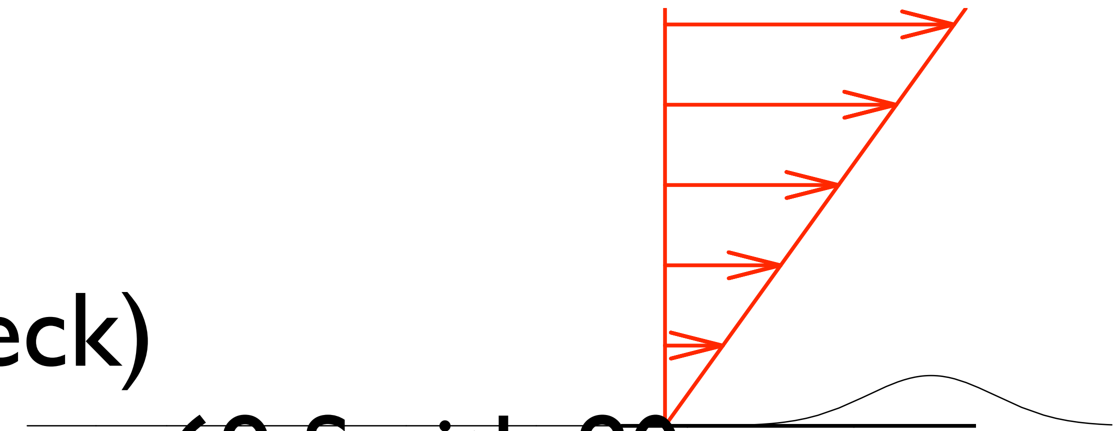

It is called Double Deck (Triple Deck)

Introduced by Neiland 69 Stewartson 69 Smith 80...

linear solution

$$\begin{cases} -ik\hat{u}_1 + \dfrac{\partial \hat{v}_1}{\partial y} = 0, \\ -iky\hat{u}_1 + \hat{v}_1 = ik\hat{p}_1 \quad + \dfrac{\partial^2 \hat{u}_1}{\partial y^2}, \end{cases}$$

$$-iky\hat{\tau}_1 = \frac{\partial^2 \hat{\tau}_1}{\partial y^2} \longrightarrow Ai((-ik)^{1/3} y)$$

$k^{1/3}$

Viscous effects are important near the wall
Perturbation of a shear flow Non linear resolution (with flow separation) possible
But first we linearise

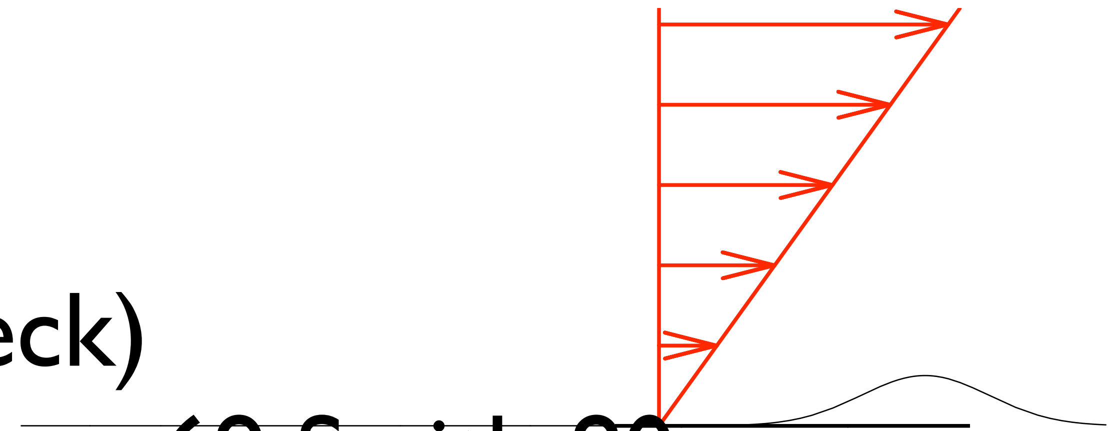

It is called Double Deck (Triple Deck)
Introduced by Neiland 69 Stewartson 69 Smith 80...

very similar to Fowler / Azerad Bouharguane $\dfrac{\partial^{1/3}}{\partial x^{1/3}}$

$$\int_0^\infty \frac{f'(x-\xi)}{\xi^{1/3}} d\xi$$

$k^{1/3}$

$\tau = \mu U_0'(\bar{U}_S'(1 + (\frac{U_0'}{\nu\lambda})^{1/3} H\tilde{c}))$, with $\tilde{c} = FT^{-1}[FT[\tilde{f}]3Ai(0)(-(i2\pi\tilde{k})\bar{U}_S')^{1/3}]$

Conclusion of the fluid part: asymptotic models

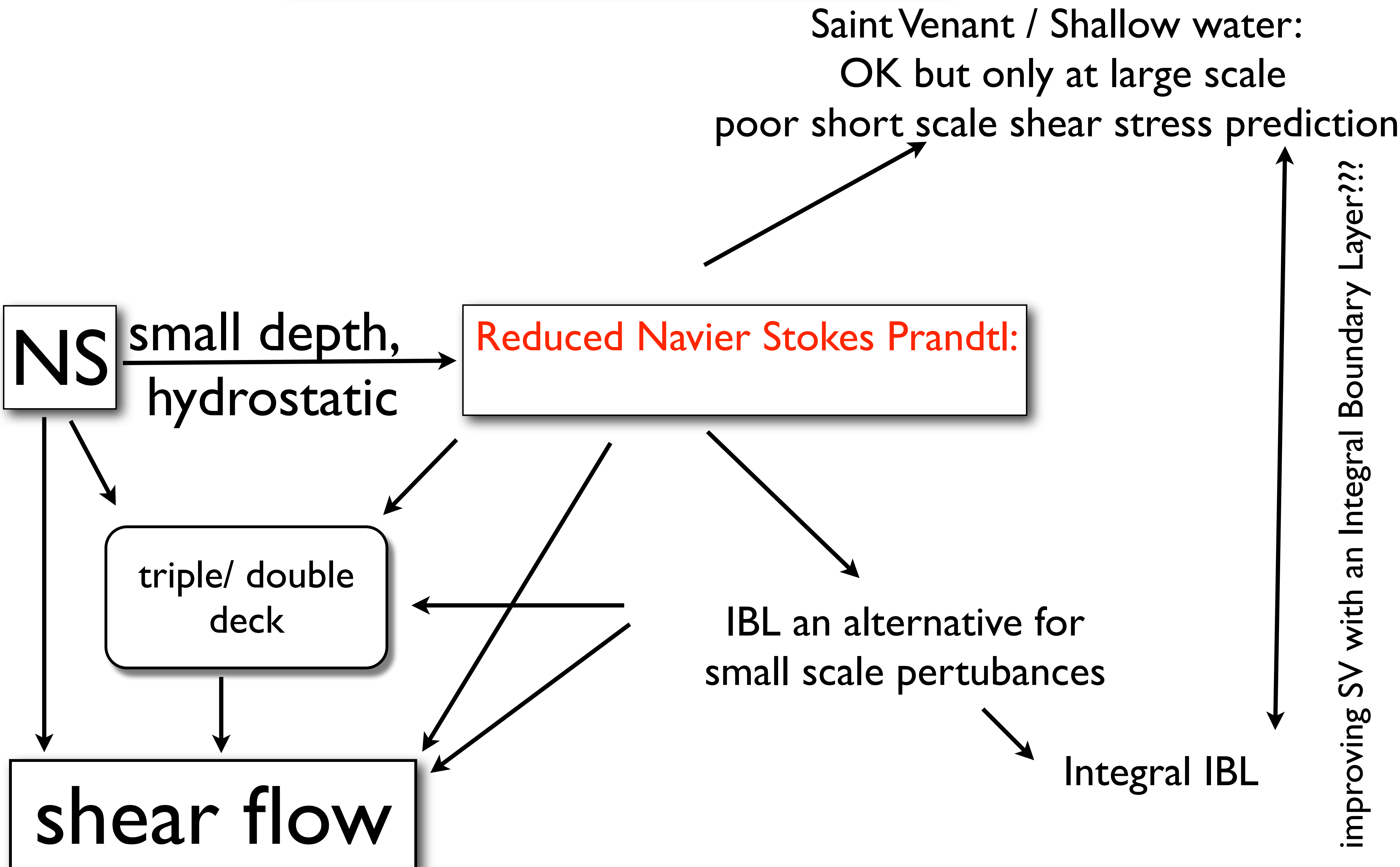

Turbulence?

The laminar model is a «good» approximation of a turbulent model

Laboratory experiments are more or less laminar

In linear Shallow Water, it changes only the value of the coefficients

difficult message

- introduction
- the problem
- the flow: Saint Venant and other
- first granular model
- first coupling: bars
- imporved granular model: saturation length
- ripples
- bars & ripples
- conclusions perspectives

Erosion Model

link between the flow of water and the flow of grains

Problem :
What is the relationship between q and the flow?
hint: the larger u the larger the erosion, the larger q
q seems to be proportional to the skin friction

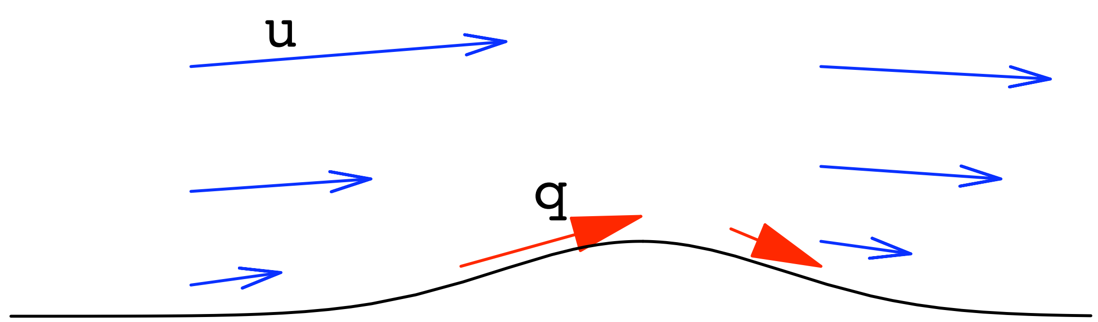

Erosion Model

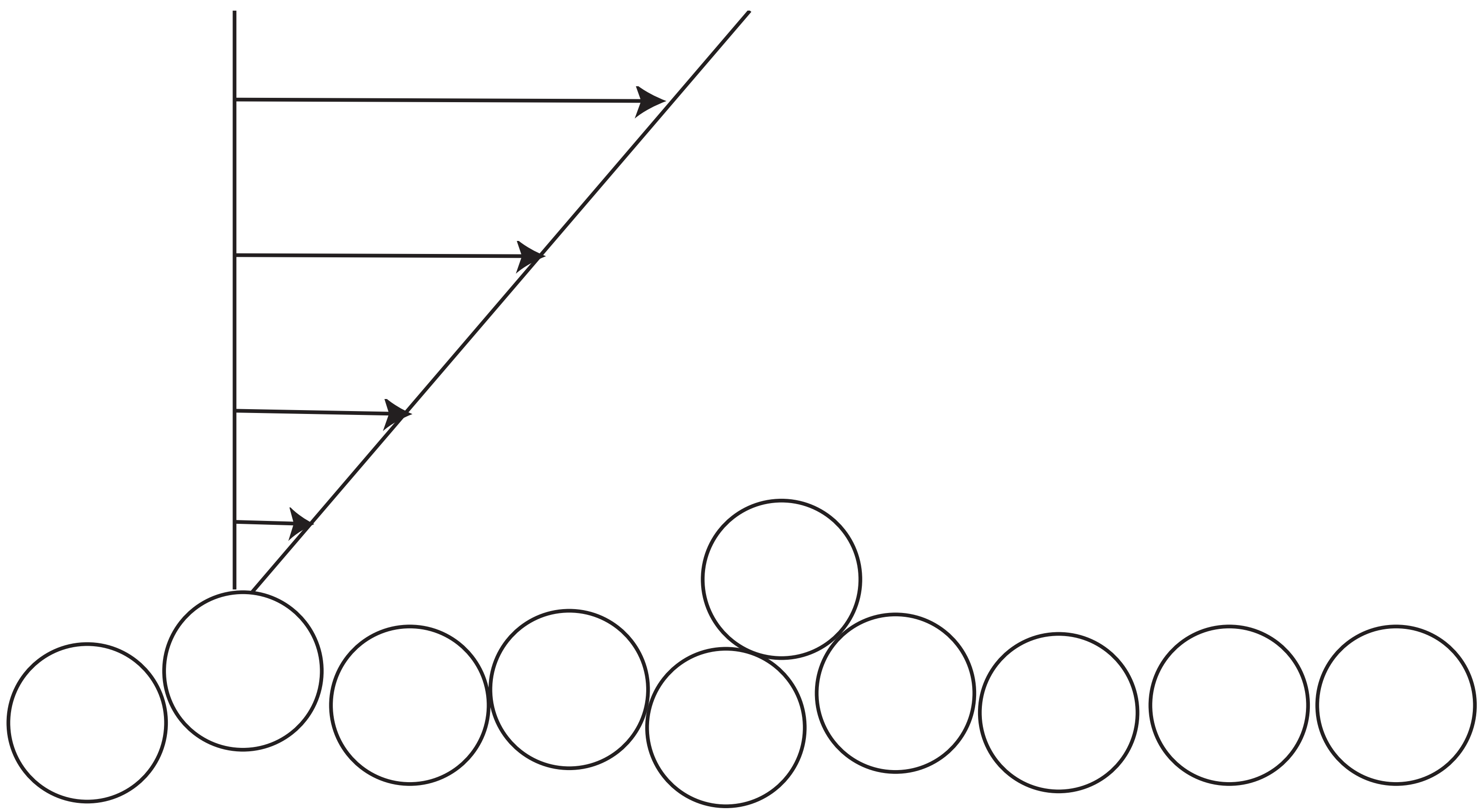

Stress larger than a threshold $\tau > \tau_s$

Shields number $$\frac{\tau}{(\rho_p - \rho) g D}$$

Erosion Model

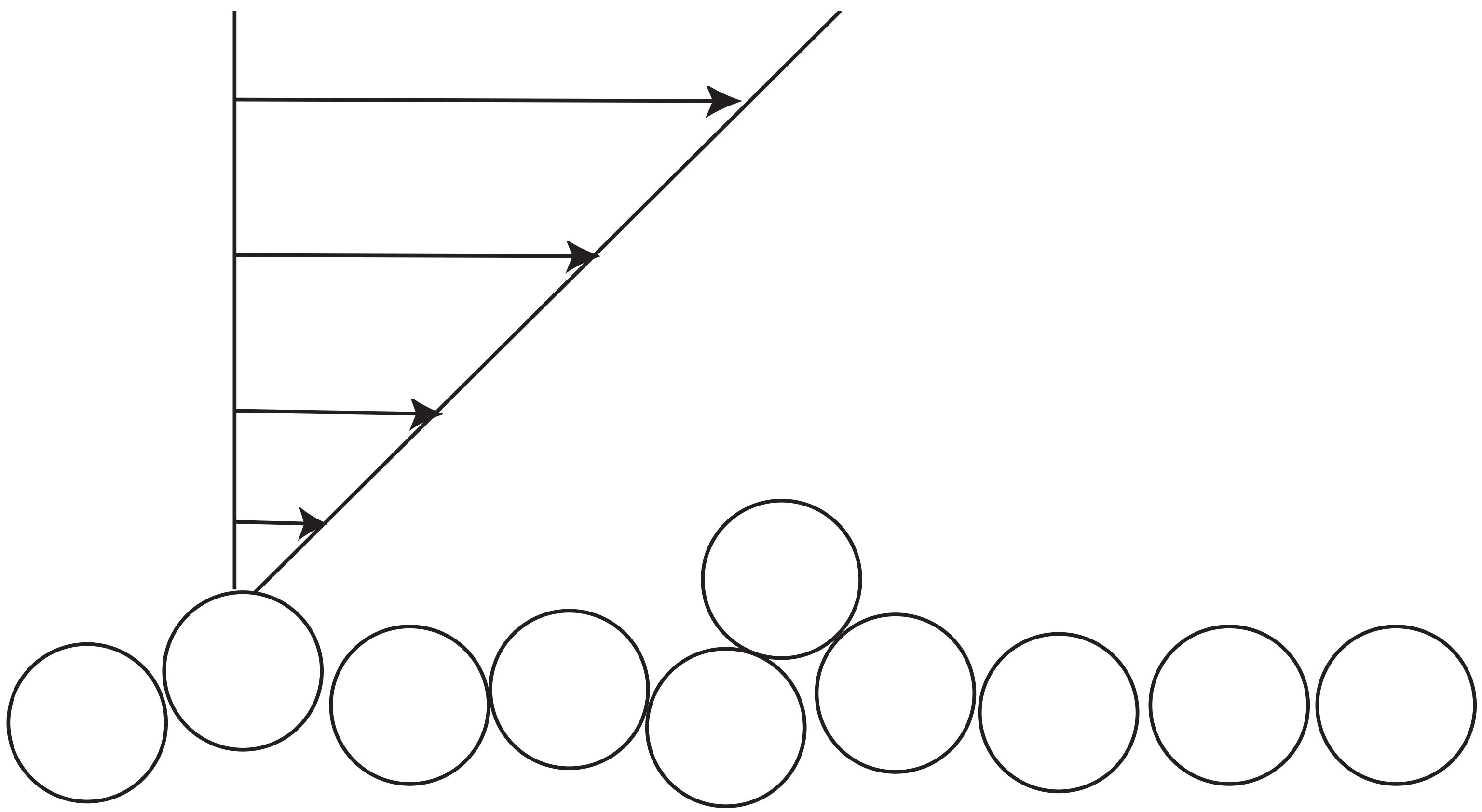

Stress larger than a threshold $\tau > \tau_s$

Shields number $$\frac{\tau}{(\rho_p - \rho) g D}$$

Erosion Model

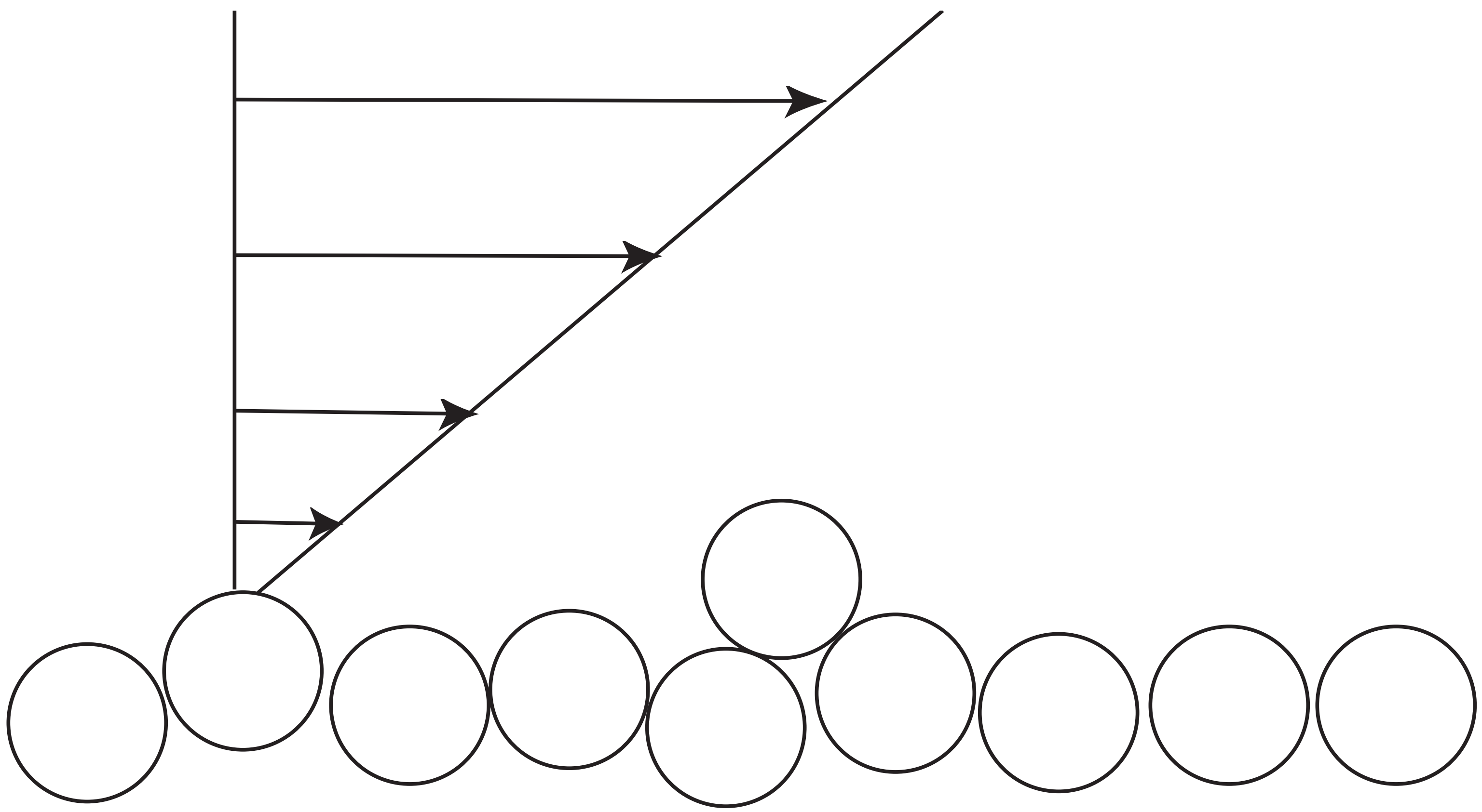

Stress larger than a threshold $\tau > \tau_s$

Shields number $\dfrac{\tau}{(\rho_p - \rho) g D}$

Erosion Model

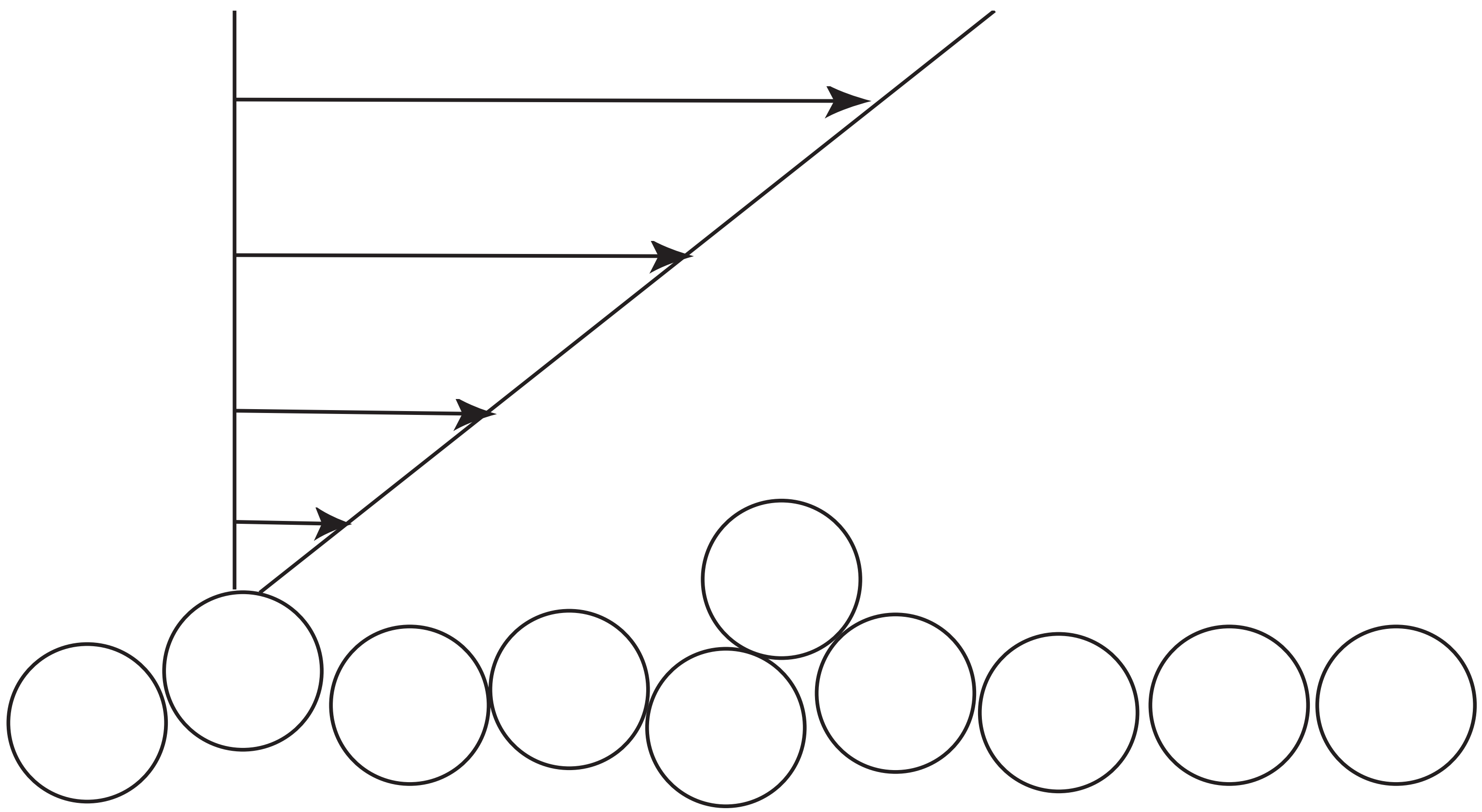

Stress larger than a threshold $\tau > \tau_s$

Shields number $$\frac{\tau}{(\rho_p - \rho) g D}$$

Erosion Model

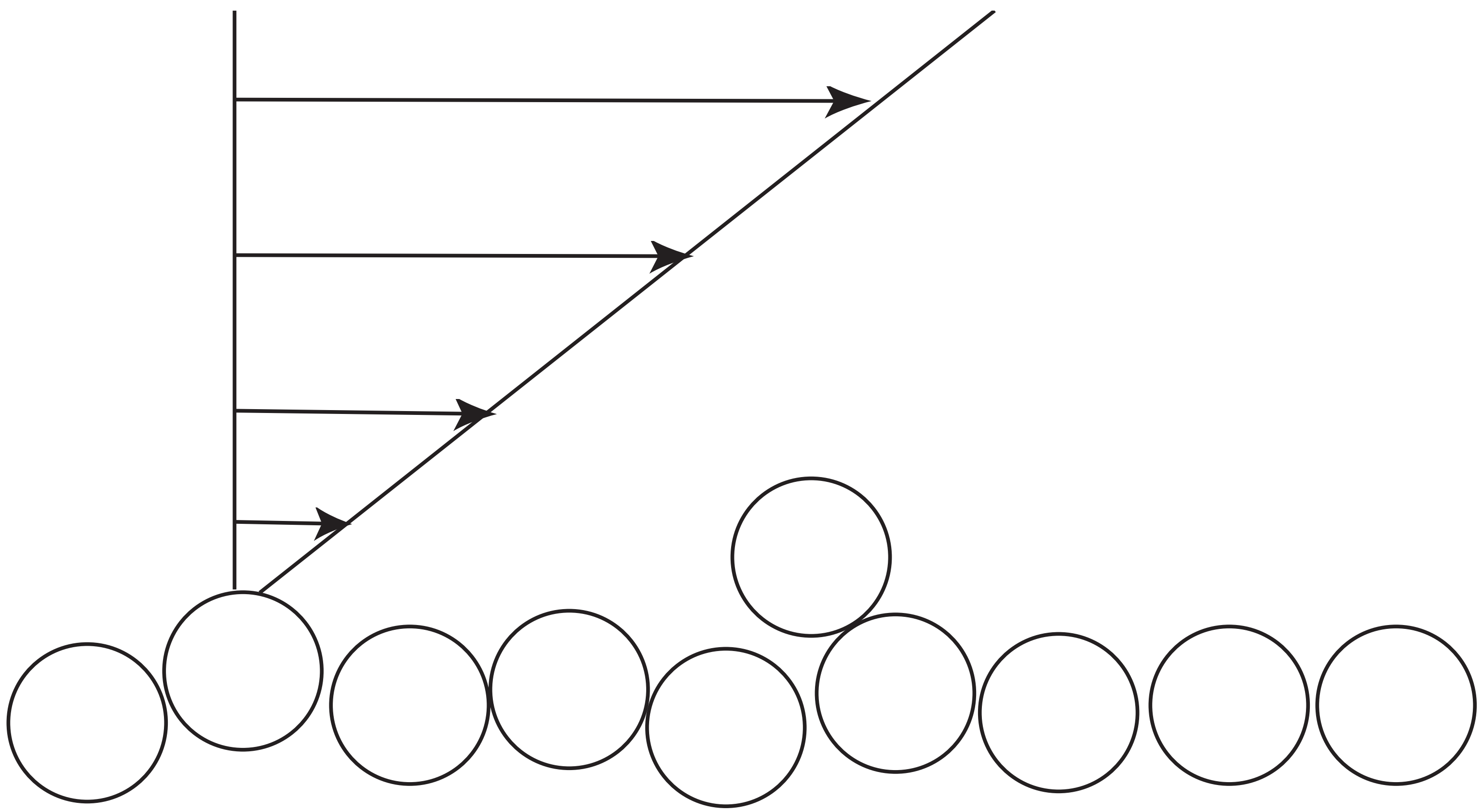

Stress larger than a threshold $\tau > \tau_s$

Shields number $$\frac{\tau}{(\rho_p - \rho) g D}$$

Erosion Model

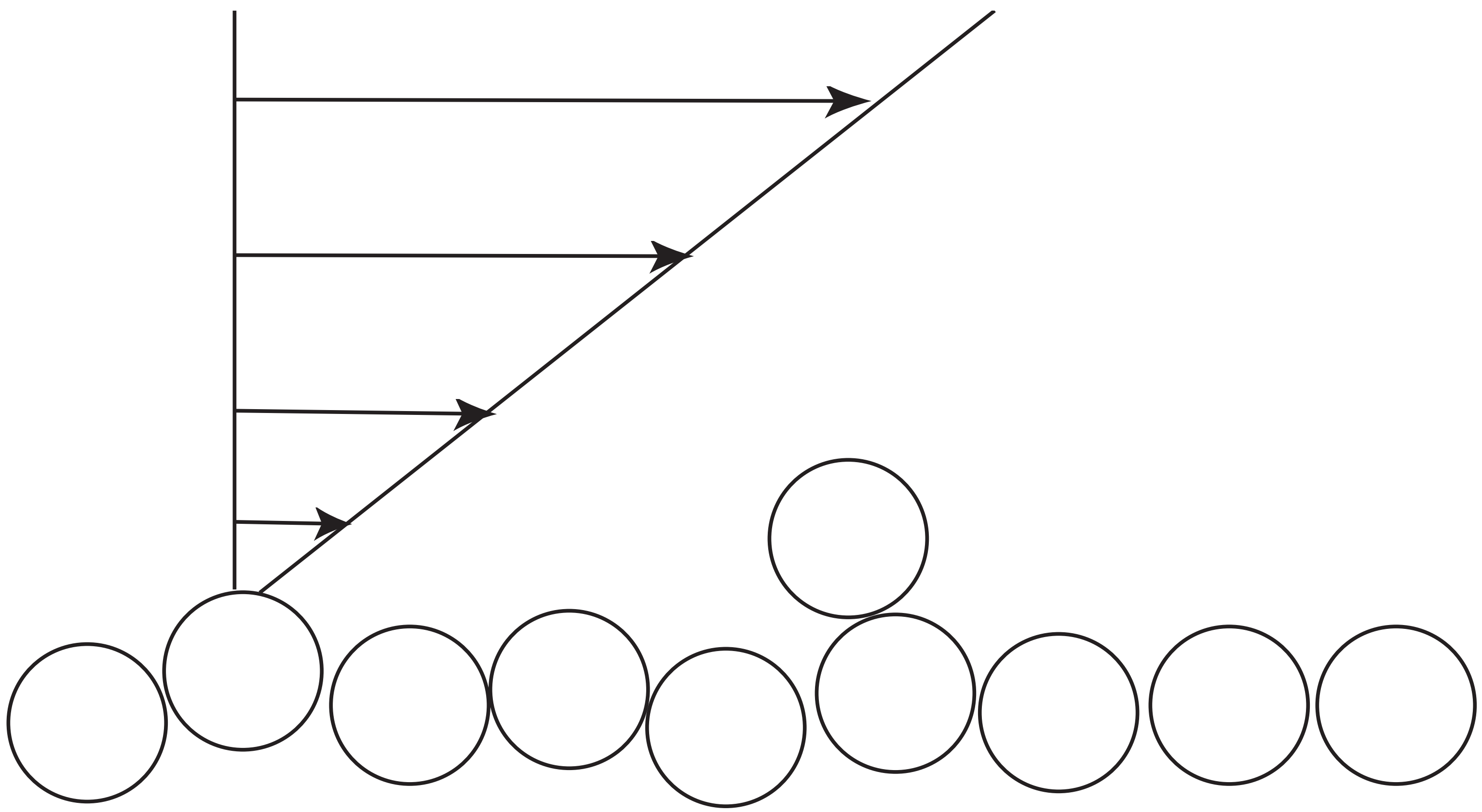

Stress larger than a threshold $\tau > \tau_s$

Shields number $\dfrac{\tau}{(\rho_p - \rho) g D}$

Erosion Model

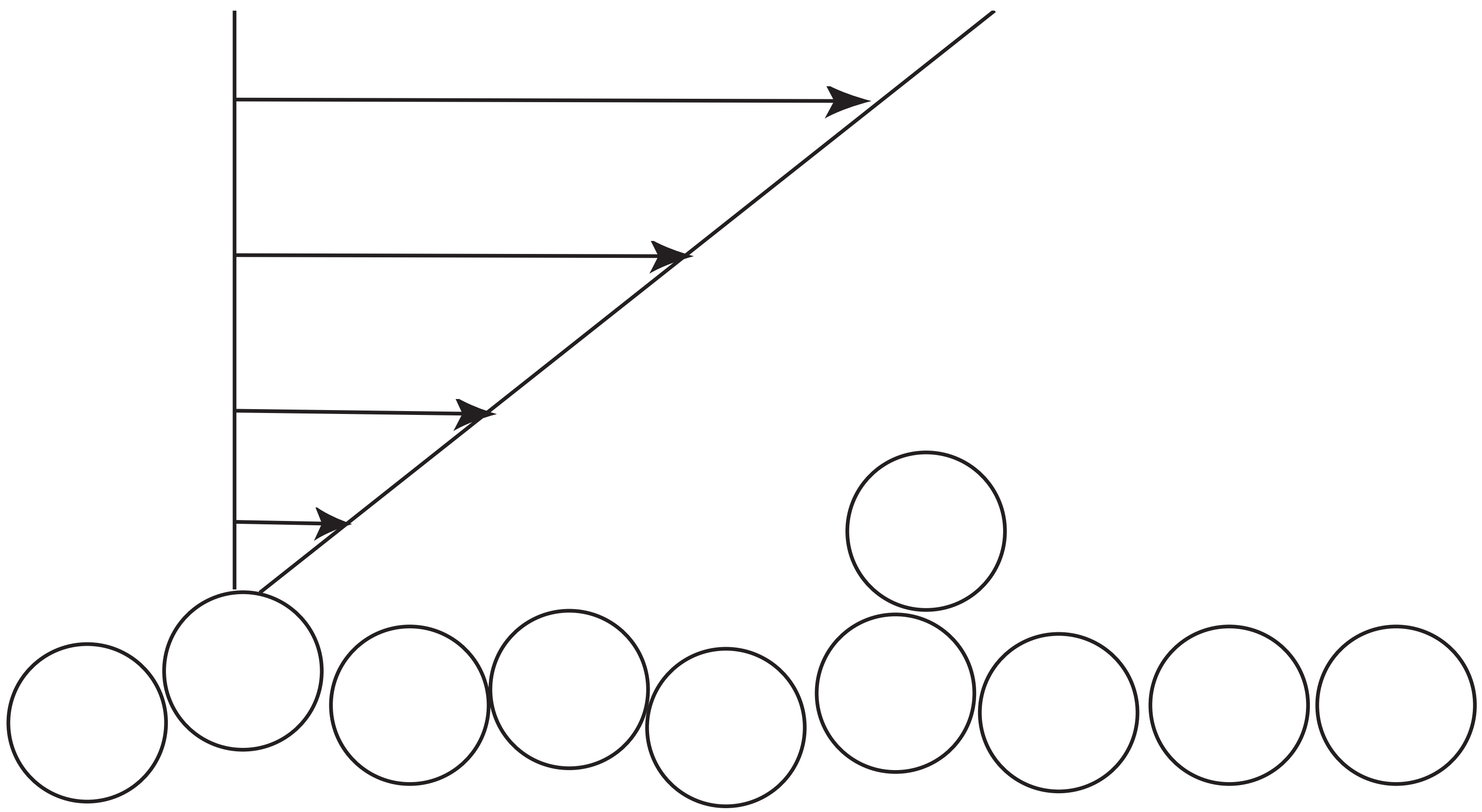

Stress larger than a threshold $\tau > \tau_s$

Shields number $$\frac{\tau}{(\rho_p - \rho) g D}$$

Erosion Model

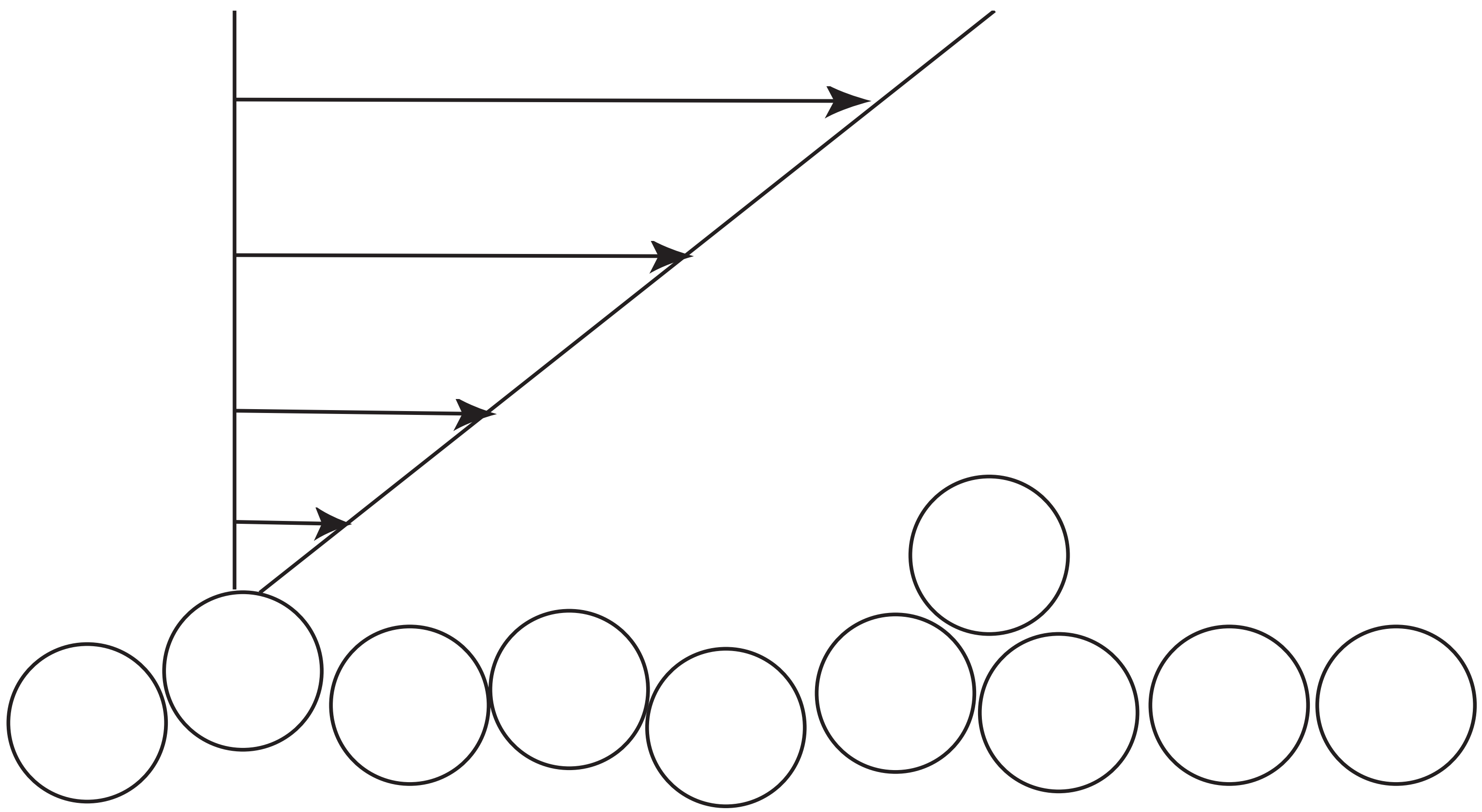

Stress larger than a threshold $\tau > \tau_s$

Shields number $$\frac{\tau}{(\rho_p - \rho) g D}$$

Erosion Model

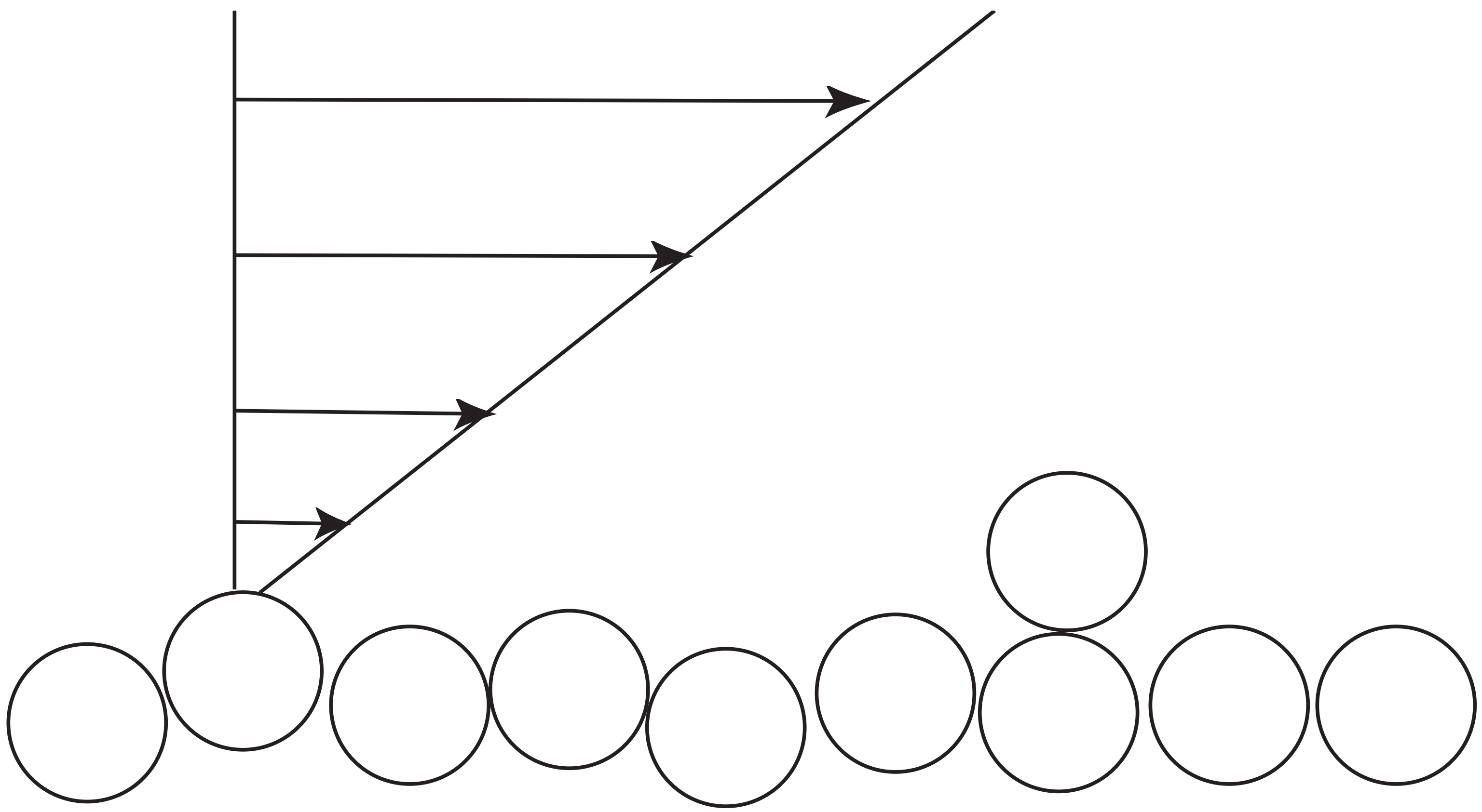

Stress larger than a threshold $\quad \tau > \tau_s$

Shields number $\quad \dfrac{\tau}{(\rho_p - \rho) g D}$

Erosion Model

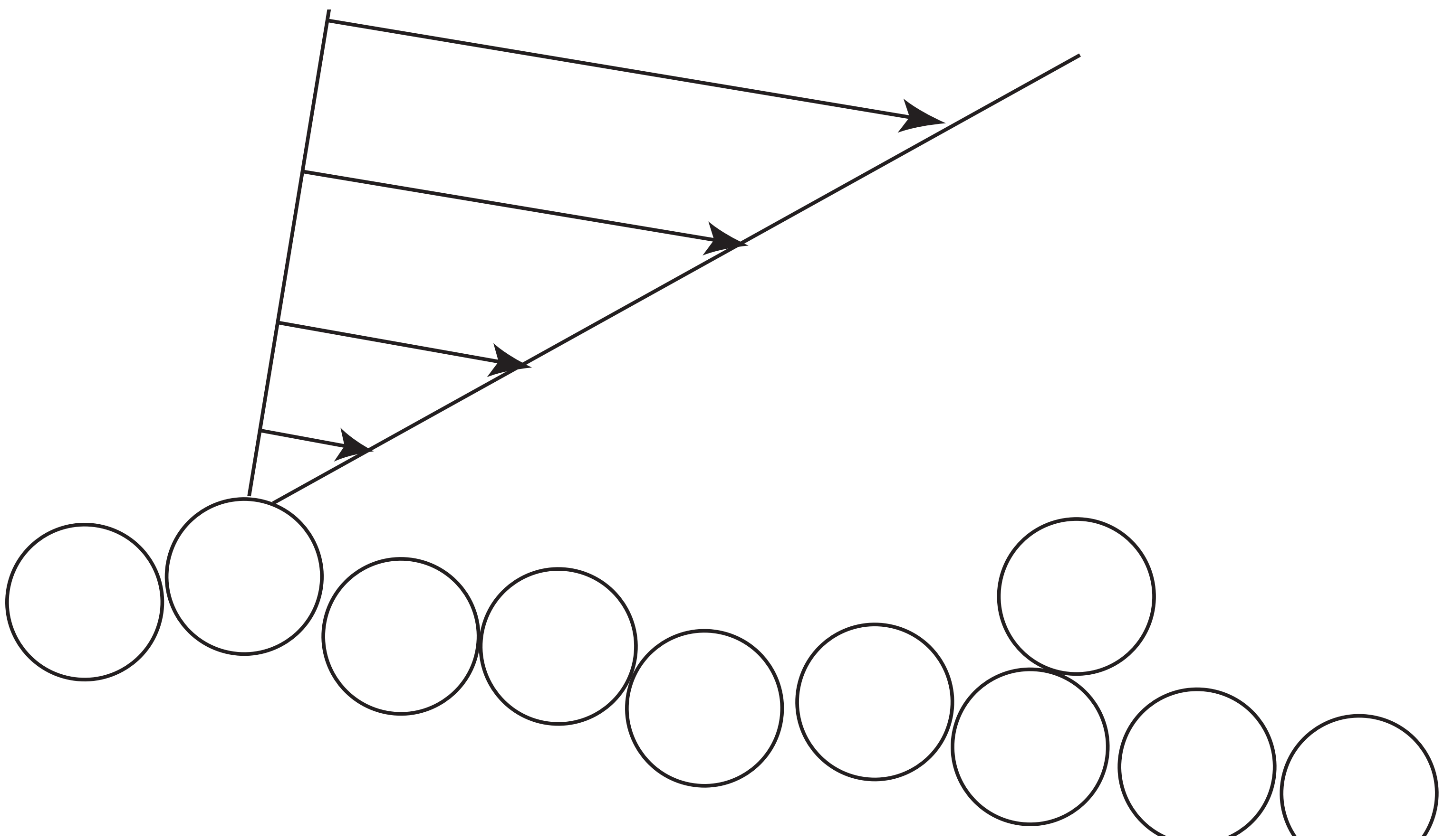

Stress larger than a threshold $\tau > \tau_s$

Shields number $\dfrac{\tau}{(\rho_p - \rho) g D}$

Erosion Model

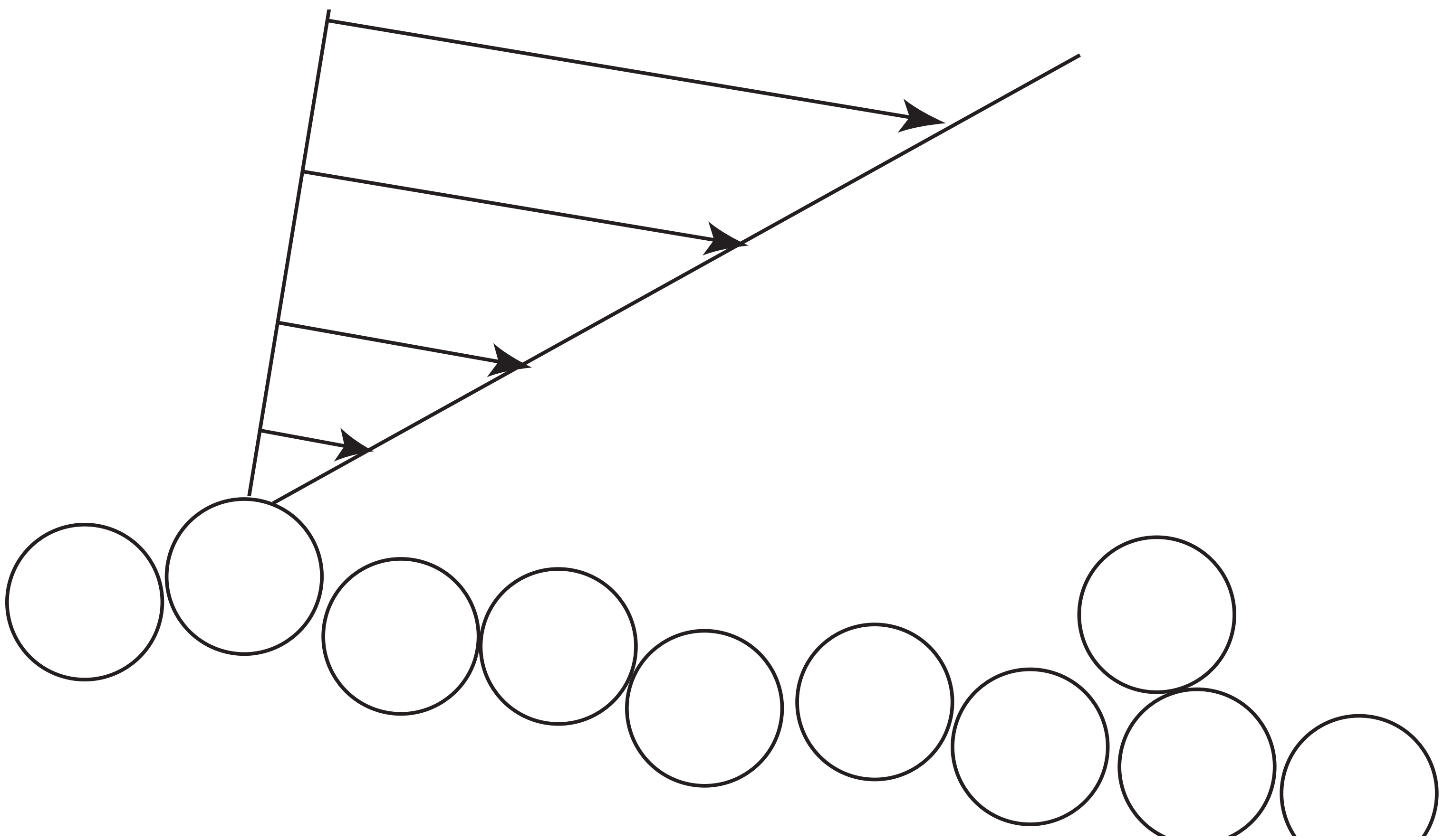

Stress larger than a threshold $\tau > \tau_s$

Shields number $$\frac{\tau}{(\rho_p - \rho) g D}$$

Erosion Model

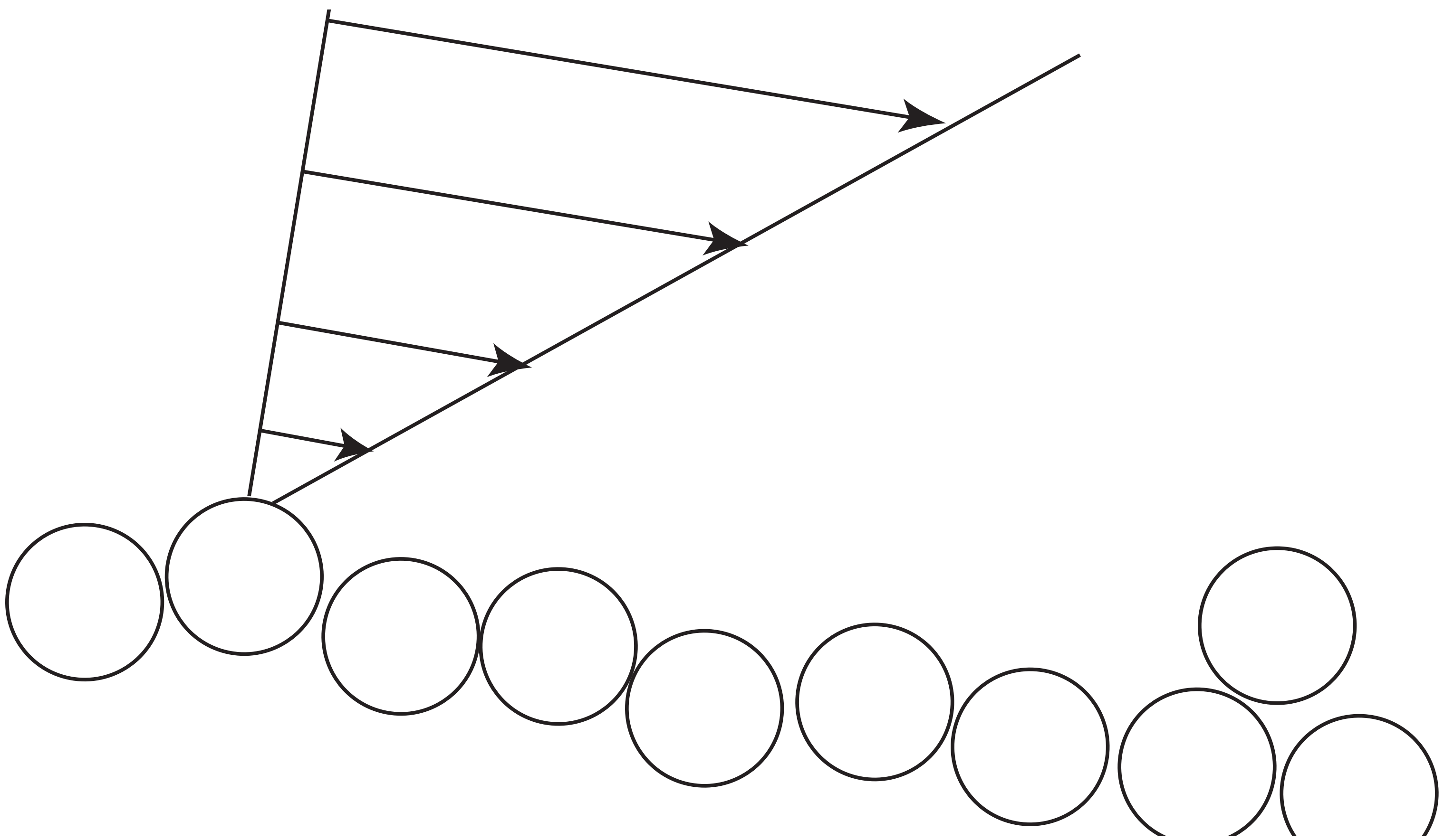

Stress larger than a threshold $\tau > \tau_s$

Shields number $$\frac{\tau}{(\rho_p - \rho) g D}$$

Erosion Model

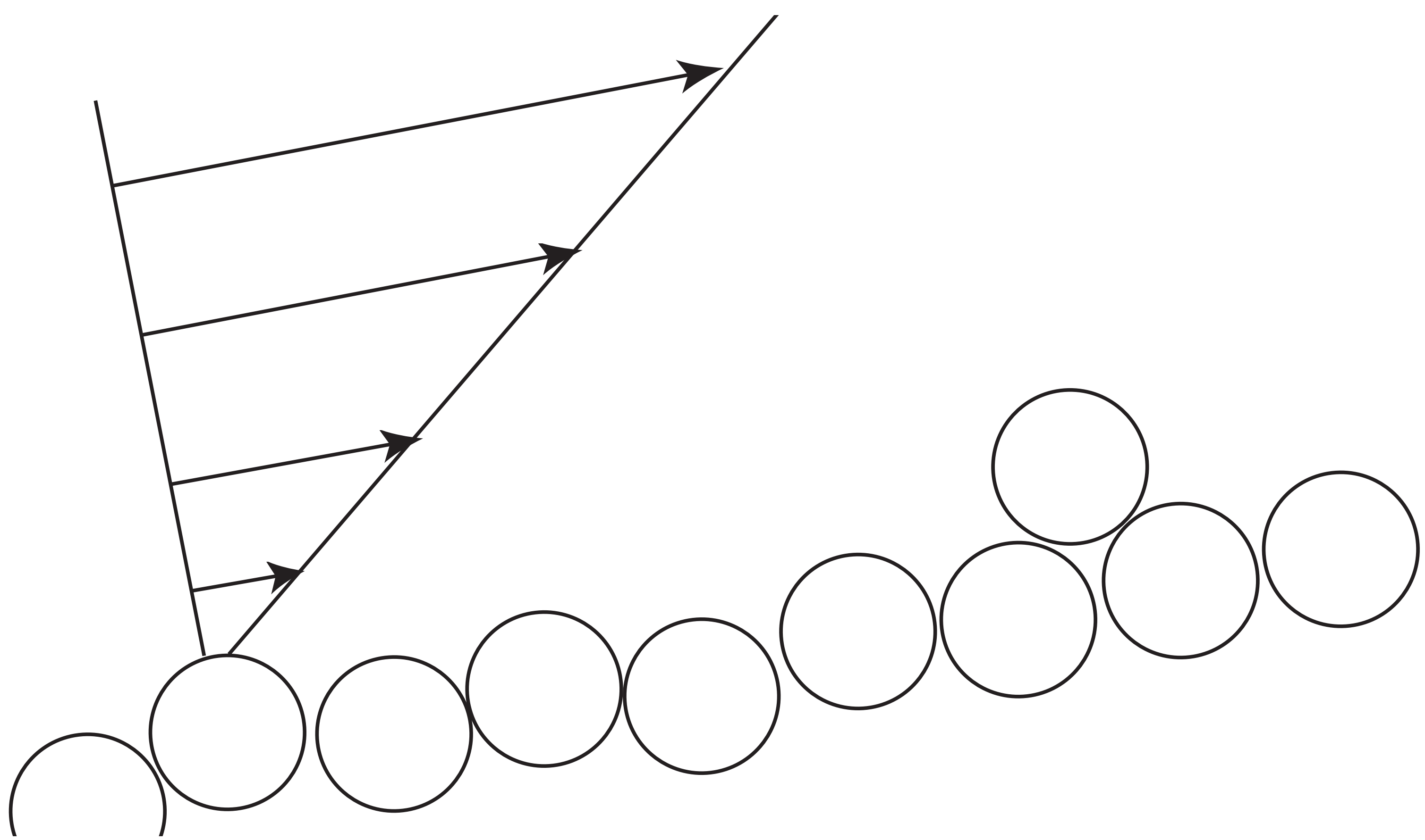

$$\tau_s + \Lambda \frac{\partial f}{\partial x}$$

Stress larger than a threshold $\tau > \tau_s$

Shields number $$\frac{\tau}{(\rho_p - \rho) g D}$$

Erosion Model

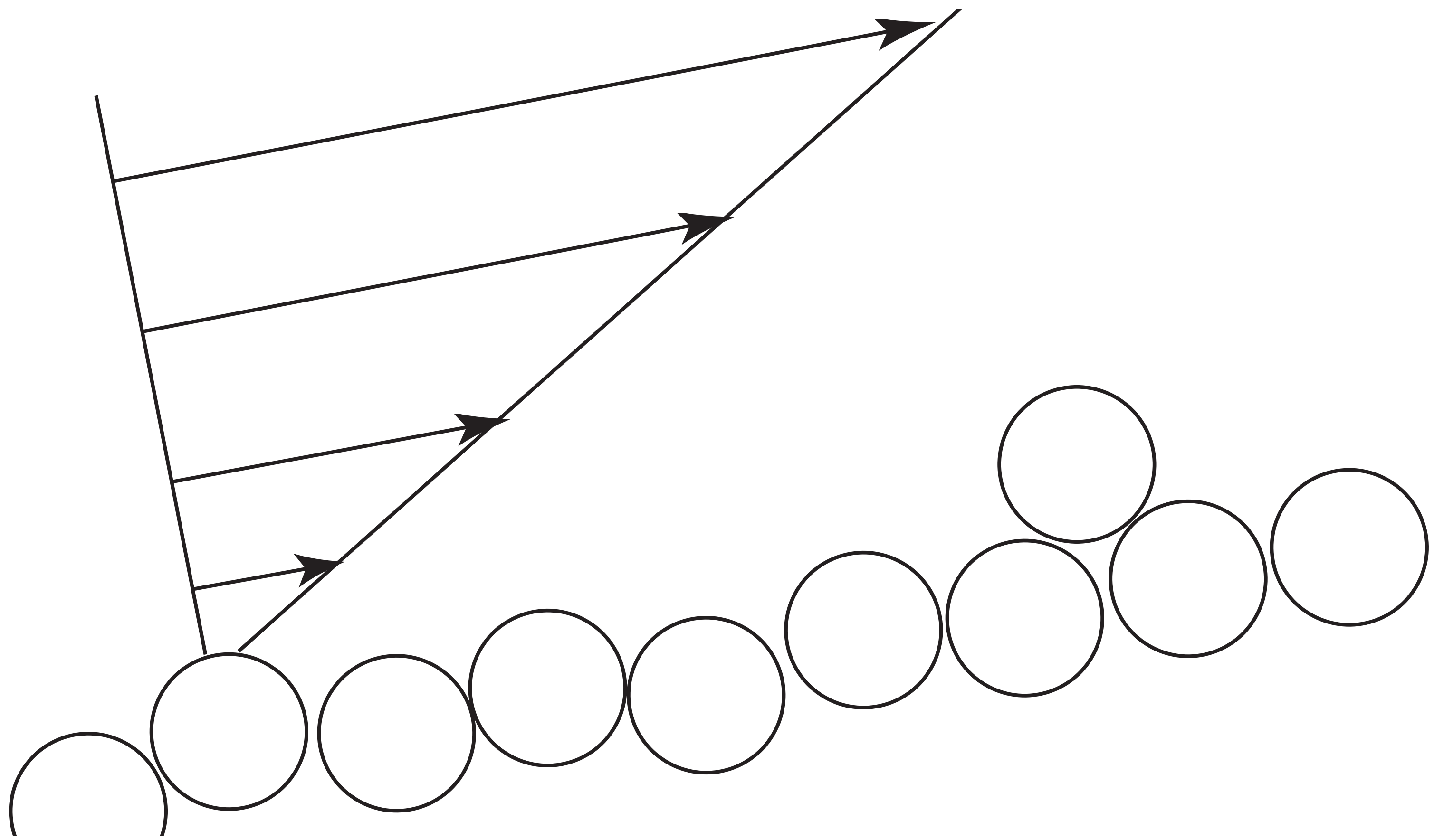

$$\tau_s + \Lambda \frac{\partial f}{\partial x}$$

Stress larger than a threshold $\tau > \tau_s$

Shields number $\dfrac{\tau}{(\rho_p - \rho) g D}$

Erosion Model

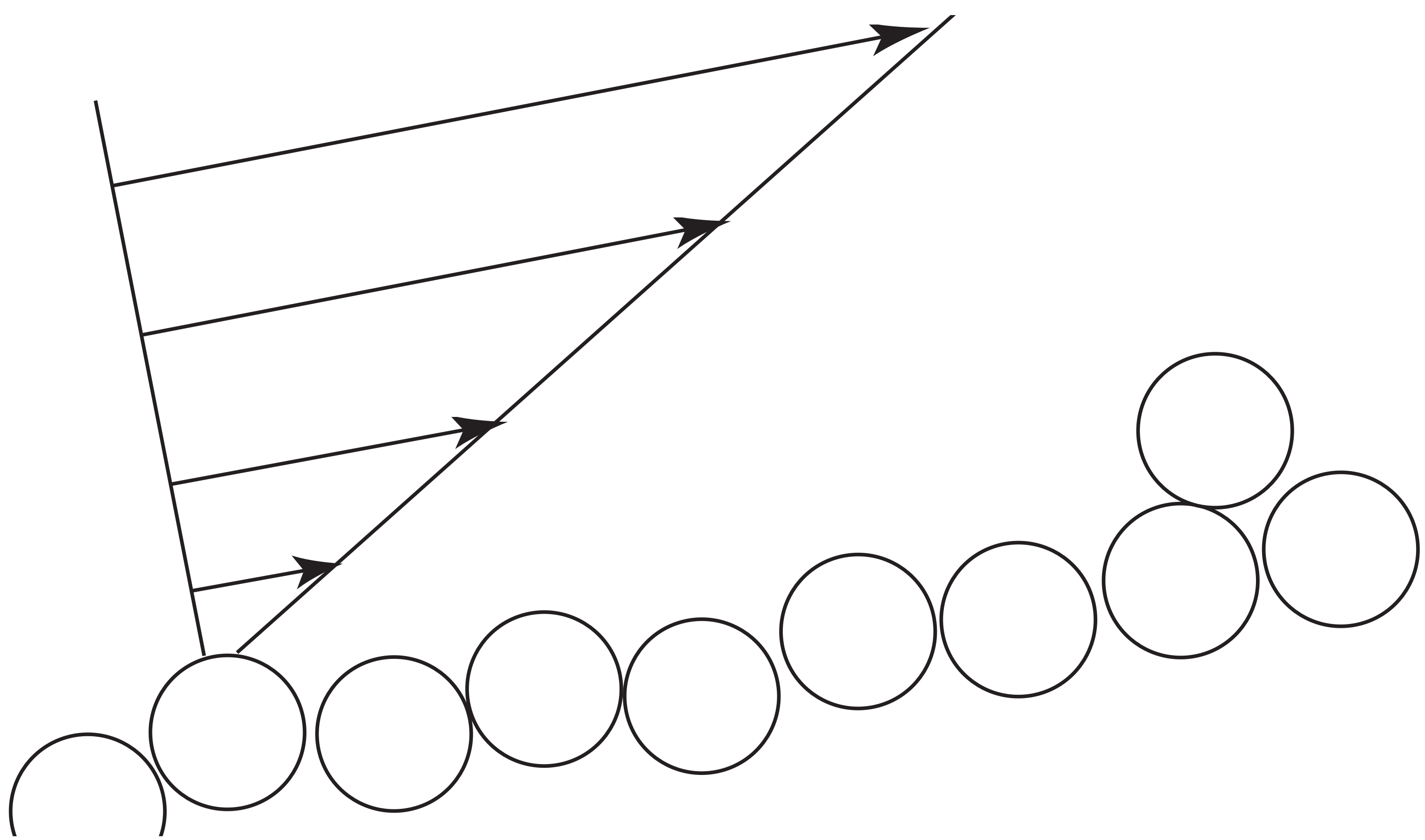

$$\tau_s + \Lambda \frac{\partial f}{\partial x}$$

Stress larger than a threshold $\tau > \tau_s$

Shields number $$\frac{\tau}{(\rho_p - \rho) g D}$$

Erosion Model

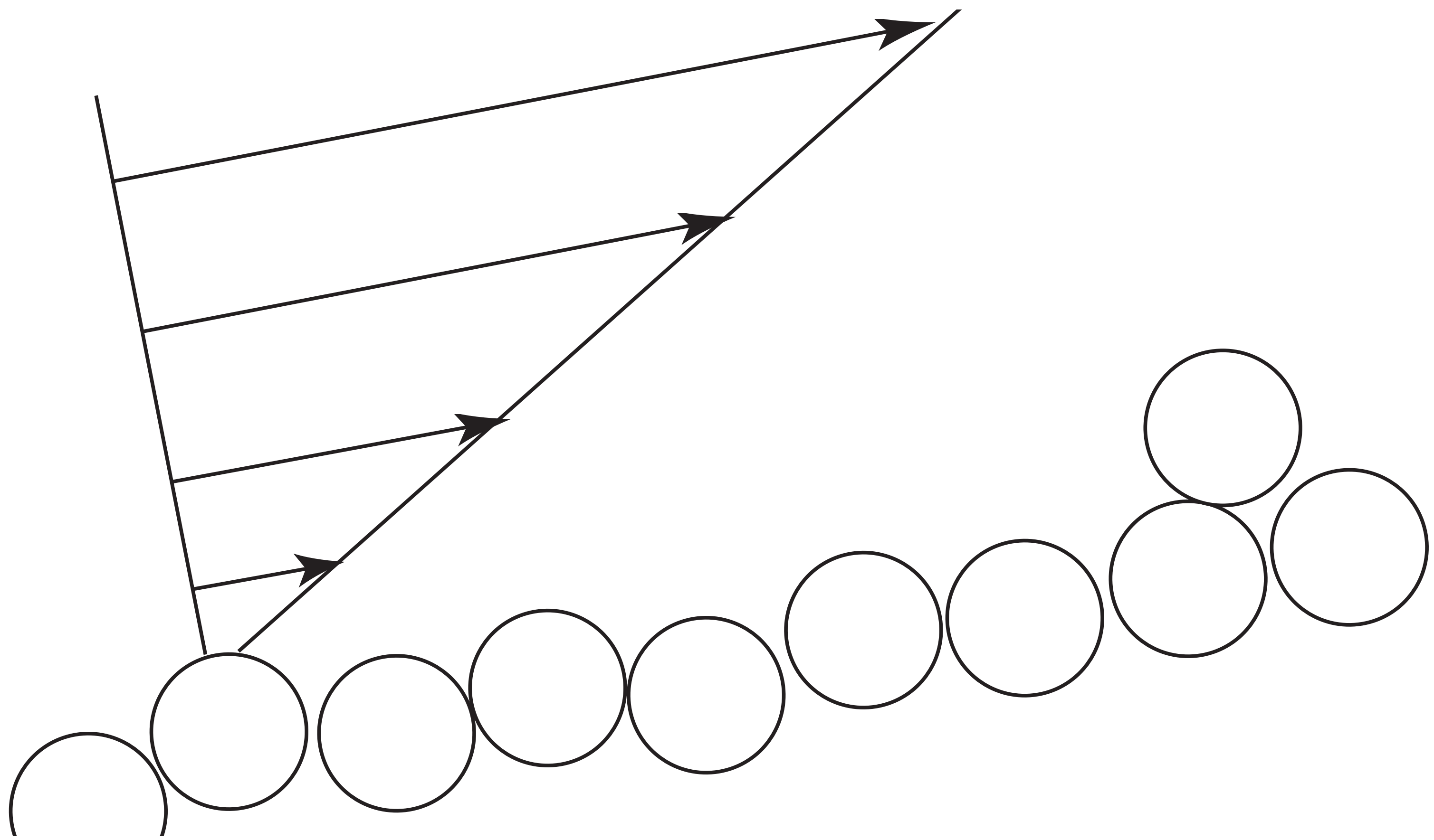

1806 Grenoble 1873

http://www.annales.org/archives/x/gras.html

Les lois d'entraînement de M. Scipion Gras
sur les torrents des Alpes (Annales des ponts et Chaussées, 1857, 2^e semestre) résumées par du Boys 1879 :

"*un caillou posé au fond d'un courant liquide, peut être déplacé par l'impulsion des filets qui le rencontrent : le mouvement aura lieu si la vitesse est supérieure à une certaine limite qu'il (S. Gras) nomme vitesse d'entraînement. Cette vitesse limite dépend de la densité, du volume et de la forme du caillou ; elle dépend aussi de la densité du liquide et de la profondeur du courant.*"

Erosion Model

In the literature one founds Charru /Izumi & Parker / Yang / Blondeau Du Boys

$$q_s = E\varpi(\tau^a(\tau - \tau_s)^b)$$

if $x > 0$ then $\varpi(x) = x$ else $\varpi(x) = 0$.

or with a slope correction for the threshold value:

a, E coefficients, $a = 0, b = 3$ or $a = b = 1$ or $a = 1/2, b = 1$ or ...

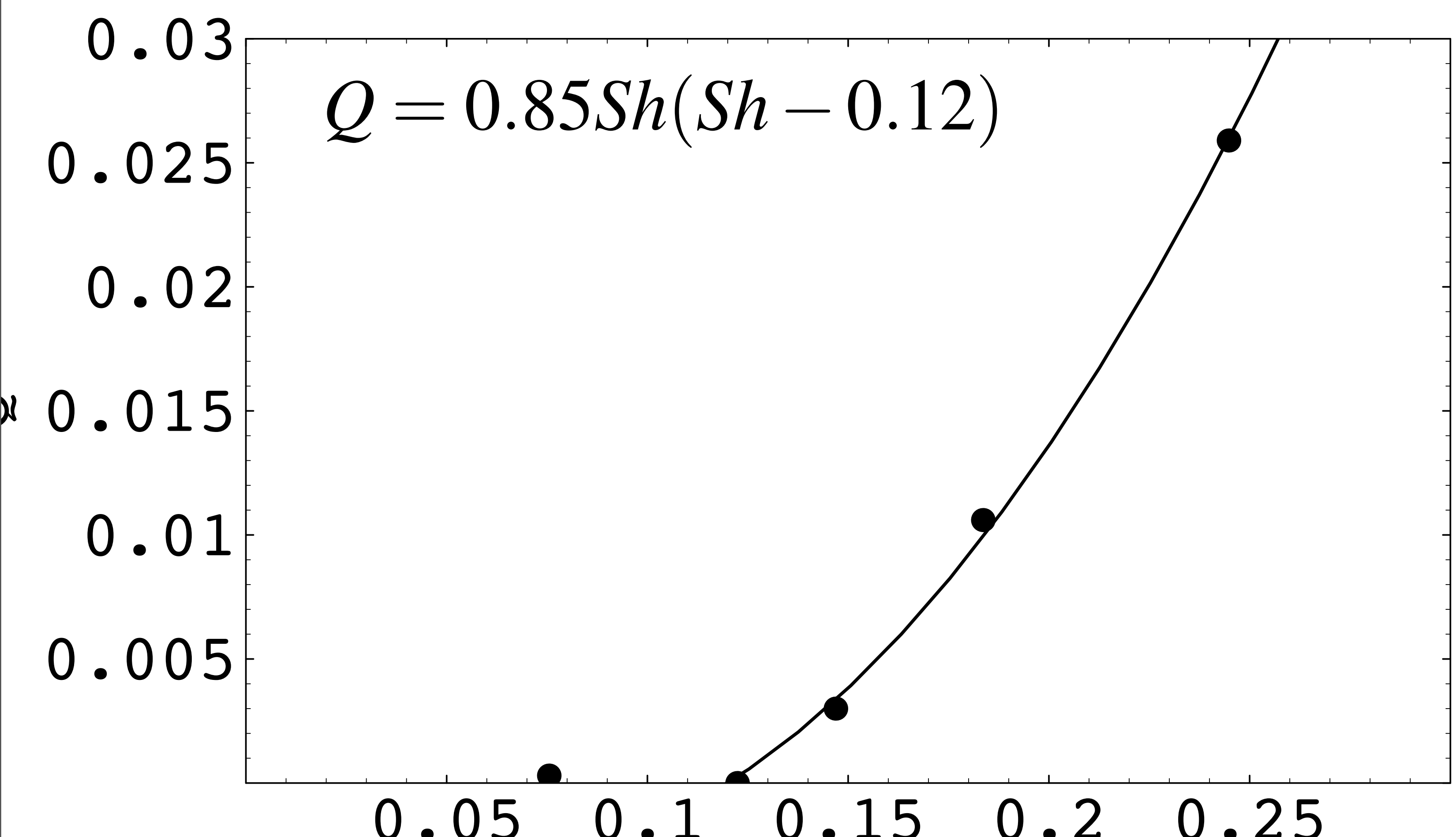

$$\theta = \frac{\eta\gamma}{(\rho_s - \rho_f)gd}$$

Charru

Sh

Erosion Model

In the literature one founds Charru /Izumi & Parker / Yang / Blondeau Du Boys

$$q_s = E\varpi(\tau^a(\tau - \tau_s)^b)$$

if $x > 0$ then $\varpi(x) = x$ else $\varpi(x) = 0$.

or with a slope correction for the threshold value:

a, E coefficients, $a = 0, b = 3$ or $a = b = 1$ or $a = 1/2, b = 1$ or ...

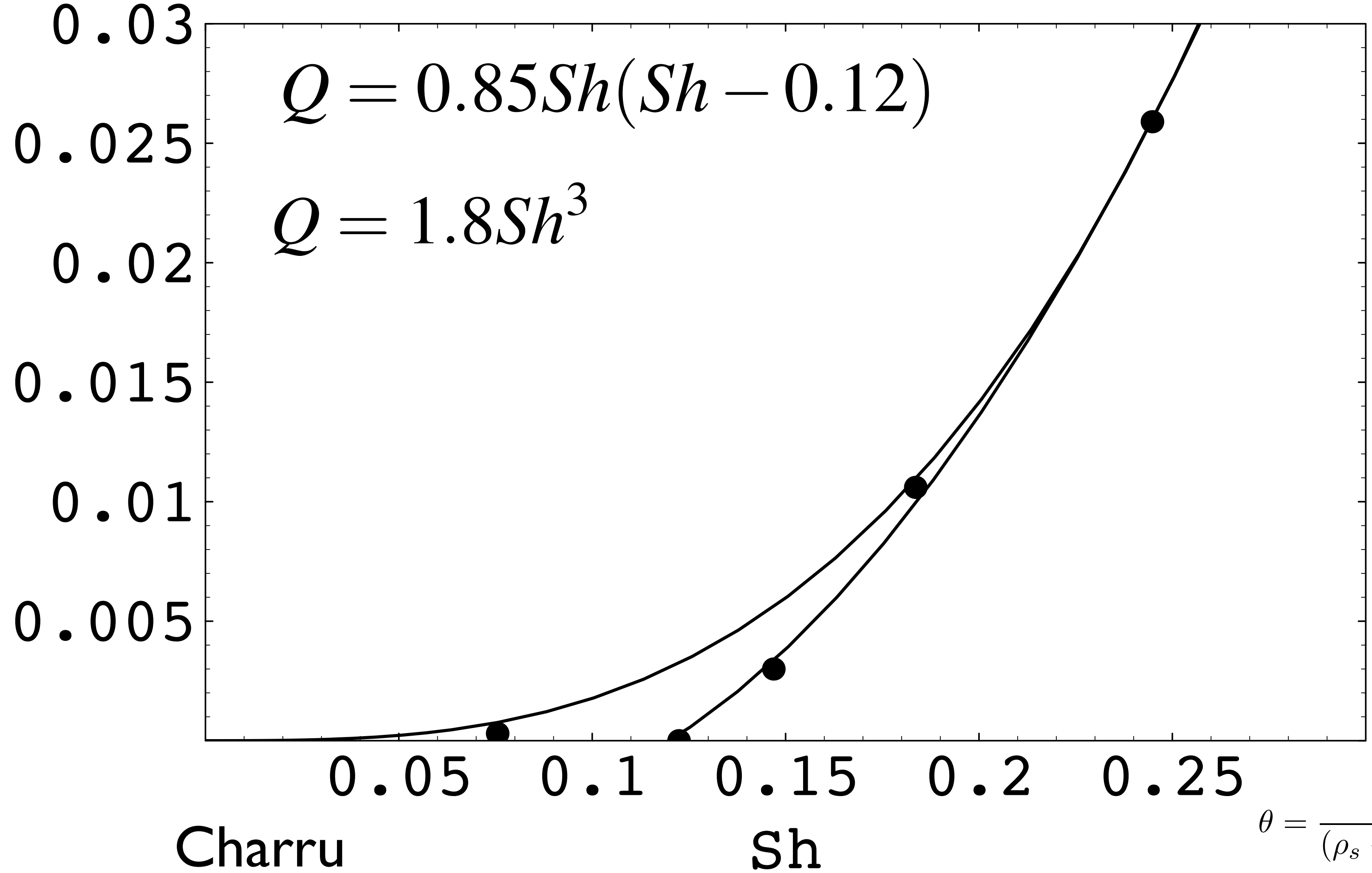

Charru

$\theta = \frac{\eta\gamma}{(\rho_s - \rho_f)gd}$

Erosion Model

In the literature one founds Charru /Izumi & Parker / Yang / Blondeau Du Boys

$$q_s = E\varpi(\tau^a(\tau - \tau_s)^b)$$

if $x > 0$ then $\varpi(x) = x$ else $\varpi(x) = 0$.

or with a slope correction for the threshold value:

a, E coefficients, $a = 0, b = 3$ or $a = b = 1$ or $a = 1/2, b = 1$ or ...

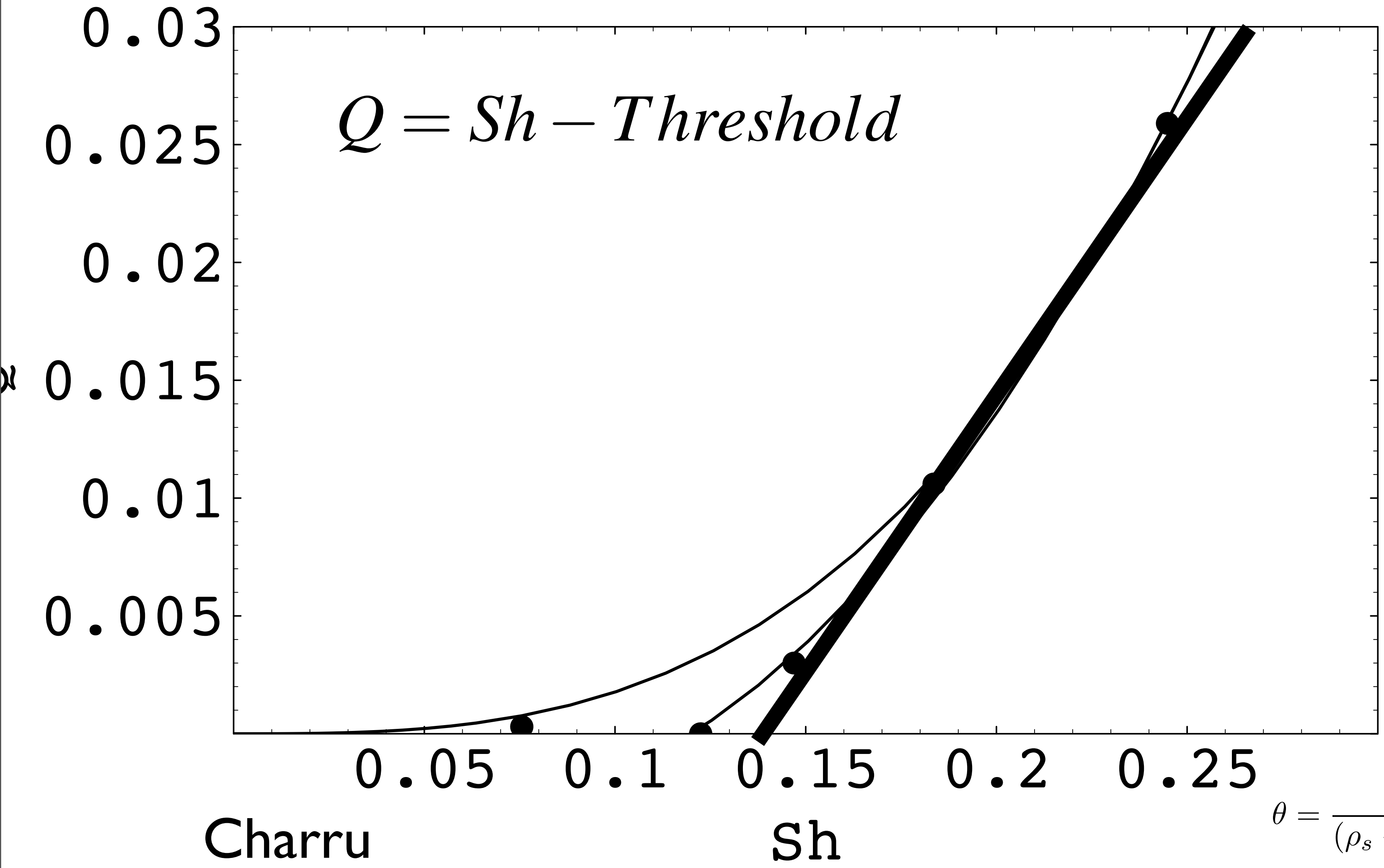

Charru

$\theta = \frac{\eta\gamma}{(\rho_s - \rho_f)gd}$

Erosion Model

In the literature one founds Charru /Izumi & Parker / Yang / Blondeau Du Boys

$$q_s = E\varpi(\tau^a(\tau-\tau_s)^b)$$

if $x>0$ then $\varpi(x)=x$ else $\varpi(x)=0$.

or with a slope correction for the threshold value:

a, E coefficients, $a=0, b=3$ or $a=b=1$ or $a=1/2, b=1$ or ...

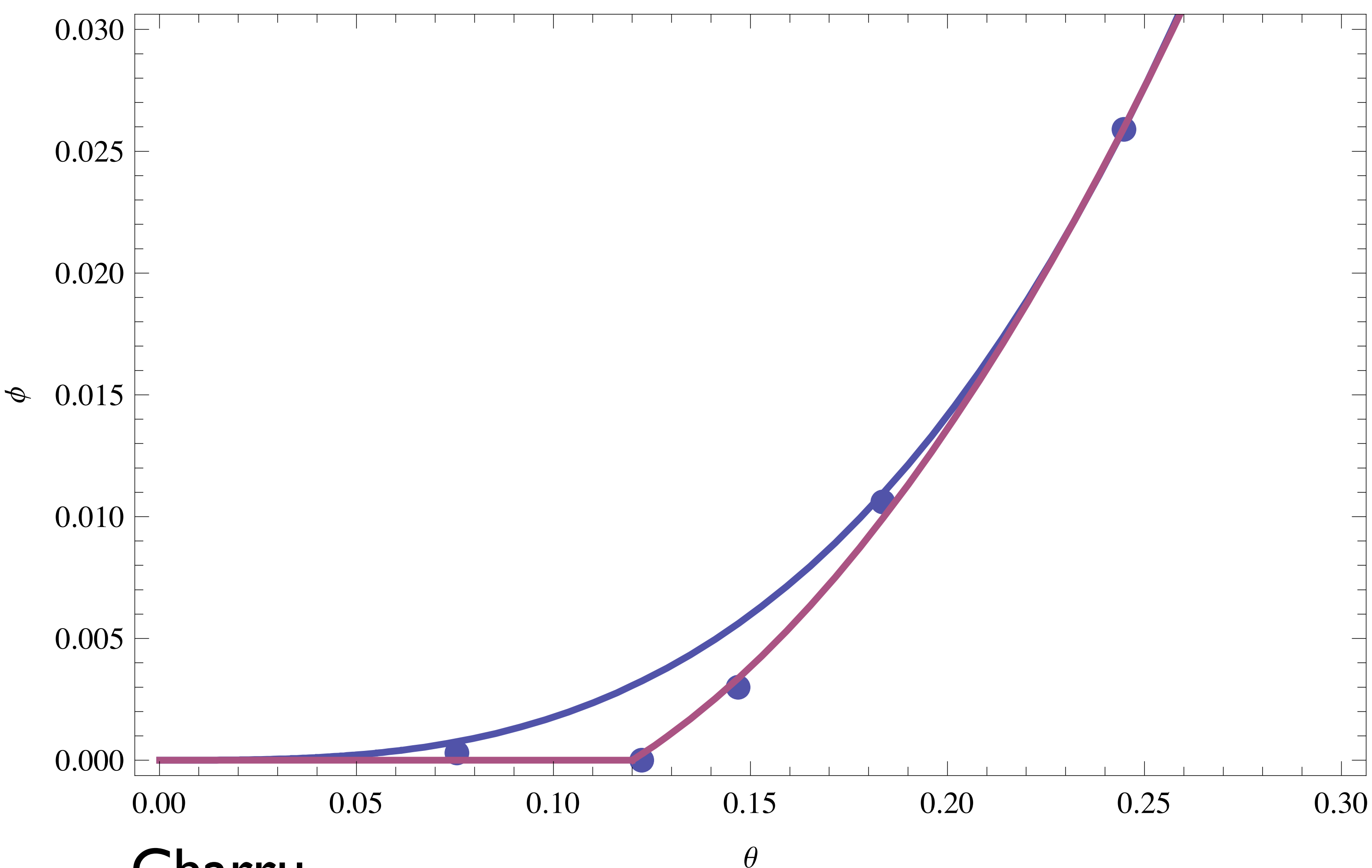

Charru

Erosion Model

In the literature one founds Charru /Izumi & Parker / Yang / Blondeau Du Boys

$$q_s = E\varpi(\tau^a(\tau-\tau_s)^b)$$

if $x>0$ then $\varpi(x)=x$ else $\varpi(x)=0$.

or with a slope correction for the threshold value:

a, E coefficients, $a=0, b=3$ or $a=b=1$ or $a=1/2, b=1$ or ...

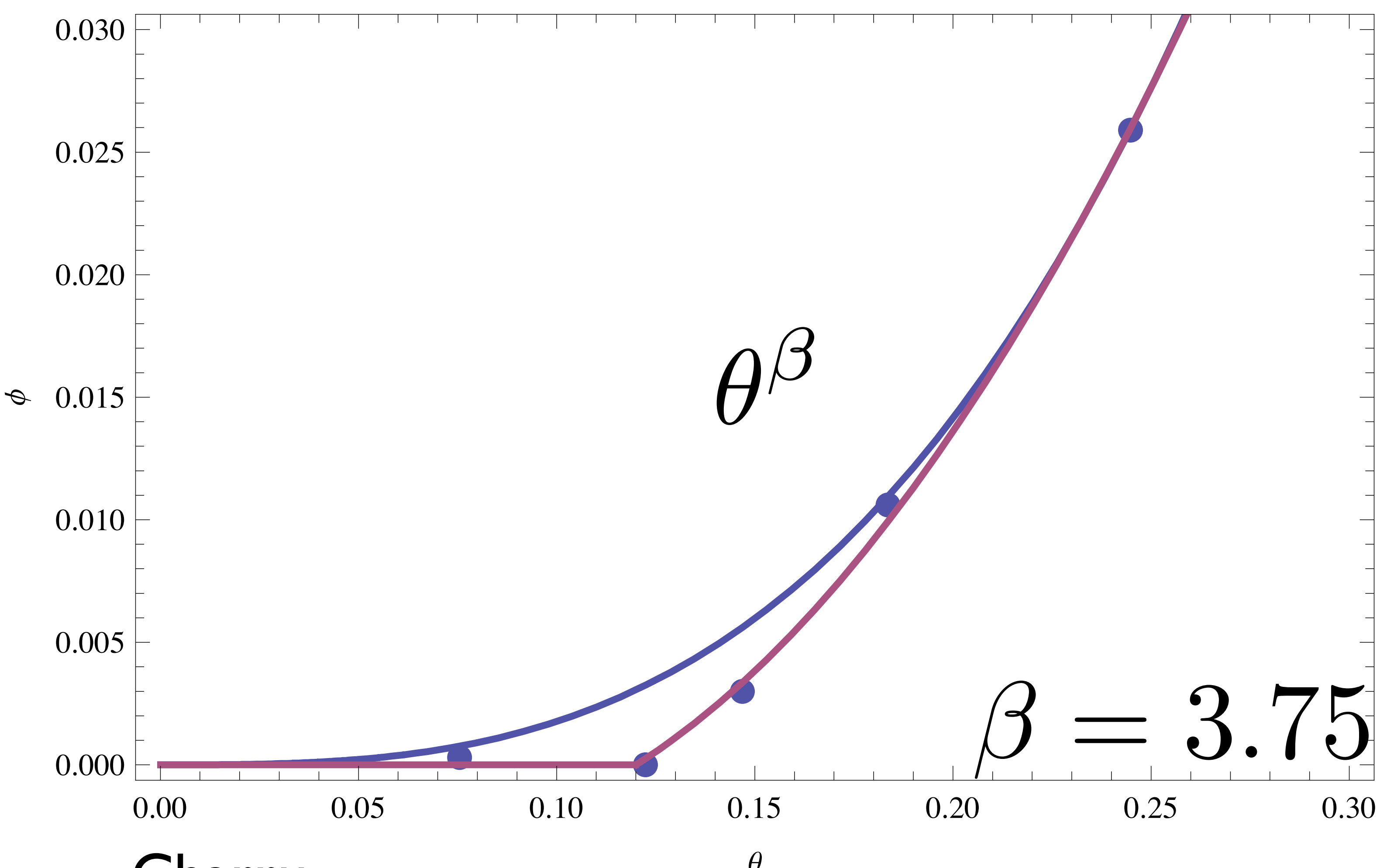

Charru

Erosion Model

In the literature one founds Charru /Izumi & Parker / Yang / Blondeau Du Boys

$$q_s = E\varpi(\tau^a(\tau - \tau_s)^b)$$

if $x > 0$ then $\varpi(x) = x$ else $\varpi(x) = 0$.

or with a slope correction for the threshold value:

a, E coefficients, $a = 0, b = 3$ or $a = b = 1$ or $a = 1/2, b = 1$ or ...

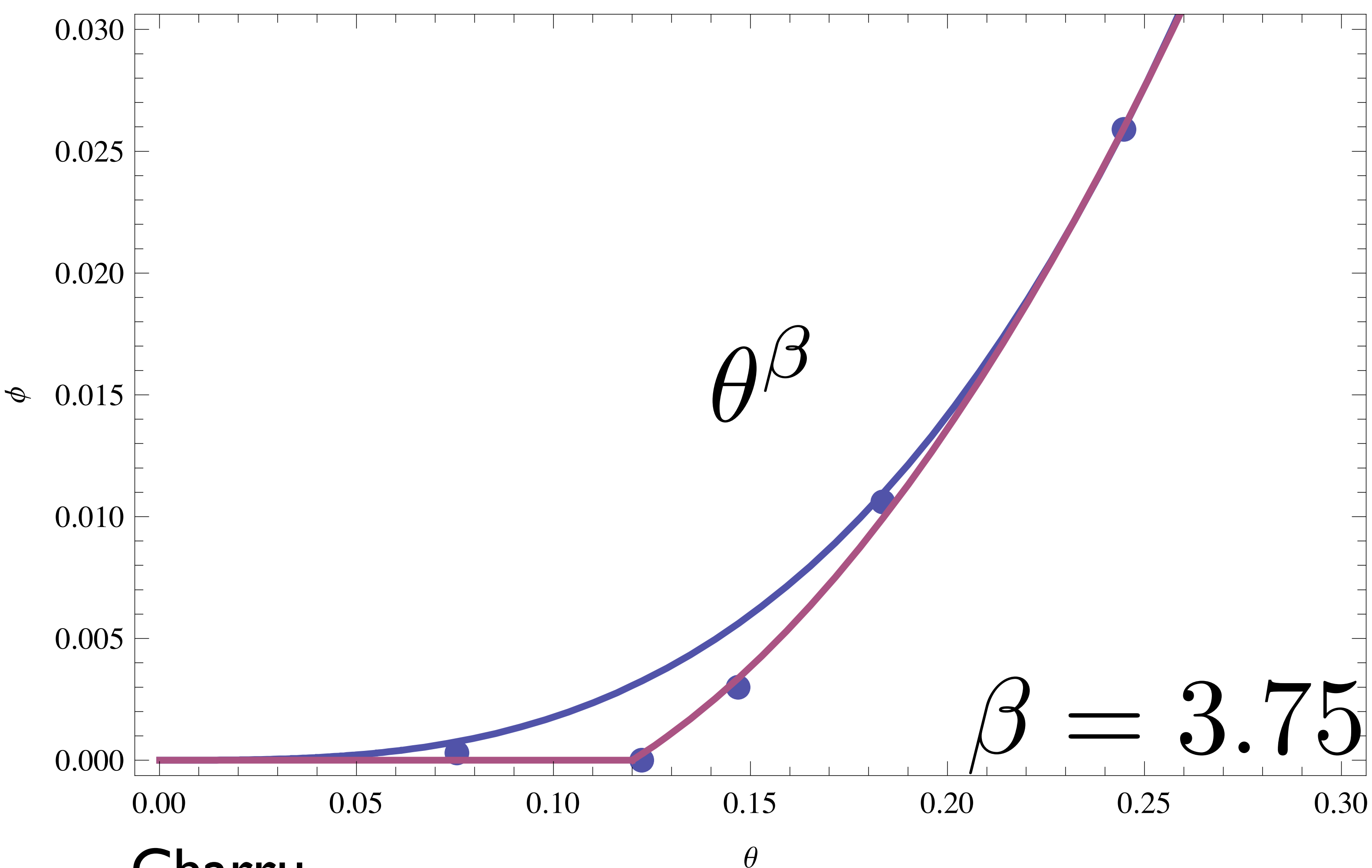

$$\vec{q} = \phi\theta^{\beta}\left(\frac{\vec{u}}{\|\vec{u}\|} - \gamma\vec{\nabla}h\right)$$

Charru

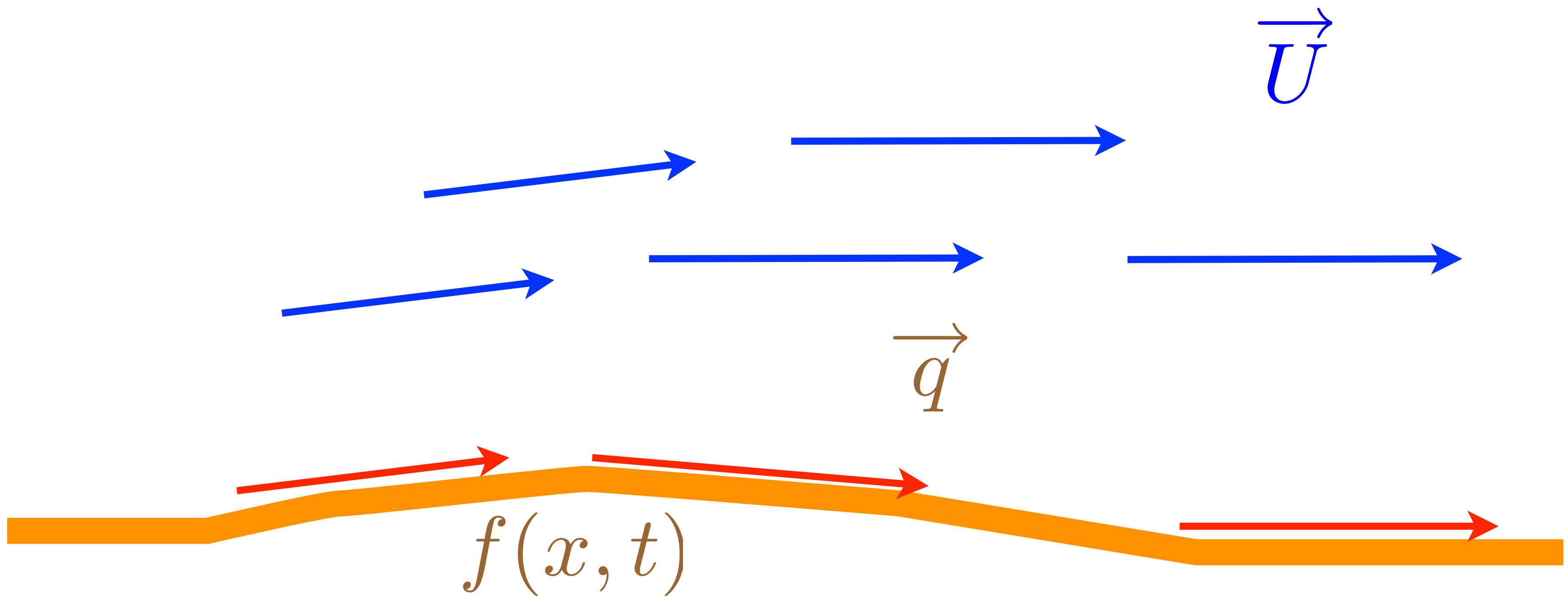

mass conservation of sediments
(Exner Law)

$$\frac{\partial f}{\partial t} = -\overrightarrow{\nabla} \cdot \overrightarrow{q}$$

- introduction
- the problem
- the flow: Saint Venant and other
- first granular model
- first coupling: bars
- imporved granular model: saturation length
- ripples
- bars & ripples
- conclusions perspectives

testing Saint Venant + erosion

testing Saint Venant + erosion

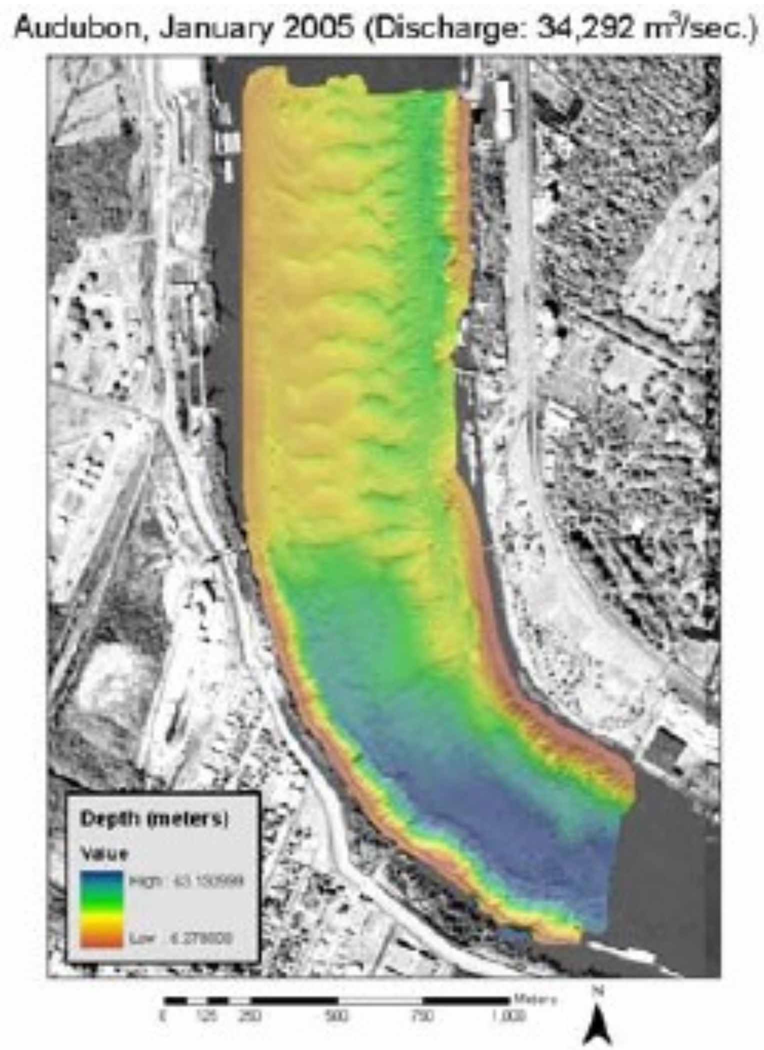

coupled system

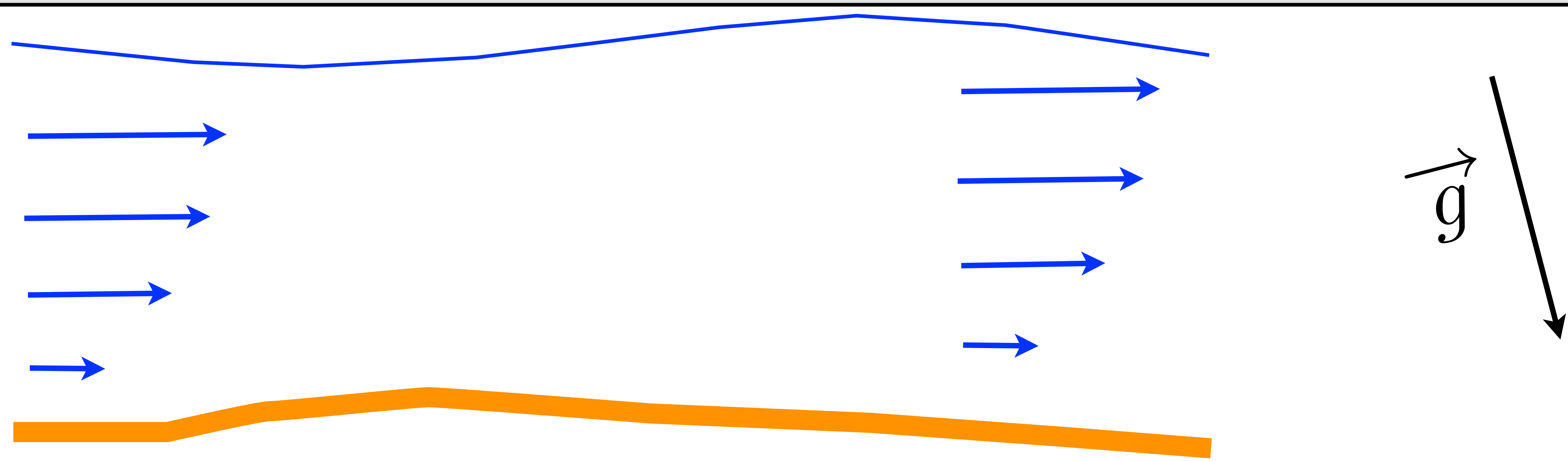

Navier Stokes

coupled system

Saint Venant

$$\frac{6}{5}(\overrightarrow{u}\cdot\overrightarrow{\nabla})\overrightarrow{u} = -g(\overrightarrow{\nabla}\eta + sin(\theta)\overrightarrow{e}_x) - \frac{3\nu\overrightarrow{u}}{(h)^2}$$

Mass conservation of fluid

$$\overrightarrow{\nabla}\cdot(h\overrightarrow{u}) = 0$$

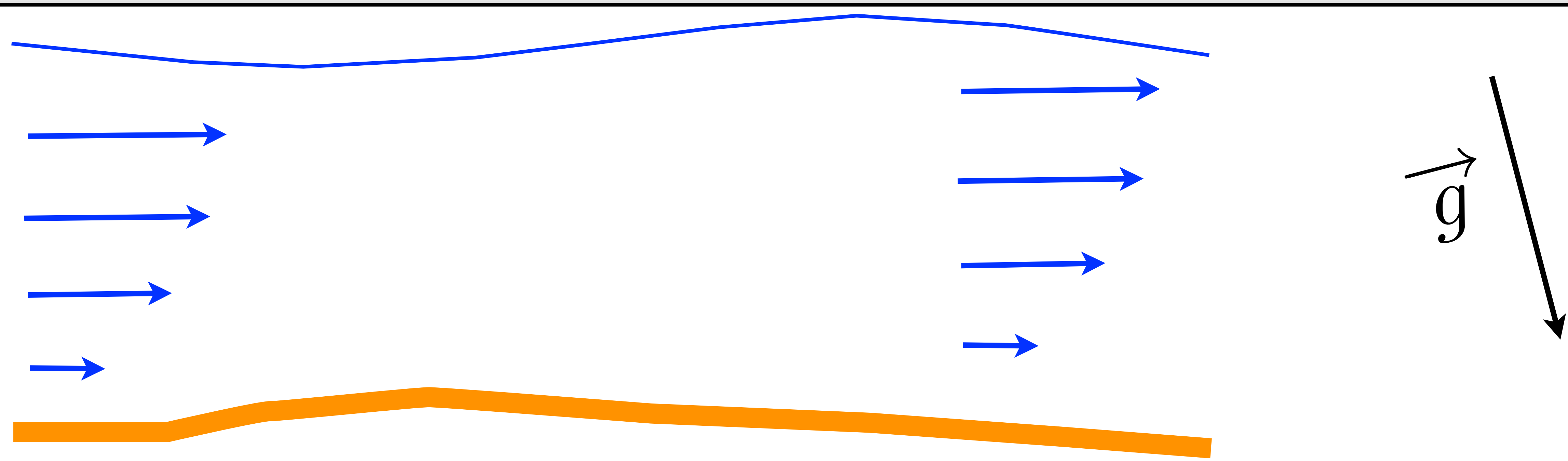

Navier Stokes — coupled system — Saint Venant

$$\frac{6}{5}(\overrightarrow{u}\cdot\overrightarrow{\nabla})\overrightarrow{u} = -g(\overrightarrow{\nabla}\eta + sin(\theta)\overrightarrow{e}_x) - \frac{3\nu\overrightarrow{u}}{(h)^2}$$

Mass conservation of fluid

$$\overrightarrow{\nabla}\cdot(h\overrightarrow{u}) = 0$$

$$\vec{q} = \phi\theta^{\beta}\left(\frac{\vec{u}}{\|\vec{u}\|} - \gamma\vec{\nabla}h\right)$$

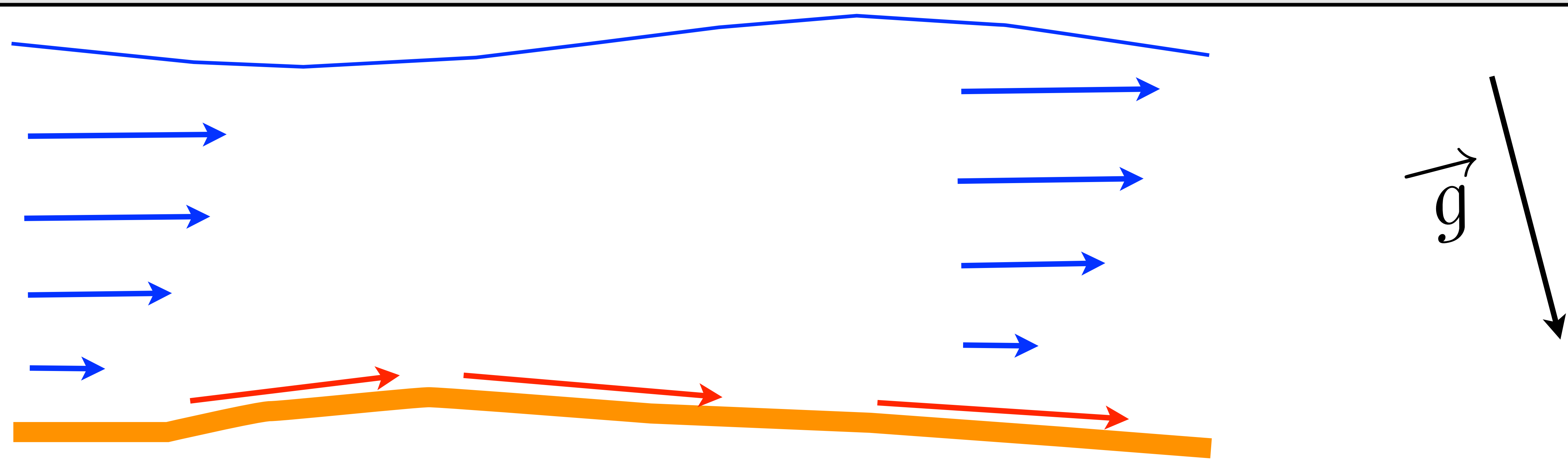

Navier Stokes — **coupled system** — Saint Venant

$$\frac{6}{5}(\overrightarrow{u}\cdot\overrightarrow{\nabla})\overrightarrow{u} = -g(\overrightarrow{\nabla}\eta + sin(\theta)\overrightarrow{e}_x) - \frac{3\nu\overrightarrow{u}}{(h)^2}$$

Mass conservation of fluid

$$\overrightarrow{\nabla}\cdot(h\overrightarrow{u}) = 0$$

$$\vec{q} = \phi\theta^{\beta}\left(\frac{\vec{u}}{\|\vec{u}\|} - \gamma\vec{\nabla}h\right)$$

$$\frac{\partial f}{\partial t} = -\overrightarrow{\nabla}\cdot\overrightarrow{q}$$

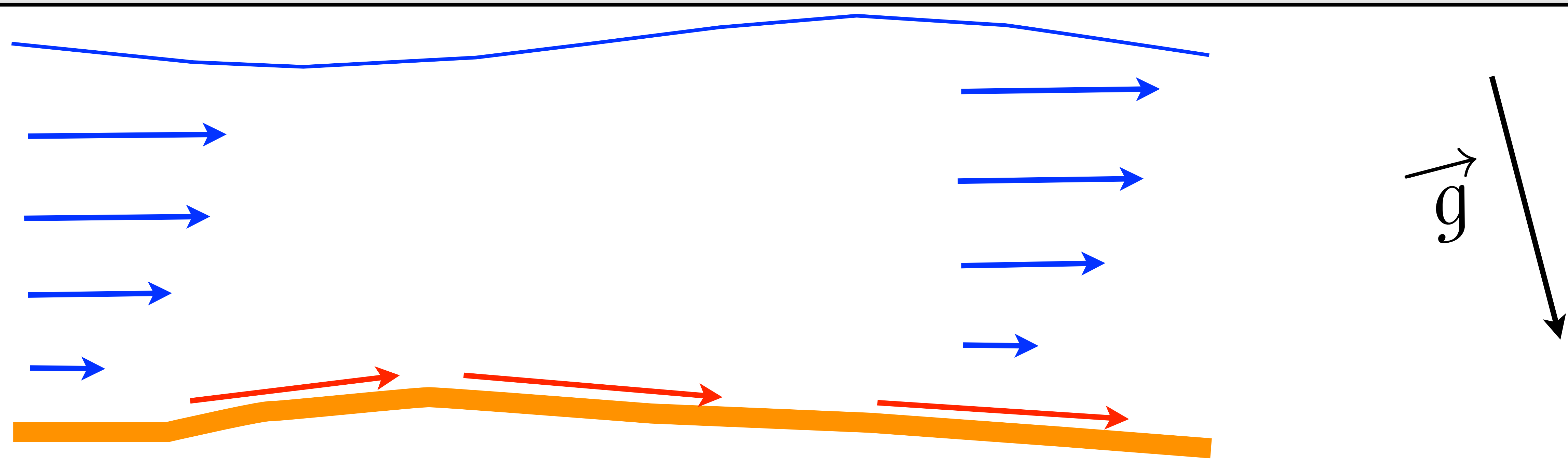

Navier Stokes

coupled system

Saint Venant

$$\frac{6}{5}(\overrightarrow{u}\cdot\overrightarrow{\nabla})\overrightarrow{u} = -g(\overrightarrow{\nabla}\eta + sin(\theta)\overrightarrow{e}_x) - \frac{3\nu\overrightarrow{u}}{(h)^2}$$

Mass conservation of fluid

$$\overrightarrow{\nabla}\cdot(h\overrightarrow{u}) = 0$$

$$\vec{q} = \phi\theta^{\beta}\left(\frac{\vec{u}}{\|\vec{u}\|} - \gamma\vec{\nabla}h\right)$$

$$\frac{\partial f}{\partial t} = -\overrightarrow{\nabla}\cdot\overrightarrow{q}$$

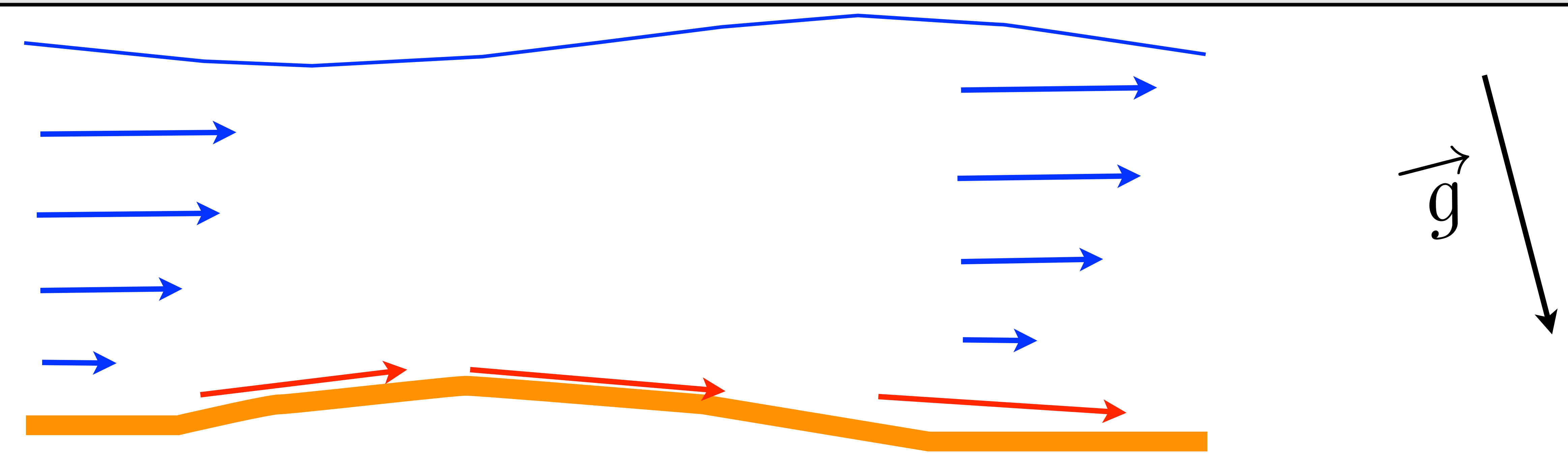

Navier Stokes

coupled system

Saint Venant

$$\frac{6}{5}(\overrightarrow{u}\cdot\overrightarrow{\nabla})\overrightarrow{u} = -g(\overrightarrow{\nabla}\eta + sin(\theta)\overrightarrow{e}_x) - \frac{3\nu\overrightarrow{u}}{(h)^2}$$

Mass conservation of fluid

$$\overrightarrow{\nabla}\cdot(h\overrightarrow{u}) = 0$$

$$\vec{q} = \phi\theta^{\beta}\left(\frac{\vec{u}}{\|\vec{u}\|} - \gamma\vec{\nabla}h\right)$$

$$\frac{\partial f}{\partial t} = -\overrightarrow{\nabla}\cdot\overrightarrow{q}$$

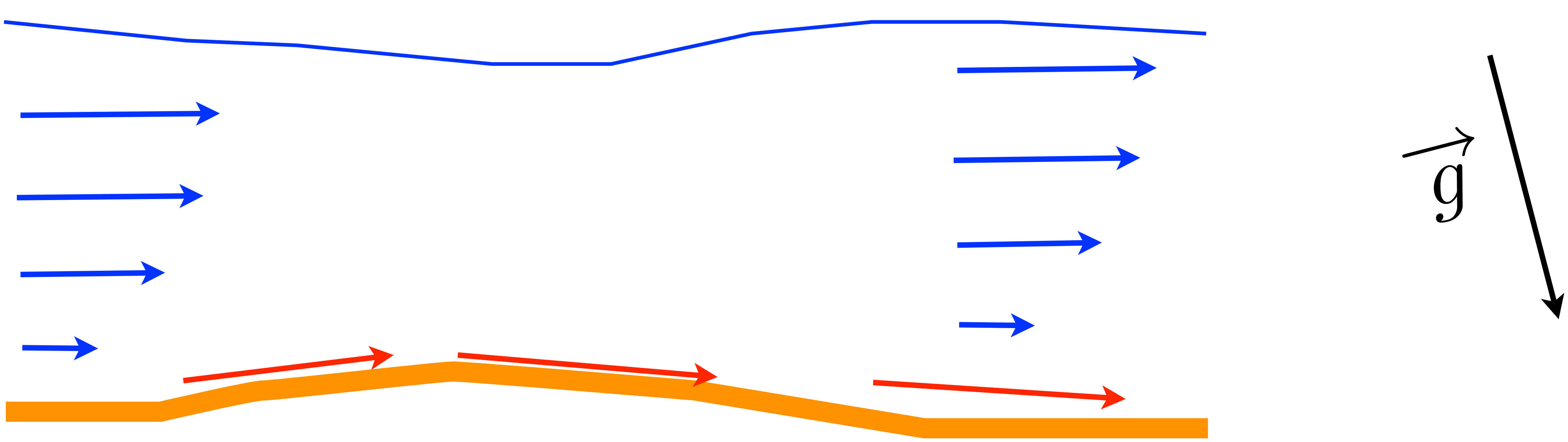

Navier Stokes

coupled system

Saint Venant

$$\frac{6}{5}(\overrightarrow{u}\cdot\overrightarrow{\nabla})\overrightarrow{u} = -g(\overrightarrow{\nabla}\eta + sin(\theta)\overrightarrow{e}_x) - \frac{3\nu\overrightarrow{u}}{(h)^2}$$

Mass conservation of fluid

$$\overrightarrow{\nabla}\cdot(h\overrightarrow{u}) = 0$$

$$\vec{q} = \phi\theta^{\beta}\left(\frac{\vec{u}}{\|\vec{u}\|} - \gamma\vec{\nabla}h\right)$$

$$\frac{\partial f}{\partial t} = -\overrightarrow{\nabla}\cdot\overrightarrow{q}$$

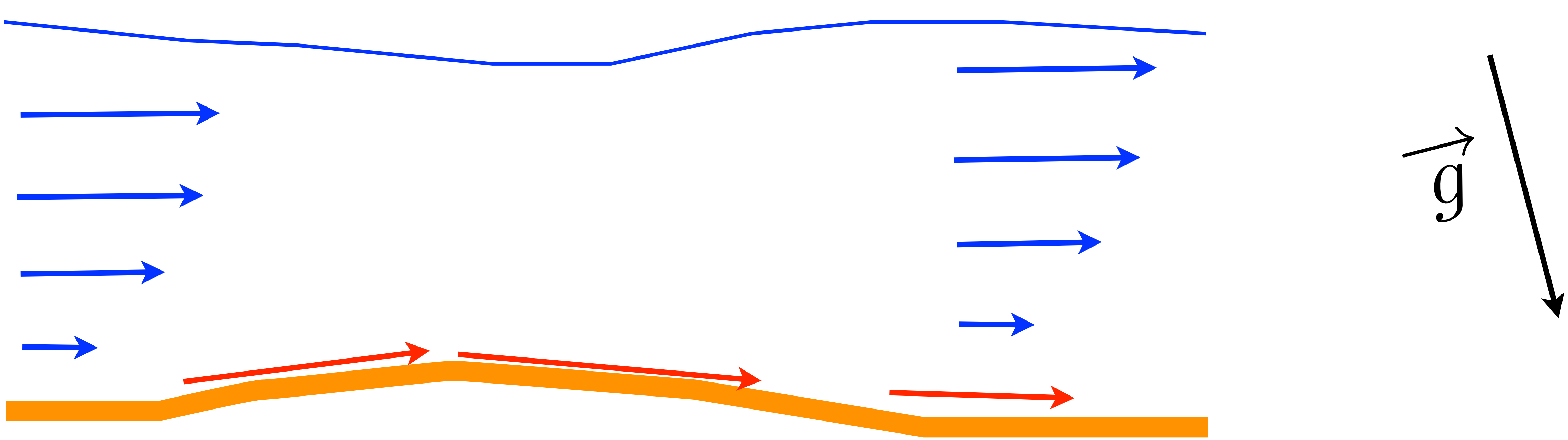

Navier Stokes

coupled system

Saint Venant

$$\frac{6}{5}(\overrightarrow{u}\cdot\overrightarrow{\nabla})\overrightarrow{u} = -g(\overrightarrow{\nabla}\eta + sin(\theta)\overrightarrow{e}_x) - \frac{3\nu\overrightarrow{u}}{(h)^2}$$

Mass conservation of fluid

$$\overrightarrow{\nabla}\cdot(h\overrightarrow{u}) = 0$$

$$\vec{q} = \phi\theta^{\beta}\left(\frac{\vec{u}}{\|\vec{u}\|} - \gamma\vec{\nabla}h\right)$$

$$\frac{\partial f}{\partial t} = -\overrightarrow{\nabla}\cdot\overrightarrow{q}$$

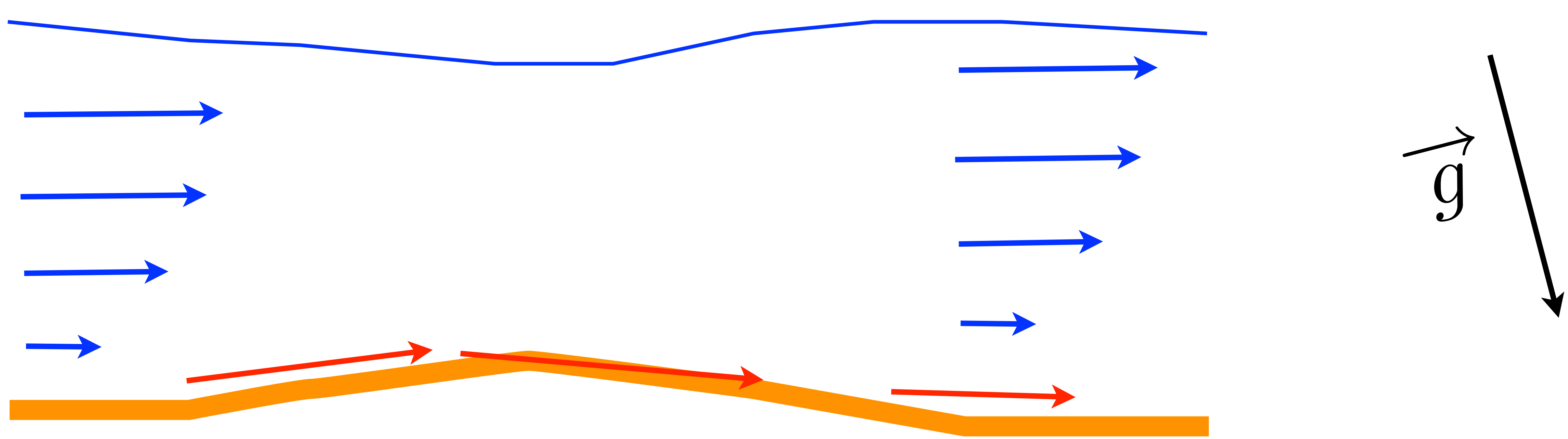

Linear Stability

Basic flow $u_0 = 1,\, d_0 = 1$

Linear Stability

Basic flow $u_0 = 1,\ d_0 = 1$

perturbations $\propto \exp(i(k_l x_l - \omega t))$

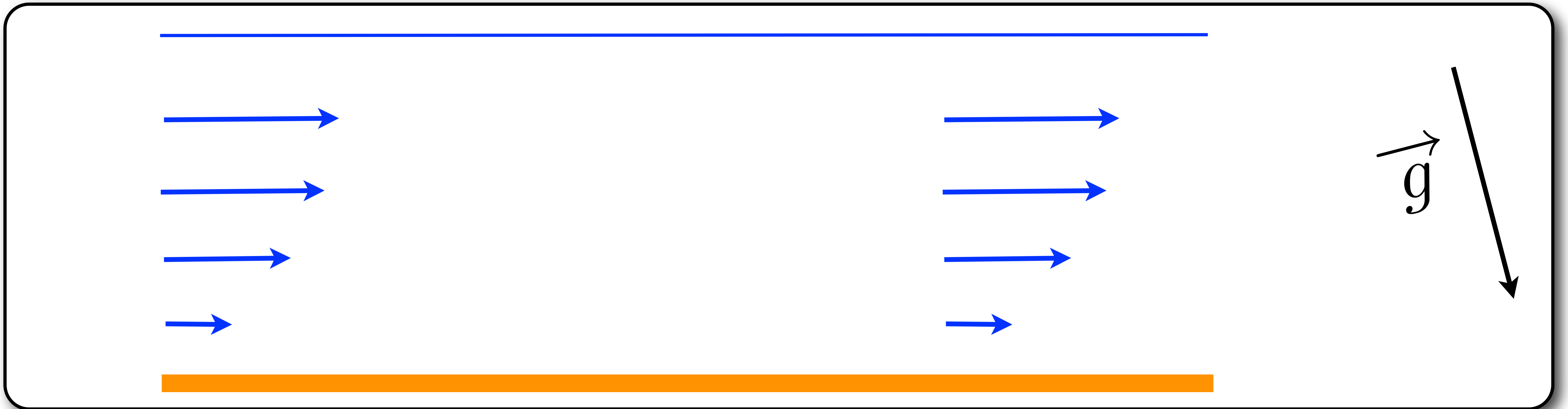

Linear Stability

Basic flow $$u_0 = 1,\ d_0 = 1$$

perturbations $$\propto \exp(i(k_l x_l - \omega t))$$

dispersion relation

$$\omega = \Big(-36iF^4k_x^3\big(k_x^2+k_y^2\big)\gamma + 30iF^2k_x\big(k_x^4\gamma + 2k_x^2k_y^2\gamma + k_y^4\gamma \\ + 2ik_x^3(\beta + S(2+\beta)\gamma) + ik_xk_y^2(1+\beta+S(4+\beta)\gamma)\big) \\ + 25S\big(k_x^4\gamma + 2k_x^2k_y^2\gamma + k_y^4\gamma - ik_xk_y^2(-3+\beta)(1+S\gamma) \\ + ik_x^3(2\beta + S(3+2\beta)\gamma)\big)\Big)/ \\ \Big(\big(6F^2k_x - 5iS\big)\Big(\big(-5+6F^2\big)k_x^2 - 5k_y^2 - 15ik_xS\big)(1+S\gamma)\Big)$$

$$\beta = \frac{\theta_0\phi'(\theta_0)}{\phi(\theta_0)}$$

Linear Stability 1D $\int$(2D)

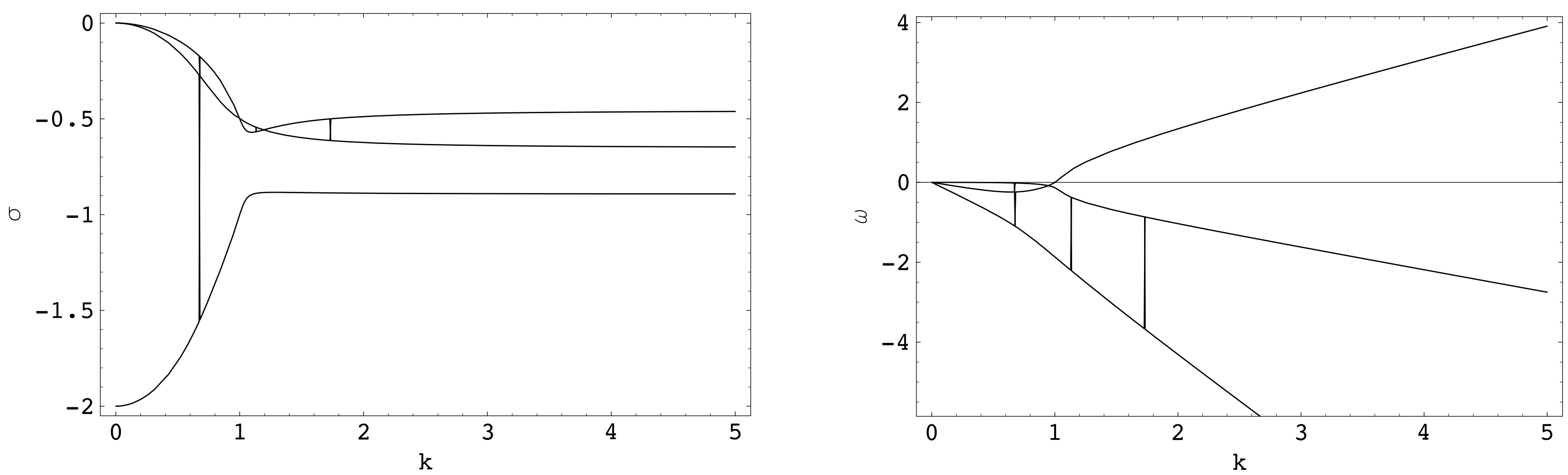

no dunes in 2D

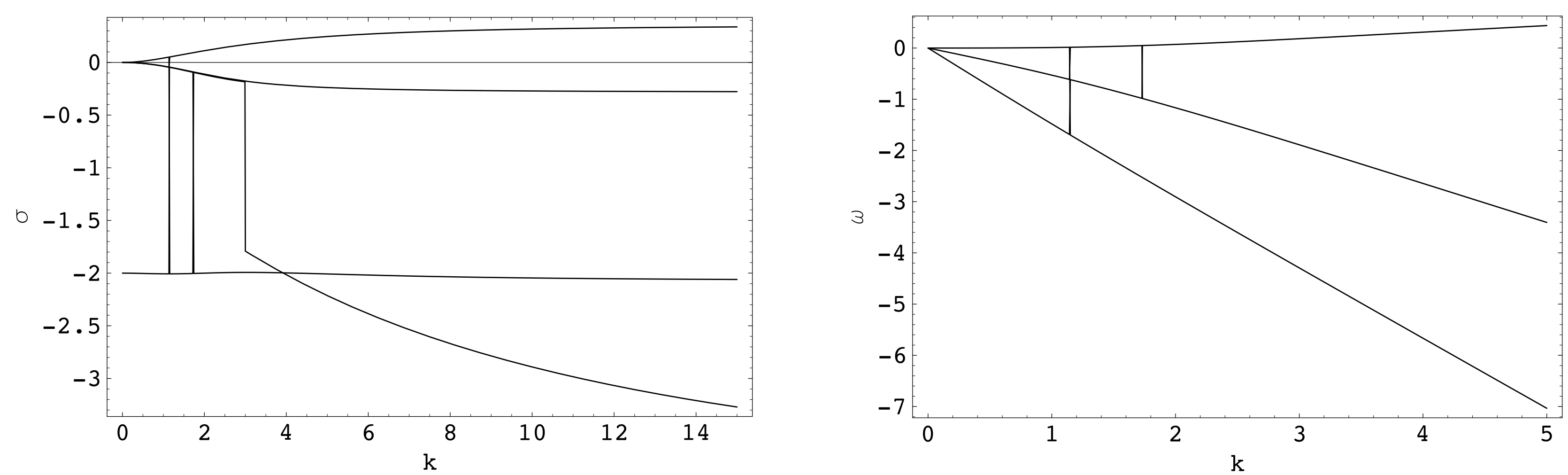

antidunes in 2D

Linear Stability 1D $\int$(2D)

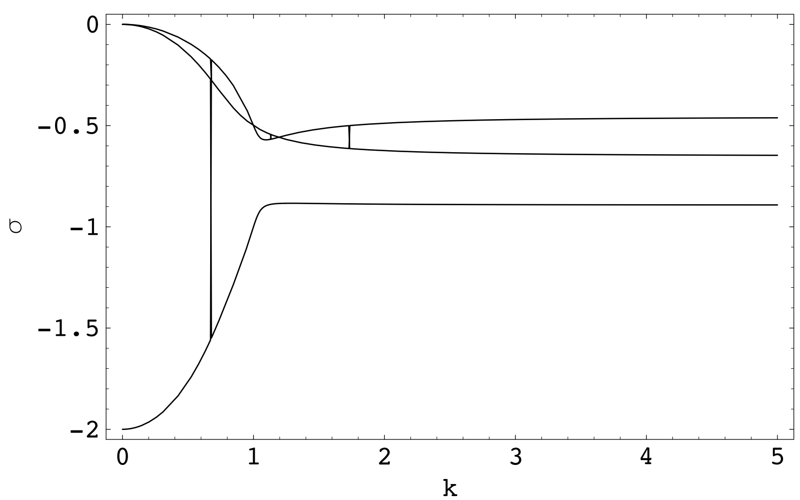

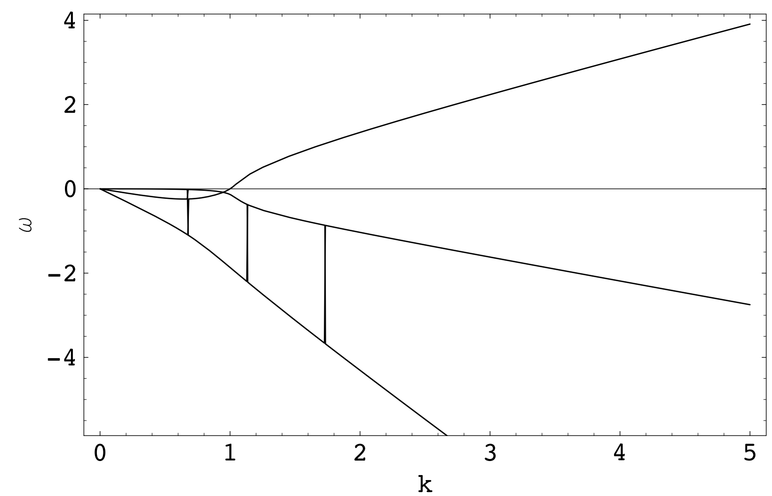

no dunes in 2D

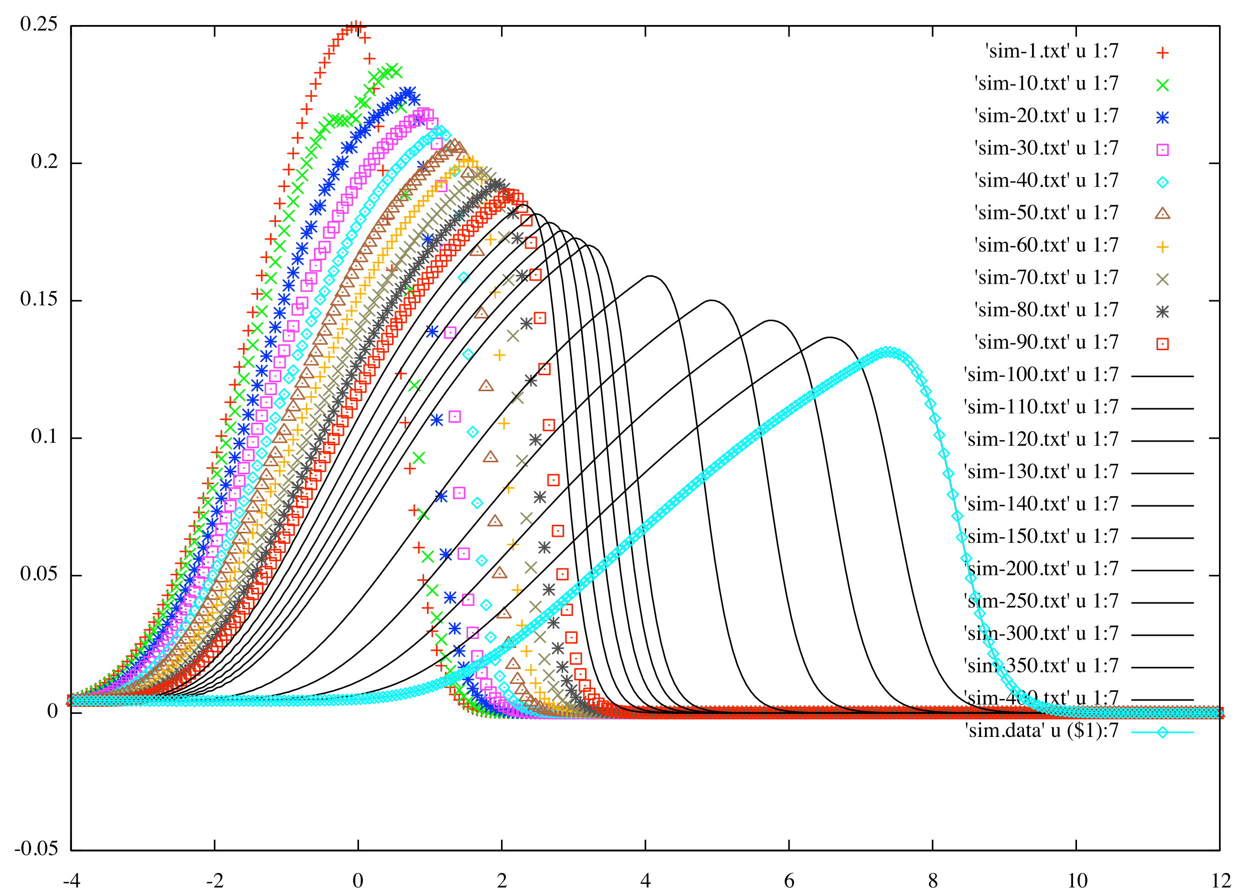

example gerris

Linear Stability 2D $\int$(3D)

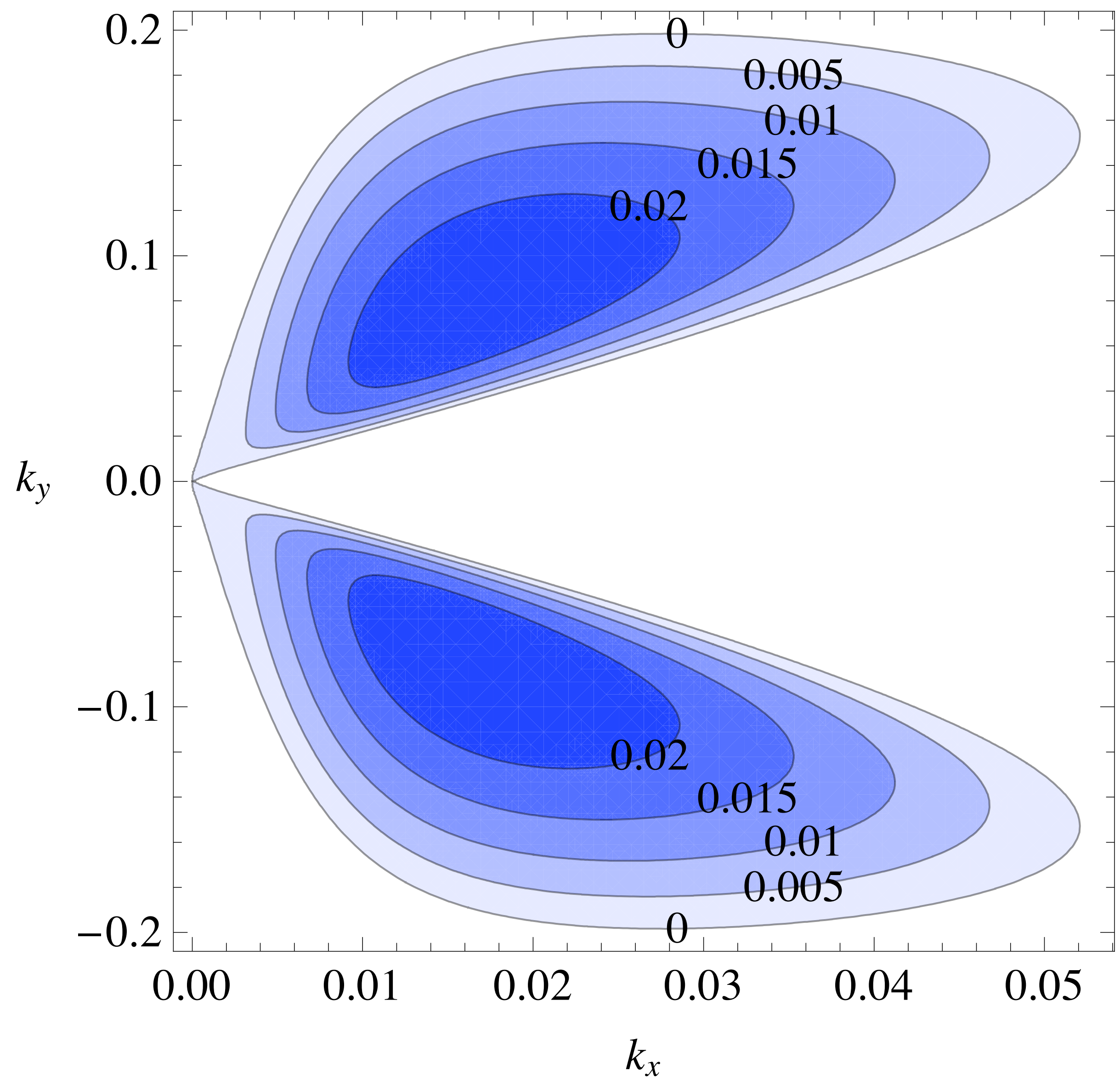

Mussel Curve

Linear Stability

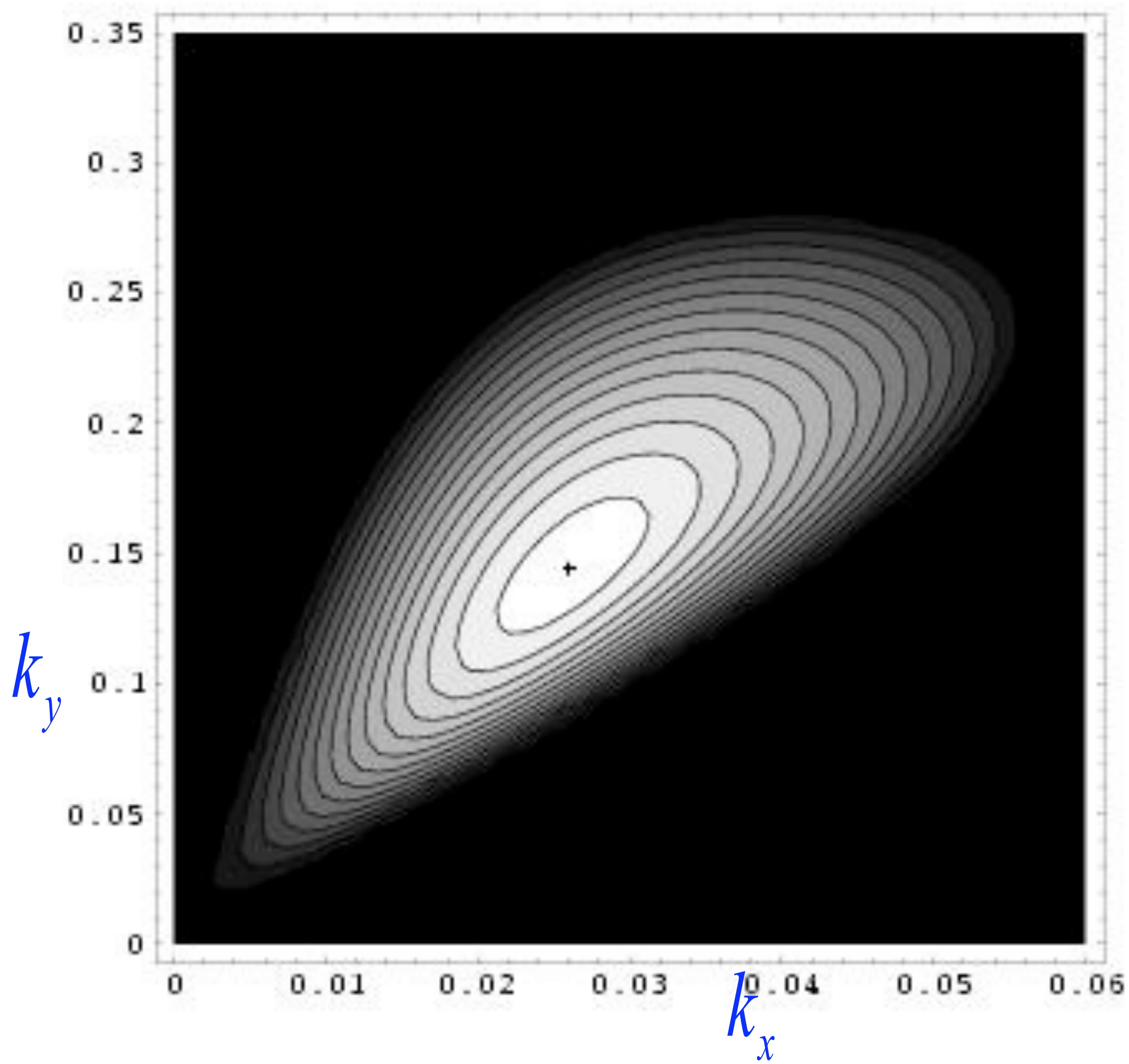

2 D Instability :
inclindes bancs

No 1D instability (k_y=0):

$F = 1,5 \quad \varphi = 3°$

$\beta = 3,75 \quad \gamma = 1$

Linear Stability

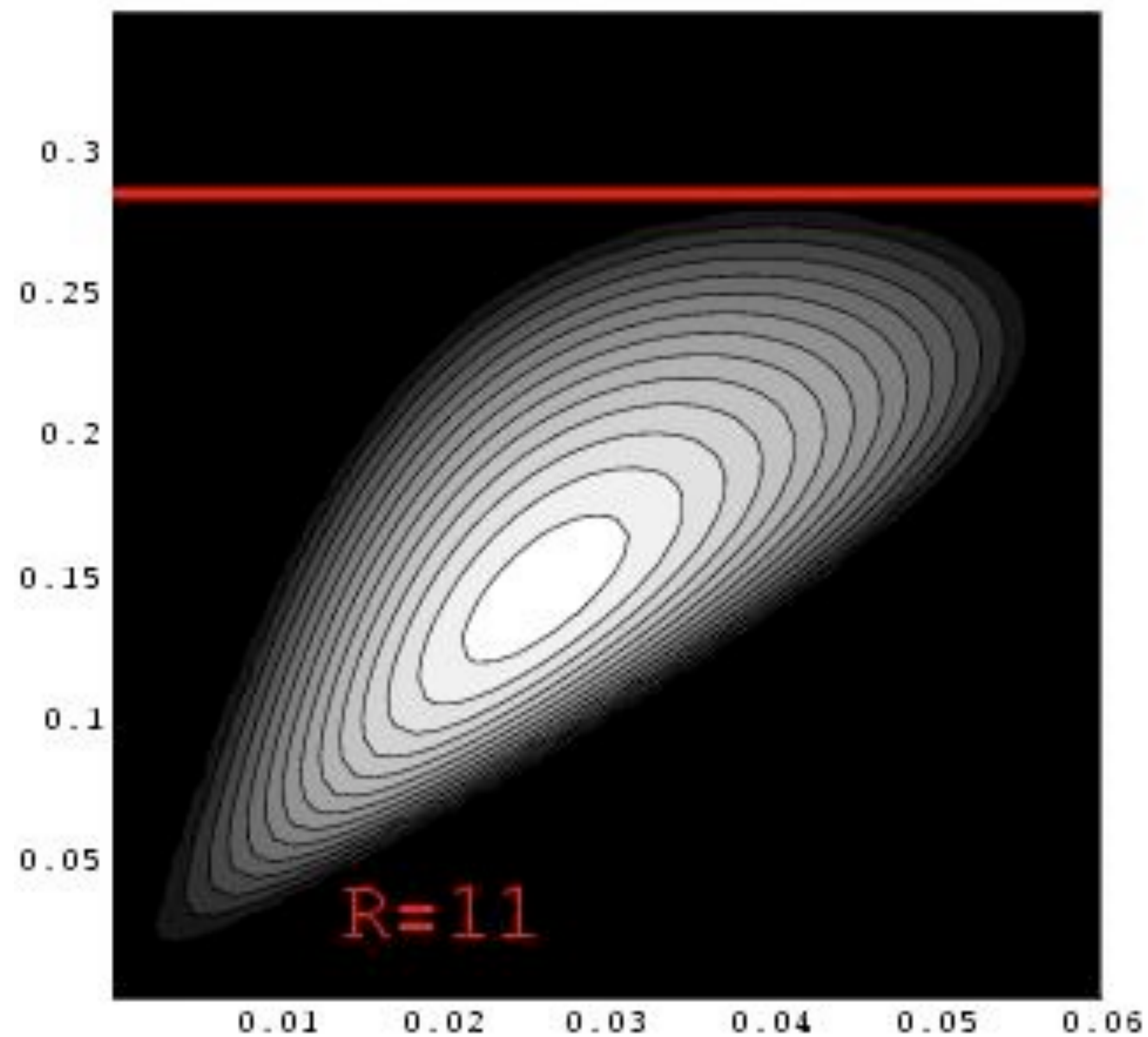

width of the river R promotes the modes

$$F = 1{,}5 \quad \varphi = 3°$$

$$\beta = 3{,}75 \quad \gamma = 1$$

Linear Stability

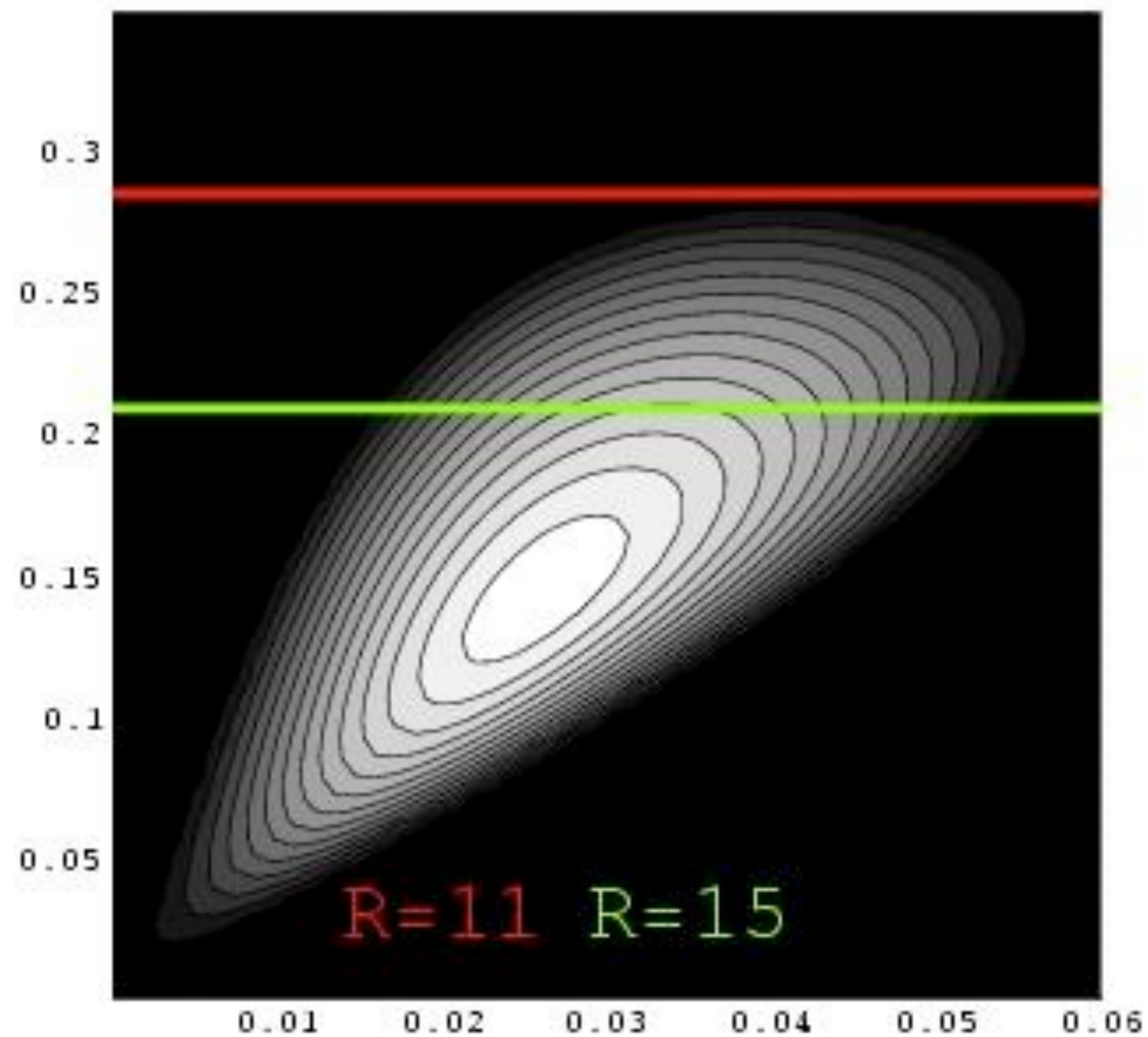

width of the river R promotes the modes

$$F = 1,5 \quad \varphi = 3°$$

$$\beta = 3,75 \quad \gamma = 1$$

Linear Stability

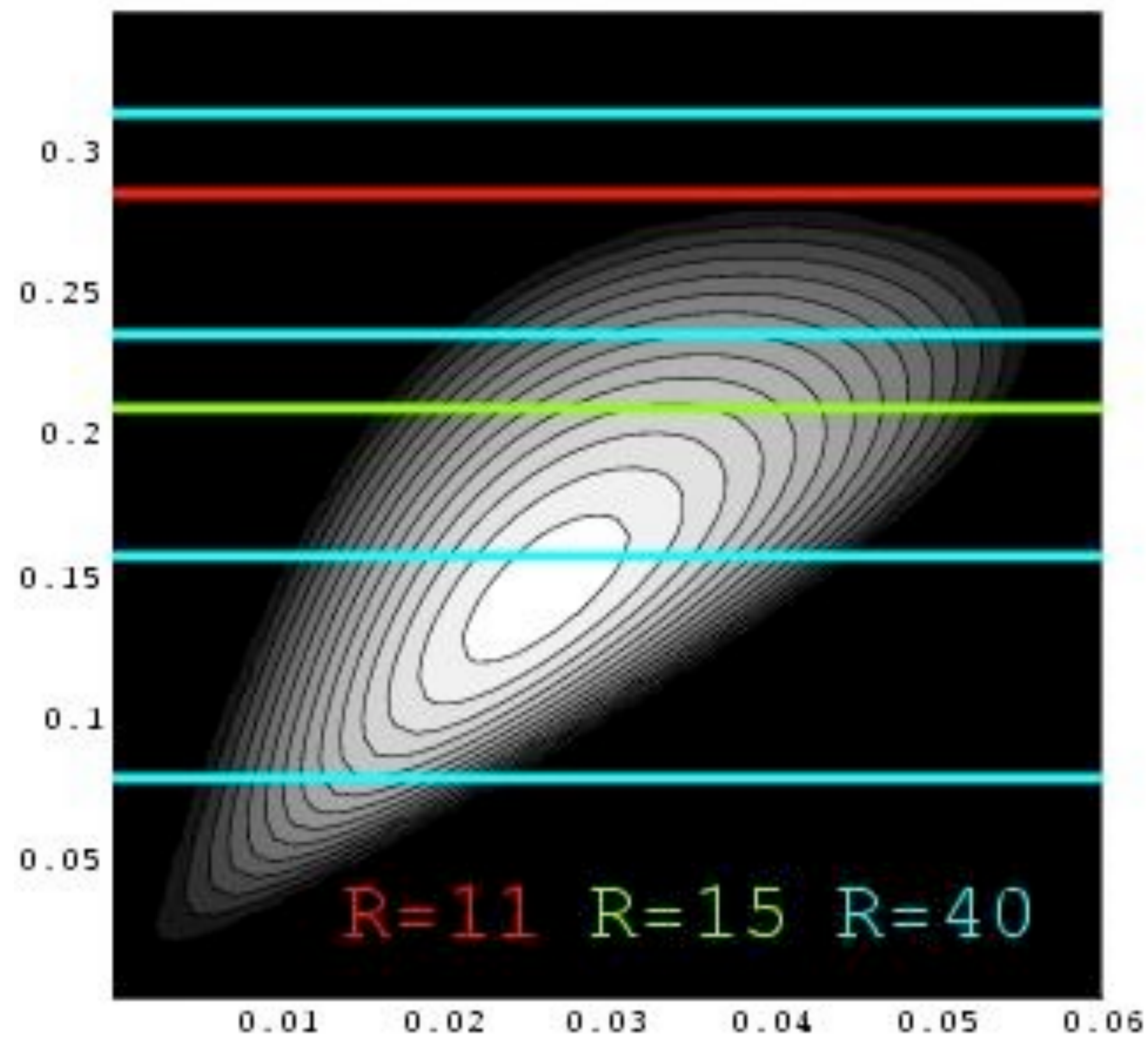

$$F = 1,5 \quad \varphi = 3°$$

width of the river R promotes the modes

$$\beta = 3,75 \quad \gamma = 1$$

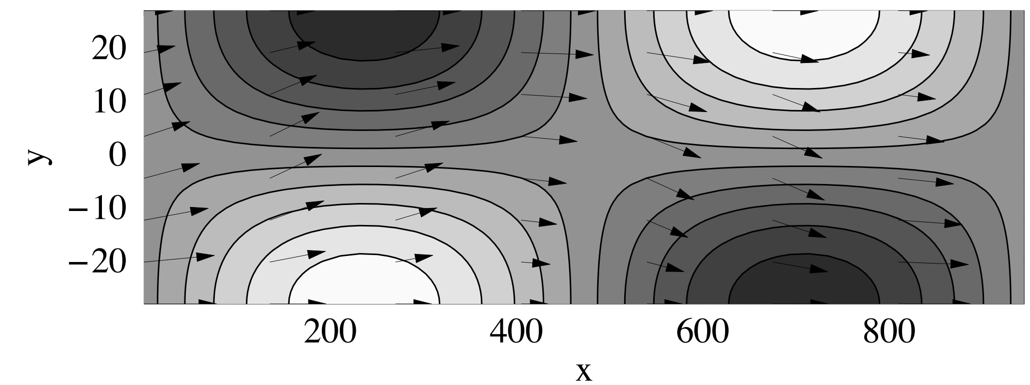

y
x

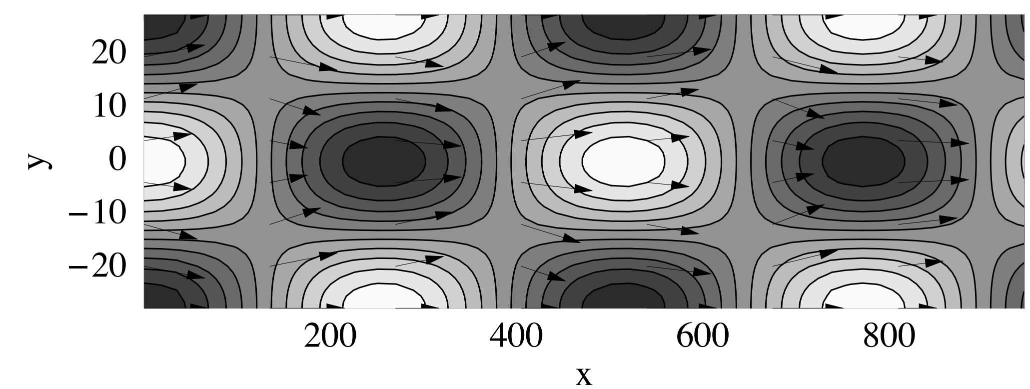

y
x

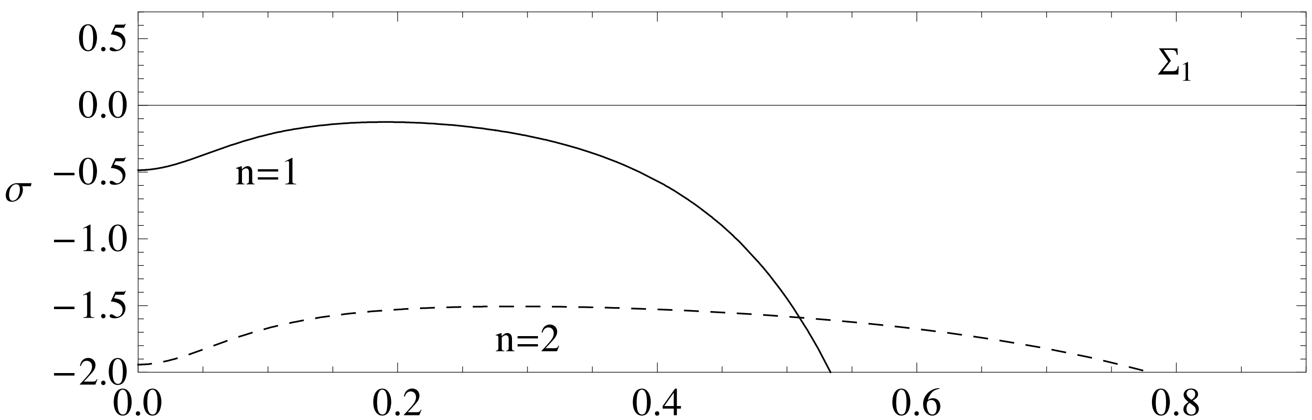

Σ_1
n=1
n=2
σ

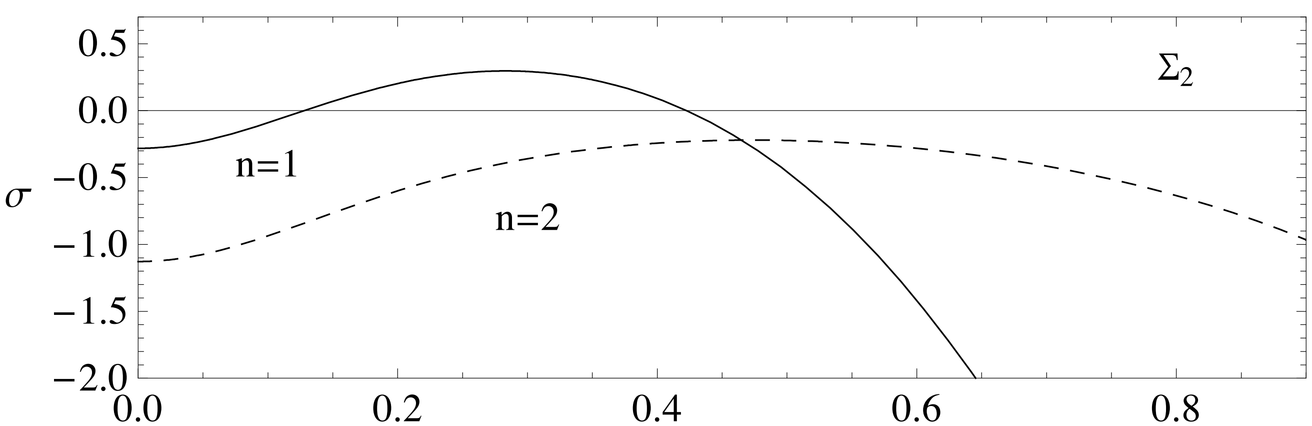

Σ_2
n=1
n=2
σ

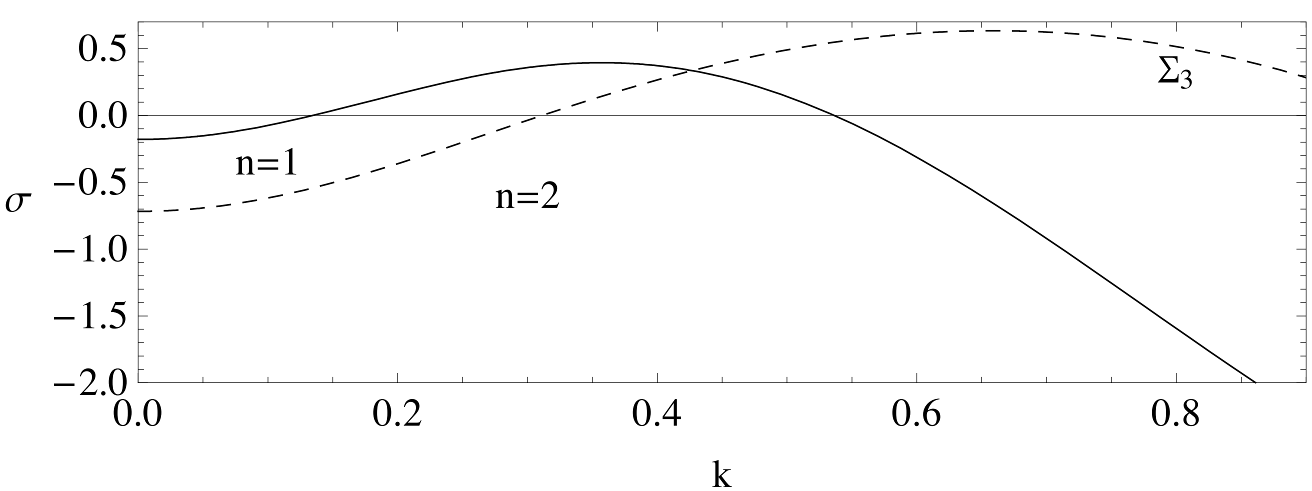

Σ_3
n=1
n=2
σ
k

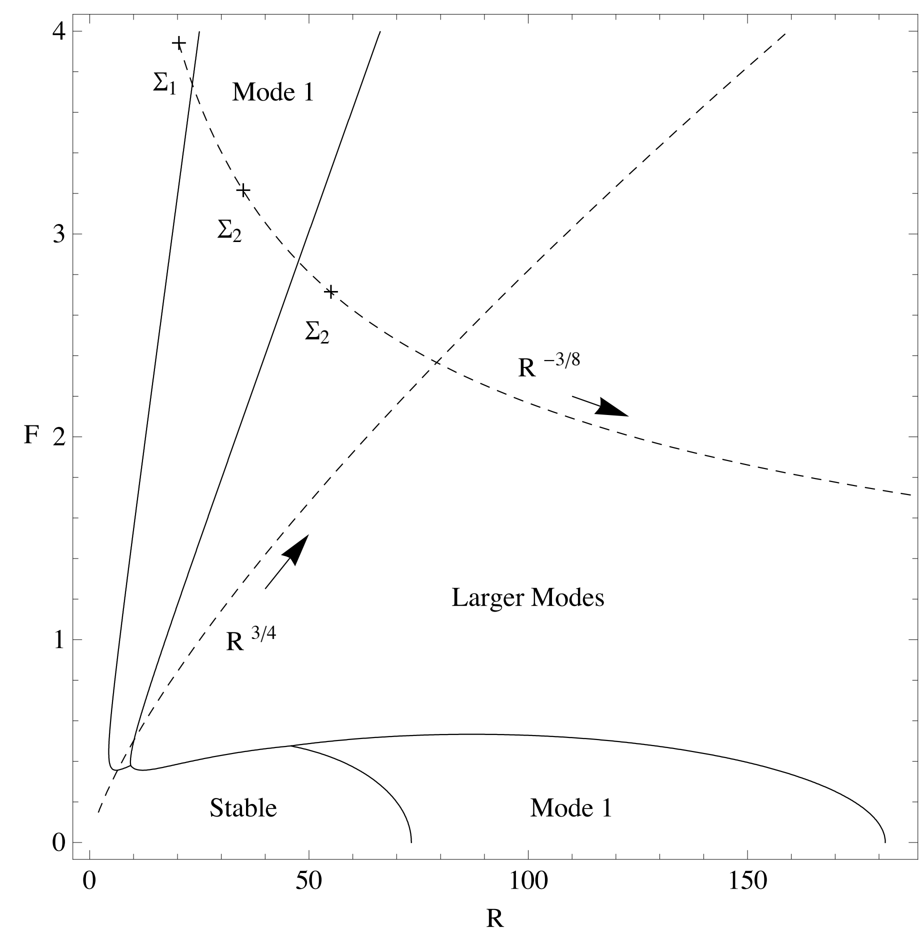

Σ_1
Mode 1
Σ_2
Σ_2
$R^{-3/8}$
F
$R^{3/4}$
Larger Modes
Stable
Mode 1
R

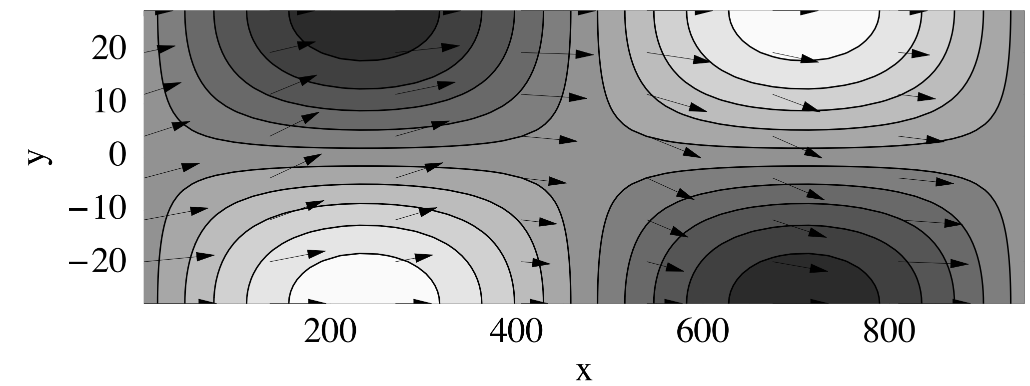

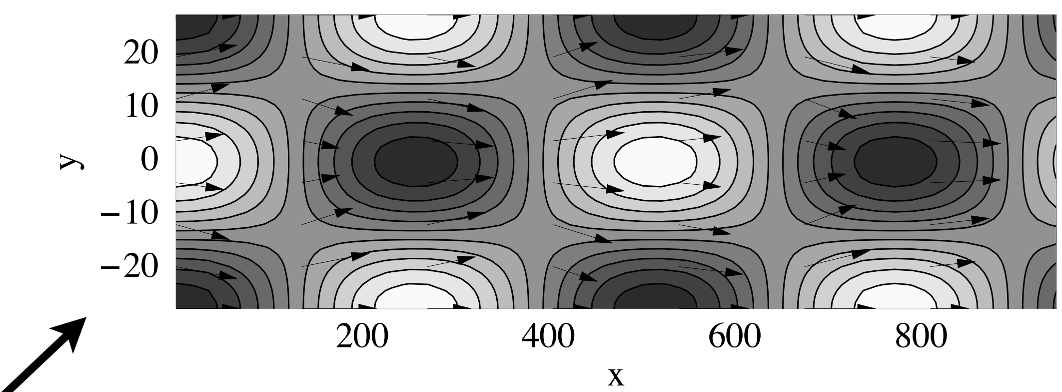

meander

braided river

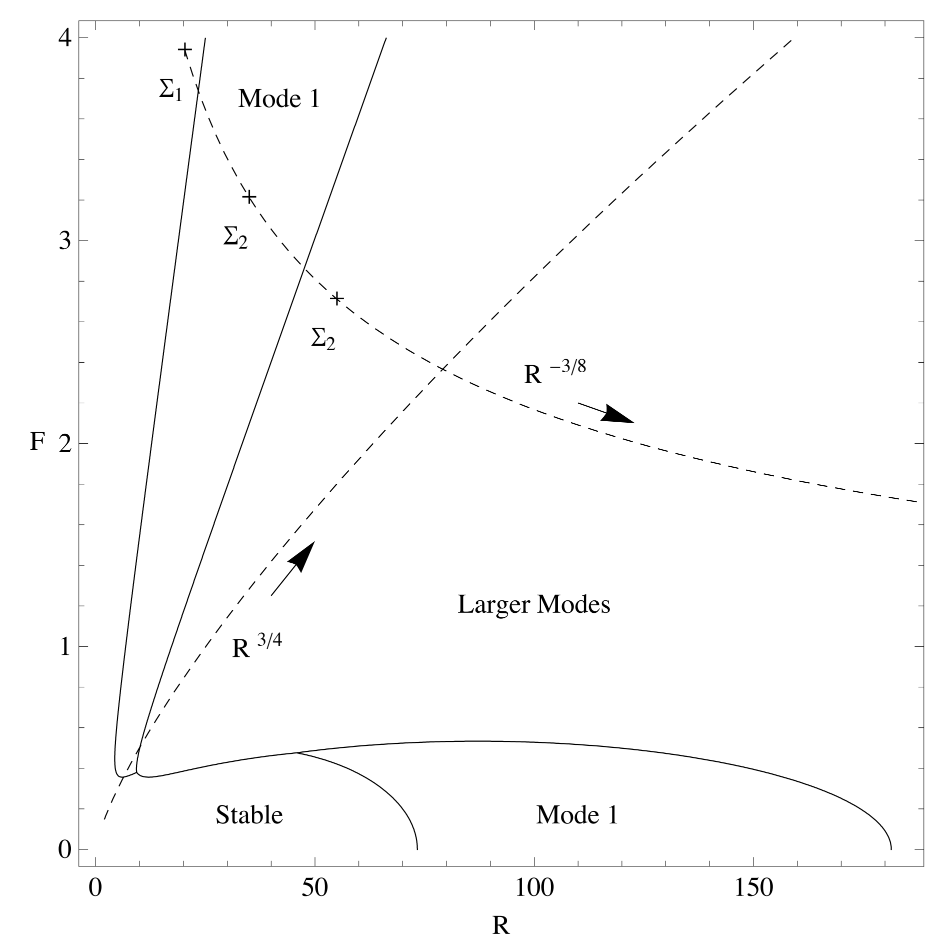

- Saint Venant + erosion gives alternate bars
- now we look at the evolution of those bars

small film of water

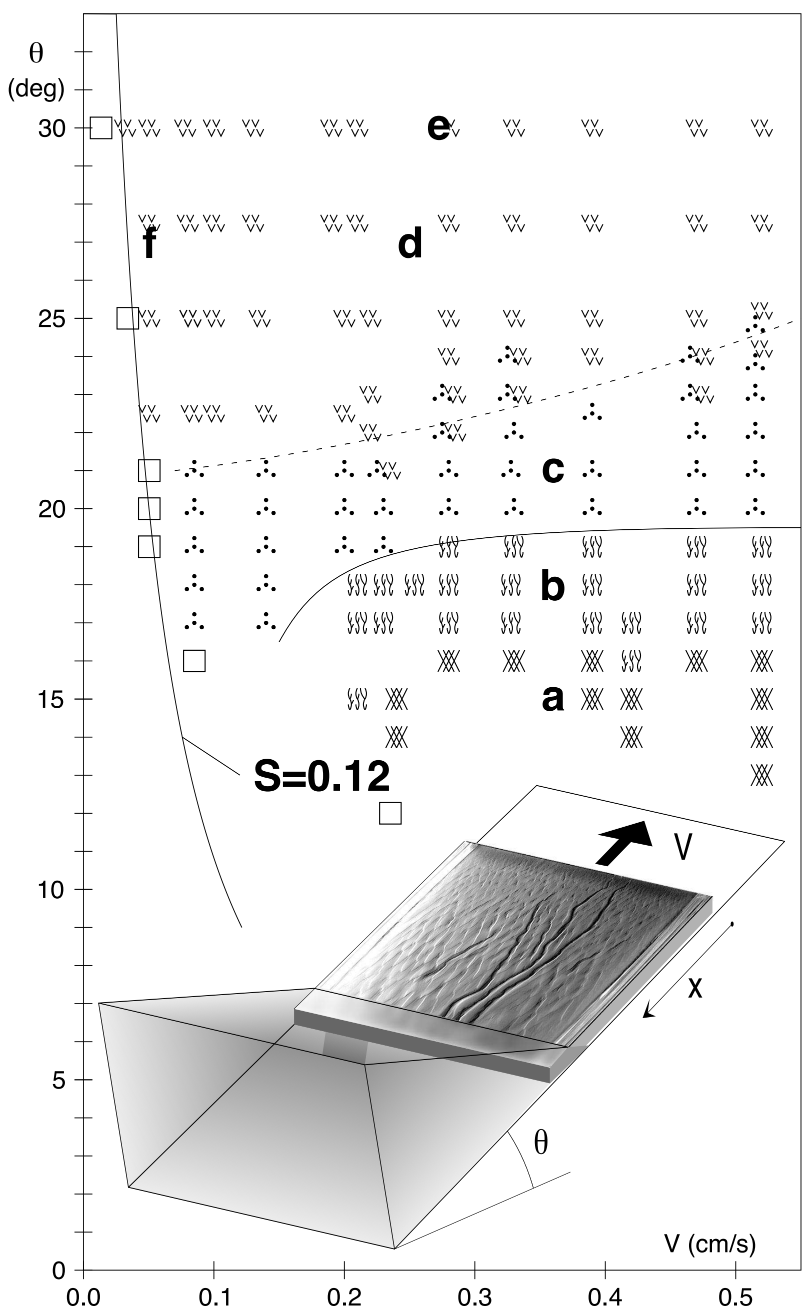

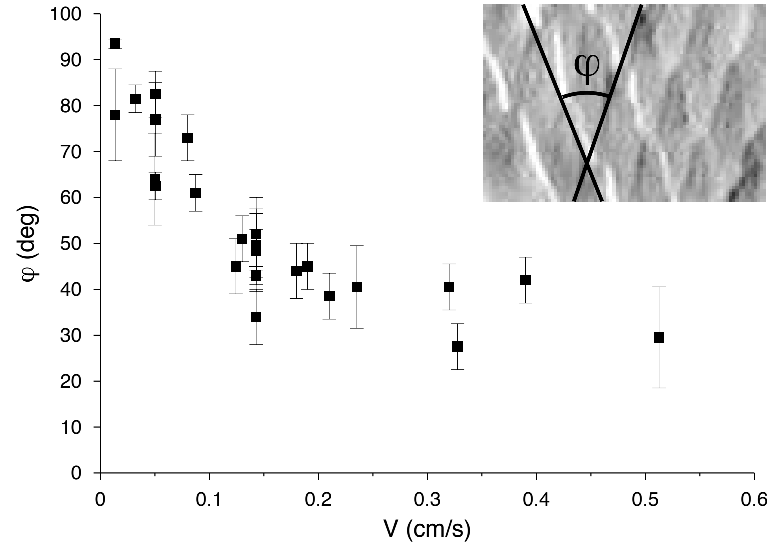

FIG. 3: Chevron alignment angle as a function of velocity. Error bars indicate measurement variations

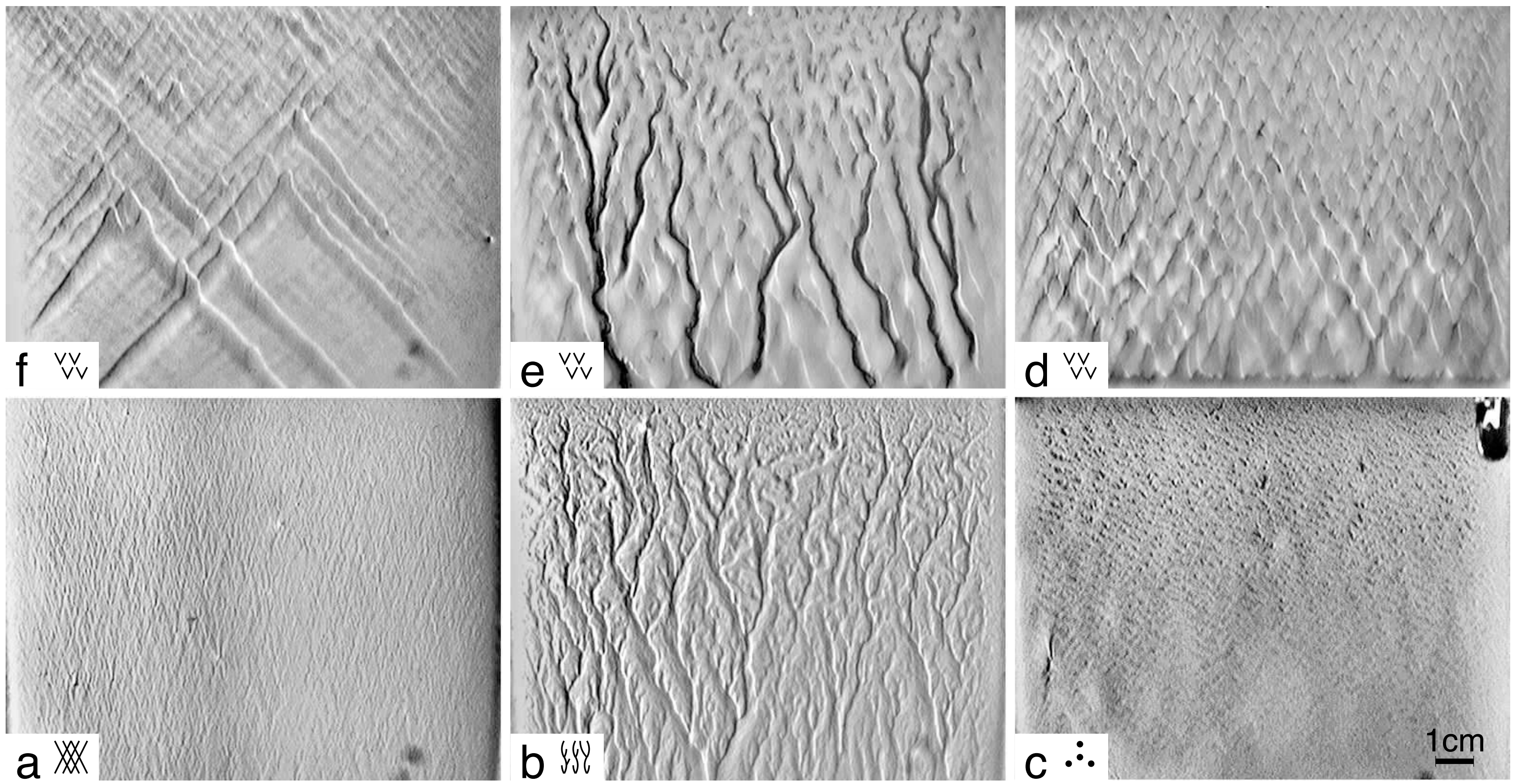

FIG. 2: Patterns observed in the erosion experiment: **a** crossed hatched pattern, **b** disordered branched pattern, **c** orange skin, **d** chevron structure, **e** chevrons with oblique channels, **f** localized pulses at chevron onset. The layer appears darker where it has been eroded because the bottom plate is black. A light source to the left creates additional shading.

Daerr, A., Lee, P., Lanuza, J. & Clement, E. 2003 Erosion patterns in a sediment layer. Physical Review E 67.

small film of water

small film of water

RHOMBOID RIPPLE MARK.

A. O. WOODFORD.

Bucher (p. 153, 1919) has proposed the term "*rhomboid (current-) ripple*" for "*small rhomboidal, scale-like tongues of sand*, arranged in a reticular pattern" produced experimentally by Engels (1905) as the first effect of transportation by a water current in gentle, uniform flow. But violent currents in water also impress rhomboidal patterns on sand, and hence, in this paper, the term *rhomboid ripple mark* will be used in a descriptive sense, to include all sharply rhomboid patterns developed on the surface of a mobile sediment. An example is given in Fig. 1. Braided rills which are not sharply and regularly rhomboid in pattern, are not included. Neither are the numerous V-shaped grooves which spread from the snouts of partly buried sand crabs (Hippidae, *Emerita analoga* in California), and which may in combination suggest an irregularly rhombic pattern.

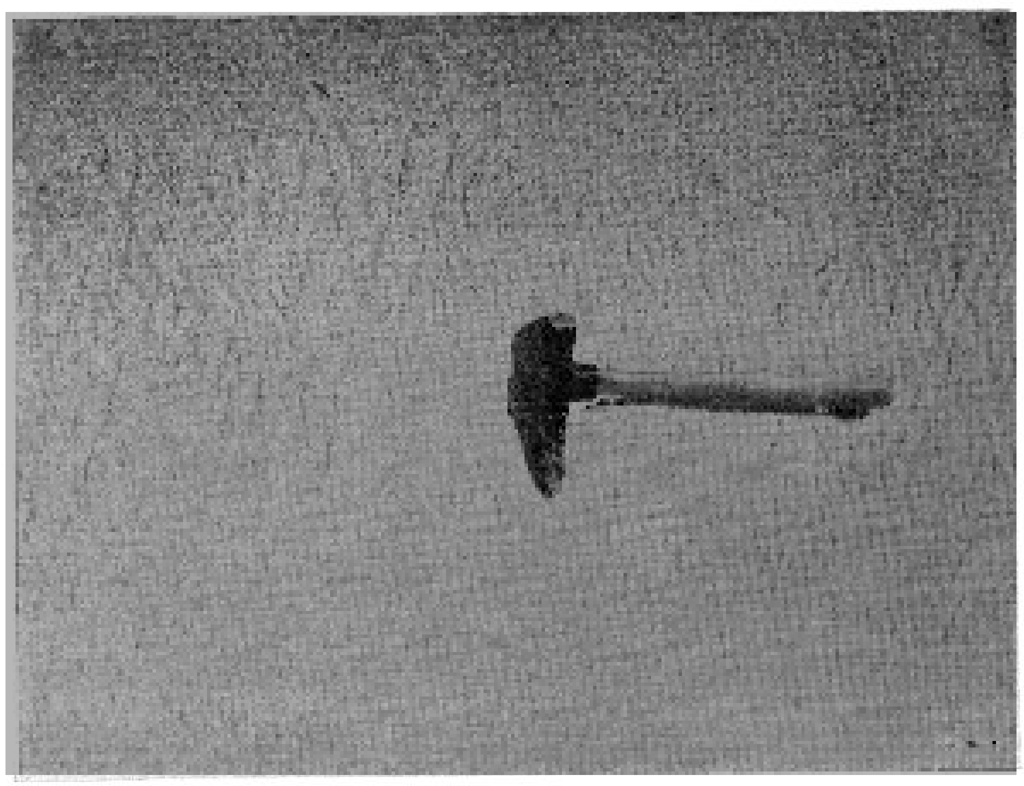

Fig. 1. Rhomboid ripple mark, Laguna Beach, Calif., March 29, 1933. The hammer gives the scale.

Several authors (Kindle: p. 34 and pl. 19b, 1917; Johnson: pp. 515-517, 1919; Kindle and Bucher: pp. 655, 656, 1932) describe and figure rhomboid ripple marks from modern beaches. In 1917 Kindle ascribed the imbricated pattern to, "The action of very small waves lapping and crossing each other from opposite sides of a miniature spit," but in 1932 Kindle and Bucher were inclined to explain the pattern in the light of the Engels' experiment mentioned above. Johnson calls the structures "backwash marks," and says (p. 517, 1919): "The thin sheet of water returning down the beach slope appeared to be split into diverging minor currents by every patch of more compact sand or particle of coarser material which impeded its progress, and the crossing of these minor currents resulted in the criss-cross pattern in the sand."

INTERFERENCE PATTERN UNDER RAPID FLOW.

The rhomboid pattern formed on sand looks very much like an interference effect. Therefore, before describing the

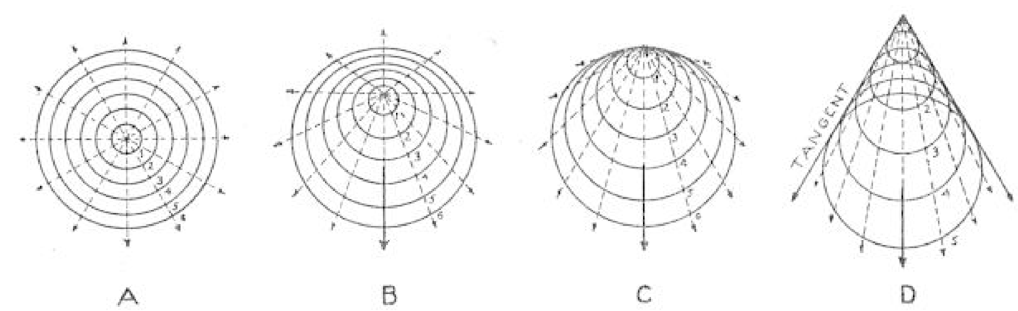

Fig. 2. Schematic sketches showing wave impulses spreading from a point, affected by various rates of flow. See text for explanation. After Rehbock.

observed pattern in detail, there will be presented some generalities concerning the waves which may form in water currents.

First of all, the distinction must be made between *tranquil flow* and *rapid flow* (Rehbock: 1930; Bakhmeteff: 1932). In tranquil flow, the average velocity of the water is less than the wave velocity for the given depth; in rapid flow it is greater. The effect on waves is shown in Fig. 2, after Rehbock. If a pebble is tossed into quiet water, concentric waves are produced (A). If the water is in tranquil flow, the ripples are distorted (B). If a certain critical velocity is equaled or exceeded, the waves cannot be propagated upstream, but only down (C and D). In D there is suggested a cause for the


gutter
sidewalk

Chang Simons JFM 70

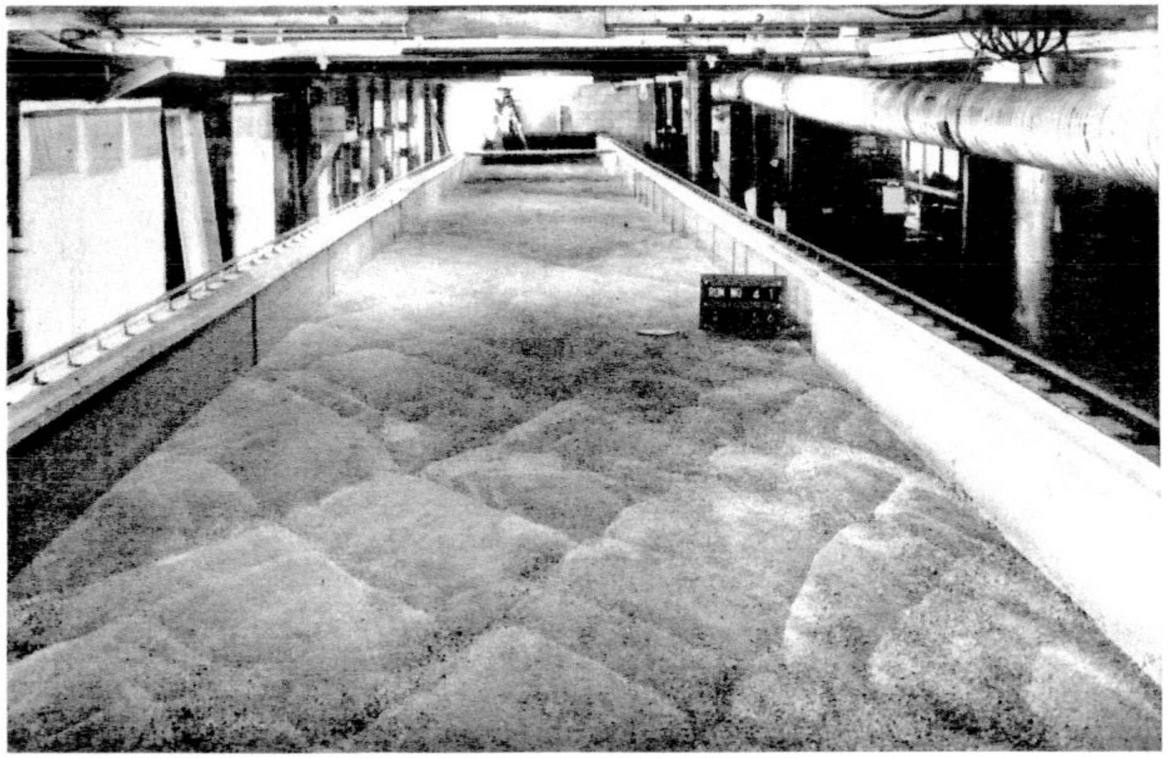

(c)

FIGURE 2. Diagonal bed patterns in a laboratory flume with large width to depth ratios and with the flow nearly critical. (a) Froude number = 0·92, width to depth ratio = 24. (b) Froude number = 0·83, width to depth ratio = 28·5. (c) Froude number = 1·12, width to depth ratio = 18.

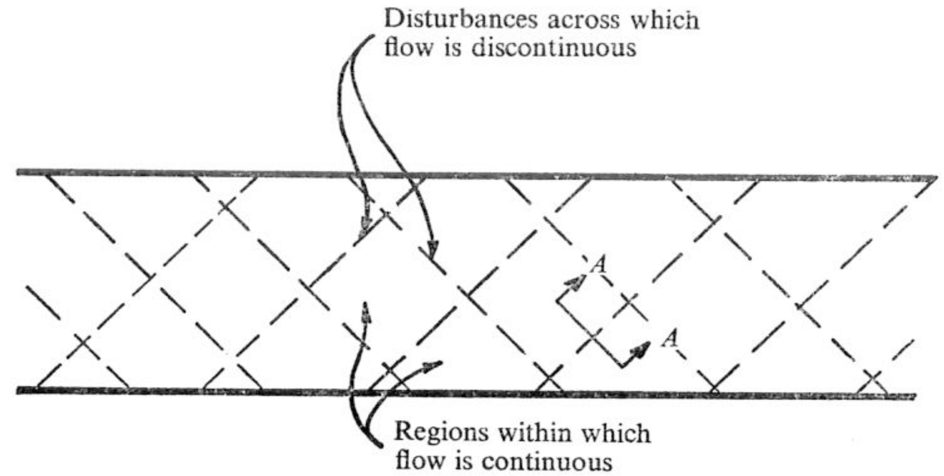

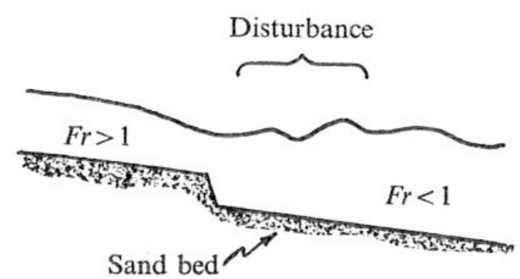

Section A–A

Schematic drawing showing diagonal lines in shallow channel flow with Froude number near unity.

$$N = \begin{vmatrix} U & W & 0 & 0 & g & 0 & 0 & 0 \\ 0 & 0 & U & W & 0 & g & 0 & 0 \\ h & 0 & 0 & h & U & W & 0 & 0 \\ 0 & \dfrac{Wq_1}{U^2} & 0 & -\dfrac{q_1}{U} & 0 & 0 & -1 & -\dfrac{W}{U} \\ dx & dz & 0 & 0 & 0 & 0 & 0 & 0 \\ 0 & 0 & dx & dz & 0 & 0 & 0 & 0 \\ 0 & 0 & 0 & 0 & dx & dz & 0 & 0 \\ 0 & 0 & 0 & 0 & 0 & 0 & dx & dz \end{vmatrix}.$$


IPGP Saint-Maur

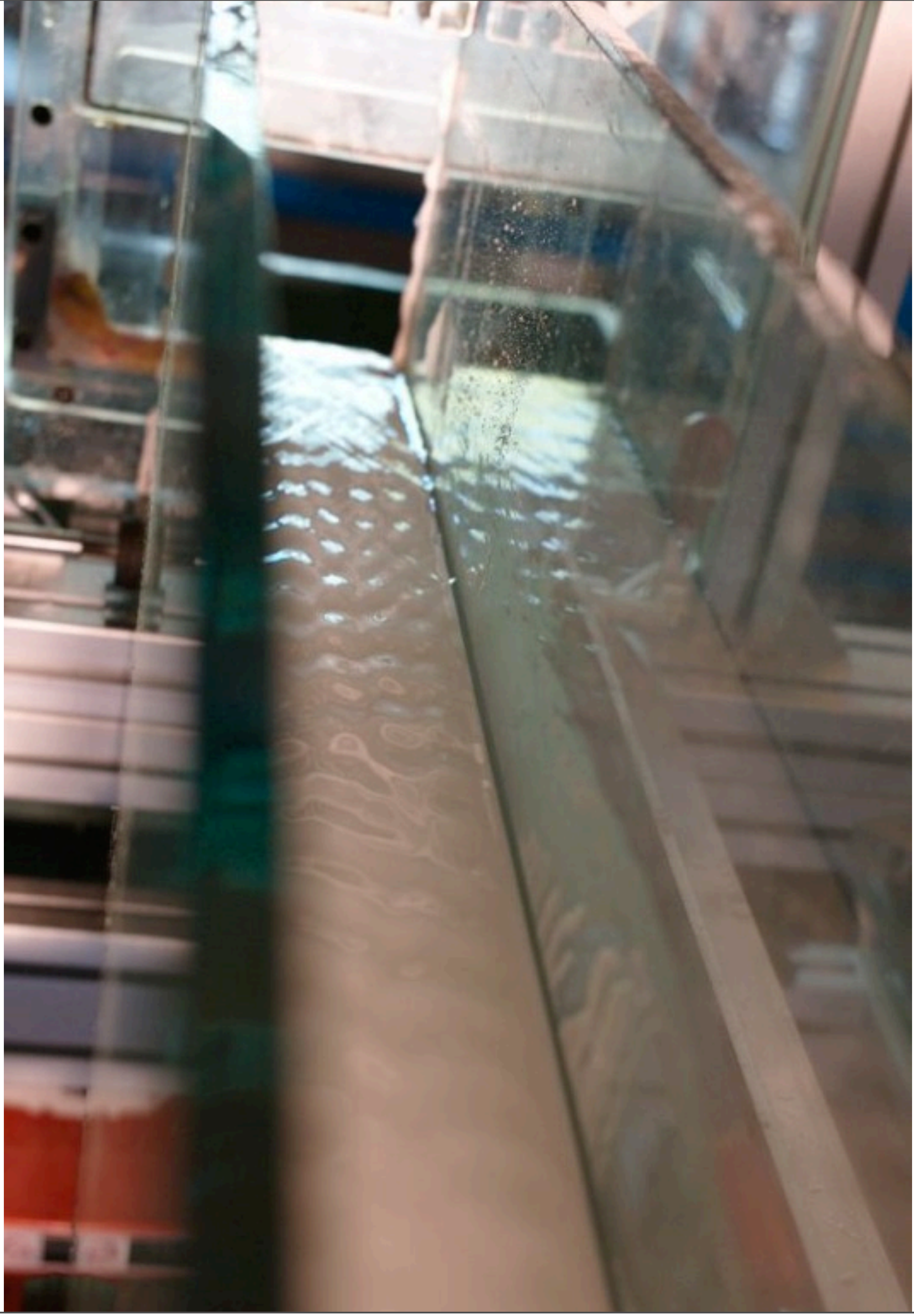

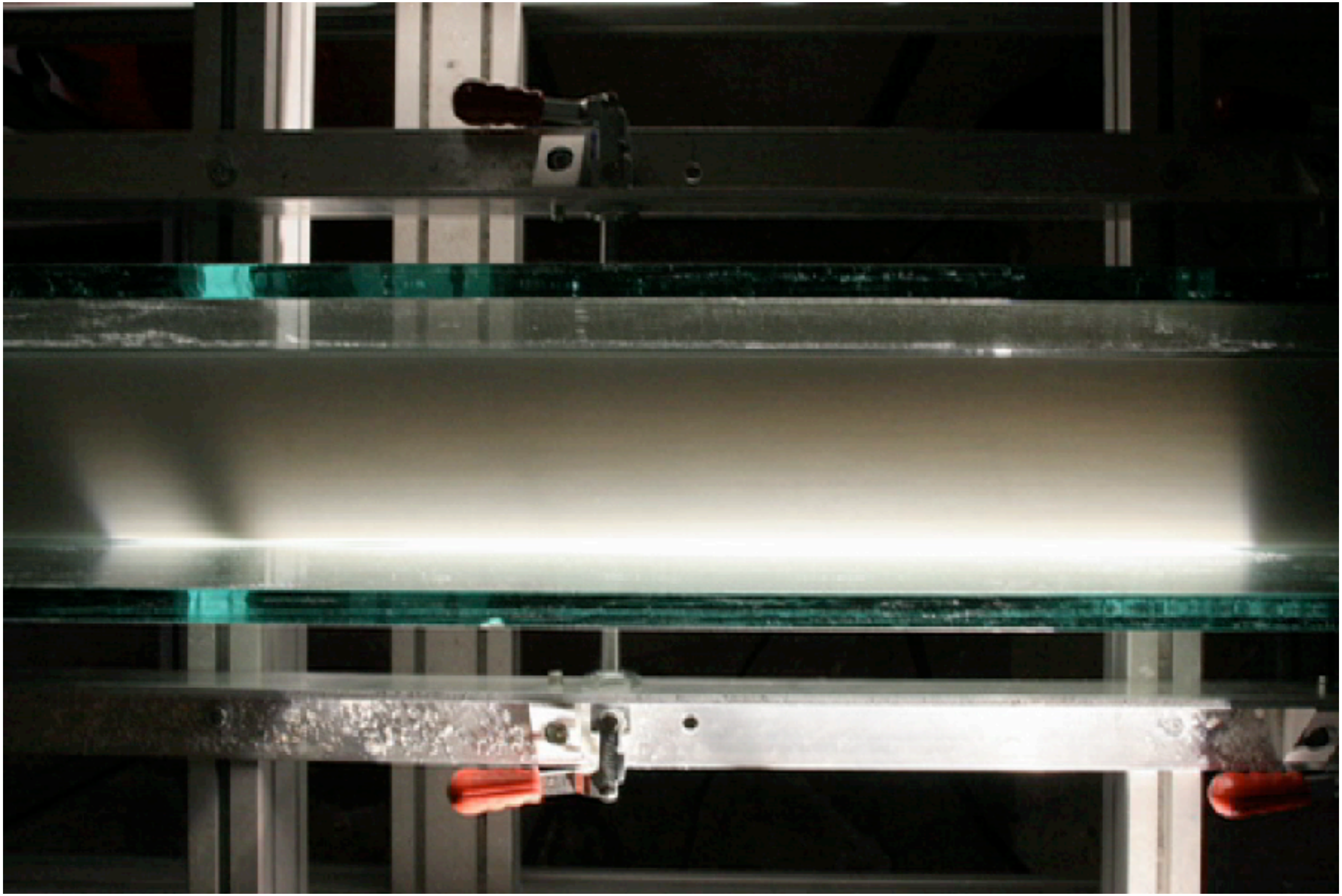

apparition des chevrons (lecture en boucle)

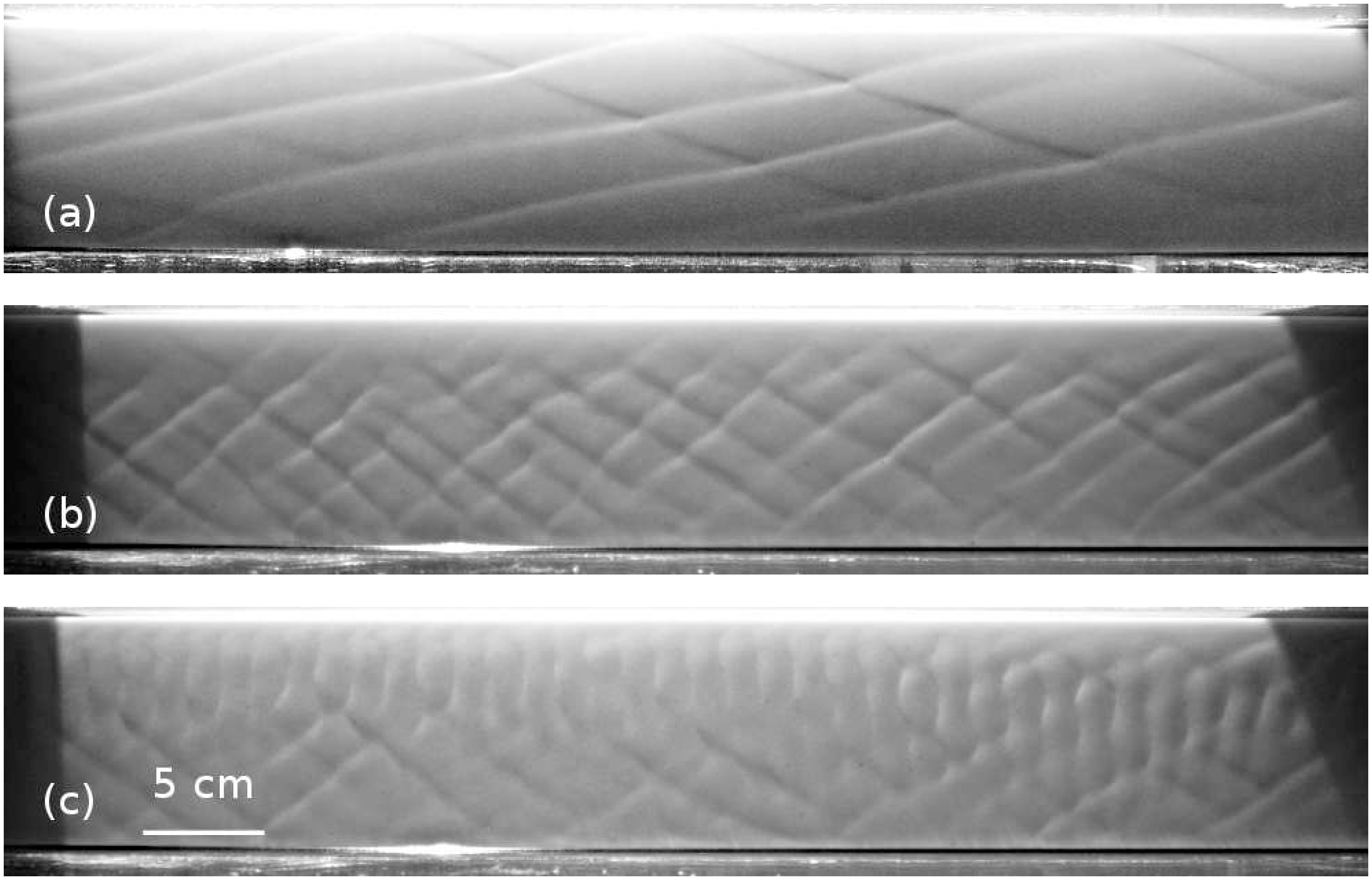
(a)
(b)
(c)
5 cm

evolution of a periodic bed with an initial random noise
it gives inclined waves and rhomboid shape

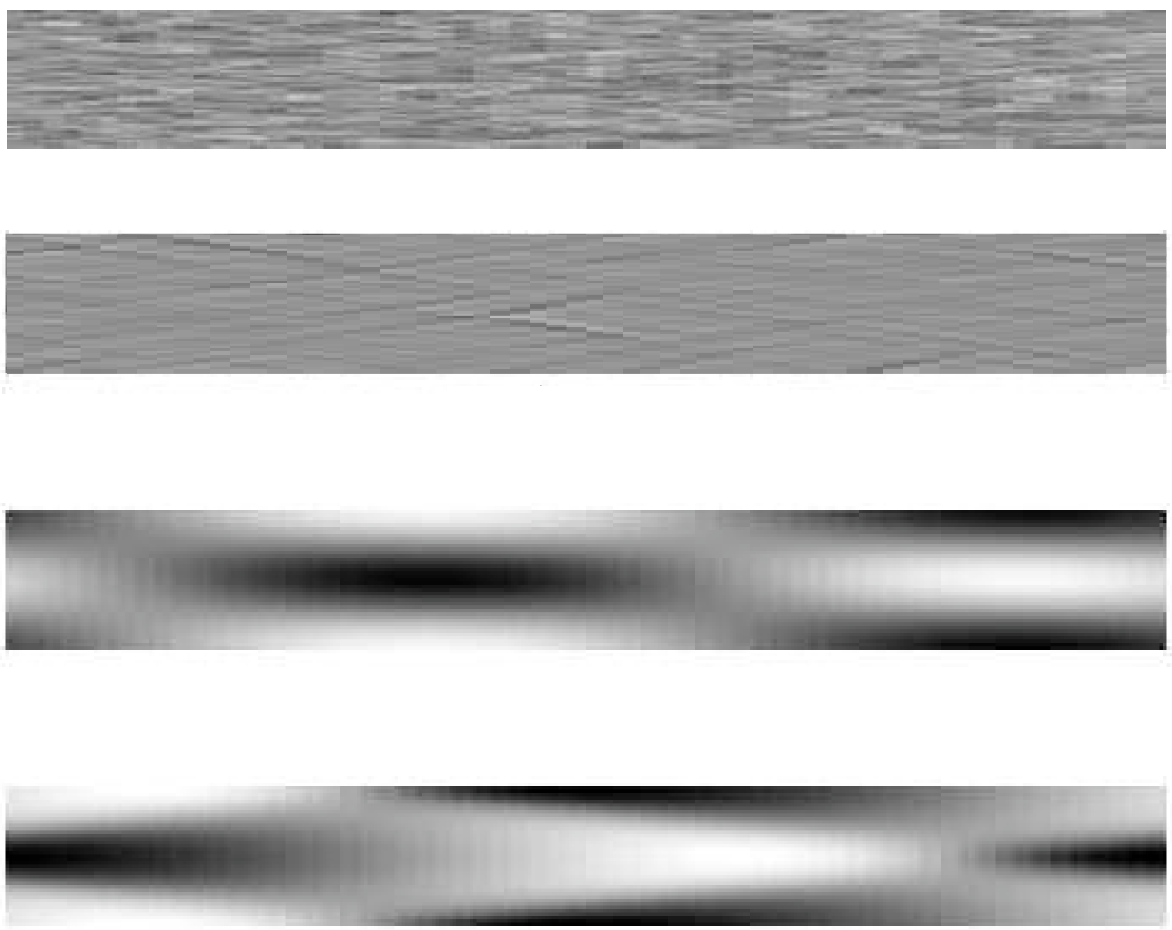

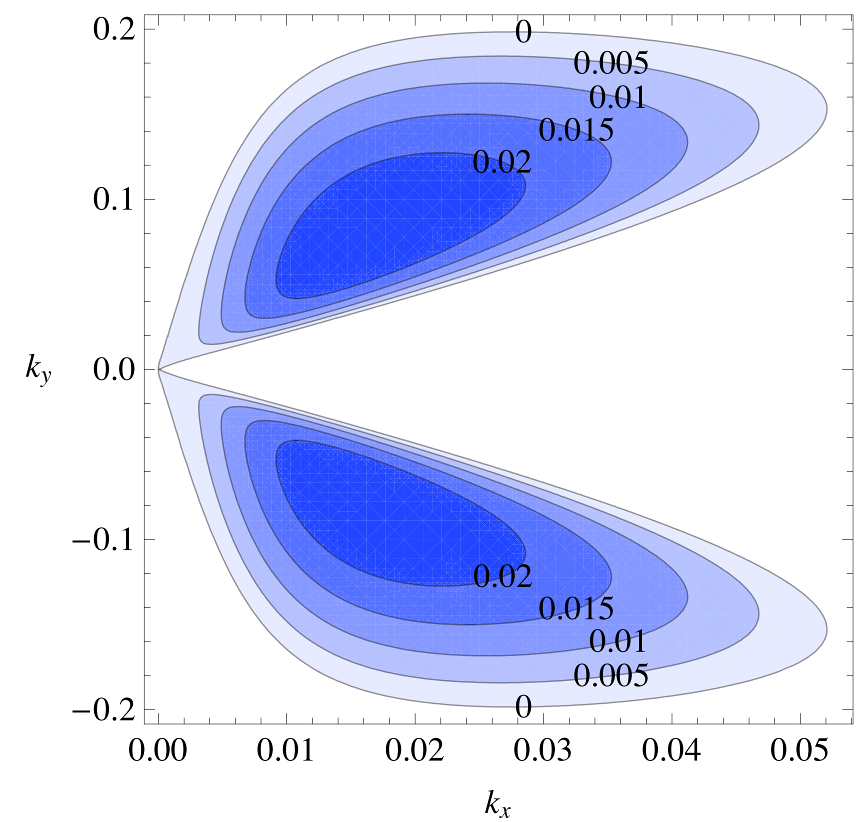

Fourier/ non linearity (θ^{β}), periodicity in x et y

Inclined ripples and diamond pattern

at first

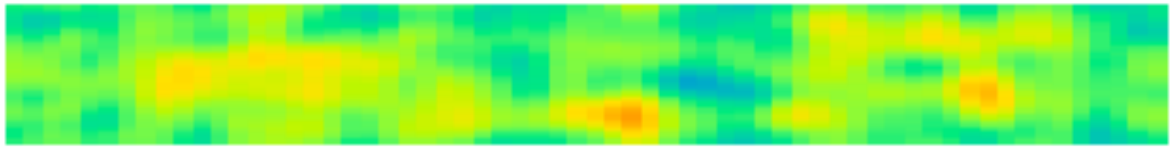

next

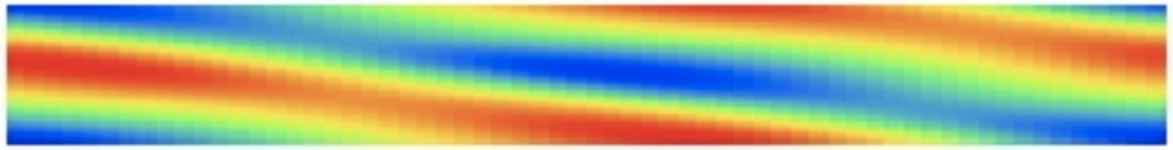

Fourier FFT/ non linearity (θ^{β}), full periodicity

Inclined ripples and diamond pattern

at first

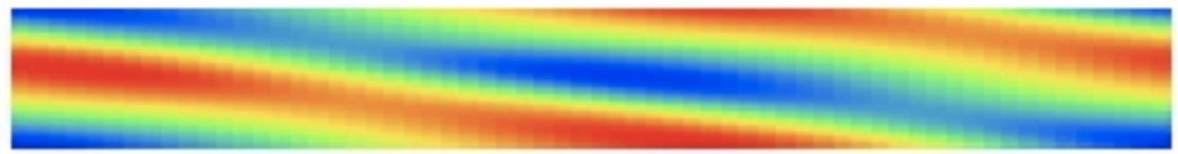

next

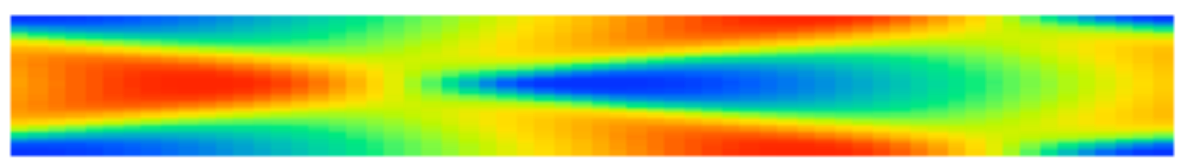

Fourier FFT/ non linearity (θ^{β}), full periodicity

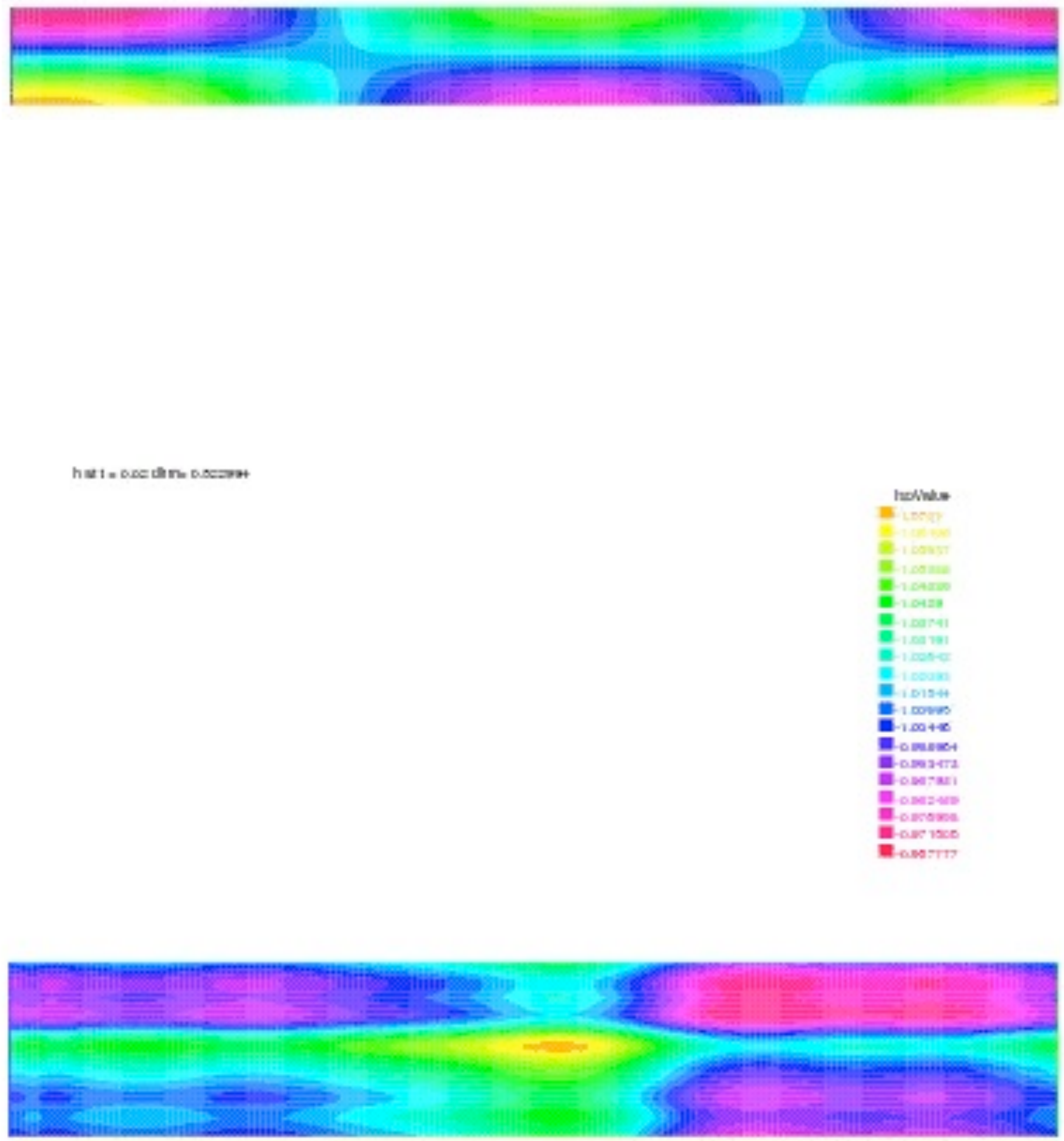

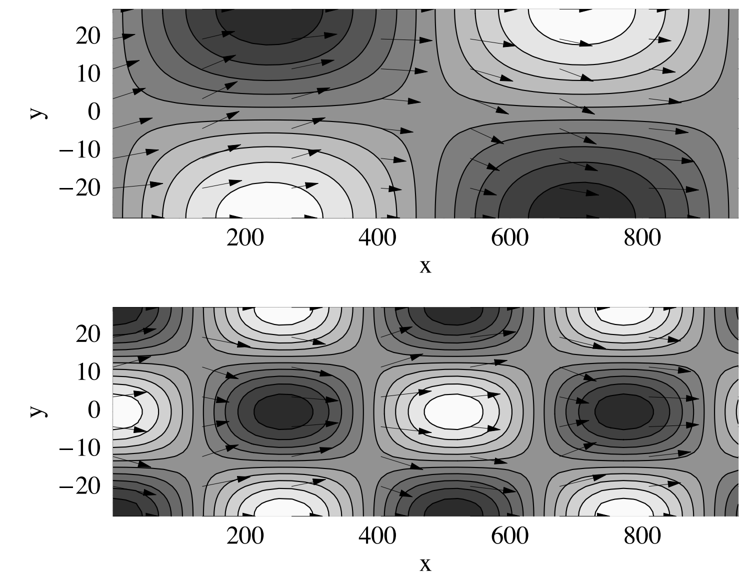

from alternate bars to diamond

FreeFem++

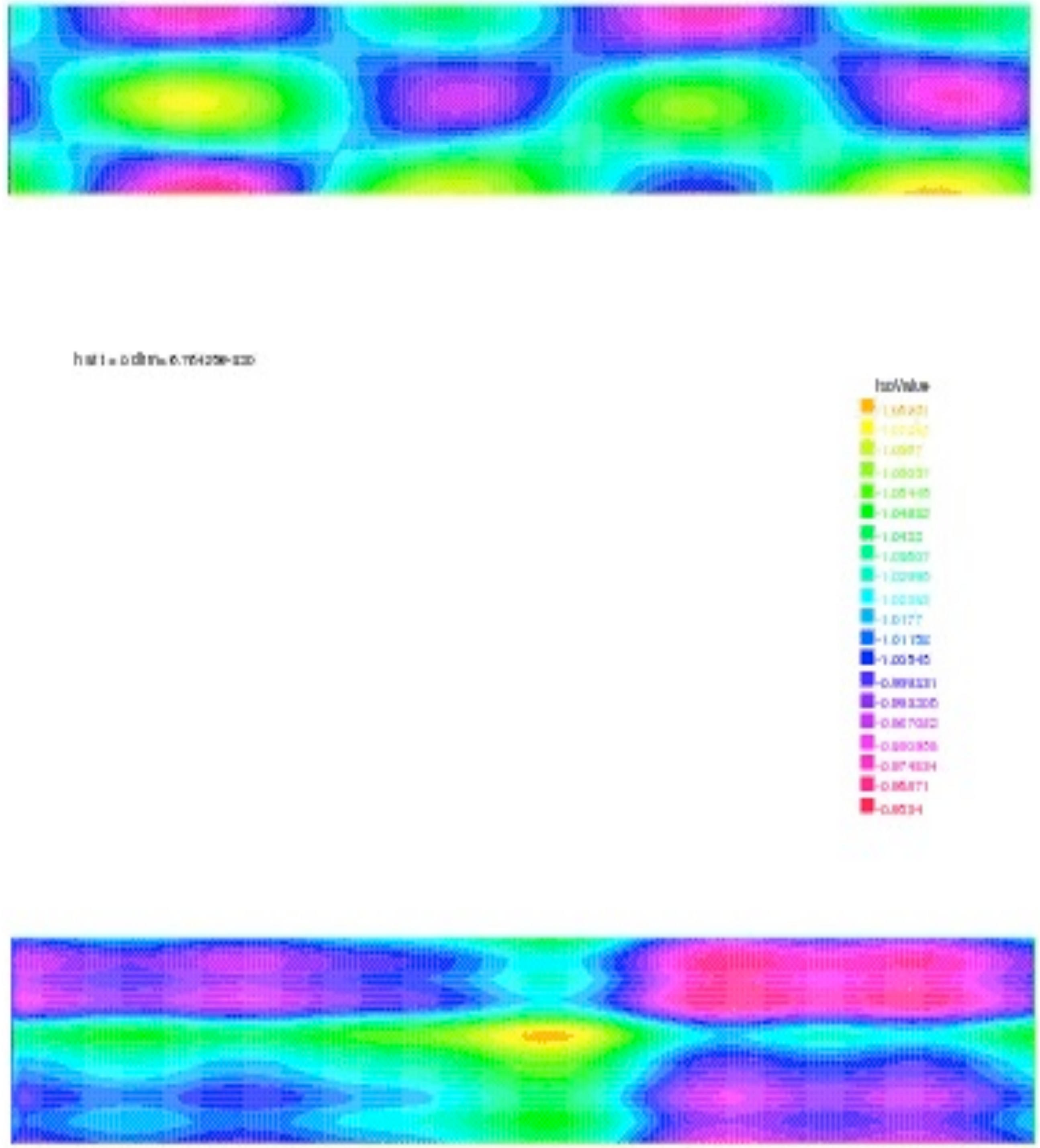

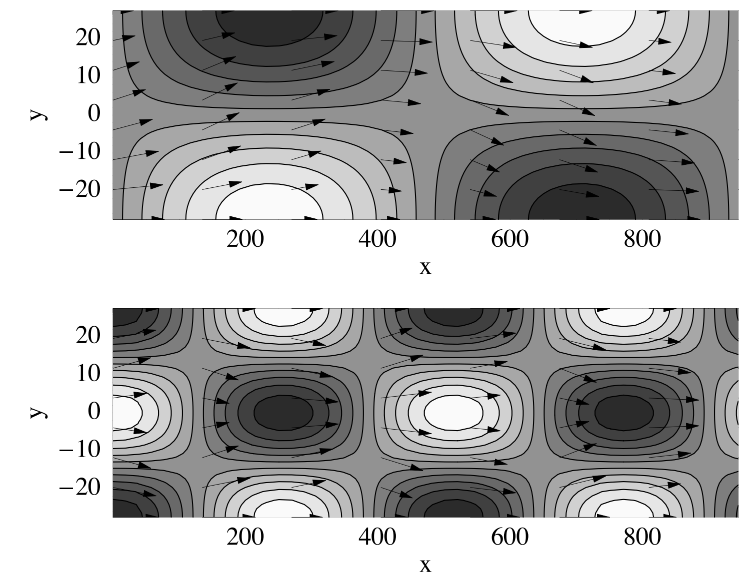

from alternate bars to diamond

FreeFem++

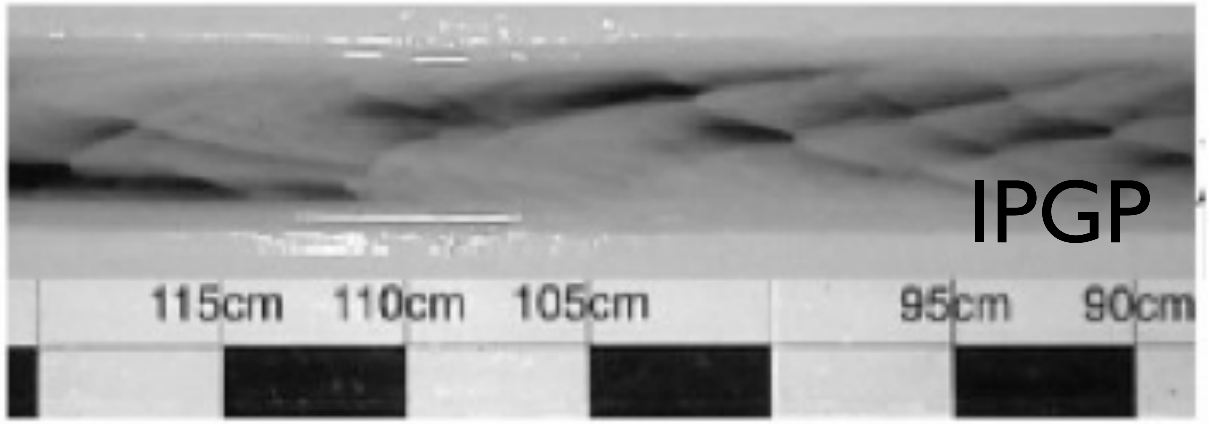

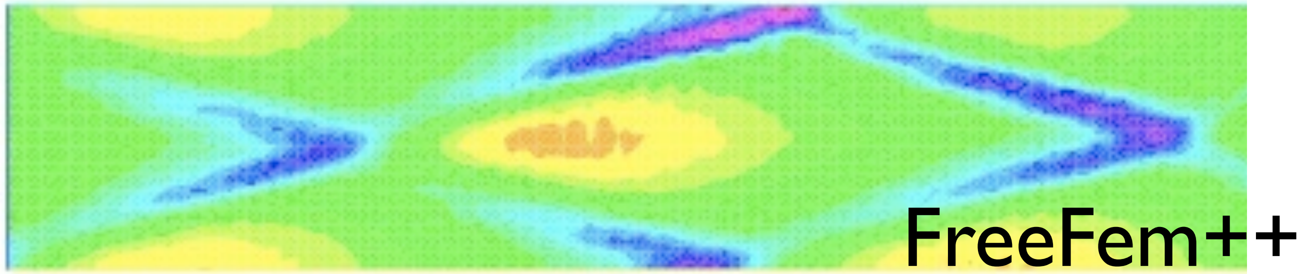

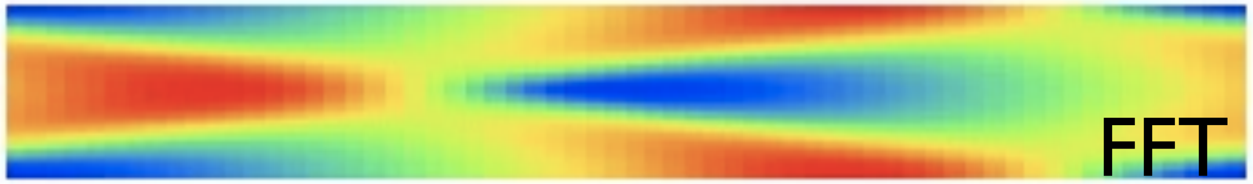

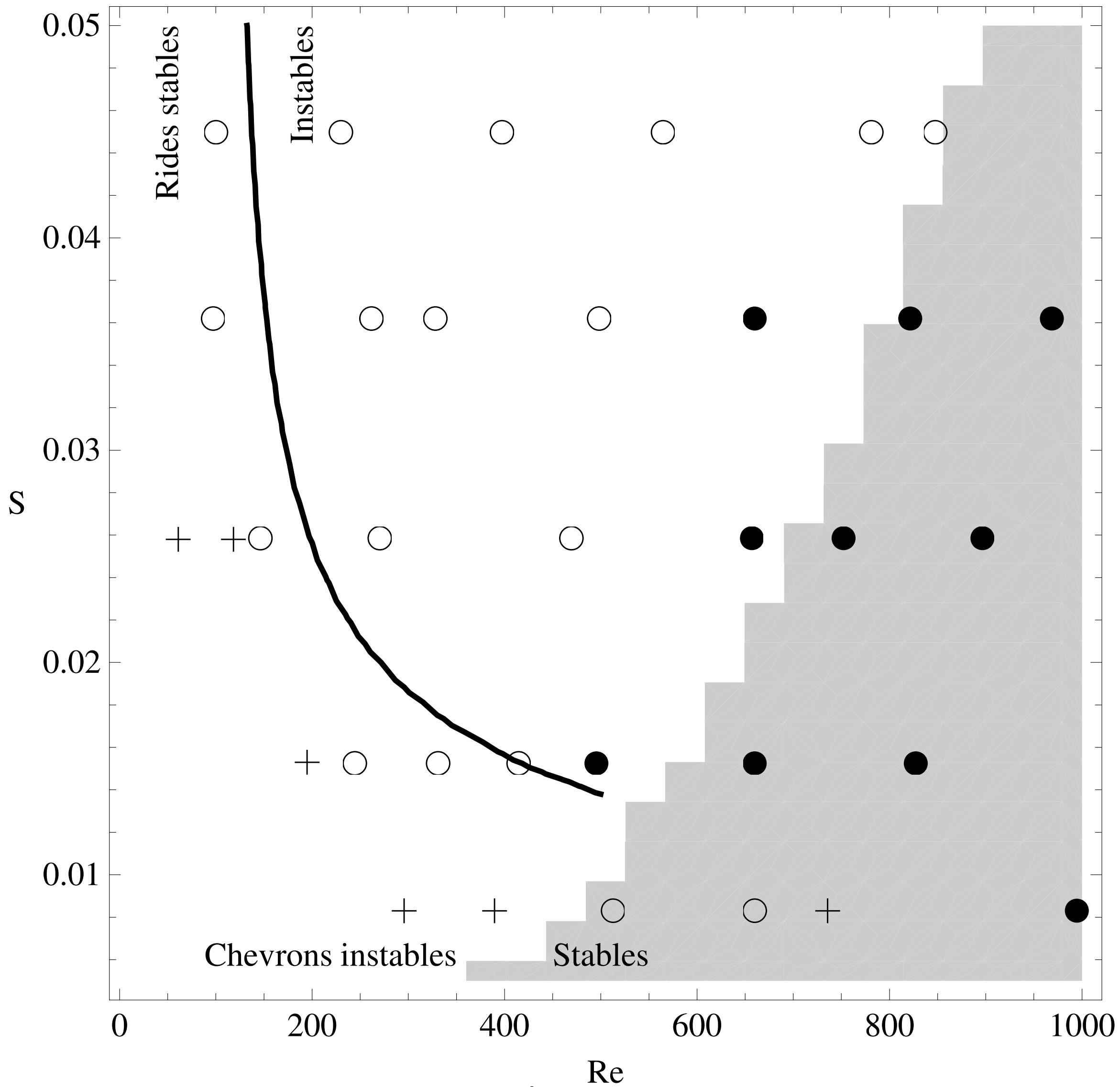

experiments at
Institut de Physique de Globe de Paris

comparisons mesurements vs theory

$$\alpha \approx \arcsin\frac{0.463}{F},$$

$$\alpha = \arcsin\frac{1}{F},$$

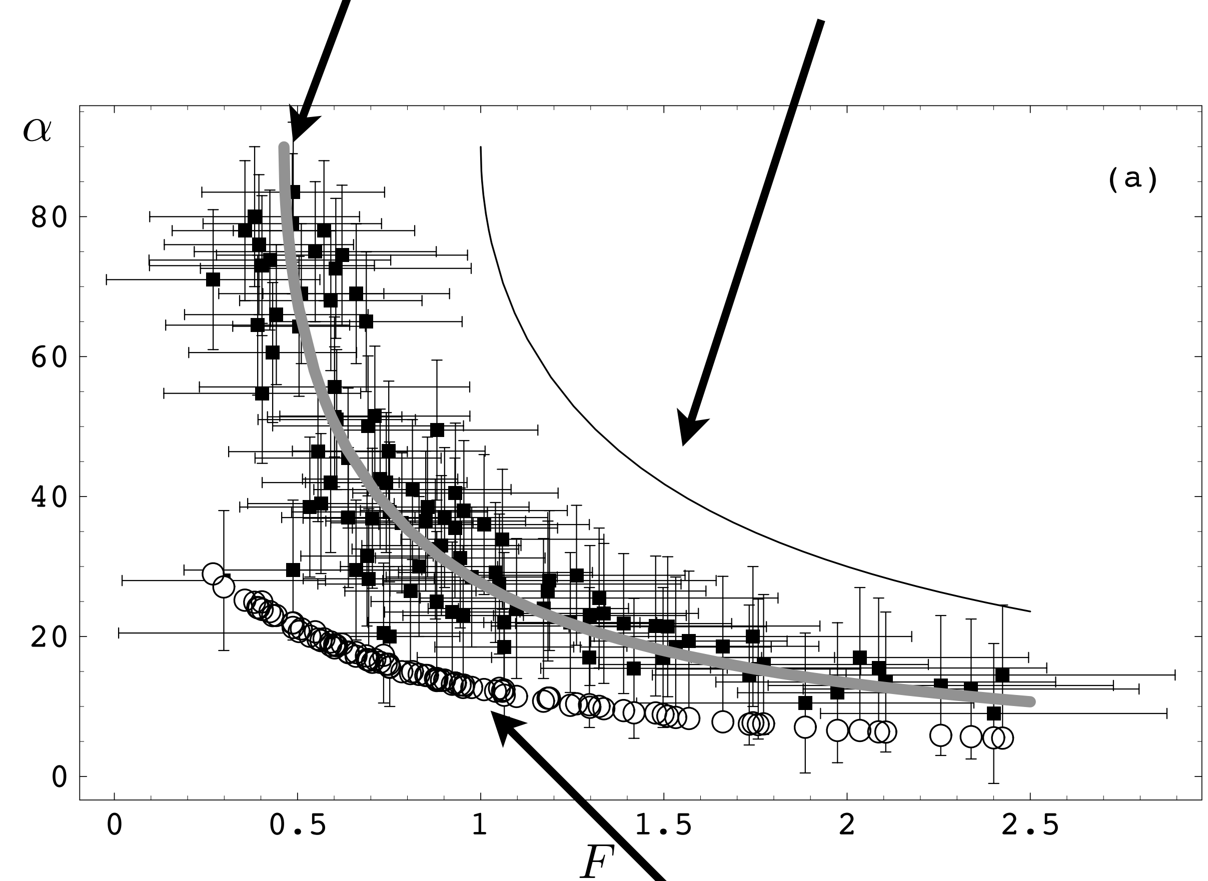

Saint Venant

problems with Saint Venant

up to now only qualitative results: realistic trends but:

Saint Venant is not enough precise for the bars...

Saint Venant is not good for the dunes...

- introduction
- the problem
- the flow: Saint Venant and other
- first granular model
- first coupling: bars
- improved granular model: saturation length
- ripples
- bars & ripples
- conclusions perspectives

Going back to mass conservation

(what goes in) - (what goes out)

Kroy/ Hermann/ Sauermann 02, Lagrée 03, Valance Langlois 05, Charru Hinch 06

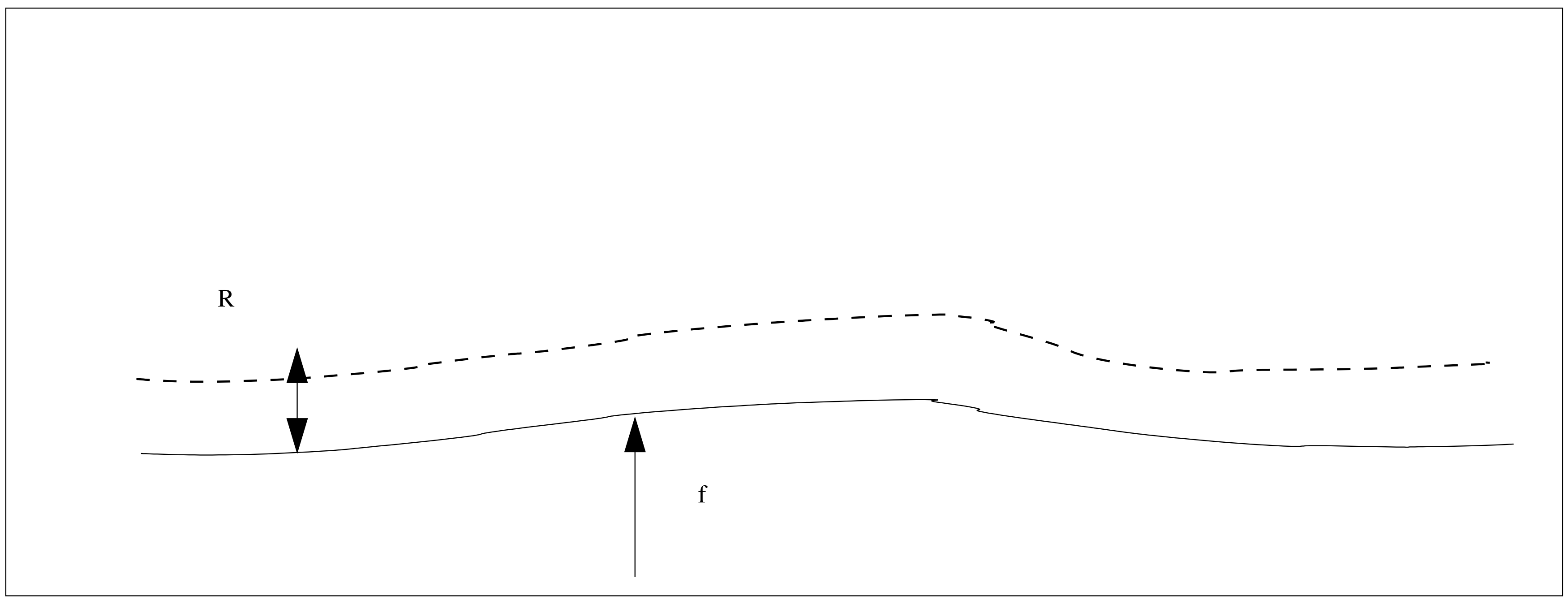

$$\frac{\partial R}{\partial t} = ...$$

$$\frac{\partial f}{\partial t} = ...$$

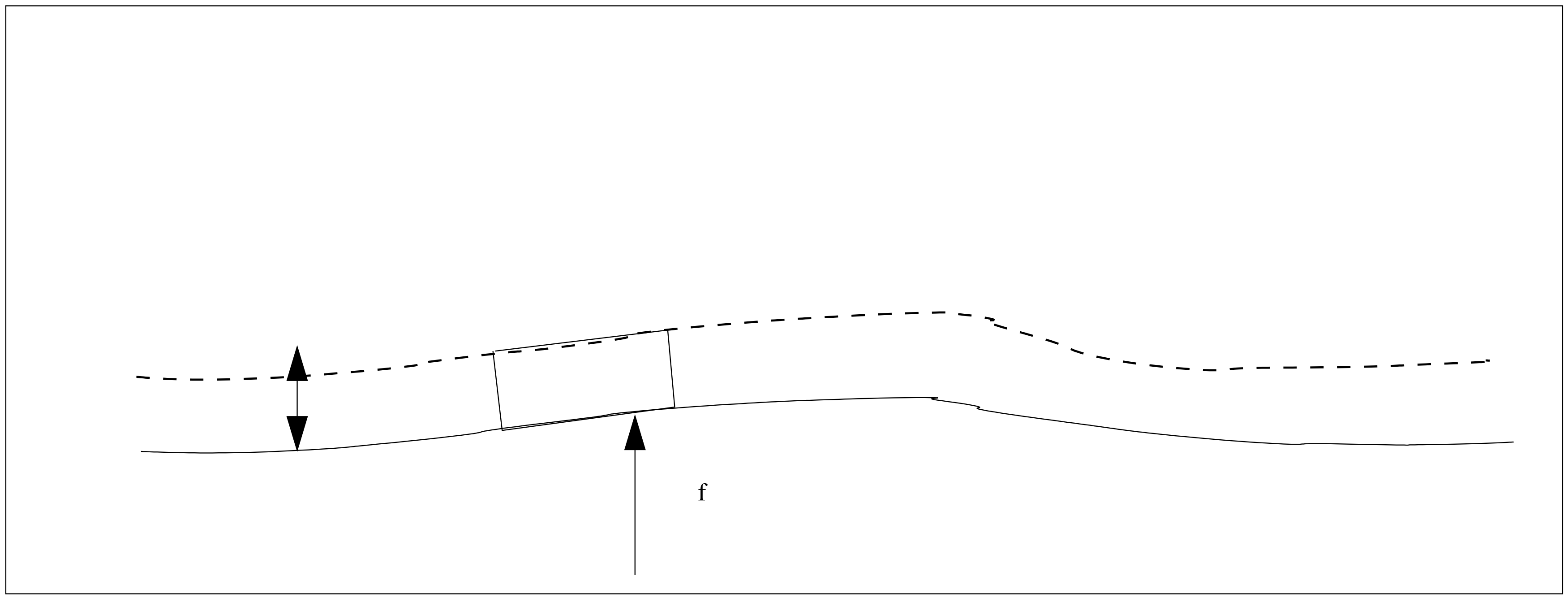

$$\frac{\partial R}{\partial t} = ...$$

$$\frac{\partial f}{\partial t} = ...$$

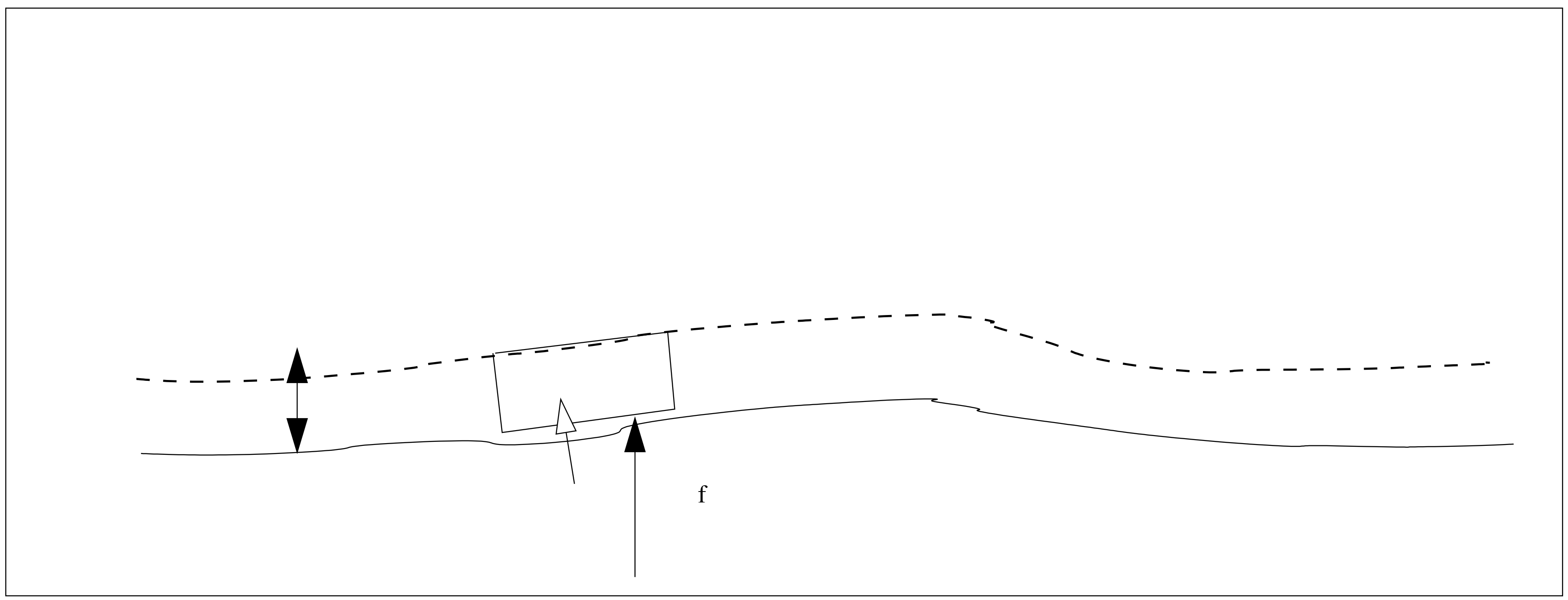

$$\frac{\partial R}{\partial t} = ... + \Gamma$$

$$\frac{\partial f}{\partial t} = -\Gamma$$

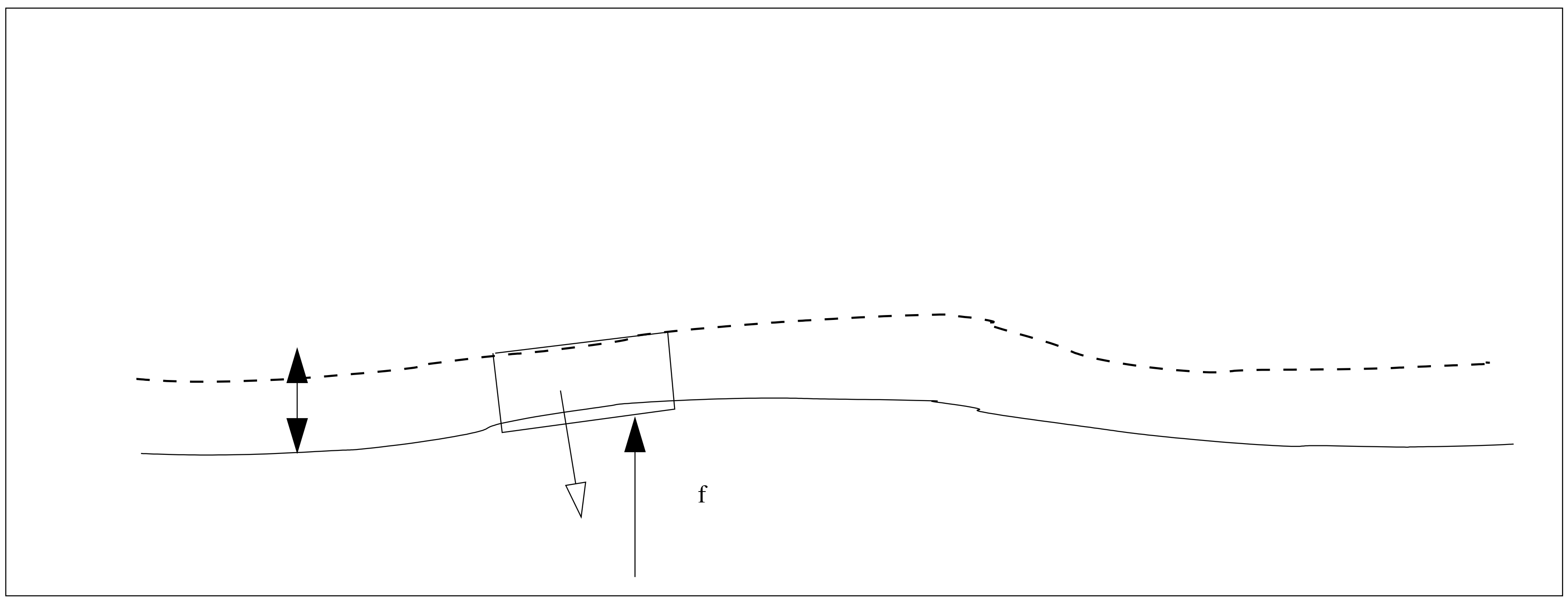

$$\frac{\partial R}{\partial t} = ... + \Gamma$$

$$\frac{\partial f}{\partial t} = -\Gamma$$

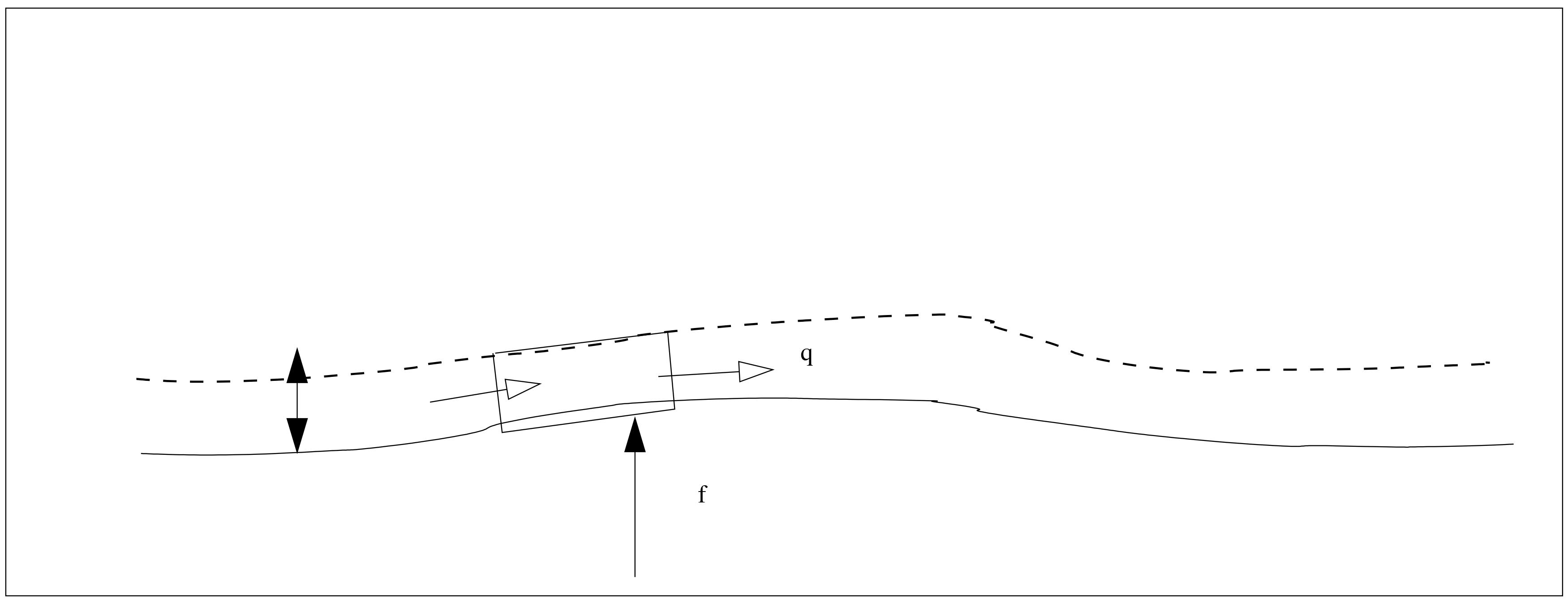

$$\frac{\partial R}{\partial t} = -\frac{\partial q}{\partial x} + \Gamma$$

$$\frac{\partial f}{\partial t} = -\Gamma$$

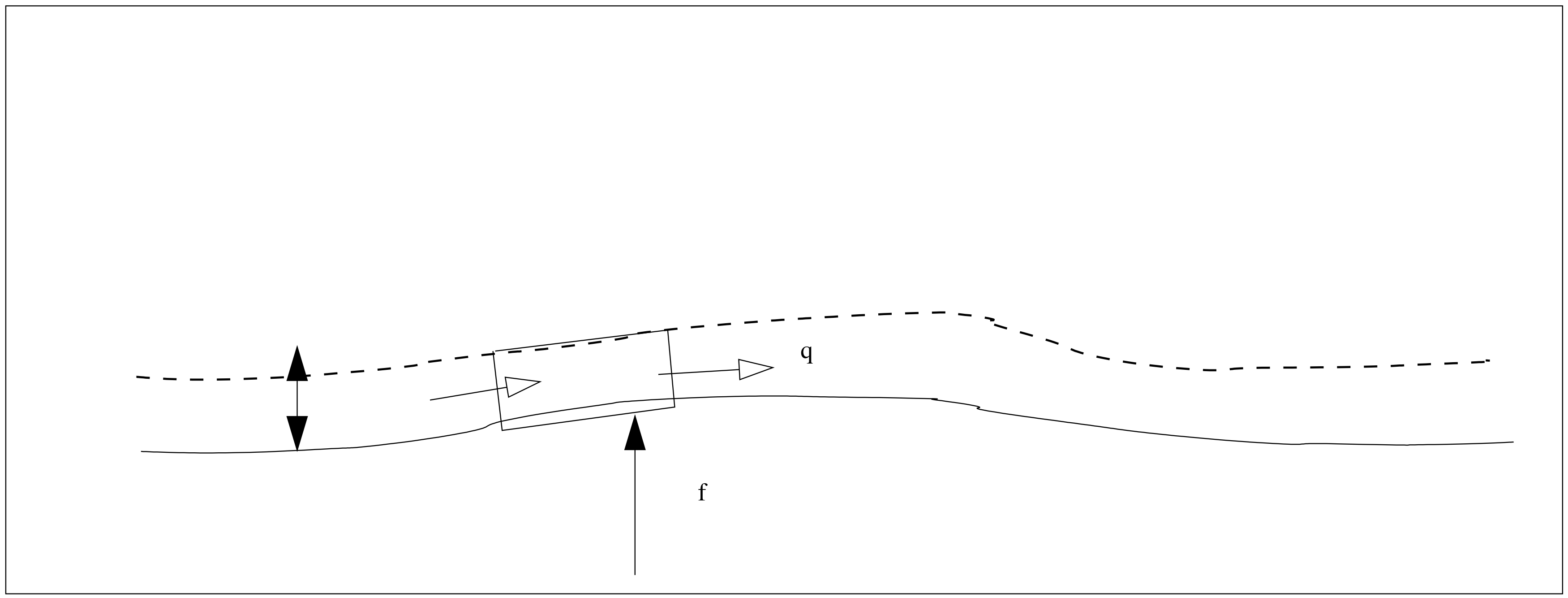

$$\frac{\partial R}{\partial t} = -\frac{\partial q}{\partial x} + \Gamma \qquad \frac{\partial f}{\partial t} = -\Gamma$$

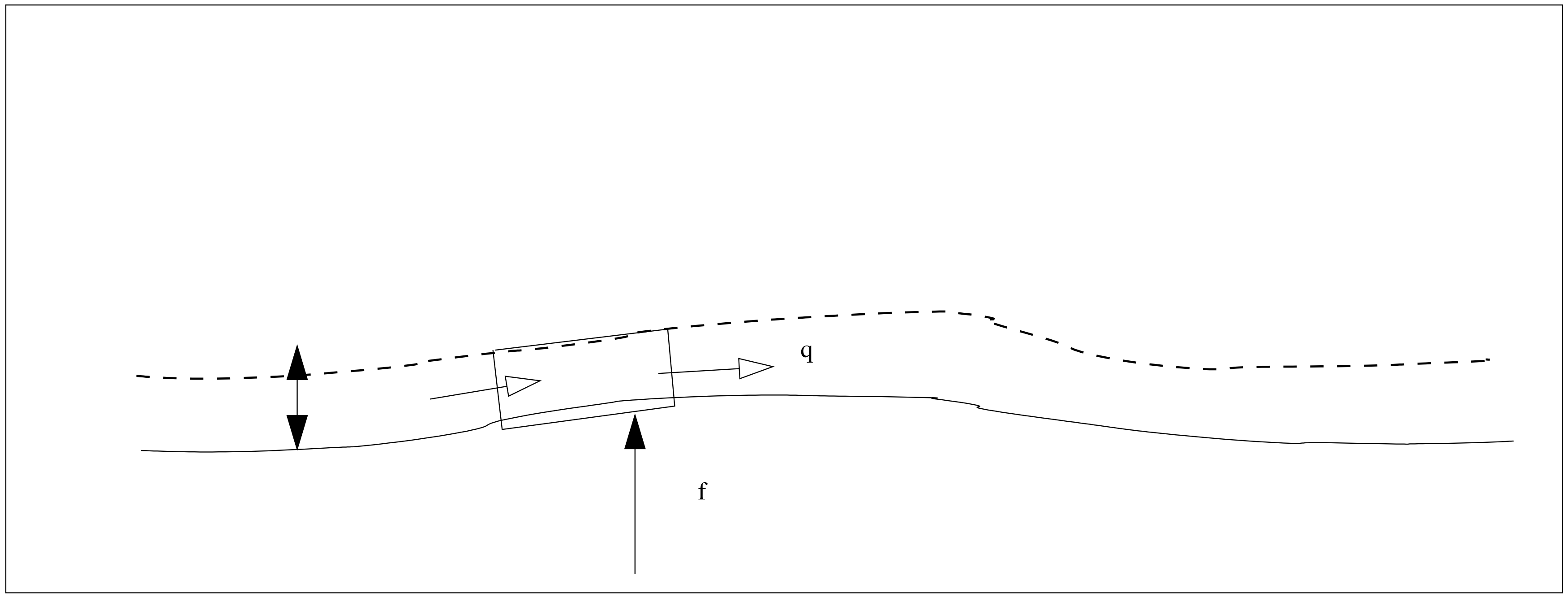

$$\frac{\partial R}{\partial t} = -\frac{\partial q}{\partial x} + \Gamma \qquad\qquad \frac{\partial f}{\partial t} = -\Gamma$$

$\Gamma =$ (érosion)-(déposition)

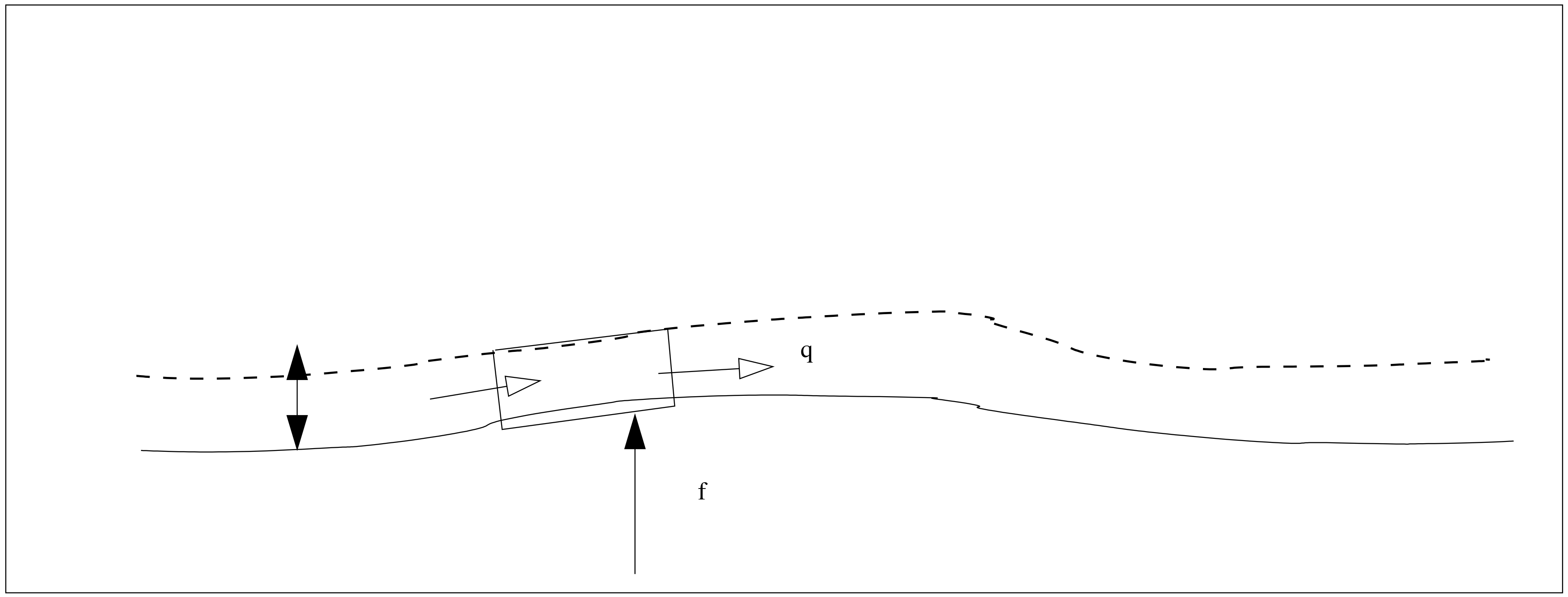

$$\frac{\partial R}{\partial t} = -\frac{\partial q}{\partial x} + \Gamma \qquad\qquad \frac{\partial f}{\partial t} = -\Gamma$$

$\Gamma =$ (érosion)-(déposition)

-(déposition) $\propto -R$ érosion $\propto (\tau - \tau_s)$ et $q \propto R\,\tau$

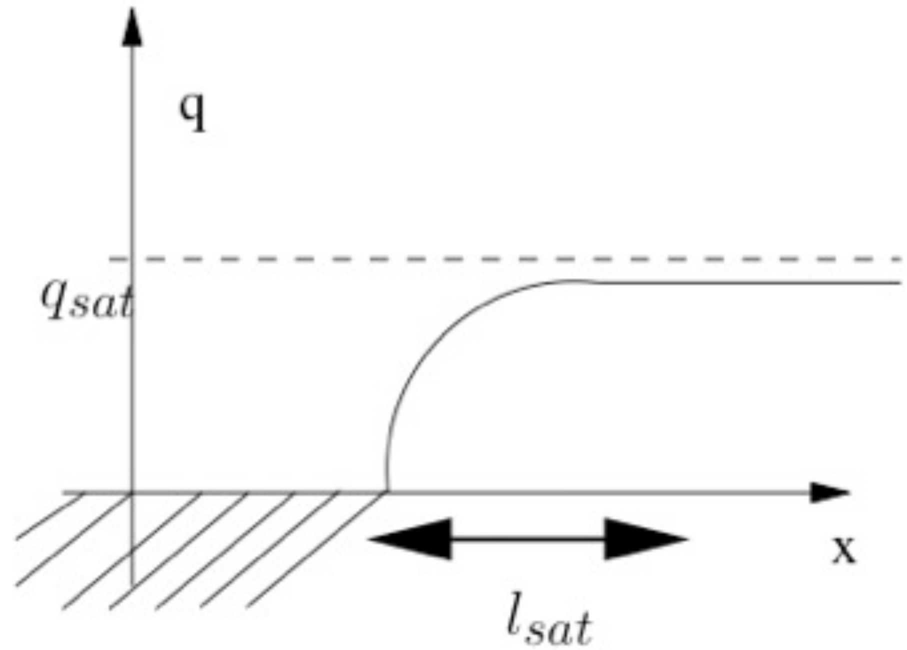

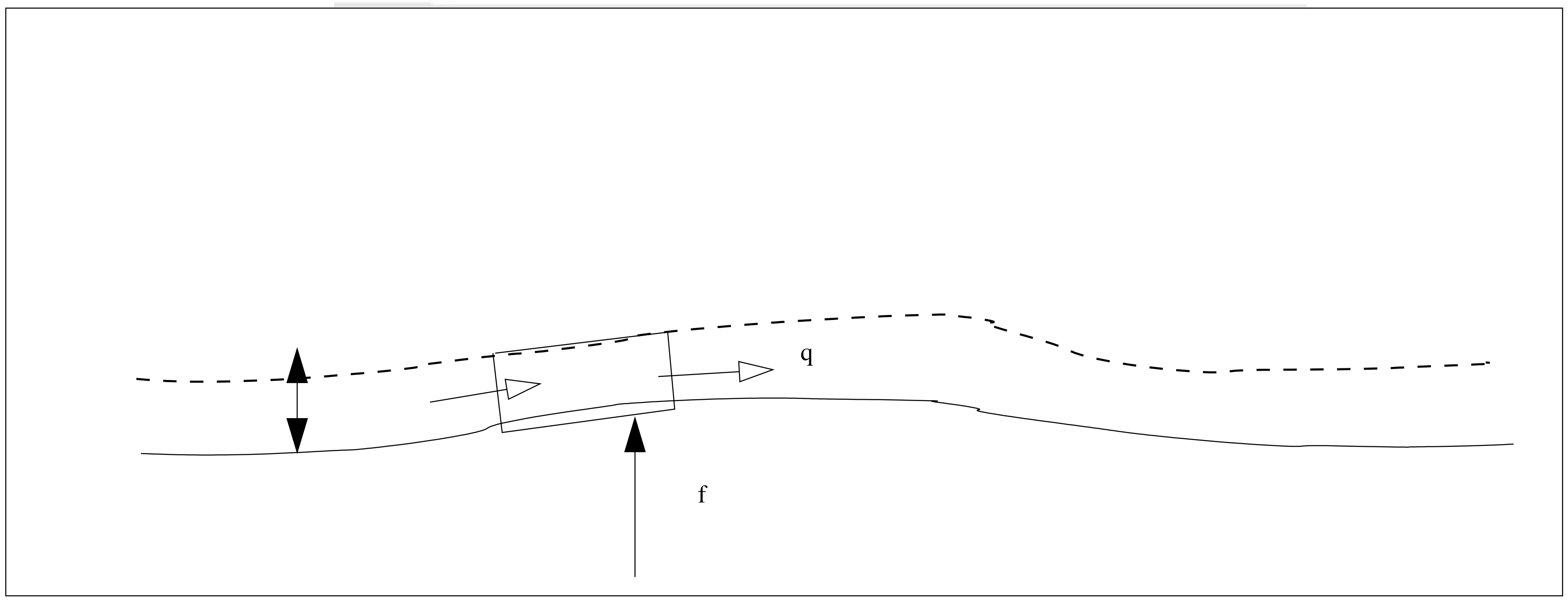

$$l_s \frac{\partial q}{\partial x} + q = q_s \qquad \frac{\partial f}{\partial t} = -\frac{\partial q}{\partial x}$$

$$q_s = E(\tau - \tau_s)_+$$

inspired from Sauerman Kroy Hermann 01: Andreotti Claudin Douady 02, Lagrée 03

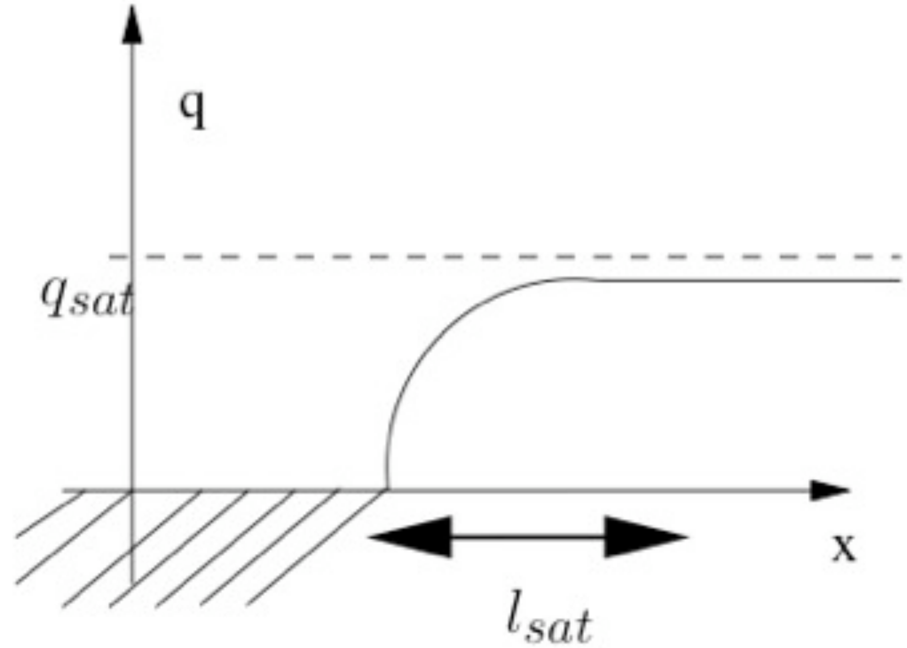

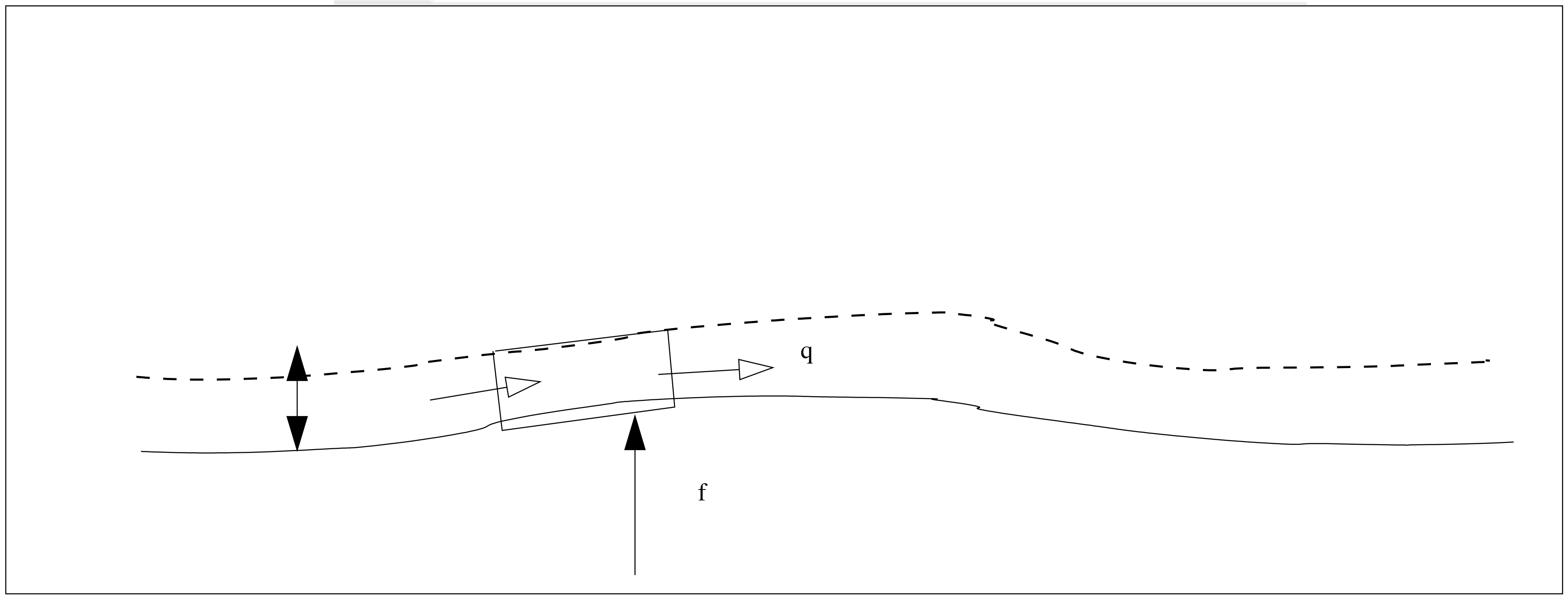

Du Boy (1879) :

"*une fois une certaine quantité de matières en mouvement sur le fond du lit, la vitesse des filets liquides devient trop faible pour entraîner davantage : le cours d'eau est alors saturé. Un cours d'eau non saturé tend à le devenir en entraînant une partie des matériaux qui composent son lit, et en choisissant de préférence les plus petits.*"

- introduction
- the problem
- the flow: Saint Venant and other
- first granular model
- first coupling: bars
- imporved granular model: saturation length
- ripples
- bars & ripples
- conclusions perspectives

we have an improved model for the bed

come back to the fluid

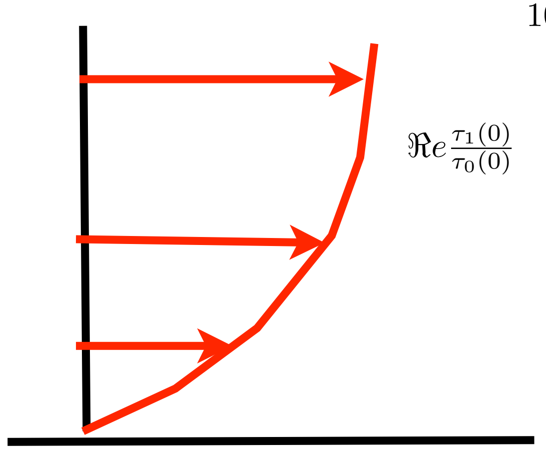

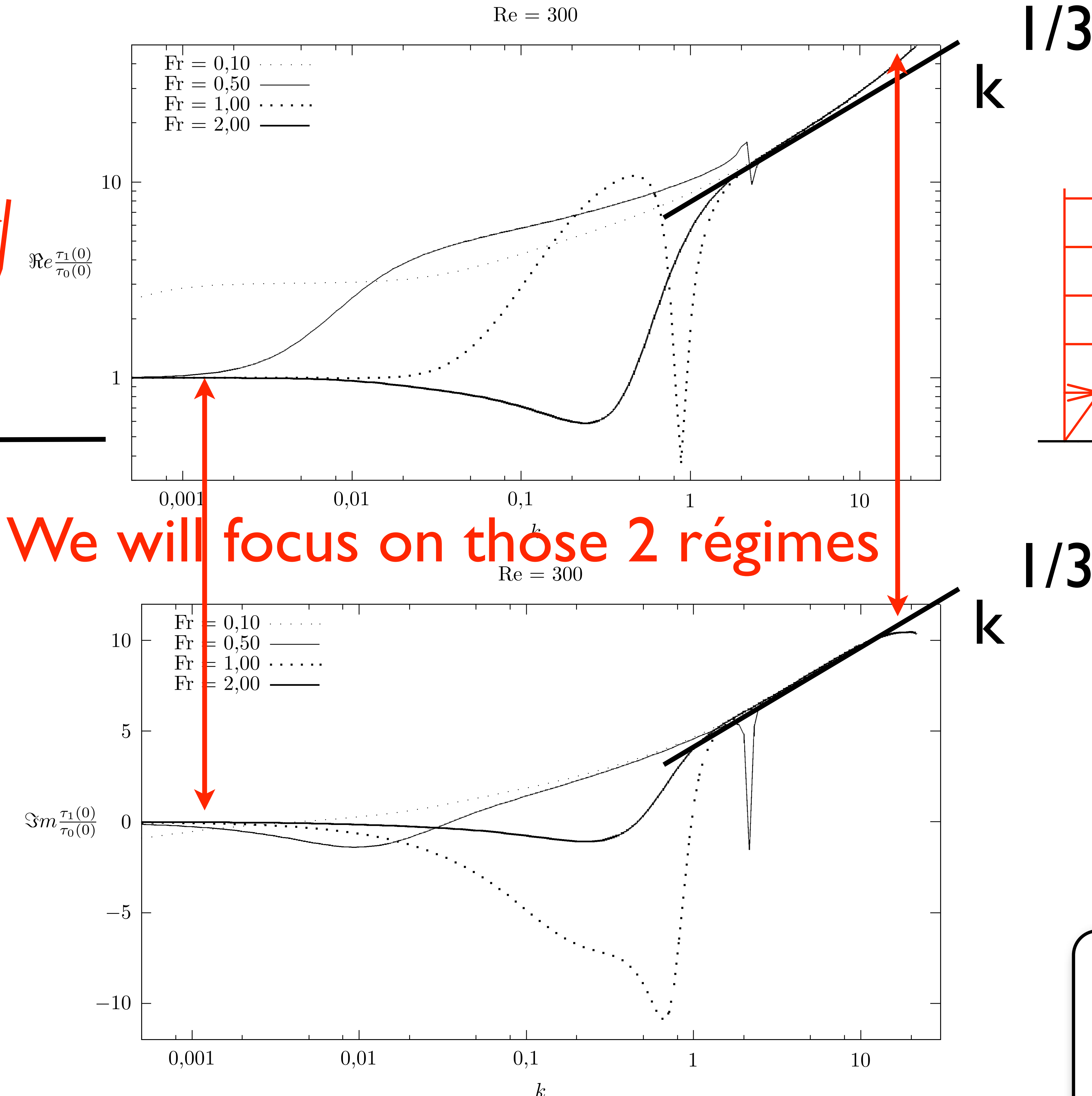

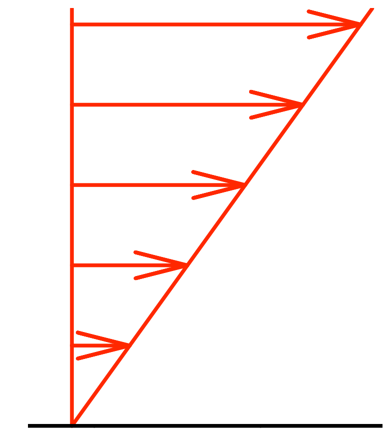

$k^{1/3}$

FIG. 2.6 – *Parties réelles (en haut) et parties imaginaires (en bas) de la perturbation du cisaillement au fond renormalisée, pour $Re = 300$ et différentes valeurs de Fr.*

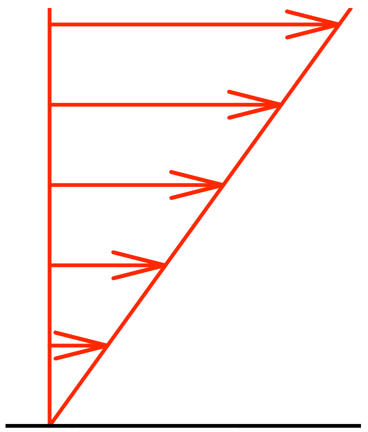

Viscous effects are important near the wall
Perturbation of a shear flow Non linear resolution (with flow separation) possible
But first we linearise

It is called Double Deck (Triple Deck)
Introduced by Neiland 69 Stewartson 69 Smith 80...

$\tau = \mu U_0'(\bar{U}_S'(1 + (\frac{U_0'}{\nu\lambda})^{1/3} H\tilde{c}))$, with $\tilde{c} = FT^{-1}[FT[\tilde{f}]3Ai(0)(-(i2\pi\tilde{k})\bar{U}_S')^{1/3}]$

- Fowler

$$\int_0^\infty \frac{f'(x-\xi)}{\xi^{1/3}} d\xi$$

$$\boxed{k^{1/3}}$$

Completely erodible soil, Linear Stability

Solution of

$$\tau = TF^{-1}[(3Ai(0))(-ik)^{1/3}TF[f]]$$
$$l_s\frac{\partial q}{\partial x} + q = \varpi(\tau - \tau_s - \Lambda\frac{\partial f}{\partial x})$$
$$\frac{\partial f}{\partial t} = -\frac{\partial q}{\partial x}$$

Completely erodible soil, Linear Stability

$Re(\sigma(k))$

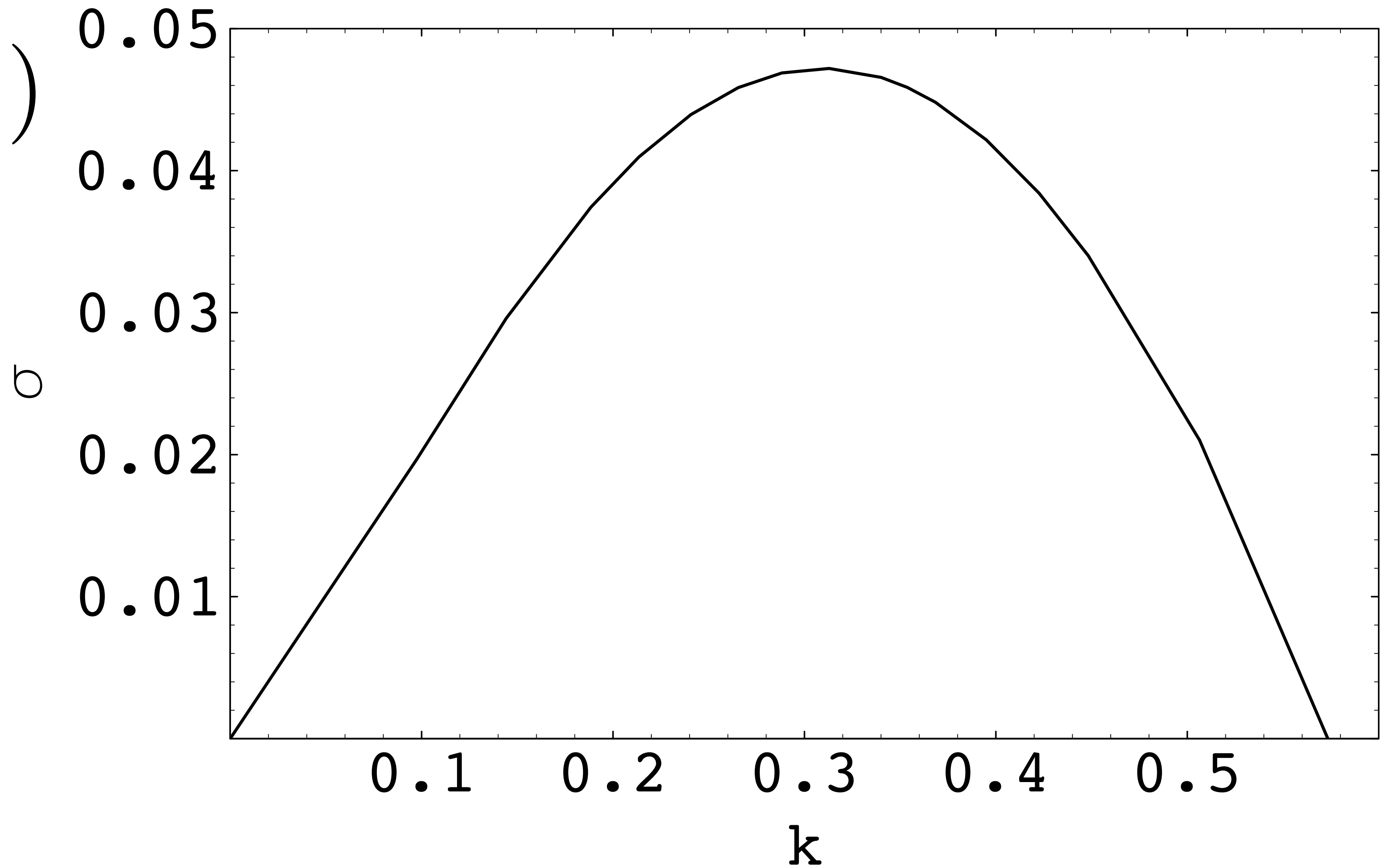

$$e^{\sigma t - ikx}$$

$\Lambda = 0,\ l_s$ increases

$$\tau = TF^{-1}[(3Ai(0))(-ik)^{1/3}TF[f]]$$
$$l_s\frac{\partial q}{\partial x} + q = \varpi(\tau - \tau_s - \Lambda\frac{\partial f}{\partial x})$$
$$\frac{\partial f}{\partial t} = -\frac{\partial q}{\partial x}$$

Fourier

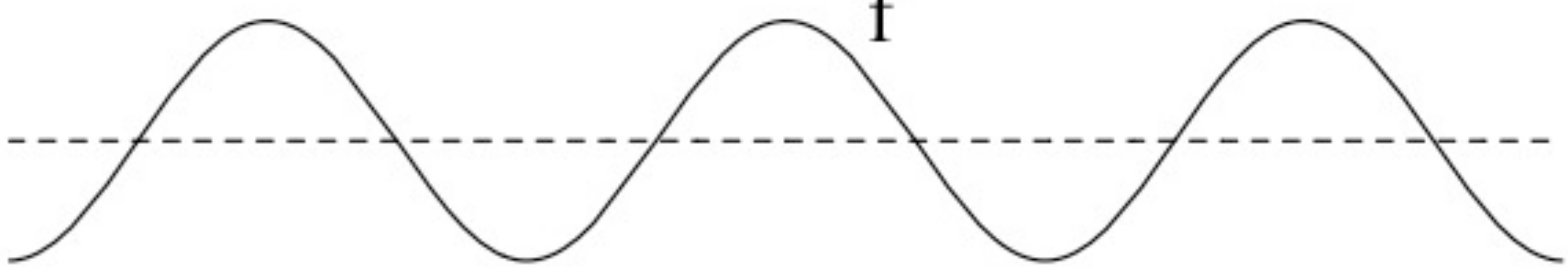

$$e^{\sigma t - ikx}$$

$$Re(\sigma(k))$$

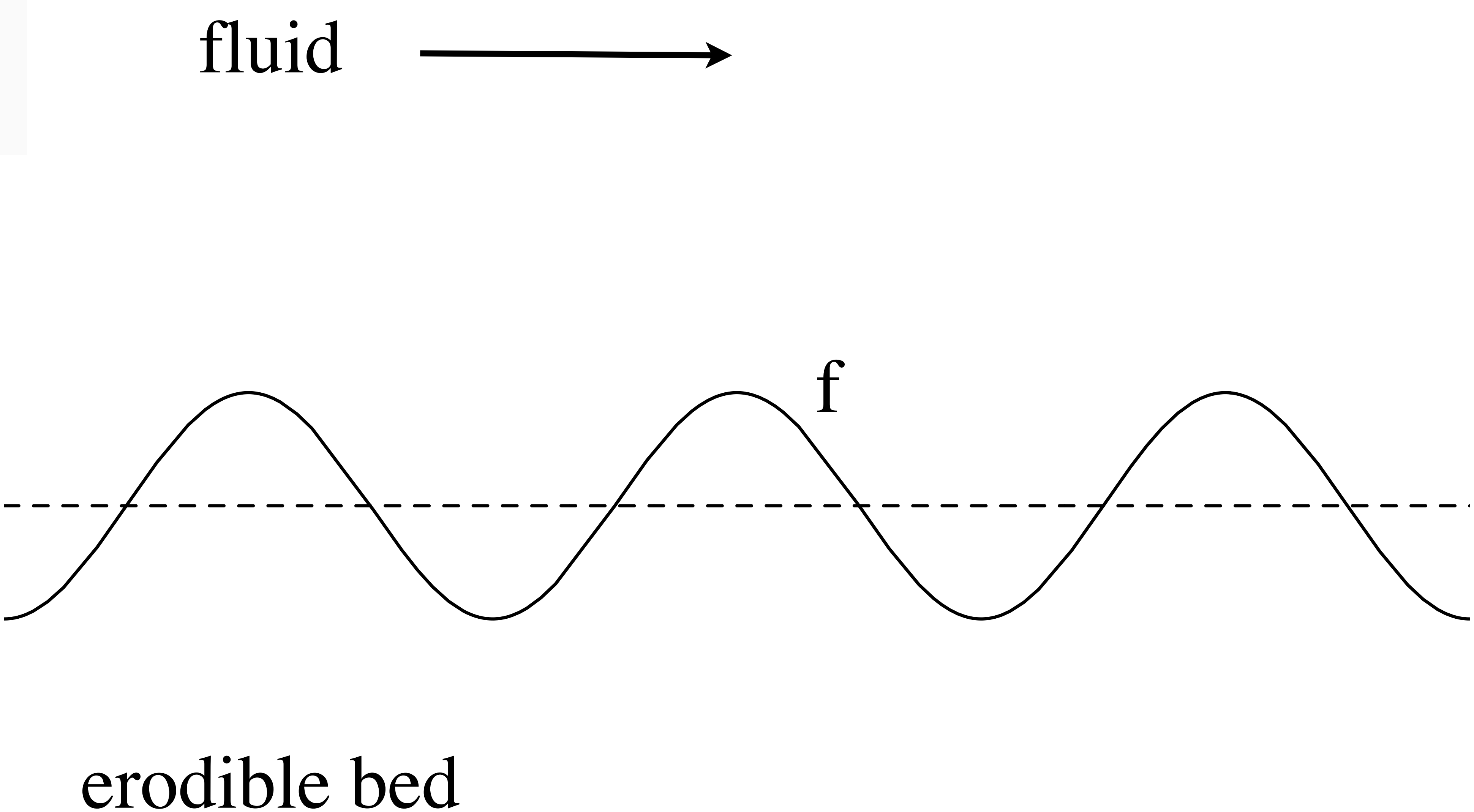
fluid
f
erodible bed

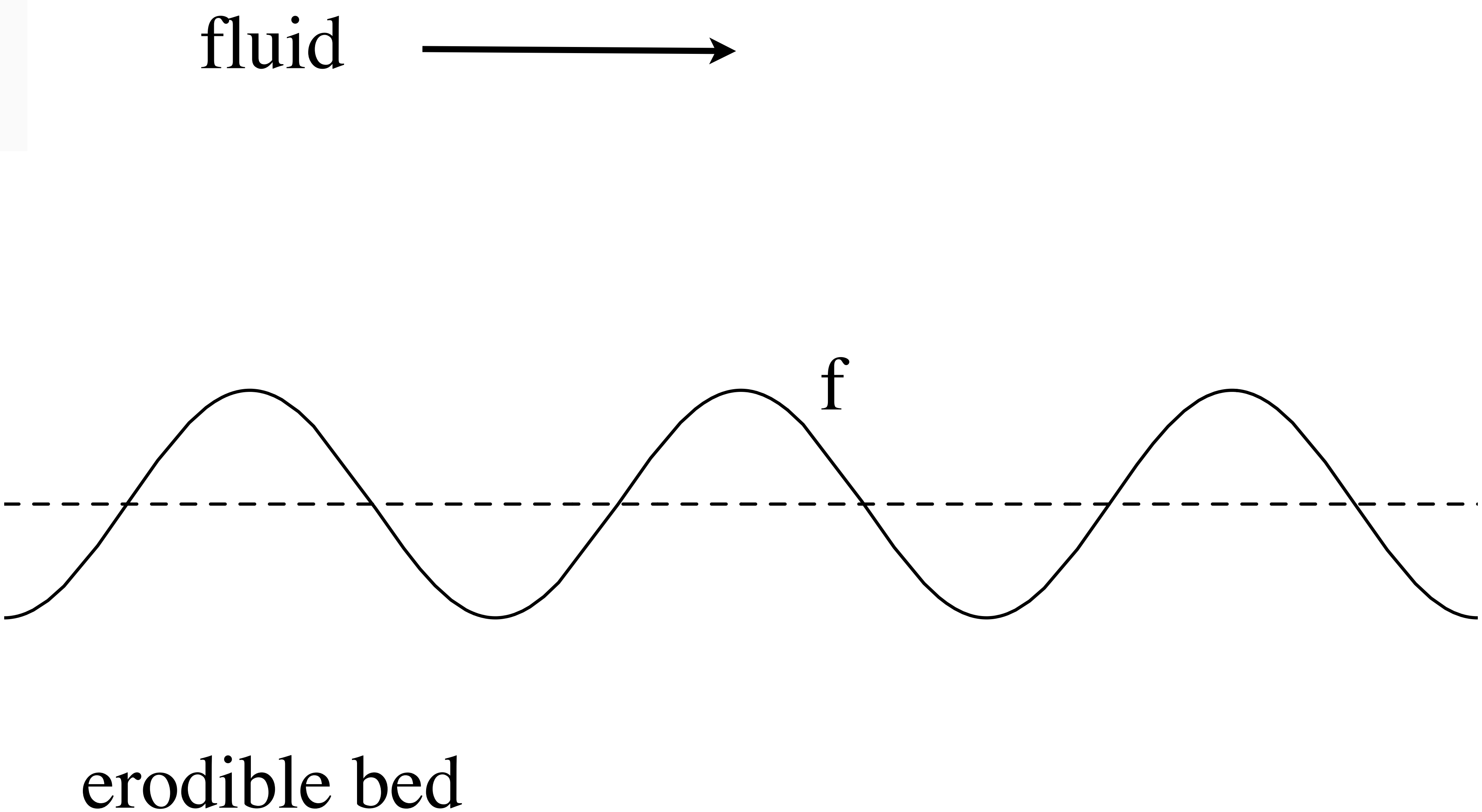

the bed

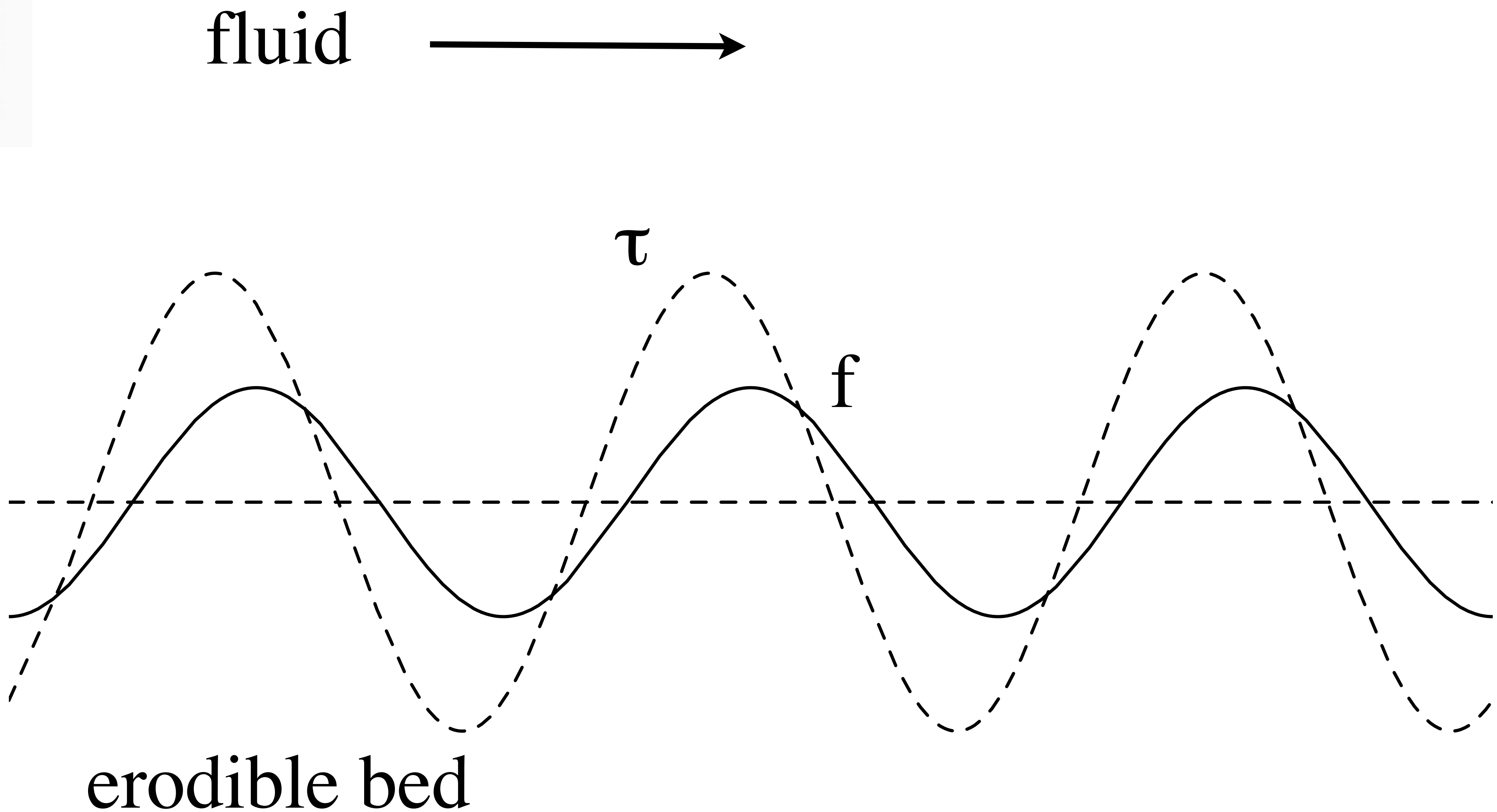

the bed The shear stress

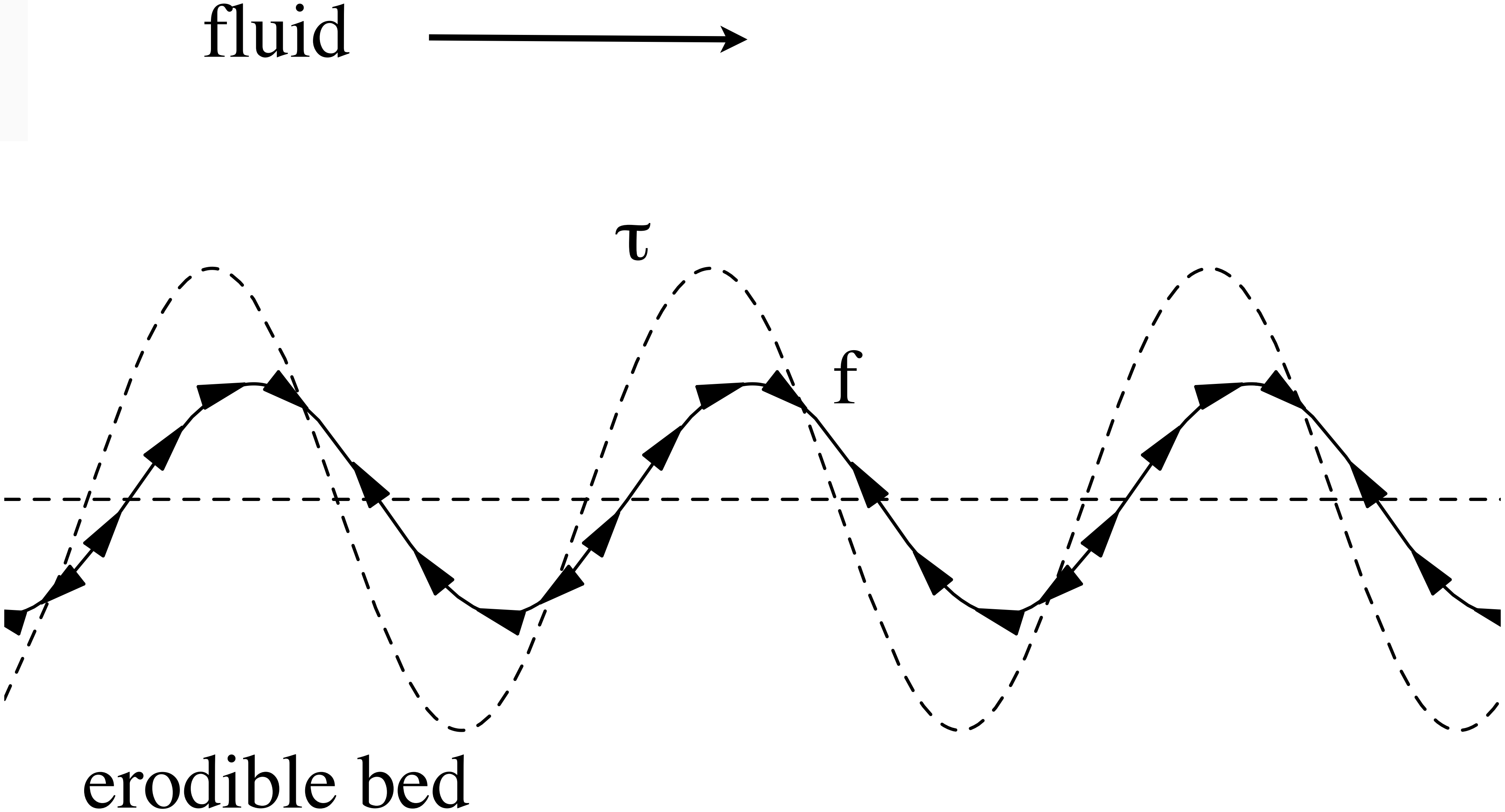

the bed The shear stress

The flux

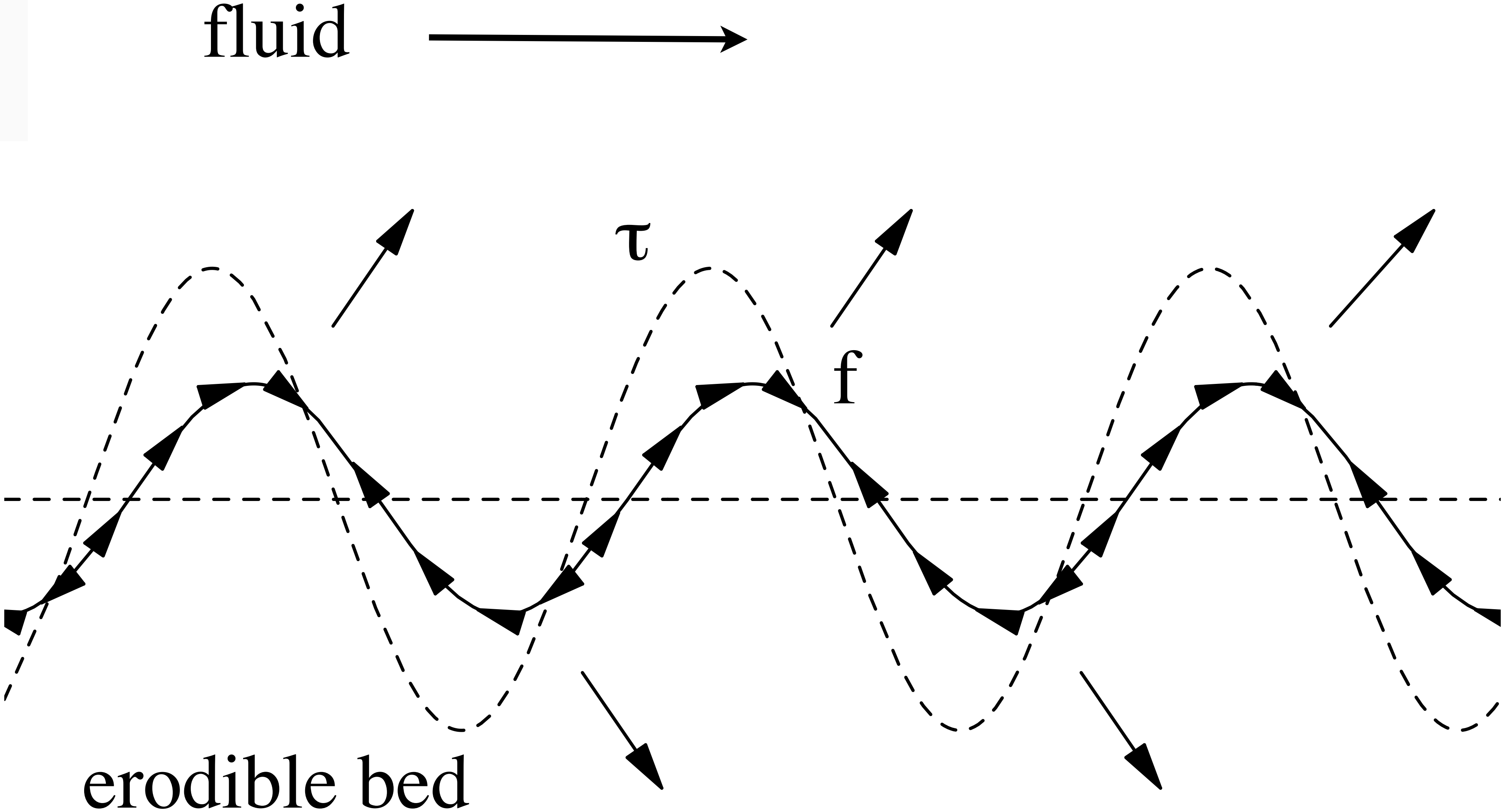

flux is positive after the top of the ripple

increase of the shear stress

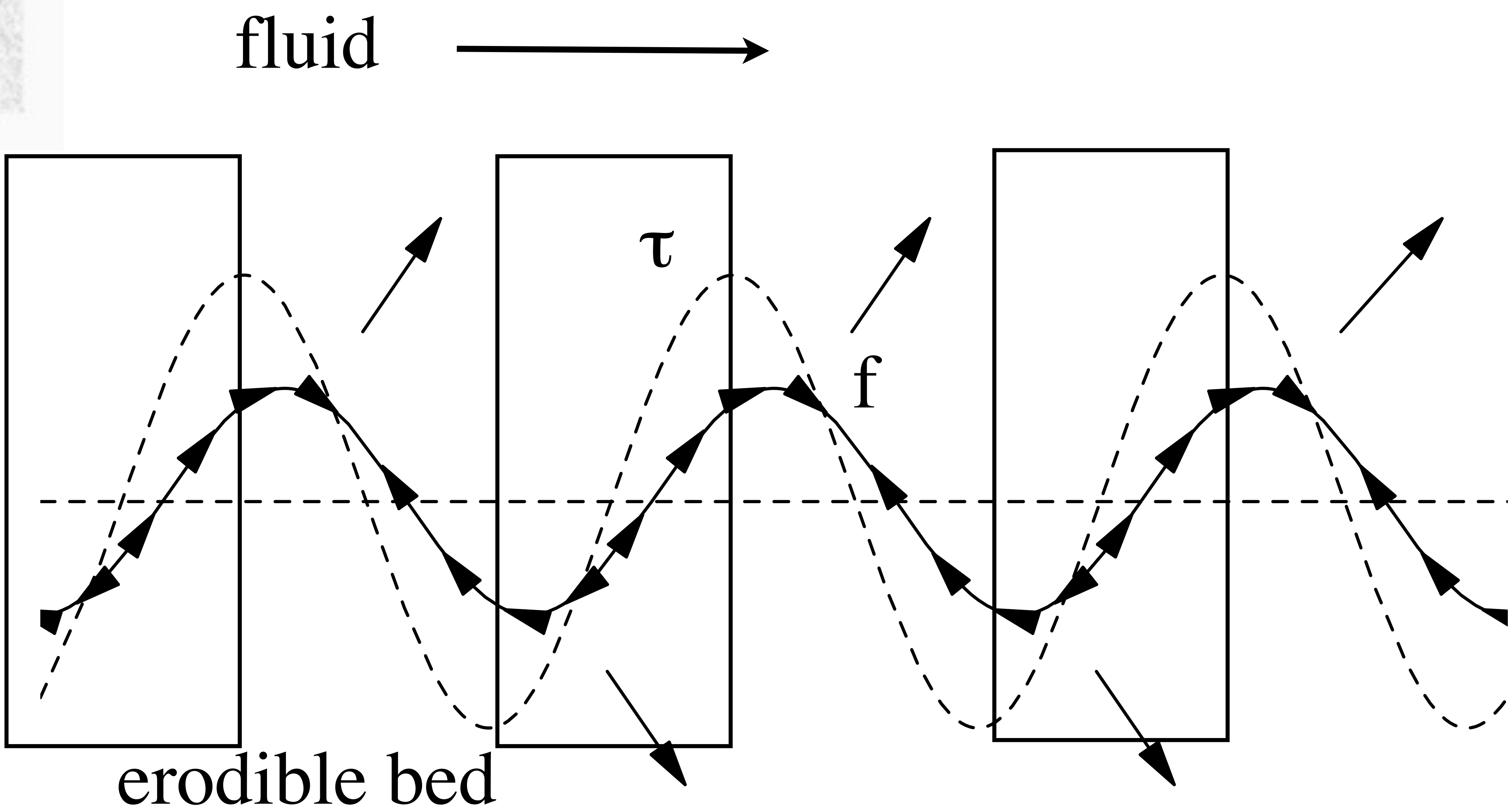

flux is positive after the top of the ripple

increase of the shear stress

erosion

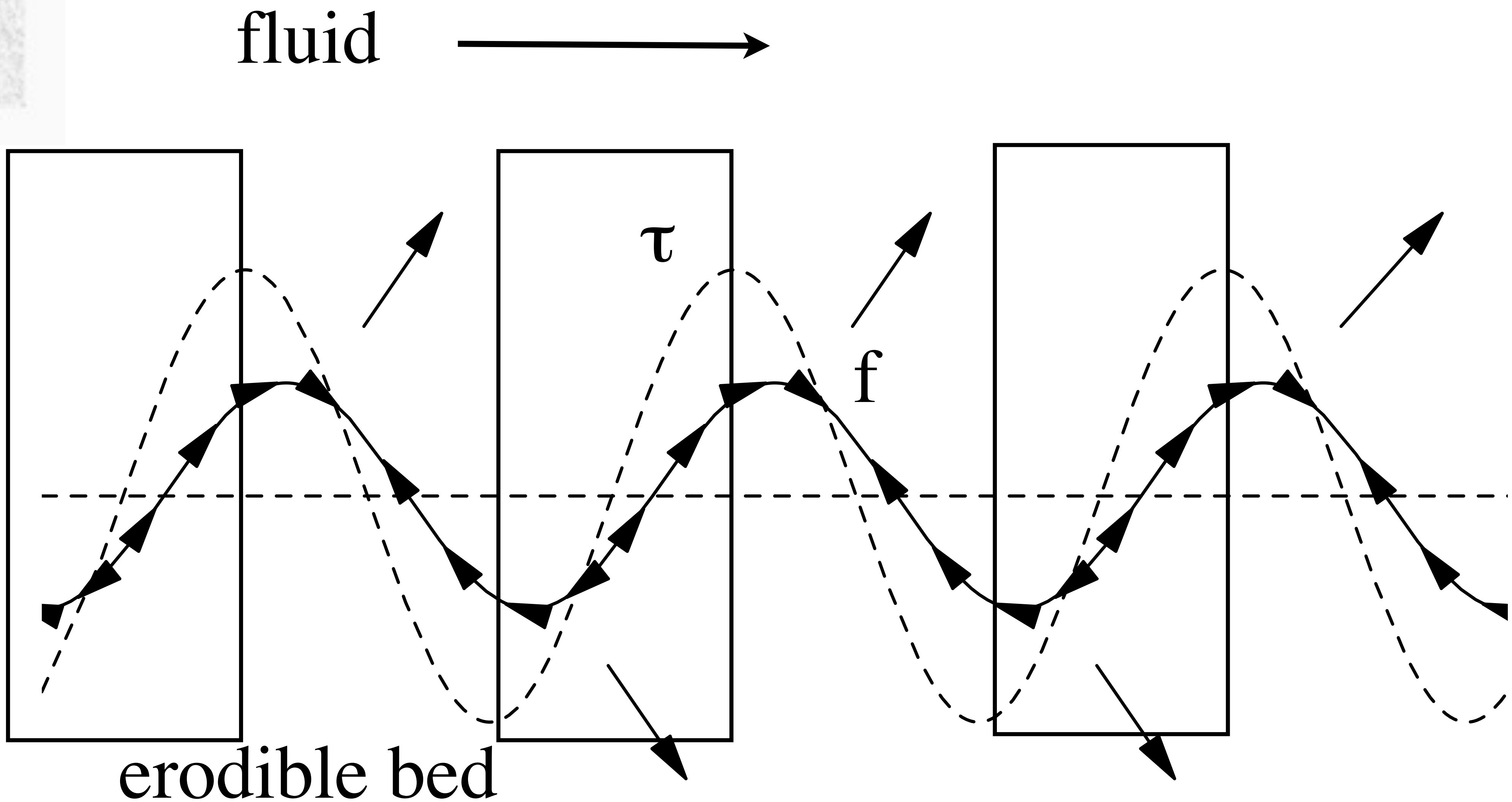

flux is positive after the top of the ripple

increase of the shear stress

erosion

decrease of the shear stress

deposition

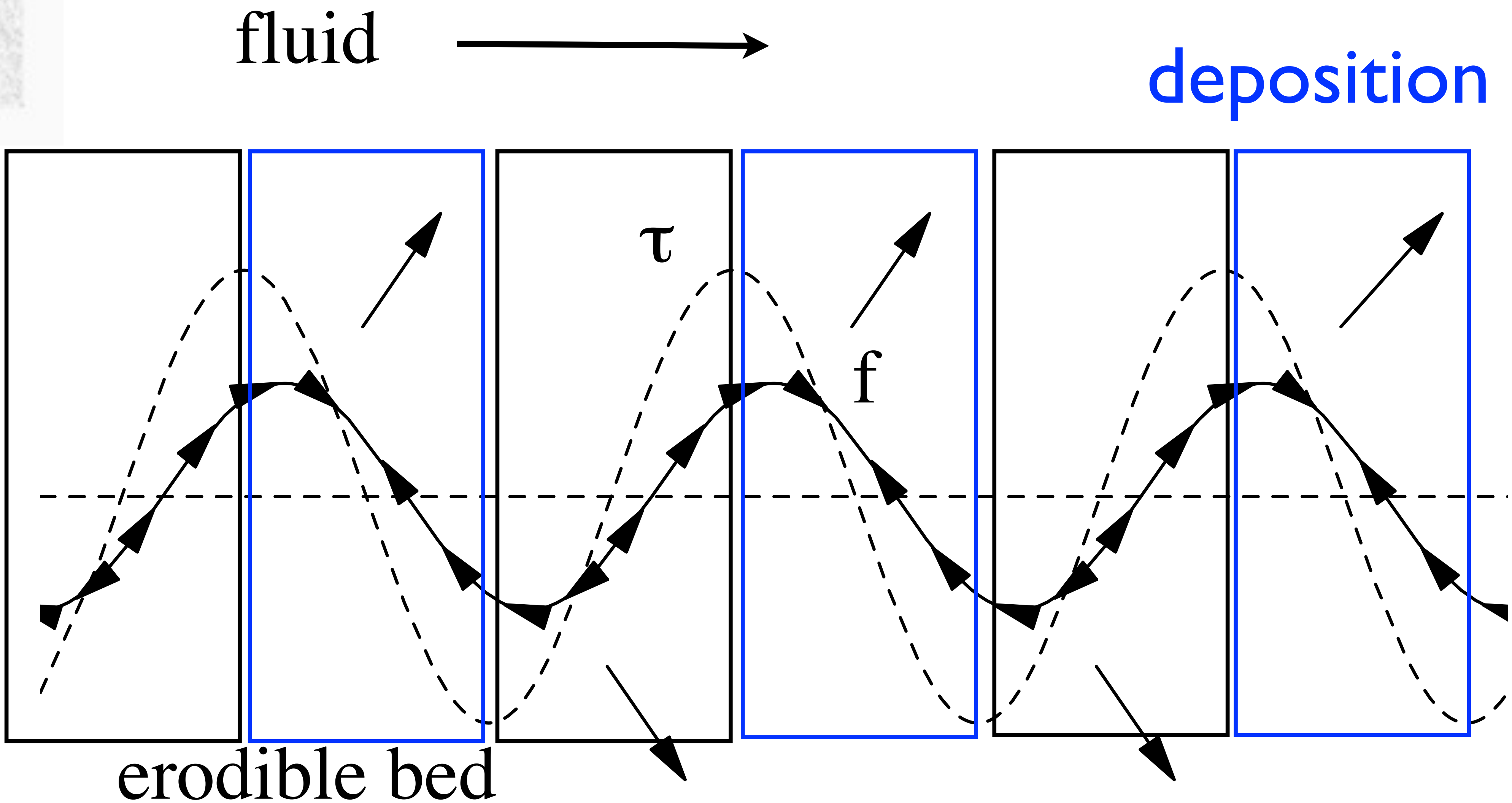

flux is positive after the top of the ripple

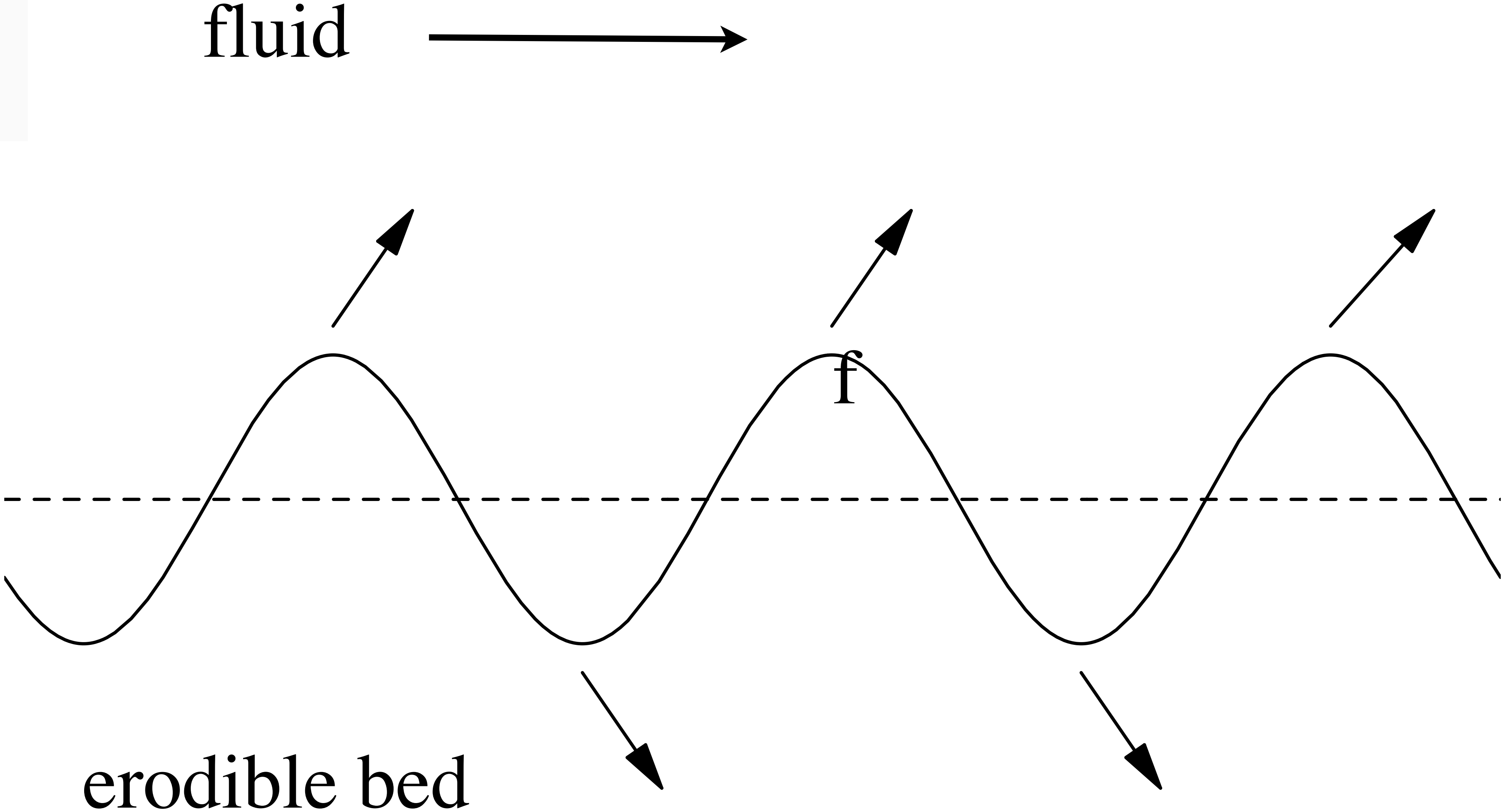
fluid
f
erodible bed

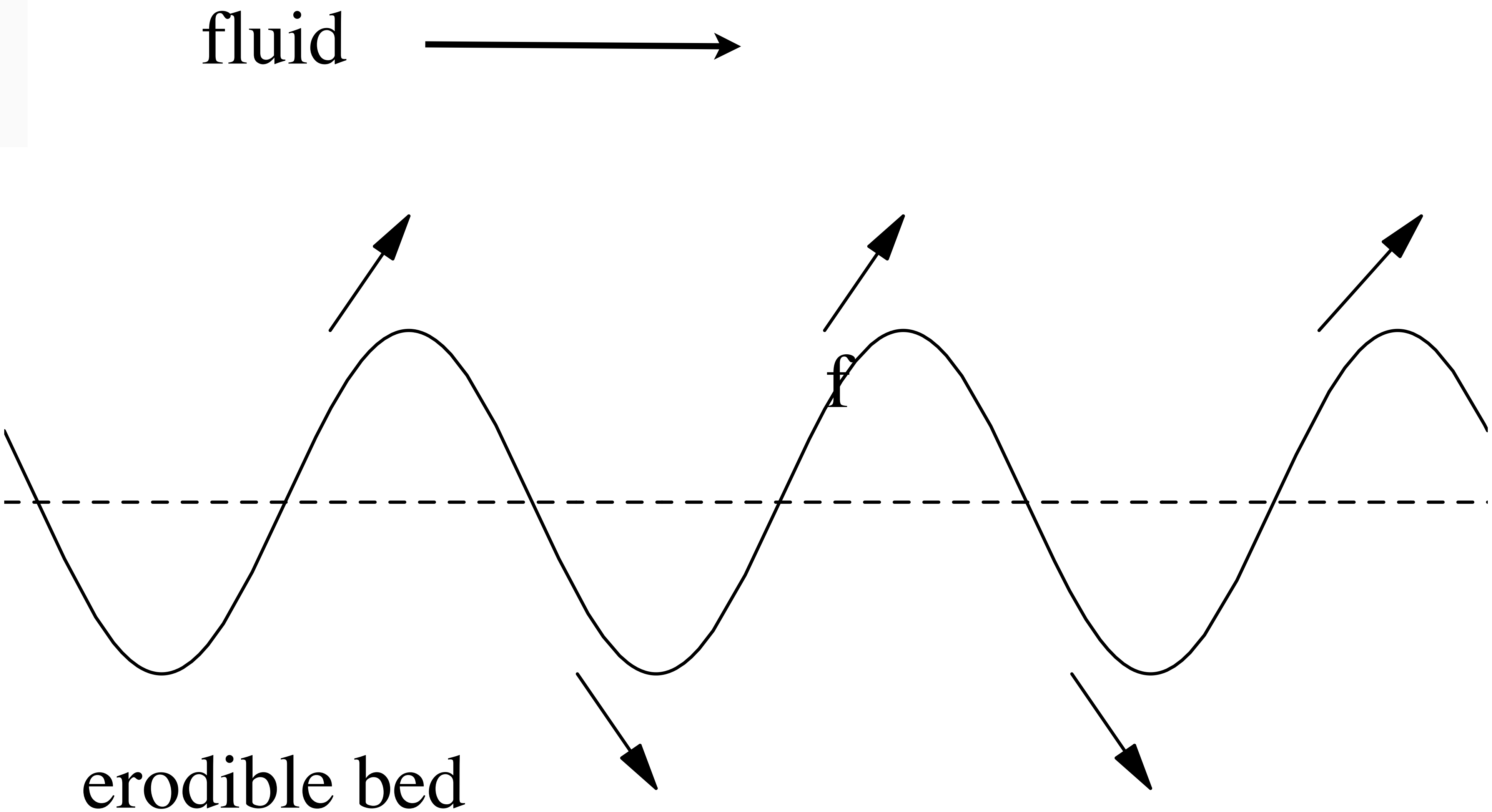

This is an instability

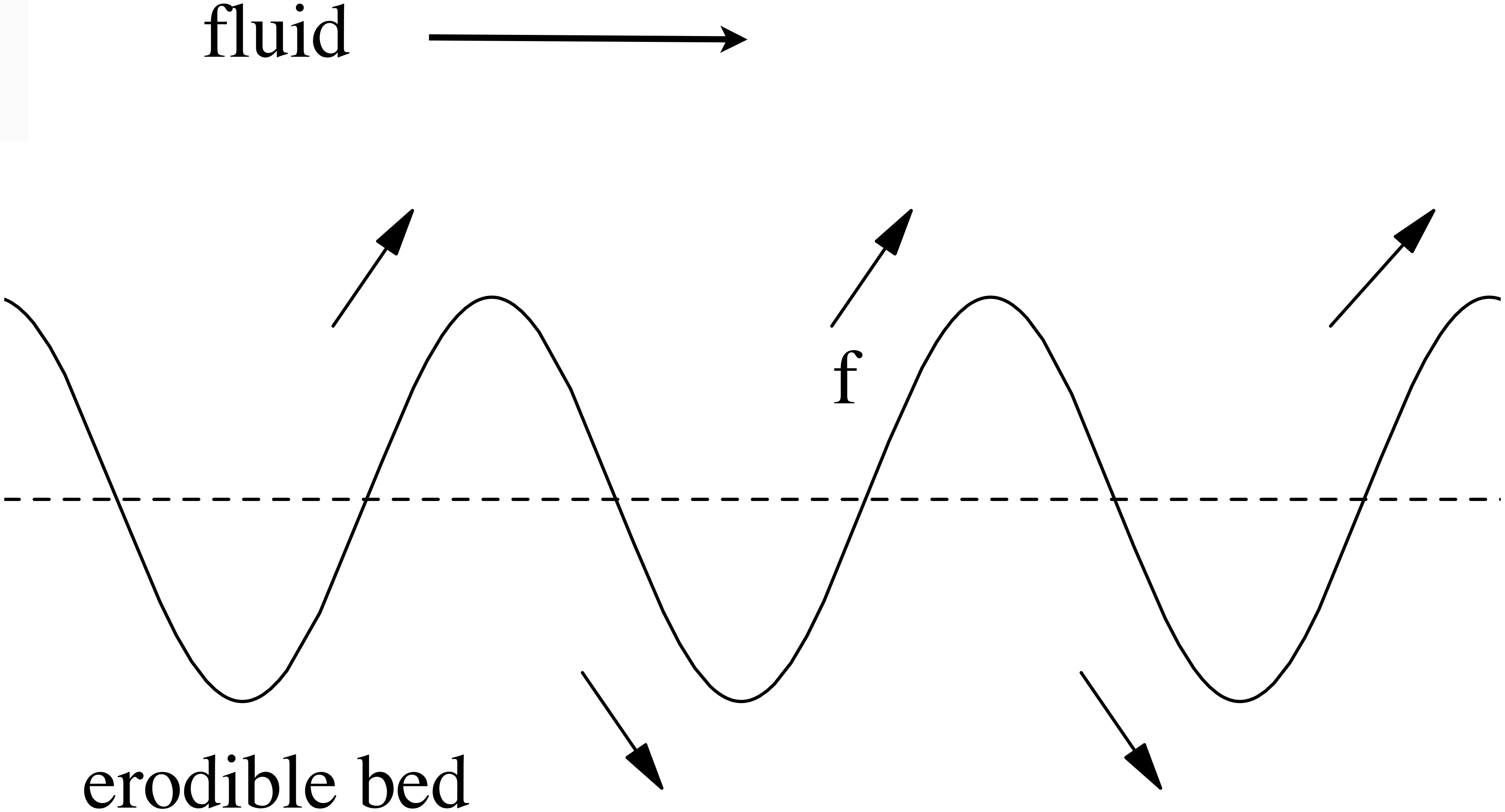

This is an instability

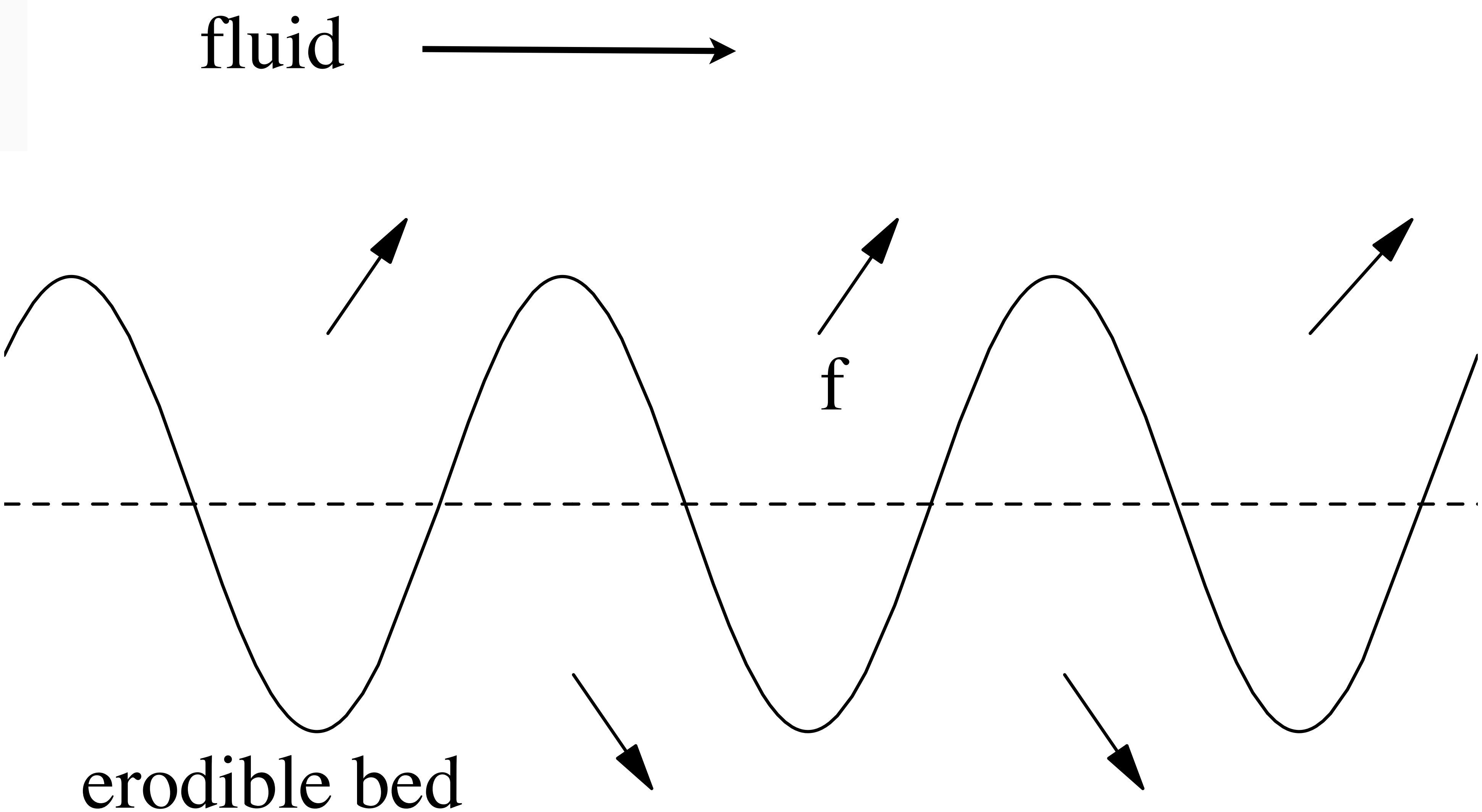

This is an instability

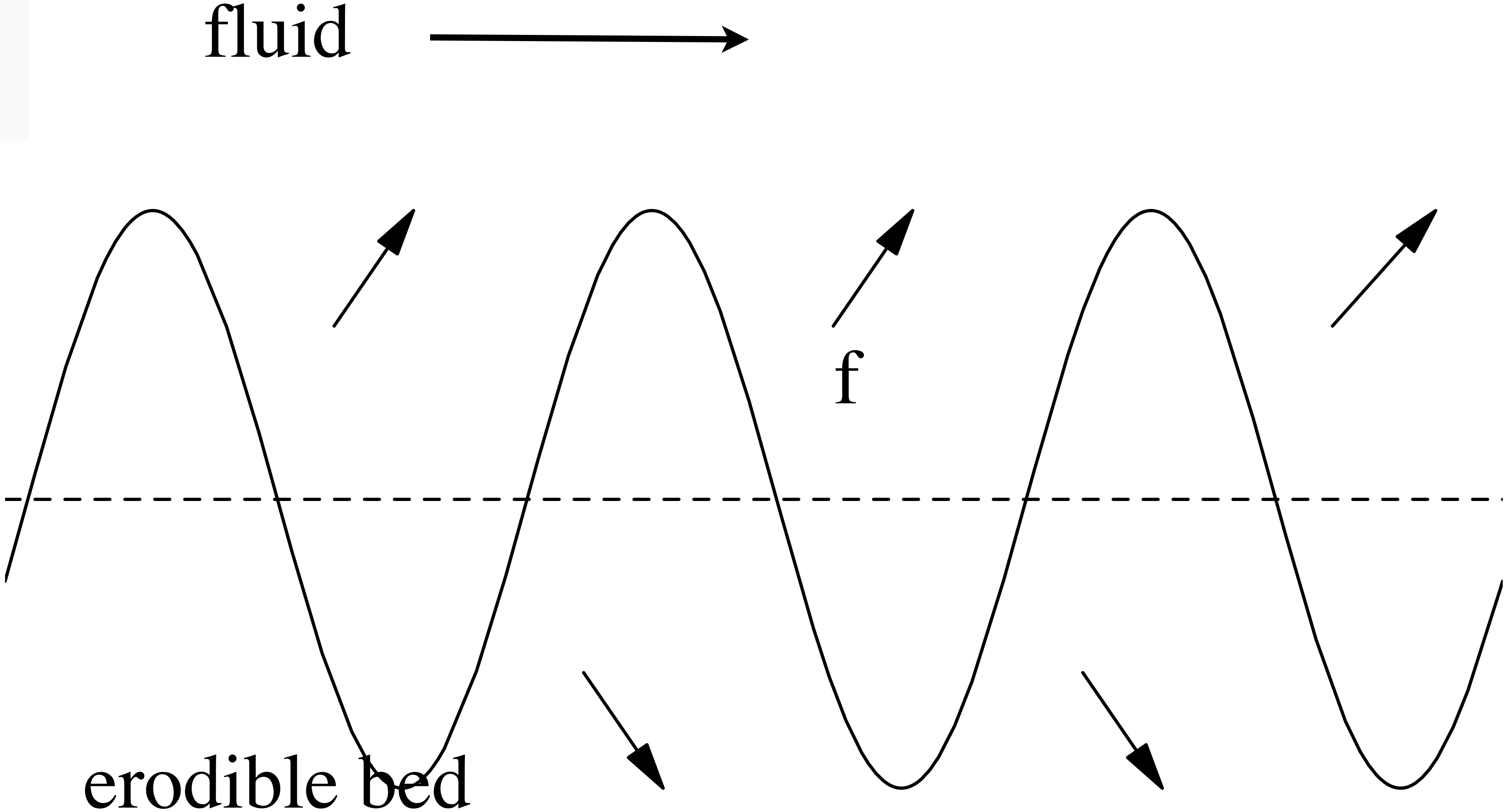

This is an instability

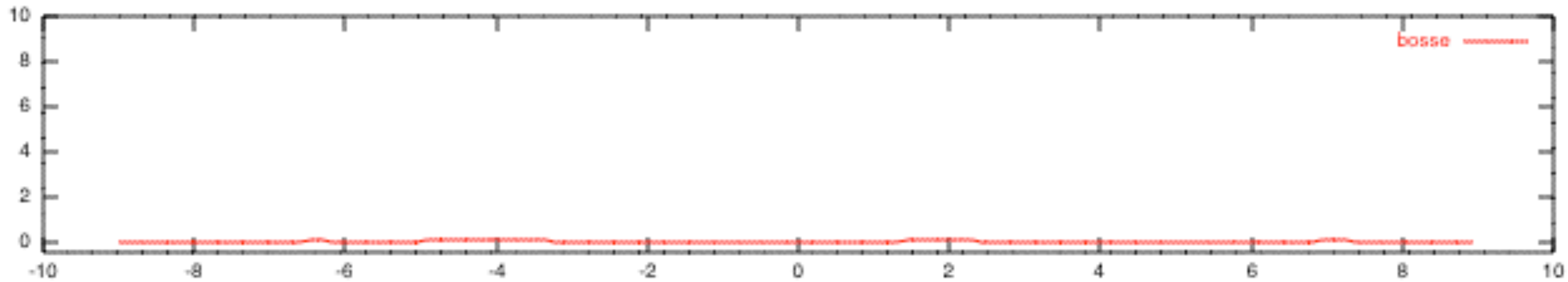

numerical simulation FFT

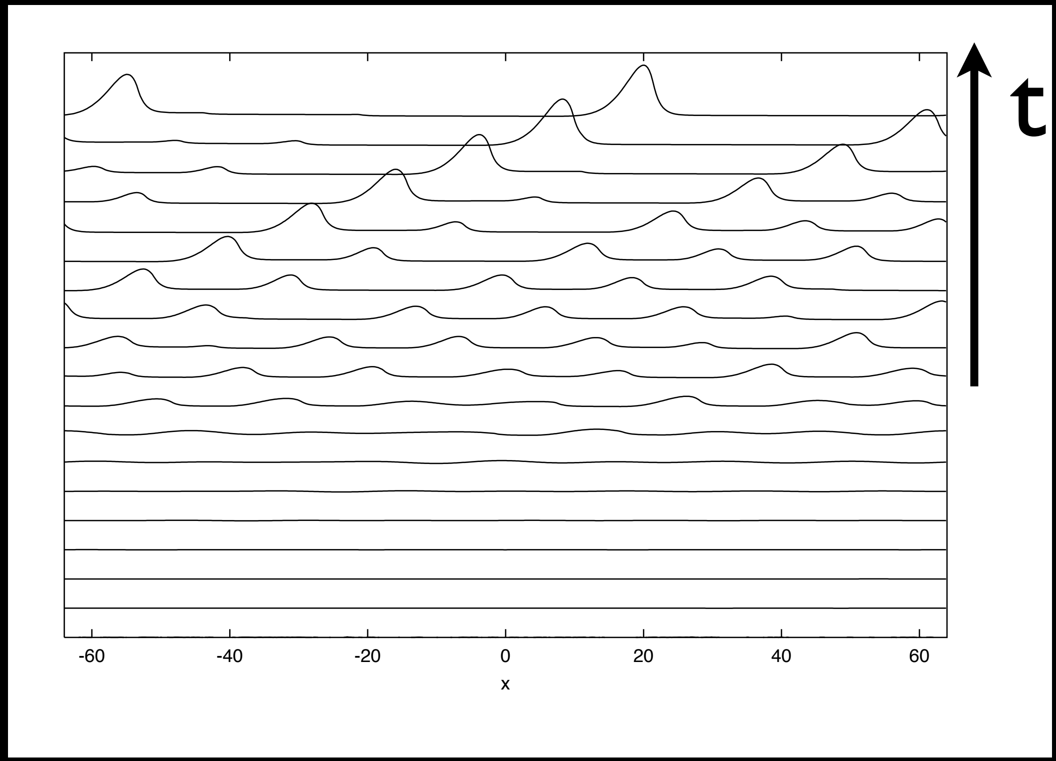
t
-60
-40
-20
0
20
40
60
x

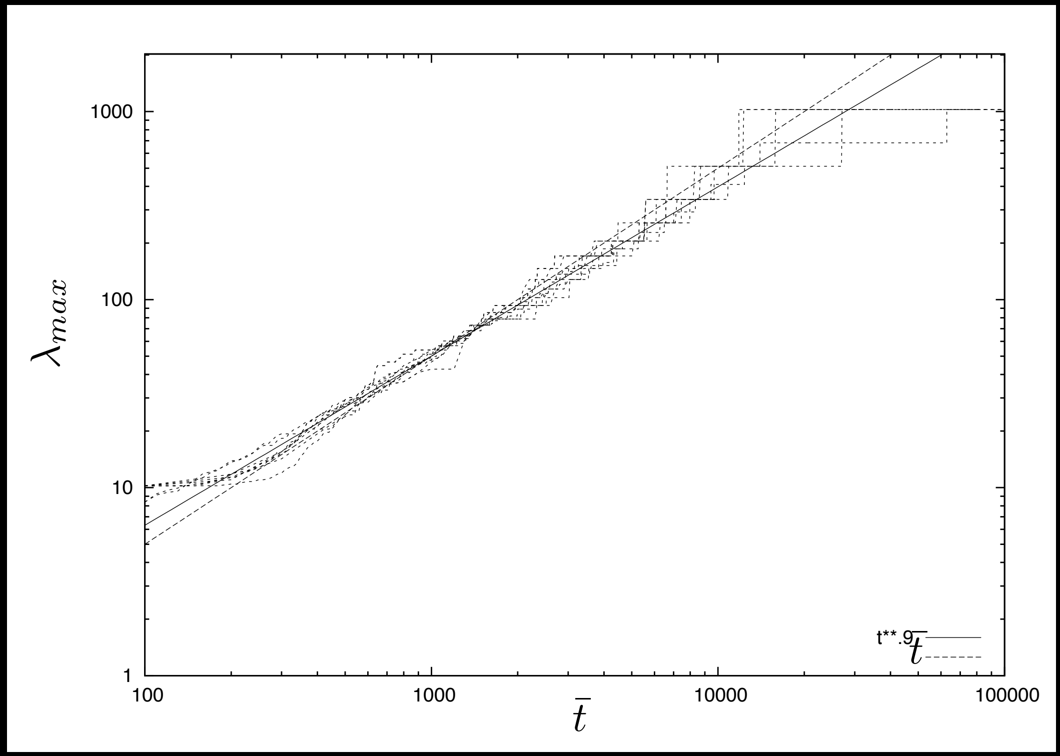
λ_{max}
1000
100
10
1
100
1000
10000
100000
$\bar{t}$
t**.9
$\bar{t}$

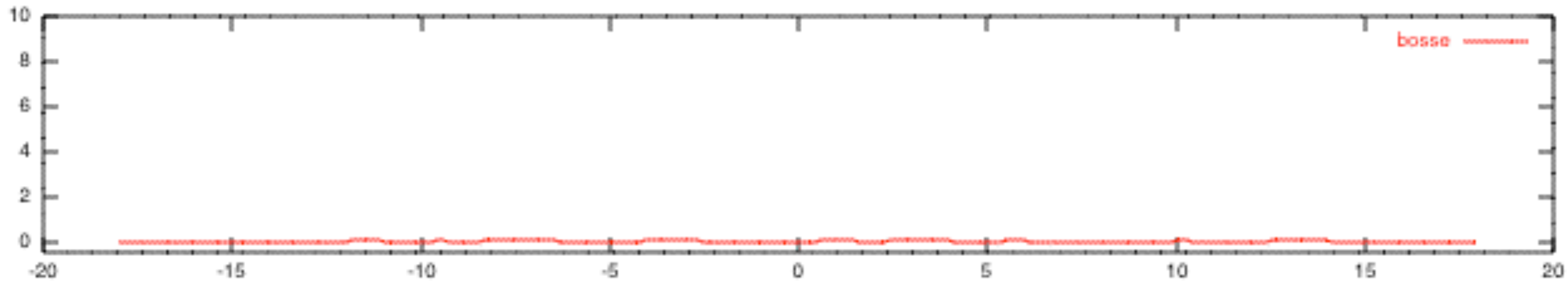
bosse
10
8
6
4
2
0
-20
-15
-10
-5
0
5
10
15
20

coarsening

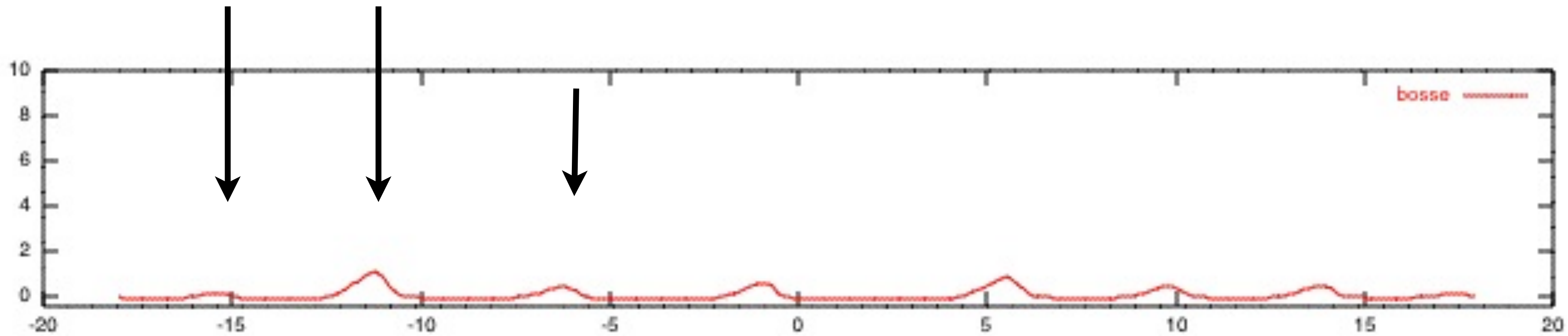

coarsening

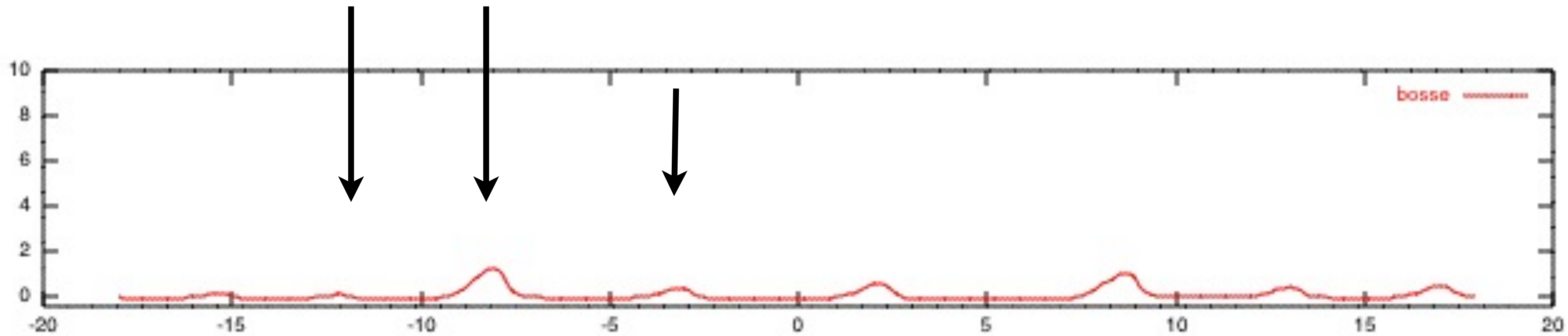

coarsening

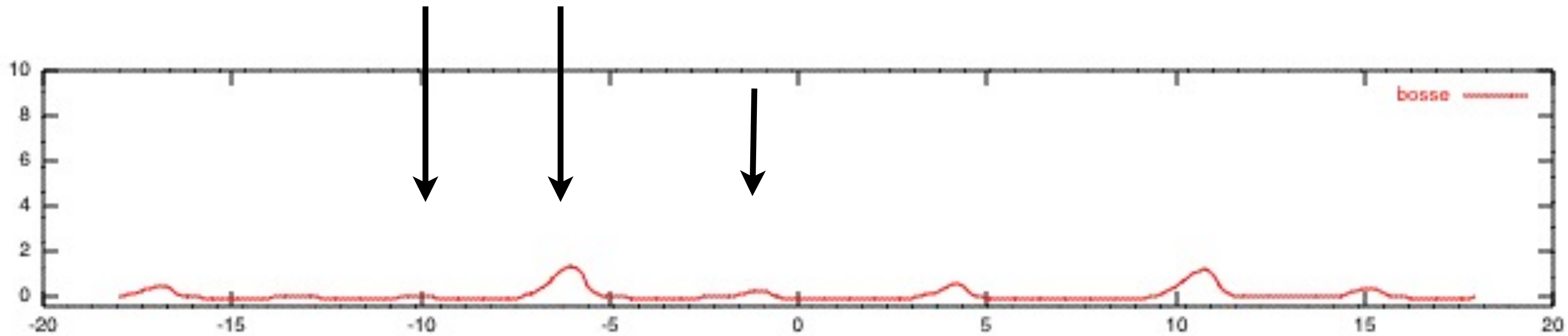

coarsening

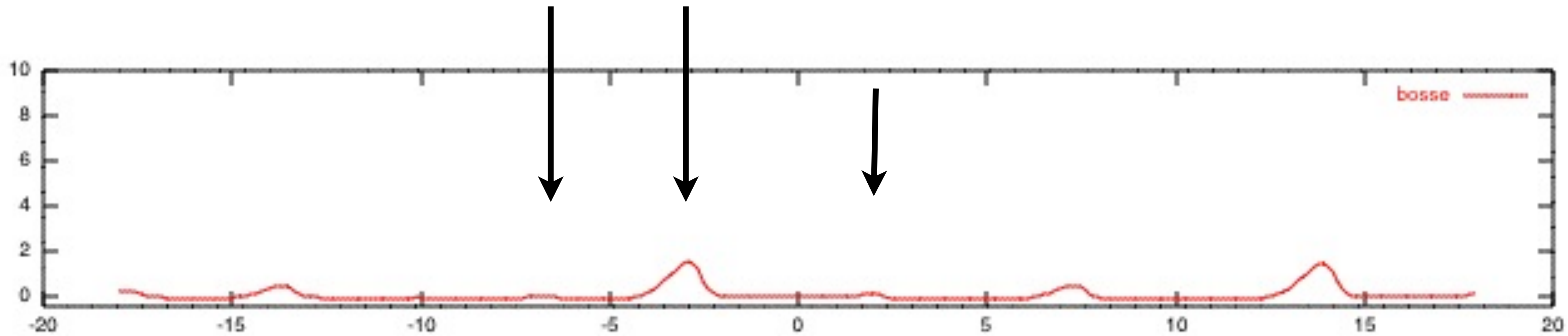

coarsening

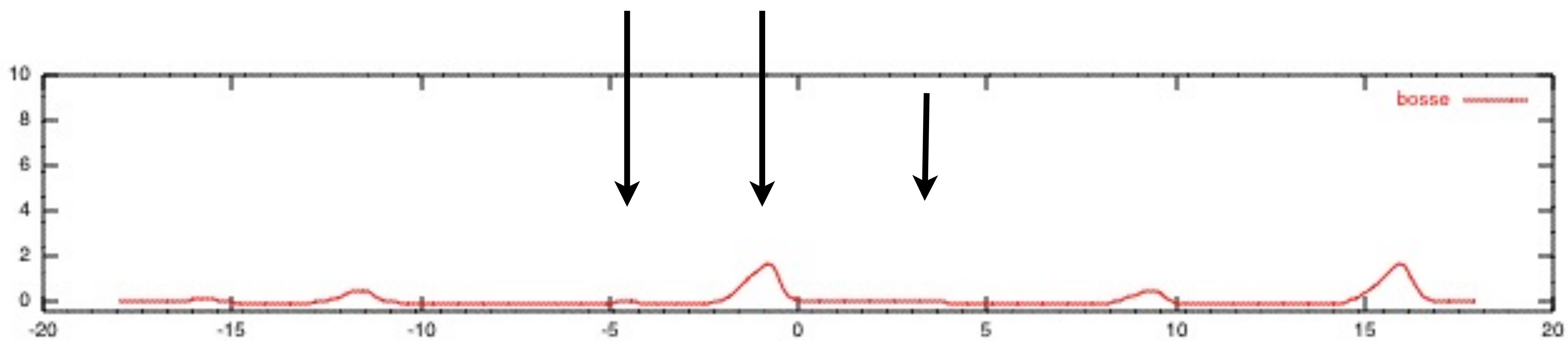

coarsening

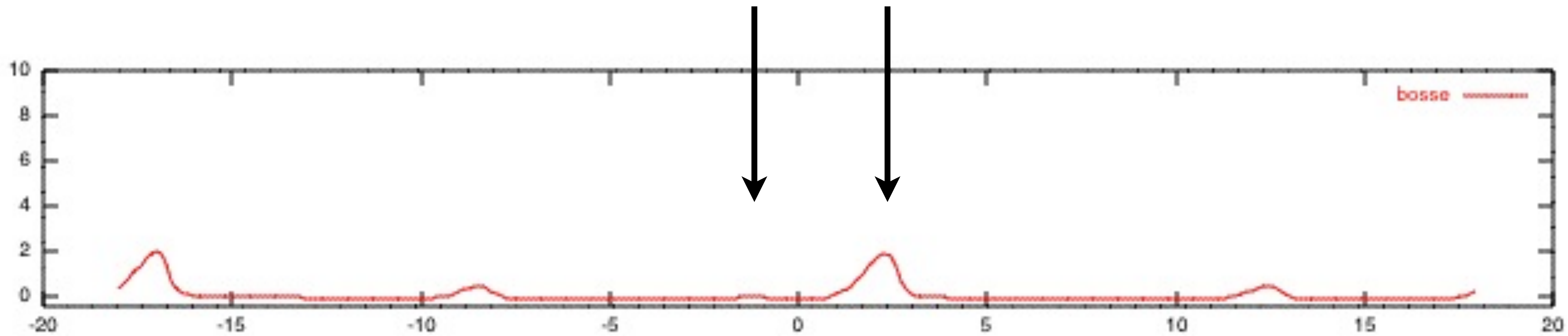

coarsening

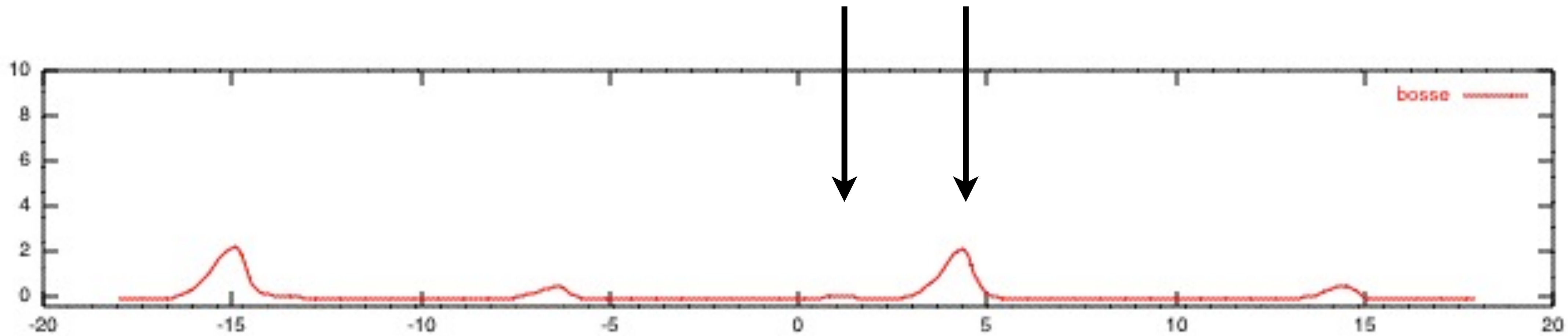

coarsening

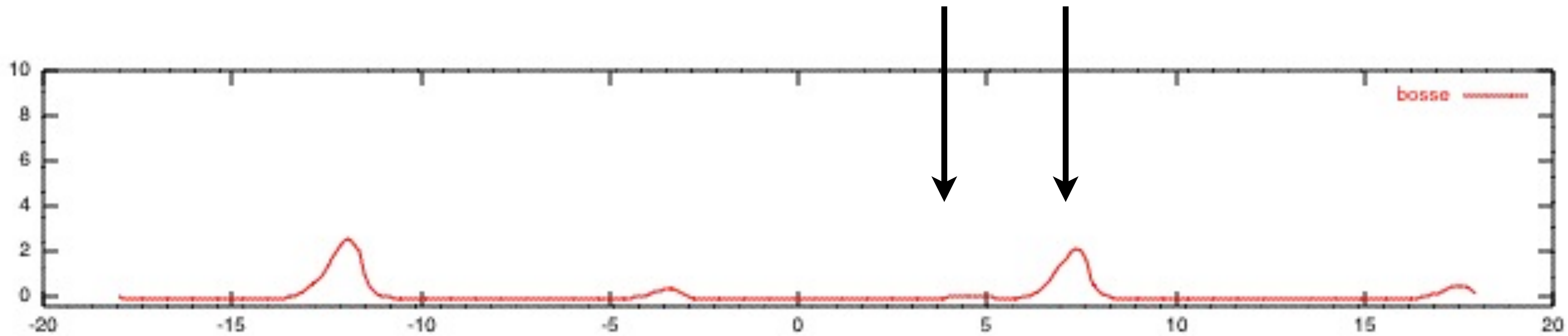

coarsening

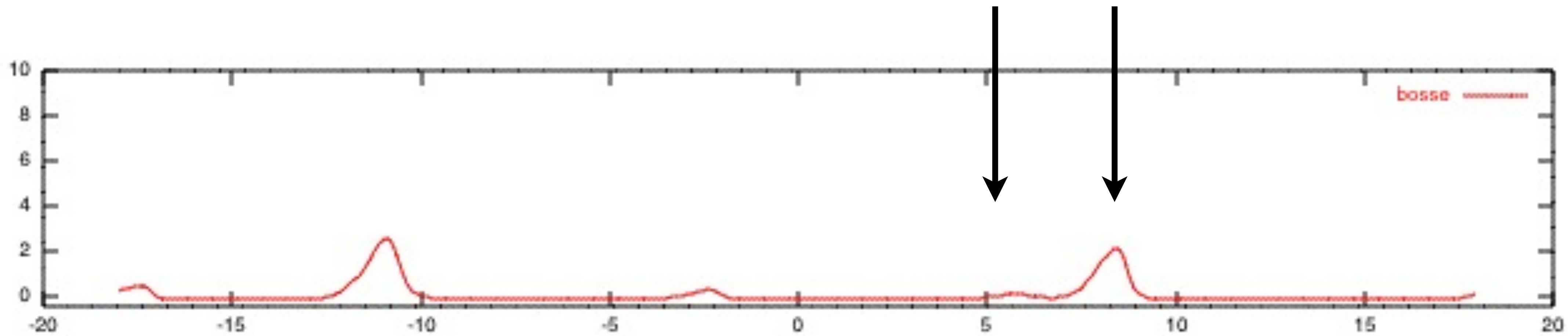

coarsening

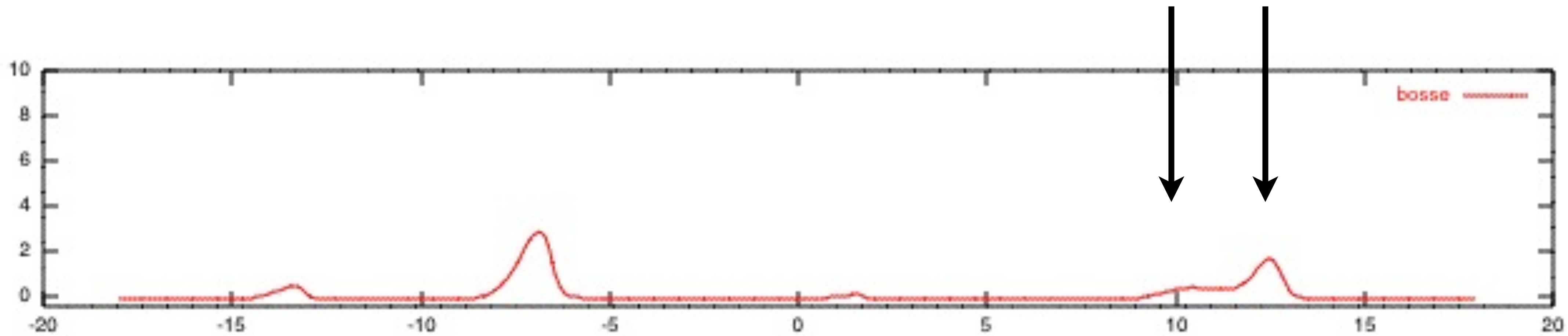

coarsening

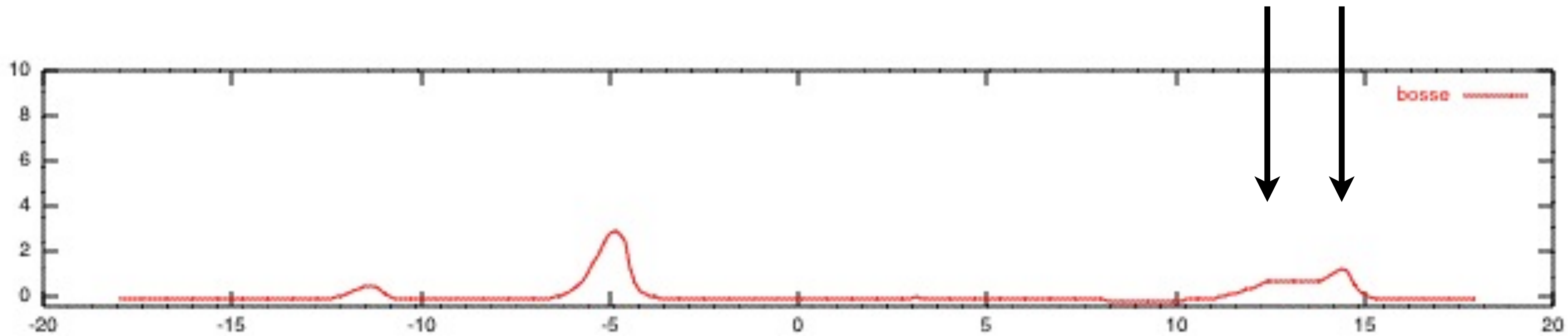

coarsening

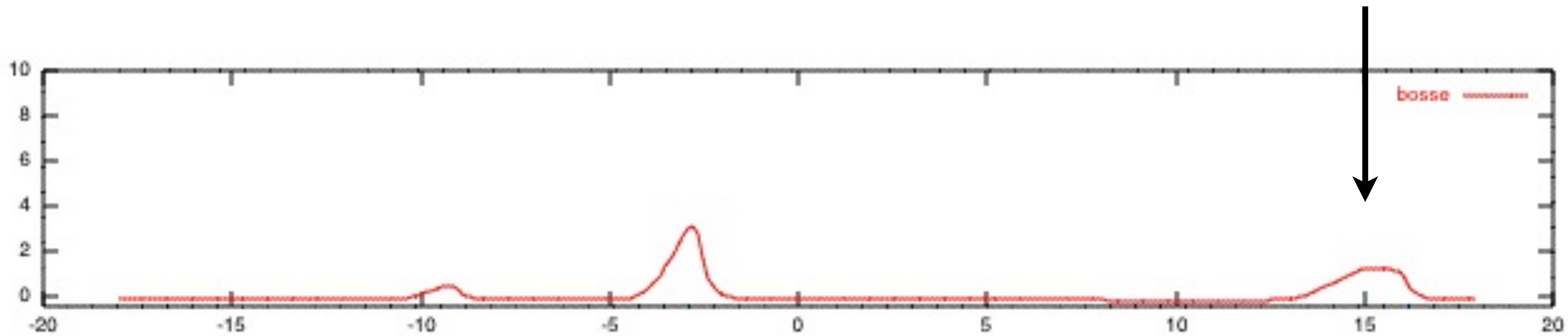

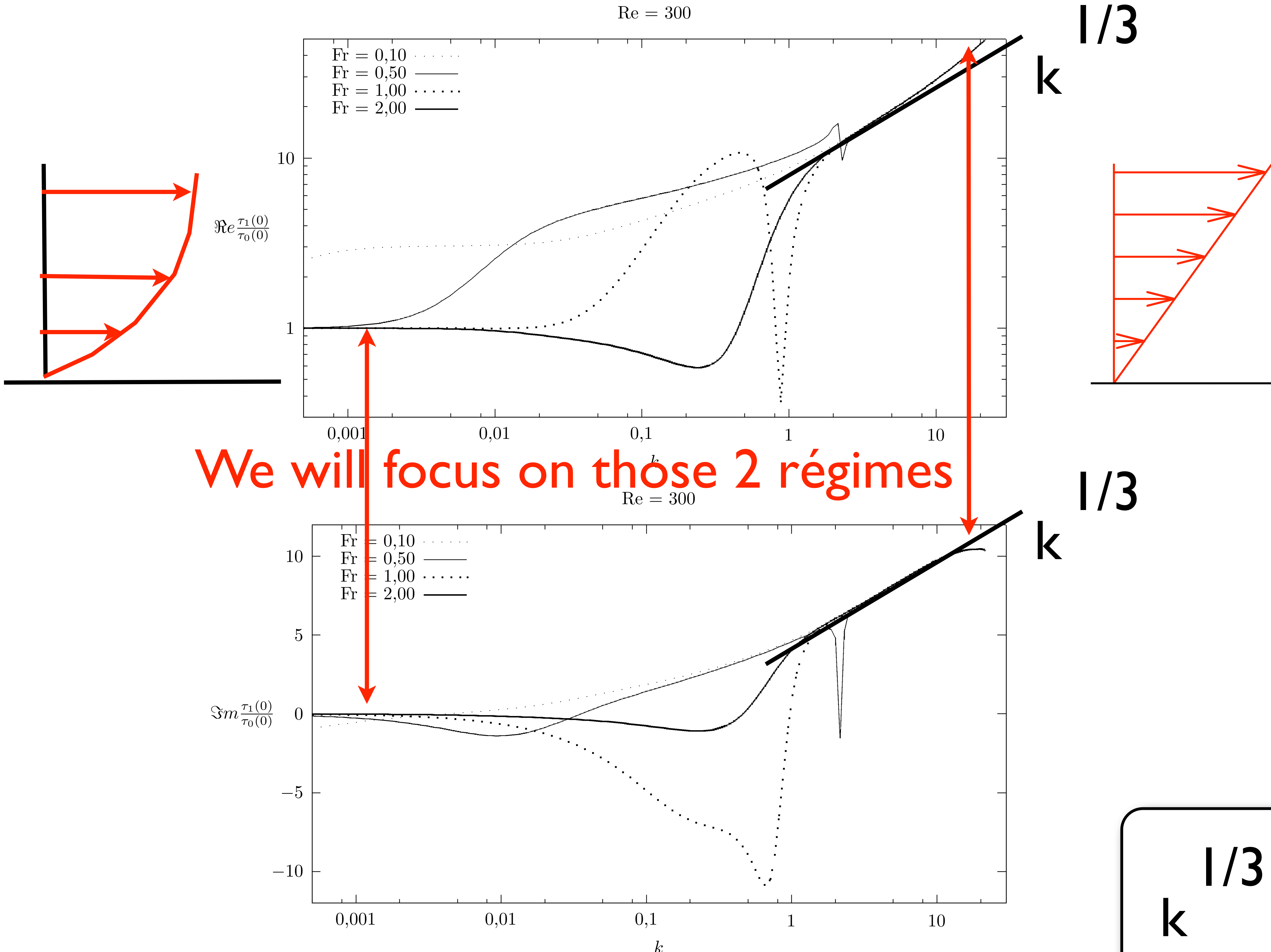

We will focus on those 2 régimes

$k^{1/3}$

> Steady Orr Sommerfeld

FIG. 2.6 – *Parties réelles (en haut) et parties imaginaires (en bas) de la perturbation du cisaillement au fond renormalisée, pour Re = 300 et différentes valeurs de Fr.*

- introduction
- the problem
- the flow: Saint Venant and other
- first granular model
- first coupling: bars
- imporved granular model: saturation length
- ripples
- bars & ripples
- conclusions perspectives

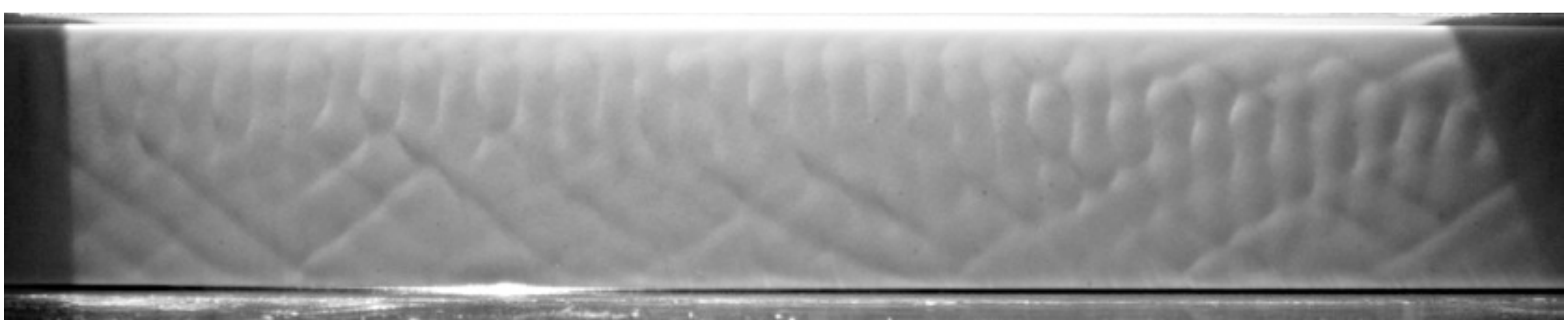

Saint-Venant

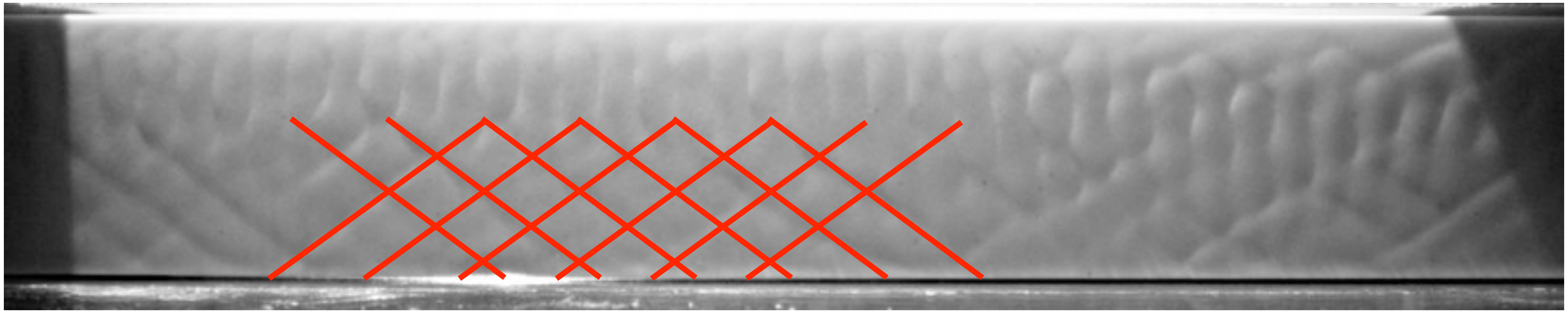

Saint-Venant

asymptotic

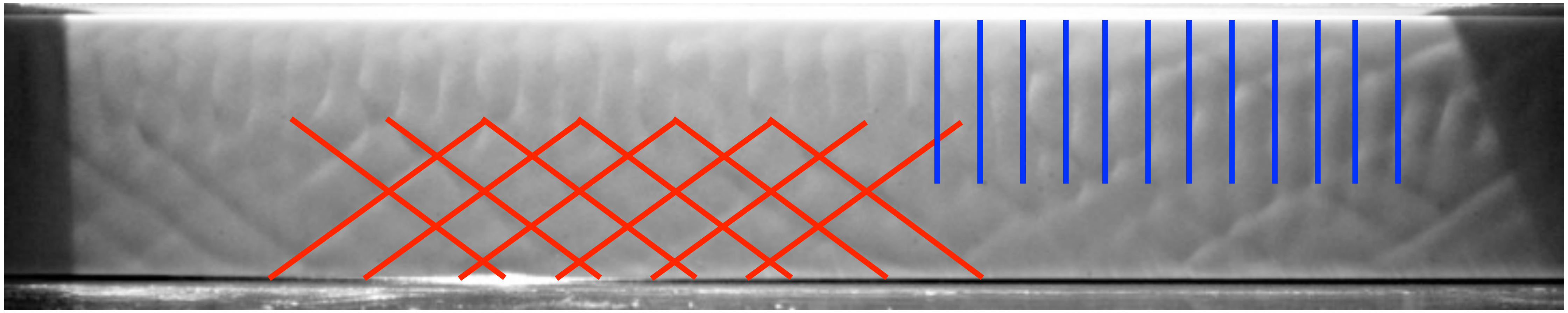

Saint-Venant

asymptotic

complete 3D linear stability approach

> Steady Orr Sommerfeld

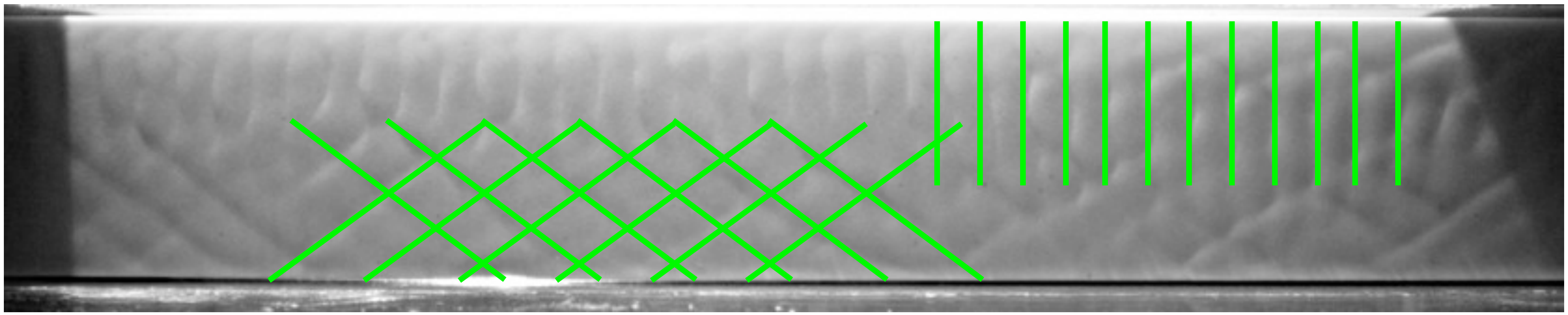

complete 3D linear stability approach

> Steady Orr Sommerfeld

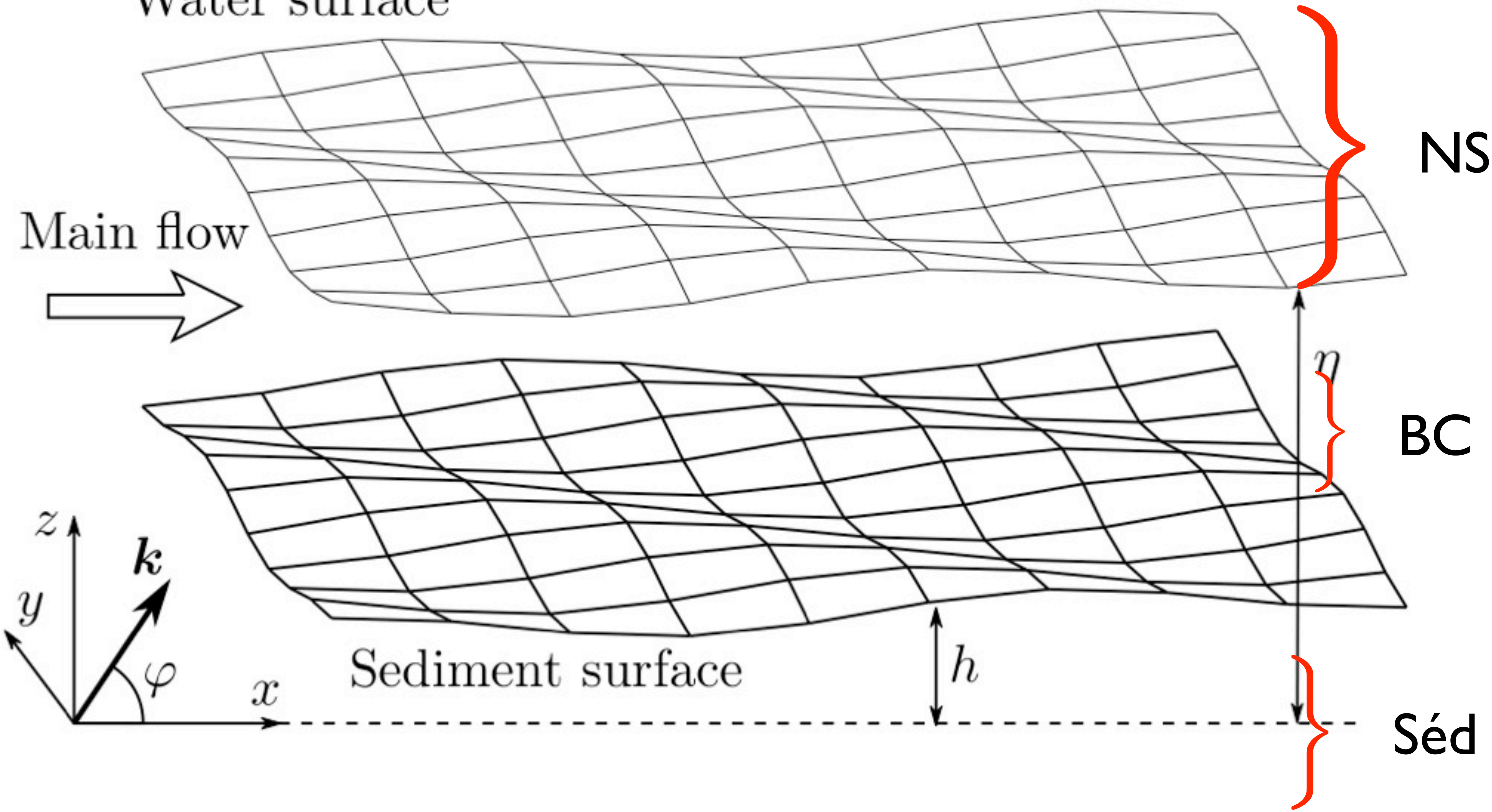

complete 3D linear stability approach

> Steady Orr Sommerfeld

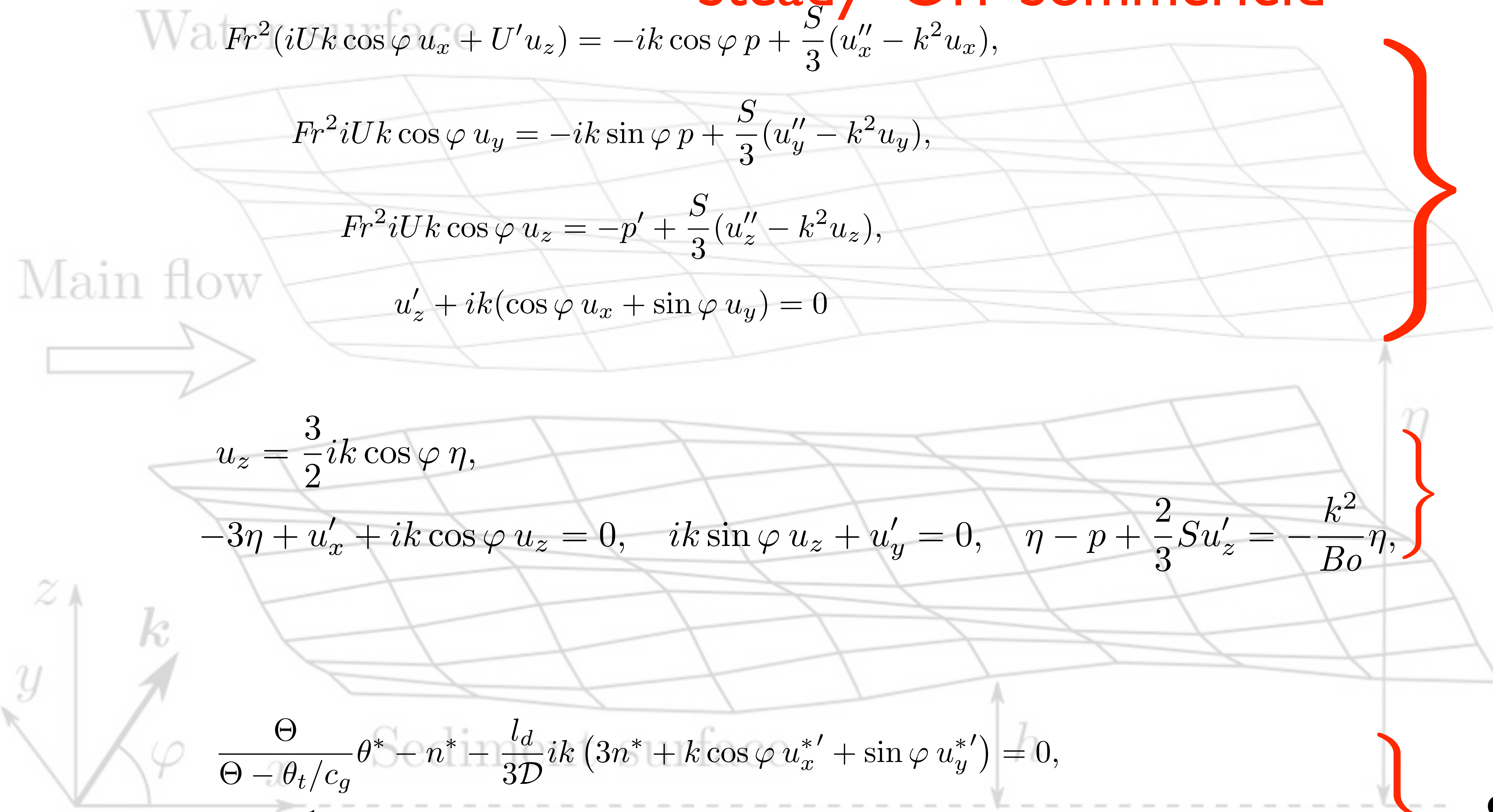

$$\left.\begin{aligned}
&Fr^2(iUk\cos\varphi\, u_x + U' u_z) = -ik\cos\varphi\, p + \frac{S}{3}(u_x'' - k^2 u_x),\\
&Fr^2 iUk\cos\varphi\, u_y = -ik\sin\varphi\, p + \frac{S}{3}(u_y'' - k^2 u_y),\\
&Fr^2 iUk\cos\varphi\, u_z = -p' + \frac{S}{3}(u_z'' - k^2 u_z),\\
&u_z' + ik(\cos\varphi\, u_x + \sin\varphi\, u_y) = 0
\end{aligned}\right\}\ \text{NS}$$

$$\left.\begin{aligned}
&u_z = \frac{3}{2} ik\cos\varphi\,\eta,\\
&-3\eta + u_x' + ik\cos\varphi\, u_z = 0, \quad ik\sin\varphi\, u_z + u_y' = 0, \quad \eta - p + \frac{2}{3} S u_z' = -\frac{k^2}{Bo}\eta,
\end{aligned}\right\}\ \text{BC}$$

$$\left.\begin{aligned}
&\frac{\Theta}{\Theta - \theta_t/c_g}\theta^* - n^* - \frac{l_d}{3\mathcal{D}} ik\left(3n^* + k\cos\varphi\, u_x^{*\prime} + \sin\varphi\, u_y^{*\prime}\right) = 0,\\
&\theta^* = \frac{1}{3}\Big(2\tilde{\theta}^2\left(u_z^{*\prime} - 3ih^* k\cos\varphi\right) - 3ih^* k\cos\varphi\ (1 + S^2) +\\
&\qquad \frac{Sh}{c_q}\left(u_x^{*\prime} + 2S u_z^{*\prime} - 3h^*(1 + 3ik\cos\varphi\, S)\right)\Big).
\end{aligned}\right\}\ \text{Séd}$$

complete 3D linear stability approach

> Steady Orr Sommerfeld

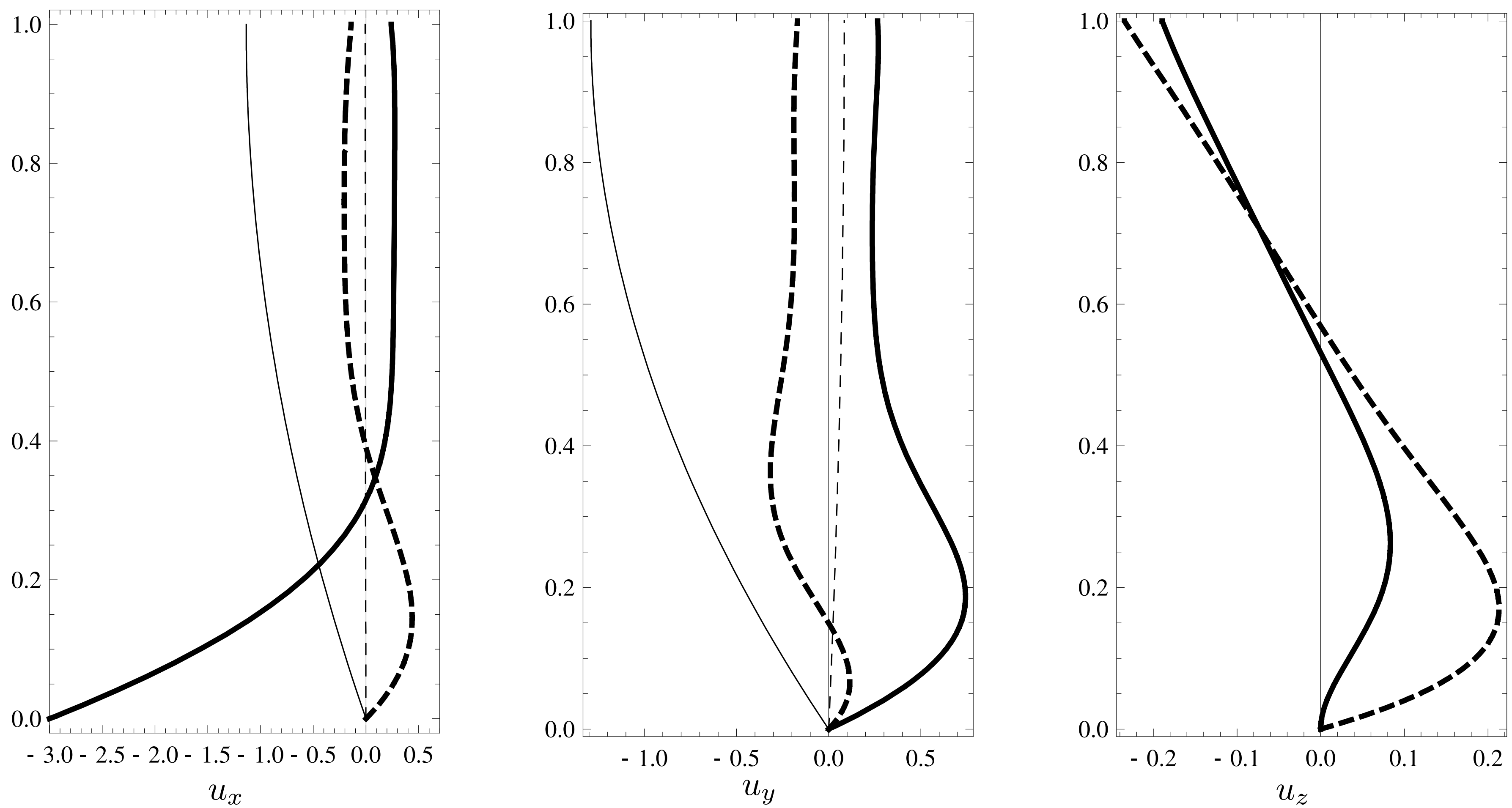

complete 3D linear stability approach

> Steady Orr Sommerfeld

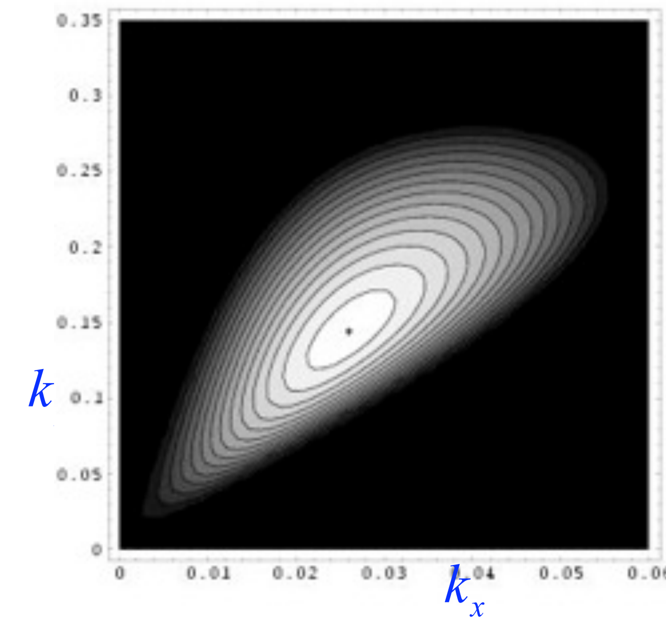

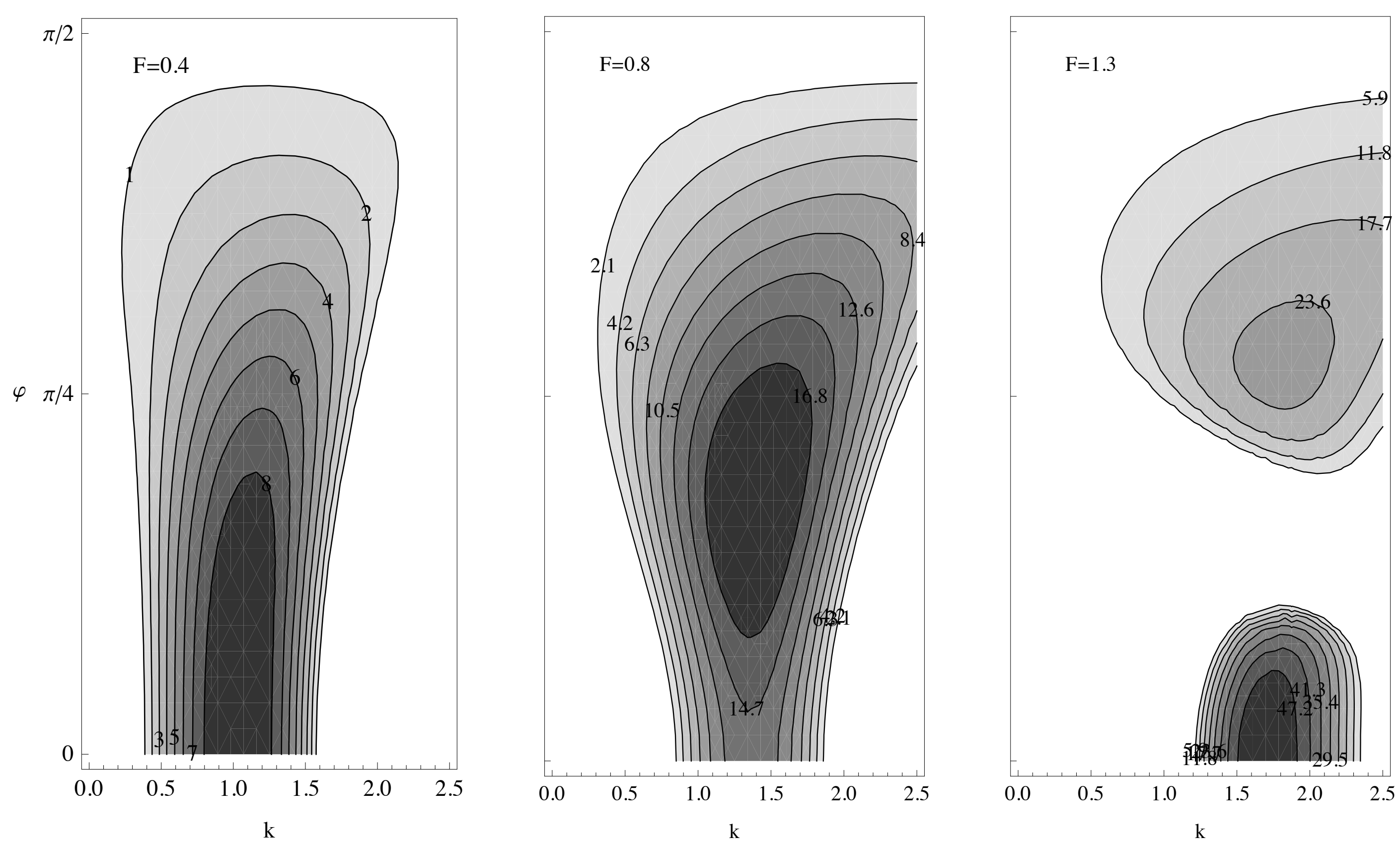

complete 3D linear stability approach

> Steady Orr Sommerfeld

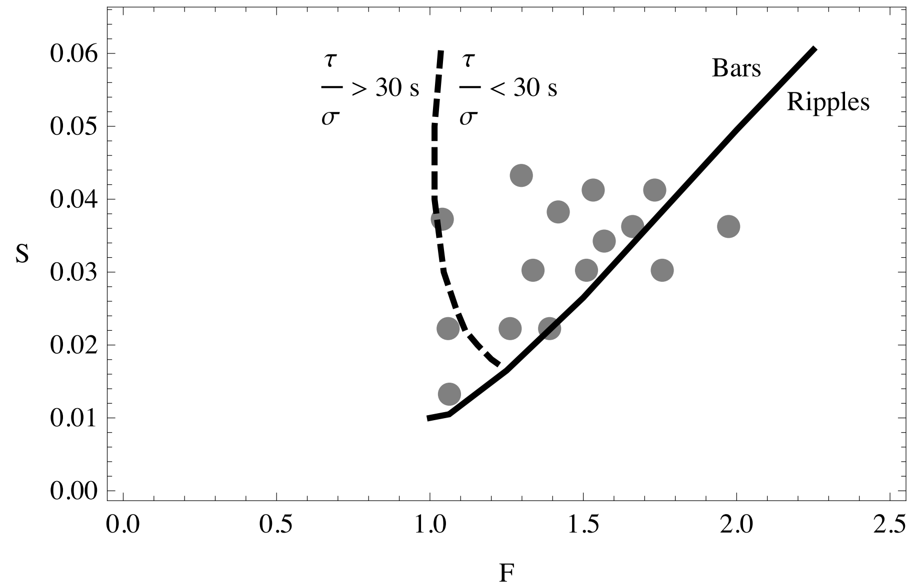

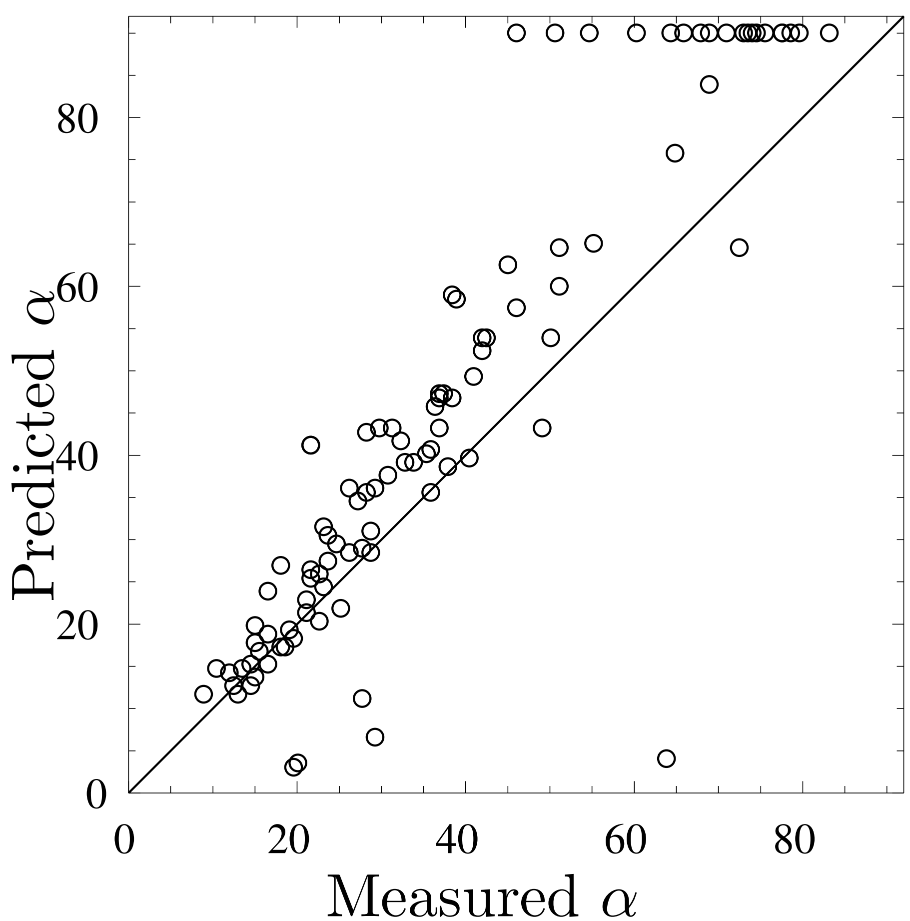

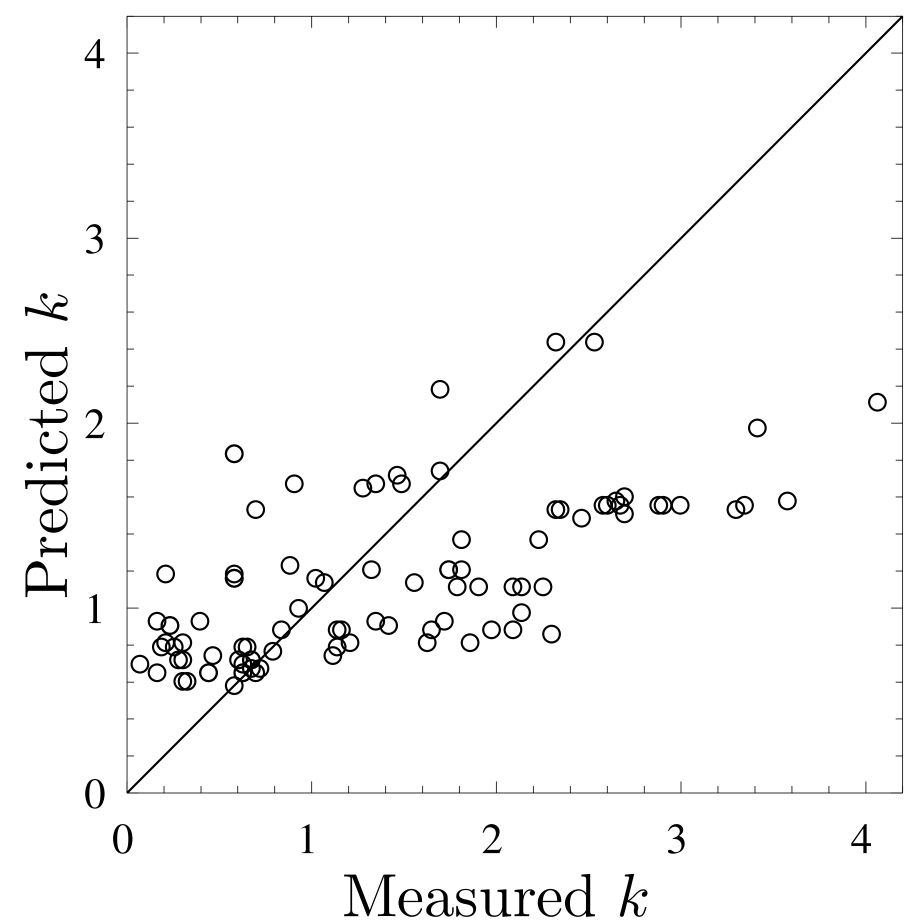

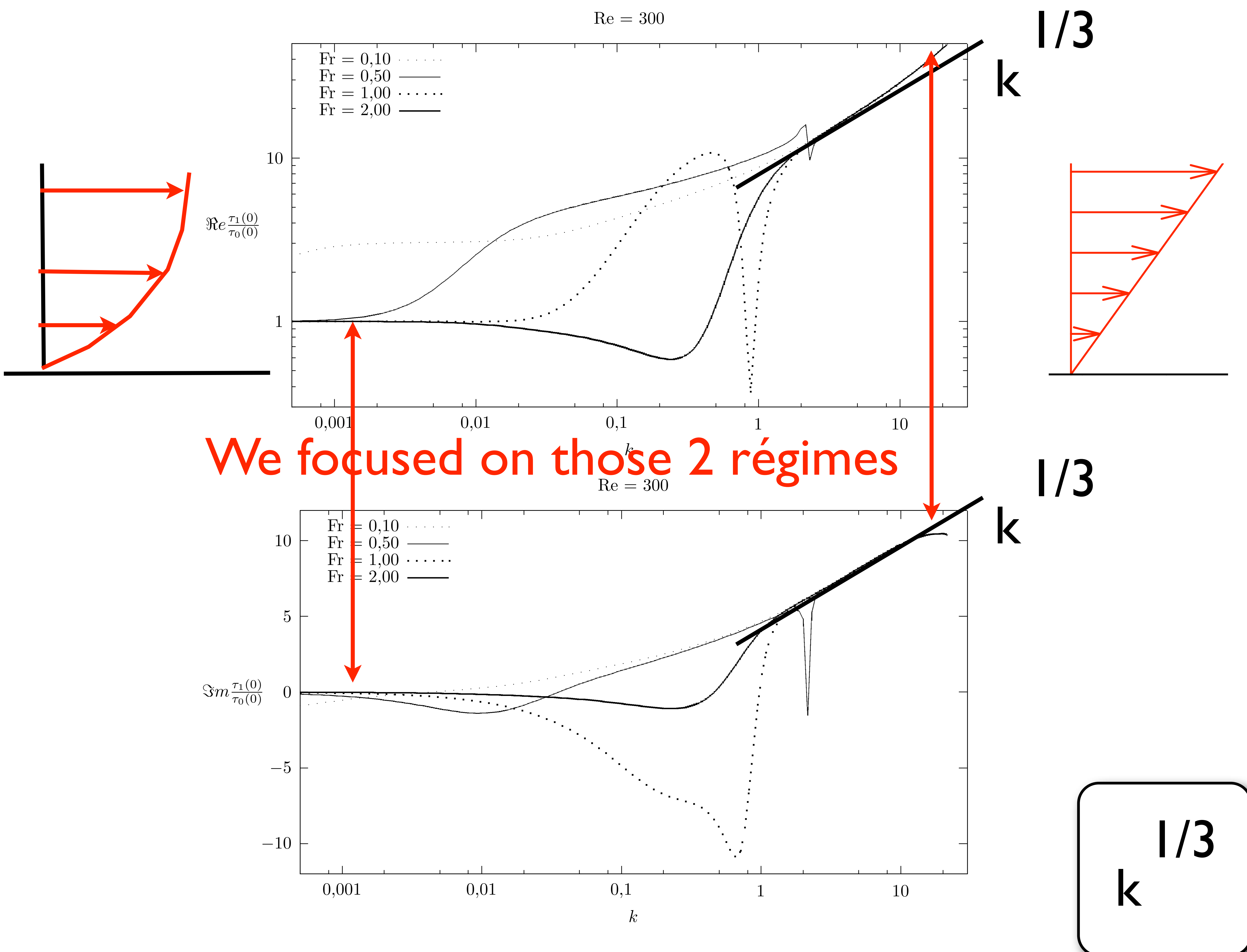

Fig. 2.6 – *Parties réelles (en haut) et parties imaginaires (en bas) de la perturbation du cisaillement au fond renormalisée, pour Re = 300 et différentes valeurs de Fr.*

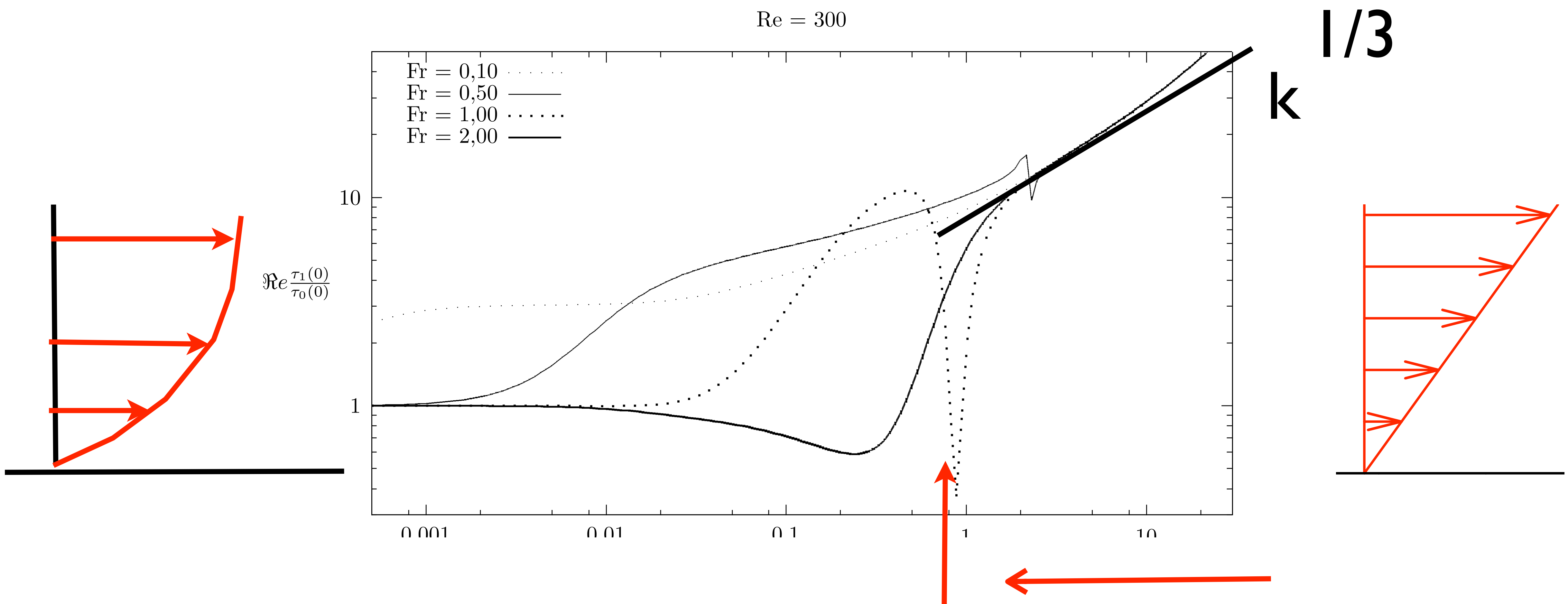

coarsening of ripples

maximum size of dunes?

- introduction
- the problem
- the flow: Saint Venant and other
- first granular model
- first coupling: bars
- improved granular model: saturation length
- ripples
- bars & ripples
- conclusions perspectives

conclusion

PATTERNS

-Saint Venant is a poor model
-need all the terms of Navier Stokes
-need a not to crude granular description

Alternate bars

Rhomboid paterns
Lingoid bars

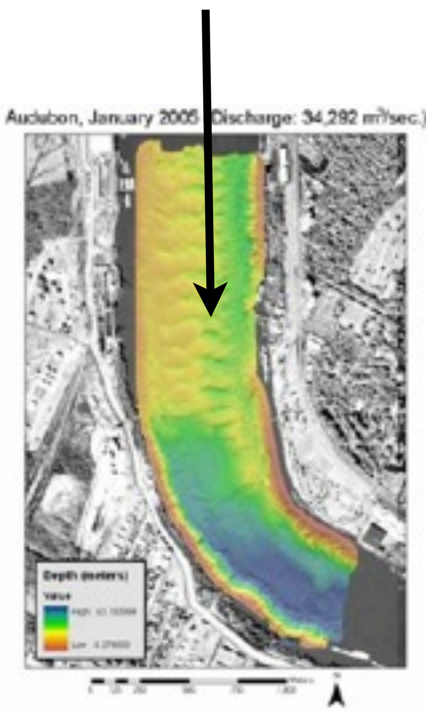

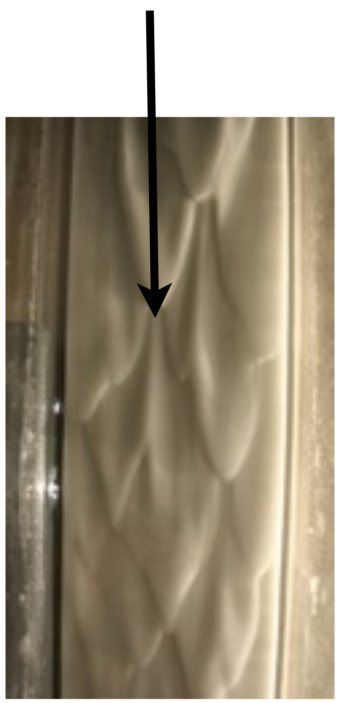

Ripples

Dunes

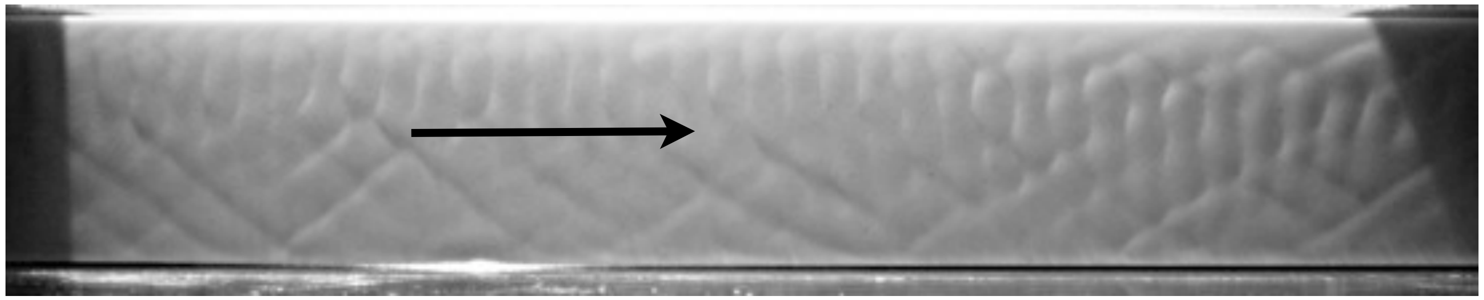

to do

- non linear evolution of the rhomboid patterns
- full asymptotic description of the wavy bed
- other flows: sloping beach?
- applications to practical configurations
- coupling with «gerris flow solver»

Publications

-O. Devauchelle, L. Malverti, É. La Jeunesse, C. Josserand, P.-Y. Lagrée, & F. Métivier
"Rhomboid Beach Pattern: a Benchmark for Shallow water Geomorphology"
to appear in JGR

- O. Devauchelle, L. Malverti, É. La Jeunesse, P.-Y. Lagrée, C. Josserand & K.-D. Nguyen Thu-Lam (2010)
Stability of bedforms in laminar flows with free-surface: from bars to ripples
Journal of Fluid Mechanics, vol 642 p 329-348

O. Devauchelle, C. Josserand, P.-Y. Lagrée and S. Zaleski (2008):
"Mobile Bank Conditions for Laminar Micro-Rivers"
C. R. Geoscience (2008), doi:10.1016/j.crte.2008.07.010

O. Devauchelle, C. Josserand, P.-Y. Lagrée, and S. Zaleski (2007):
"Morphodynamic modeling of erodible laminar channels"
Phys. Rev. E 76, 056318

P.-Y. Lagrée (2007):
"Interactive Boundary Layer in a Hele Shaw cell".
Z. Angew. Math. Mech. 87, No. 7, pp. 486-498

K.K.J. Kouakou & P.-Y. Lagrée (2006):
"Evolution of a model dune in a shear flow".
European Journal of Mechanics B/ Fluids Vol 25 (2006) pp 348-359.

C. Josserand, P.-Y. Lagrée, D. Lhuillier (2006):
" Granular pressure and the thickness of a layer jamming on a rough incline"
Europhys. Lett., 73 (3), pp. 363–369 (2006)

K.K.J. Kouakou & P.-Y. Lagrée (2005):
"Stability of an erodible bed in various shear flow".
European Physical Journal B - Condensed Matter, Volume 47, Issue 1, Sep 2005, Pages 115 - 125

P.-Y. Lagrée, K.K.J. Kouakou & E. Danho (2003):
"Effet dispersif de la loi d'Exner menant à l'équation de Benjamin-Ono: formation de rides sur un sol meuble",
C. R. Acad. Sci. Paris, vol 331/3 pp 231 - 235

P.-Y. Lagrée (2003):
"A Triple Deck model of ripple formation and evolution",
Physics of Fluids, Vol 15 n 8, pp. 2355-2368.

Lagrée P.-Y. (2000):
" Erosion and sedimentation of a bump in fluvial flow",
C. R. Acad. Sci. Paris, t328, Série II b, p869-874, 2000